PHONON OPTICAL PROPERTIES OF MIXED FLUORITE SYSTEMS: RAMAN SCATTERING FROM $Ca_{1-x}Sr_xF_2$ AND $Ba_{1-x}Sr_xF_2$

by

William B. Lacina

Technical Report No. ARPA-36

Contract ARPA SD-88

March 1969

Submitted to:

Advanced Research Projects Agency

The Department of Defense

Division of Engineering and Applied Physics

Harvard University

Cambridge, Massachusetts

PHONON OPTICAL PROPERTIES OF MIXED FLUORITE SYSTEMS: RAMAN SCATTERING FROM $Ca_{1-x}Sr_xF_2$ AND $Ba_{1-x}Sr_xF_2$

By

William B. Lacina

Division of Engineering and Applied Physics

Harvard University · Cambridge, Massachusetts

ABSTRACT

The general problem of the effects of impurities on the vibrational, electronic, and magnetic properties of crystalline solids has currently attracted much interest. One aspect of this problem has been the study of random disordered systems, and in recent years, there have been numerous experimental and theoretical investigations of the phonon optical properties of mixed crystal systems. We have studied experimentally the Raman scattering (at $\sim 4^{\circ}K$, $77^{\circ}K$, and $300^{\circ}K$) from the mixed fluorite systems, $Ca_{1-c}Sr_cF_2$ and $Ba_{1-c}Sr_cF_2$, using laser excitation and a photon counting detection system. Analogous work on the far-infrared reflectivity spectra for these systems has been carried out by Verleur and Barker.

The Green's function methods which have been extensively employed for the isolated defect and random disorder problems are reviewed, and it is shown how the phonon optical properties can be expressed using this formalism. These techniques have been very useful for qualitative and quantitative understanding of impurity effects, although they usually involve cumbersome computational difficulties for physically realistic models

of the impurity and the host lattice. A low concentration theory for Raman scattering and infrared absorption in mixed crystals, based on an average Green's function $\langle G \rangle$, is described and applied to the $Ca_{1-c}Sr_cF_2$ system; theoretical calculations are presented and compared with experimental measurements. The "proper self-energy" functions which arise in this formalism are calculated to first order in the concentration c, and involve certain unperturbed phonon Green's functions $G^o_{\alpha\beta}(\ell\kappa, \ell'\kappa';\omega + i\varepsilon)$, which have been computed numerically for a rigid ion model of a harmonic fluorite lattice. These Green's functions, which would be useful for many other studies of phonon impurity properties in CaF_2, are included in an appendix.

TABLE OF CONTENTS

I. INTRODUCTION

The study of the physical effects that impurities have on the vibrational, electronic, and magnetic properties of a crystal lattice has recently attracted much experimental and theoretical interest. The work in this field has had a variety of objectives, which can be broadly characterized as: 1) a study of new effects, such as local and resonance modes, which can arise when suitable impurities are present, 2) the use of impurities to induce new effects, through a breakdown in the selection rules applicable to a perfect crystal, 3) the study of dynamical properties of the impurity itself, 4) the study of the modification of existing properties with the addition of defects. Furthermore, there has been a wide range of experimental techniques which have been employed for these investigations. Such work has included Raman and infrared spectroscopy, the Mössbauer effect, neutron scattering, measurement of thermal and electrical conductivity, etc.

The literature in this field has been expanding so rapidly that it would be futile to attempt to cite all of the work that has been done. An excellent and extremely thorough review article on the effects of point defects and disorder on lattice vibrational properties has been given by Maradudin[1]. Although the emphasis in the present work shall be specifically on the phonon problem, some further references to work on the electronic and magnetic impurity problems will be given at appropriate places later. Many of the review articles can often be consulted for numerous references on specific aspects of this general field.

The mathematical techniques which have been most useful for describing and understanding impurity effects in crystalline solids involve Green's function methods, analogous to those used in many-body problems. These techniques, which can be used to relate the properties of an imperfect crystal lattice to those of a perfect lattice, are convenient for analyzing the "isolated impurity" problem, and can be successfully applied whenever the perturbation caused by the defect is spatially localized. Because of their generality, Green's function techniques can be used to describe a wide variety of impurity effects on the physical properties of solids. The underlying unity that characterizes these methods allows the mathematical formulation of many physically diverse phenomena to be carried out in essentially the same way. We shall discuss some of the basic aspects of the Green's function formalism in a later chapter.

Because the problem of a single impurity is now reasonably well understood, qualitatively and quantitatively, much of the current interest in this field has shifted to studies--both experimental and theoretical--of mixed crystal systems. The most extensive (analytical) theoretical work on random disordered crystals has consisted of attempts to extend those methods of Green's functions which have proved so successful for describing the isolated local impurity problem. These "average Green's function" techniques have been fruitful for explaining many of the features of a disordered system, although they are often limited by the approximations that must be imposed for even the simplest models. In some respects, these approximations have not been completely satisfactory; for example, they are inadequate to explain or predict many of the complicated "spike" effects which exact machine solutions have shown can exist

(in the density of states) for even the simplest systems. These difficulties may be related either to the limitations of the numerical approximations, or possibly even to the inadequacy of the assumptions made on the analyticity properties of the average Green's function as a function of the concentration c. Furthermore, even in situations where these methods have been applied with reasonable assurance of validity, they usually involve tedious numerical calculations for realistic models of the lattice and defect. Nevertheless, despite some of the shortcomings in certain pathological cases, or the problems of computational difficulty, these techniques have had great success in describing many of the impurity effects observed in physical systems. The method of Green's functions as applied to the study of a random disordered crystal will be discussed more fully for the vibrational problem in a subsequent chapter. At that time, we shall also give a survey of the variety of other (non-Green's function) approaches that have been taken to analyze this problem, and some of the results that have been obtained.

One aspect of this general problem is the investigation of the effects of disordering on the behavior of the long-wavelength optical vibrations of mixed crystals. There has recently been numerous experimental work on Raman scattering and infrared absorption from phonons in a wide variety of mixed crystal systems. The present work is concerned with a study of the mixed-fluorite systems, $Ca_{1-x}Sr_xF_2$ and $Ba_{1-x}Sr_xF_2$. We have investigated experimentally[2] the first order Raman scattering from these systems, and Verleur and Barker[3] have done analogous work on the infrared reflectivity. The work to be reported here is an attempt to discuss, qualitatively and quantitatively, the observed experimental effects of

disordering on the optical vibration modes for the mixed-fluorite systems.

The experimental literature on phonon optical properties in mixed crystal systems is extensive; several examples of other systems that have been studied by Raman and infrared spectroscopy include $GaAs_{1-x}Sb_x$[4], $Ni_{1-x}Co_xO$[5], $Zn_{1-x}Cd_xS$[6], $ZnSe_{1-x}Te_x$[7], $Na_{1-x}K_xCl$[8], $KCl_{1-x}Br_x$[9], $K_{1-x}Rb_xCl$[9], $KMg_{1-x}Ni_xF_3$[10], $Si_{1-x}Ge_x$[11], $InP_{1-x}As_x$[12], $GaP_{1-x}As_x$[13, 14], $CdS_{1-x}Se_x$[15-17], $ZnS_{1-x}Se_x$[18], $NaCl^{35}_{1-x}Cl^{37}_x$[19], $LiH_{1-x}D_x$[20]. There would be many more examples if the list were enlarged to include work on other than phonon optical properties. There are also some general articles which are a useful review of the experimental results on mixed crystal systems[21] and a discussion of the behavior of the long-wavelength optical modes[22].

Experimental observations on Raman scattering and infrared absorption from such crystals has yielded, basically, two characteristic types of behavior. Assume that a mixed crystal $A_{1-x}B_xC$ can be formed from AC and BC, each of which are characterized by one optically active mode, with frequency ω_A and ω_B respectively. Then in the first (Type I) behavior, the mixed crystal $A_{1-x}B_xC$ continues to exhibit[2-10] a single $\vec{k} \sim 0$ optic mode which shifts linearly with the concentration x from the frequency ω_A (that characterizes pure AC) to ω_B (that for pure BC). The intensity of the mode remains approximately constant, and the linewidth increases and peaks near the center ($x \sim .5$) of the mixture. For the second (Type II) behavior[11-19], the mixed crystal exhibits two modes which are close to those which characterize pure AC and pure BC. The intensity of these modes varies in approximate proportion to the fraction of each component present. As the (molar) concentration x increases, the inten-

sity of the BC mode increases, while that of AC decreases, with both shifting slightly.

The experimental observations on Raman scattering from the mixed-fluorites[2] represents a good example of Type I behavior, and since this system constitutes the subject of the present study, these results will be described in more detail later. A good example of Type II behavior is represented by the Raman spectrum of $Si_{1-x}Ge_x$, shown in Fig. 1.1 (taken from the work of Feldman, Ashkin, and Parker, Phys. Rev. Lett. 17, 1209 (1966), Ref. 11), and the infrared reflectivity spectrum of $CdS_{1-x}Se_x$, shown in Fig. 1.2 (taken from the work of Verleur and Barker, Phys. Rev. 155, 750 (1967), Ref. 17).

It is possible for some modes of a crystal to exhibit a behavior intermediate between types I and II, and it is also possible for different modes of the same mixed crystal system to display different behavior [10,18]. The theory for the optical phonon properties of a mixed crystal will be formulated in terms of "average Green's functions," which will be described later, and then applied later to calculations for the mixed-fluorite system, $Ca_{1-x}Sr_xF_2$. These methods, although formidable to apply, are useful for both a qualitative and quantitative understanding of the effects of disordering on the optical properties. They provide a criterion for the "virtual crystal approximation" that characterizes the linear shift (type I) behavior, and are also capable of explaining the "local mode" behavior that characterizes type II spectra.

A brief outline of the presentation of material to follow should be helpful to define the scope of the present study. In Chapter II, some elementary topics related to crystal structure, space group symmetry, the

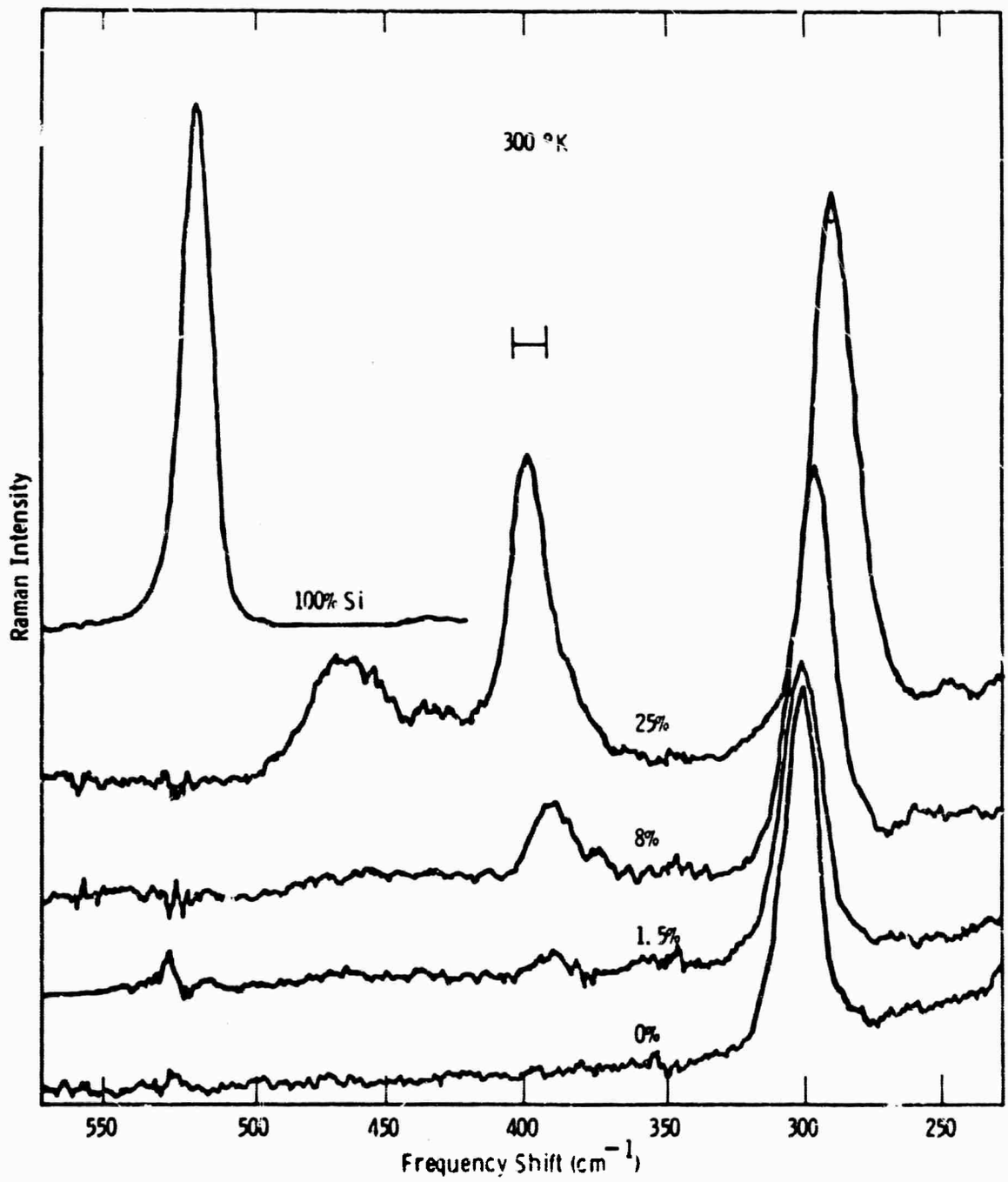

Fig. 1.1: Raman spectra of germanium-silicon alloys for several compositions (Taken from the work of Feldman, Ashkin, and Parker, Phys. Rev. Lett. 17, 1209 (1966), Ref. 11.)

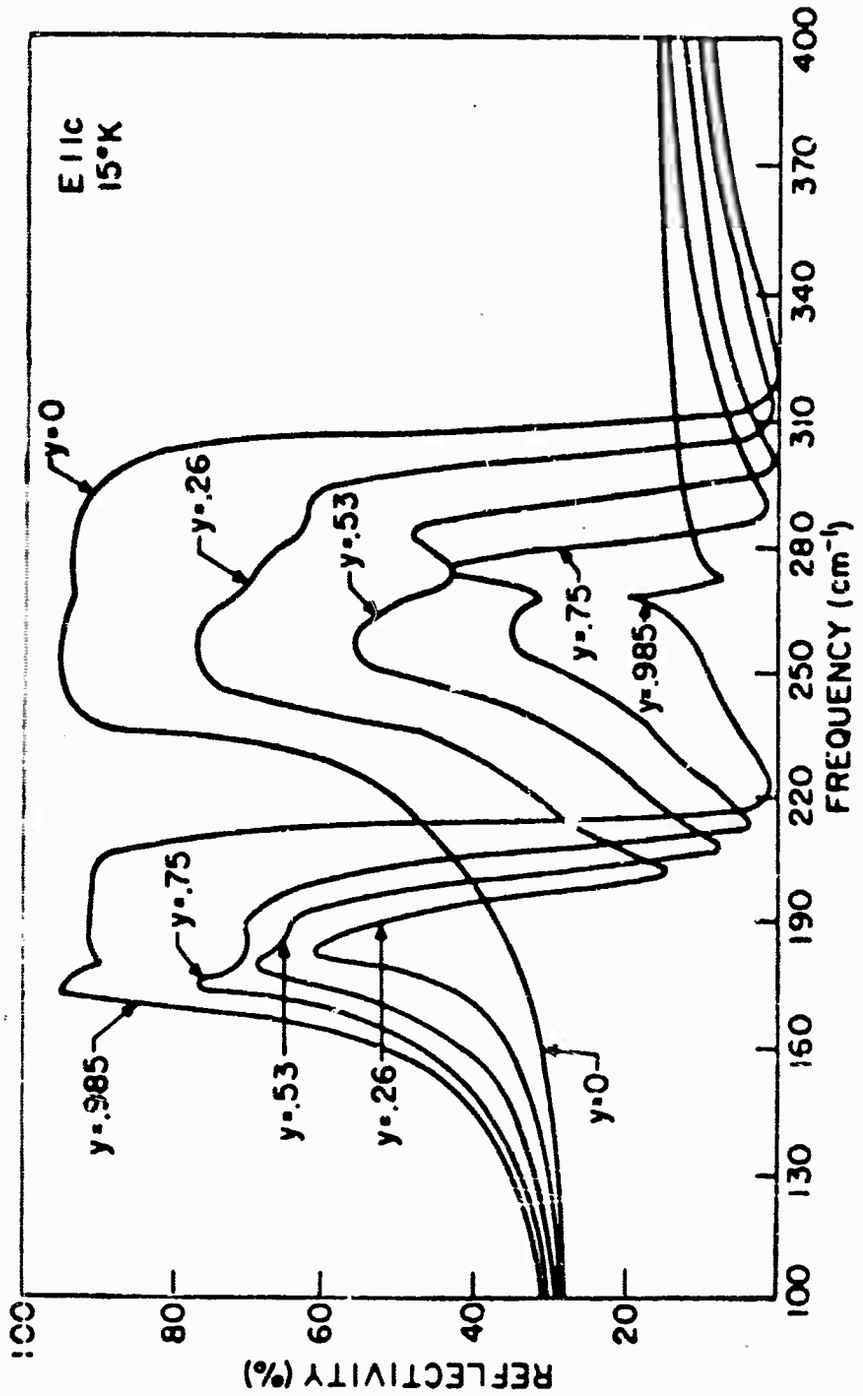

Fig. 1.2: Experimentally determined far-infrared reflectivity spectra of $CdS_{1-x}Se_x$ at 15°K, with $\vec{E} \perp c$-axis. A smooth line was drawn through experimental points. (Taken from the work of Verleur and Barker, Phys. Rev. 155, 750 (1967), Ref. 17.)

reciprocal lattice and Brillouin zone, etc. will be reviewed, with the fluorite lattice as an illustration. The normal modes of a crystal lattice in the harmonic approximation will be discussed from a phenomenological viewpoint, in order to provide a foundation for the work to follow. A brief qualitative discussion of anharmonic effects and mode broadening will conclude this chapter. Chapter III will be devoted to a development of the (classical and quantum mechanical) Green's function methods that are useful for treating the vibrational impurity problem. The interesting "local mode" and "resonance mode" phenomena serve to illustrate the usefulness that Green's function methods have for defect lattice dynamical problems. The formal properties of Green's functions are reviewed, and their physical significance illustrated; it will be shown how they arise in the expression for thermodynamically averaged correlation functions. In Chapter IV, it will be shown how the phonon optical properties--Raman scattering and infrared absorption--can be related to phonon Green's functions. Some of the general aspects of these processes, e.g., selection rules, will also be discussed. In Chapter V, we shall take up the subject of disordered systems, with a brief survey of the variety of methods that have been attempted for this type of problem. A reasonably complete discussion of the failures, successes, and usefulness of a number of approaches will be presented, and a number of the results reviewed. The description of disordered systems in terms of average Green's functions is developed, and the relatively cumbersome diagrammatic techniques that have been used by many authors to calculate these average Green's functions is replaced by a simpler differential technique. We are ultimately interested in describing the effects of disordering on the long-

wavelength vibrational properties of a random, mixed crystal. This will require the calculation of phonon "proper self-energy" functions, as well as certain unperturbed phonon Green's functions for the perfect lattice. Finally, in Chapter VI, we present the experimental observations that we have obtained for Raman scattering for the mixed-fluorite systems. Based on the formalism developed in Chapter II-V, theoretical calculations are carried out (using the average Green's function) for the $Ca_{1-x}Sr_xF_2$ system and compared with experiment. These calculations are based on a rigid ion model for CaF_2 which is discussed thoroughly in that chapter. Some of the computational aspects of this type of calculation are somewhat tedious, and the (grubbier) details (and some of the computer program listings) are relegated to the appendix.

II. NORMAL MODES OF A CRYSTAL LATTICE

2.1 Introduction

A brief discussion of lattice dynamics in the harmonic approximation will be given in Sec. 2.2, and some of the notation that will be useful for describing lattice structure is introduced here. Since the fluorite structure is the object of the present work, it shall serve as an illustration.

A perfect crystal lattice is considered to be composed of an infinite number of primitive cells, each of which is a parallelopiped bounded by three non-coplanar vectors $\vec{t}_1$, $\vec{t}_2$, and $\vec{t}_3$, called the primitive translation vectors. Each primitive cell will be assumed to contain r atoms, labeled by a basis index $\kappa = 1, 2, 3, \ldots, r$. If $\vec{R}_\kappa$ denotes the relative location of atom κ within the cell, then the equilibrium position of any atom can be expressed as

$$\vec{R}_{\ell\kappa} = \vec{R}_\ell + \vec{R}_\kappa \tag{2.1}$$

where $\vec{R}_\ell$ is a lattice vector consisting of integral numbers of primitive translations from some (arbitrary) origin,

$$\vec{R}_\ell = \ell_1\vec{t}_1 + \ell_2\vec{t}_2 + \ell_3\vec{t}_3. \tag{2.2}$$

ℓ represents a triplet of integers, (ℓ_1, ℓ_2, ℓ_3). The crystal can be described as consisting of r interpenetrating sublattices, each of which possesses translational periodicity under the lattice vectors $\vec{R}_\ell$. Two atoms of a lattice will be said to be equivalent if they are separated by some lattice vector $\vec{R}_\ell$ --i.e., if they have the same basis index κ.

Of course, identical atoms can have different basis indices, as, for example, the two fluorines do in the CaF_2 structure.

The rotational and translational symmetries of a perfect crystal form the operations of a space group. Space groups are special cases (i.e., subgroups, of the general group of linear, inhomogeneous coordinate transformations,

$$\vec{r}' = \alpha.\vec{r} + \vec{v}$$

and this operation is conveniently denoted by $(\alpha \mid \vec{v})$. The group of transformations $(\alpha \mid \vec{v})$ has two general properties: (i) the matrix parts α of the operations $(\alpha \mid \vec{v})$ themselves form a group, and (ii) the pure translations, which are of the form $(1 \mid \vec{v})$, form an invariant subgroup. A space group is a subgroup of these general coordinate transformations, and consists of all operations $(S \mid \vec{t})$ that obey further restrictions. First of all, the rotational operations S must be real, orthogonal matrices. Secondly, a space group is characterized by the property that it must possess a particular type of invariant subgroup: all of the pure translations $(1 \mid \vec{t})$ must be of the form $(1 \mid \vec{R}_\ell)$, where $\vec{R}_\ell$ is a lattice vector defined by (2.2). Of the several consequences implied by these two restrictions, one of the most important is the fact that the rotational parts S of a space group must form one of the 32 point groups.

For the fluorite structure, the space group is O_h^5-Fm3m. The crystal consists of three interpenetrating face-centered cubic lattices, and can be alternatively pictured as a cubic lattice of fluorine ions with metal ++ ions in every other body-centered position. The lattice structure is shown in Fig. 2.1. In terms of cartesian unit vectors $\hat{i}$, $\hat{j}$, $\hat{k}$, the primitive translation vectors are given by

$$\vec{t}_1 = r_o(\hat{j} + \hat{k}), \quad \vec{t}_2 = r_o(\hat{i} + \hat{k}), \quad \vec{t}_3 = r_o(\hat{i} + \hat{j}) \tag{2.3}$$

which defines a face-centered cubic lattice. Thu unit cell contains r = 3 basis ions--two (inequivalent) fluorines, and one calcium. We can arbitrarily choose the basis vectors to be

$$\begin{aligned} &\text{Ca:} \quad K = 1, \quad \vec{R}_1 = \tfrac{1}{2}r_o(\hat{i} + \hat{j} + \hat{k}) \\ &F_1\text{:} \quad K = 2, \quad \vec{R}_2 = 0 \\ &F_2\text{:} \quad K = 3, \quad \vec{R}_3 = r_o\hat{i} \end{aligned} \tag{2.4}$$

where $r_o = a/2$, and a is the "lattice constant" (cf. Fig. 2.1).

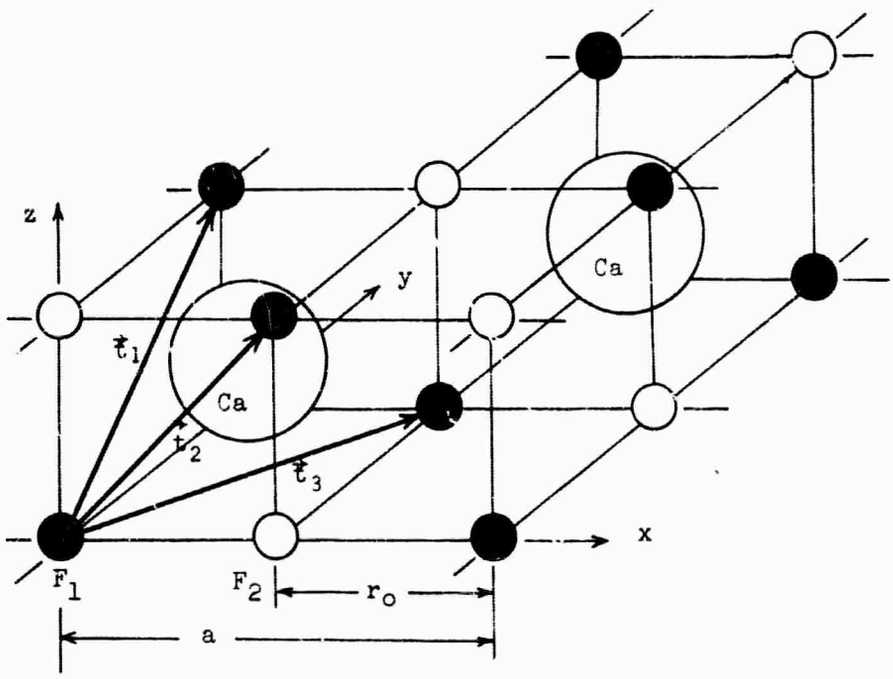

Fig. 2.1: Crystal structure of the (fcc) CaF_2 lattice, with the primitive translation vectors $\vec{t}_1$, $\vec{t}_2$, $\vec{t}_3$ shown.

The reciprocal lattice is defined in the usual way, in terms of a set of vectors,

$$\vec{b}_1 = 2\pi \frac{\vec{t}_2 \times \vec{t}_3}{v_a} = \frac{\pi}{r_o}(-\hat{i} + \hat{j} + \hat{k})$$

$$\vec{b}_2 = 2\pi \frac{\vec{t}_3 \times \vec{t}_1}{v_a} = \frac{\pi}{r_o}(\hat{i} - \hat{j} + \hat{k}) \qquad (2.5)$$

$$\vec{b}_3 = 2\pi \frac{\vec{t}_1 \times \vec{t}_2}{v_a} = \frac{\pi}{r_o}(\hat{i} + \hat{j} - \hat{k})$$

where $v_a = 2r_o^3 = (\vec{t}_1 \times \vec{t}_2)\cdot\vec{t}_3$ is the volume of the primitive cell. The reciprocal systems of vectors satisfy $\vec{b}_i \cdot \vec{t}_j = 2\pi\delta_{ij}$. A general reciprocal lattice vector, $\vec{h}_\lambda$, is defined to be the sum of integer multiples of the vectors $\vec{b}_i$:

$$\vec{h}_\lambda = \lambda_1\vec{b}_1 + \lambda_2\vec{b}_2 + \lambda_3\vec{b}_3 \qquad (2.6)$$

where λ denotes a triplet of integers, $(\lambda_1, \lambda_2, \lambda_3)$.

If we introduce the cyclic Born-von Karmen boundary conditions, and assume that the infinite crystal has a periodicity of G for each of the primitive translations $\vec{t}_1$, $\vec{t}_2$, or $\vec{t}_3$, then there will be a total of $N = G \times G \times G = G^3$ primitive cells. In the usual way, the general wave-vectors $\vec{k}$ which label the irreducible representations of the translation group for the lattice are defined by

$$\vec{k} = \frac{1}{G}(\lambda_1 b_1 + \lambda_2 b_2 + \lambda_3 b_3) \qquad (2.7)$$

where $(\lambda_1, \lambda_2, \lambda_3)$ are integers. The first Brillouin zone is defined to be the symmetrical cell in reciprocal space which contains, in and on its surface, the $N (=G^3)$ values of $\vec{k}$ which label the distinct and non-equiva-

lent representations. There are two relations which are often useful;

$$\frac{1}{N}\sum_{\vec{k}} e^{i\vec{k}\cdot(\vec{R}_\ell - \vec{R}_{\ell'})} = \delta_{\ell\ell'} \tag{2.8a}$$

and

$$\frac{1}{N}\sum_{\ell} e^{i(\vec{k}-\vec{k}')\cdot\vec{R}_\ell} = \delta_{\vec{k},\vec{k}'} \tag{2.8b}$$

For the latter relation, we have tacitly assumed that $\vec{k}$ and $\vec{k}'$ both lie in the first Brillouin zone; in general, the right-hand side of (2.8b) would be $\delta_{\vec{k},\ \vec{k}+\vec{K}}$, where $\vec{K}$ is some reciprocal lattice vector of the form (2.6).

For the fluorite structure, a $\vec{k}$-vector in the first Brillouin zone can be written

$$\vec{k} = \frac{\pi}{Gr_o}(K_x, K_y, K_z),$$

where

$$\begin{aligned} &\text{i)} && K_X,\ K_Y,\ K_Z \text{ are integers} \\ &\text{ii)} && K_x,\ K_y,\ K_z \text{ are } \underline{\text{all}} \text{ even, or } \underline{\text{all}} \text{ odd} \\ &\text{iii)} && |K_x|,\ |K_y|,\ |K_z| \le G \\ &\text{iv)} && (|K_x| + |K_y| + |K_z|) \le 3G/2 \end{aligned} \tag{2.9}$$

The first Brillouin Zone is taken to be the familiar truncated octohedron that characterizes a face-centered lattice, and is shown in Fig. 2.2. Various points and lines of high symmetry have been labeled according to the standard notation. The details of the Brillouin zone structure are very important in later calculations of phonon Green's functions for pure CaF_2.

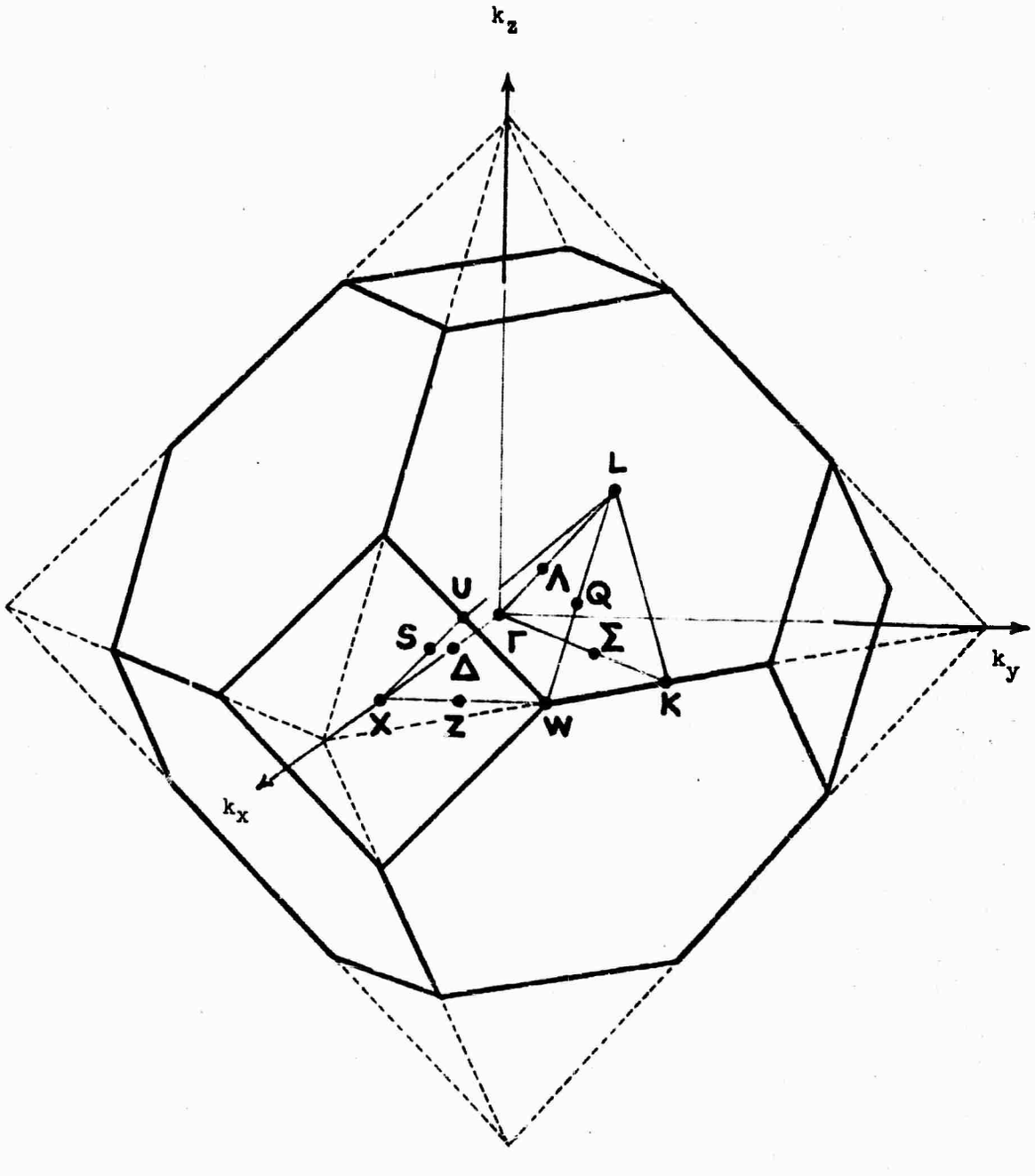

L: $\frac{\pi}{2r_o}(1,1,1)$ W: $\frac{\pi}{2r_o}(2,1,0)$ X: $\frac{\pi}{2r_o}(2,0,0)$

K: $\frac{\pi}{4r_o}(3,3,0)$ U: $\frac{\pi}{2r_o}(2,\frac{1}{2},\frac{1}{2})$

Fig. 2.2: First Brillouin zone for the (fcc) CaF_2 lattice, with points and lines of high symmetry (r_o = F-F distance).

2.2 The Harmonic Approximation

There are many good sources[23-26] on the general topic of lattice dynamics, but a short summary will be useful as a background for the later discussions. The treatment here will be phenomenological, with no attempt to describe the fundamental electronic interactions which are responsible for the "force constants" that bind the lattice together. This would involve a discussion of the Born-Oppenheimer approximation, which is covered in more detail in the book by Born and Huang[25].

It will be assumed in the subsequent development that the introduction of impurities does not distort the lattice. This is not strictly true, of course, but the assumption can be justified--or at least made plausible--by pointing out that lattice distortion effects will be implicitly incorporated into any realistic model of the lattice and defect site. For the discussion of dynamical properties of the crystal, the force constants are the fundamentally important quantities, and lattice spacings do not appear explicitly in the results. The new force constants that result when an impurity is introduced will depend on both distortion and on a possible change in the fundamental interactions that characterize the impurity. In any case, both of these effects are implicitly incorporated when the force constants are determined from experimentally measured quantities. This assumption is, in fact, always made for this type of problem, since it desireable to be able to continue to describe the lattice at equilibrium by a set of vectors $\vec{R}_{\ell\kappa}$.

If the atoms of a general lattice (perhaps containing impurities) are subjected to displacements $\vec{u}(\ell\kappa)$ from their equilibrium positions, the total potential φ (which depends upon all of the electronic and nu-

clear coordinates of the system) will change†:

$$\varphi = \varphi_0 + \frac{1}{2} \sum_{\ell\kappa, \ell'\kappa'} \vec{u}(\ell\kappa) \cdot \overleftrightarrow{\Phi}(\ell\kappa, \ell'\kappa') \cdot \vec{u}(\ell'\kappa') + \cdots$$

where

$$\Phi_{\alpha\beta}(\ell\kappa, \ell'\kappa') = \left. \frac{\partial^2 \varphi}{\partial u_\alpha(\ell\kappa) \partial u_\beta(\ell'\kappa')} \right|_0 \qquad (2.10)$$

are the second derivatives of φ evaluated for the equilibrium configuration. There is no linear term in $\vec{u}(\ell\kappa)$, since its coefficient would be $\partial\varphi/\partial\vec{u}(\ell\kappa)|_0$, which must vanish in the equilibrium configuration, since it represents the force on atom $(\ell\kappa)$. The first term for φ is an unimportant constant which can be discarded. If only the quadratic terms in the displacement are retained, the vibrational Hamiltonian for a general crystal lattice can be written

$$\mathcal{H} = \frac{1}{2} \sum_{\ell\kappa} M_{\ell\kappa} \dot{\vec{u}}(\ell\kappa)^2 + \frac{1}{2} \sum_{\ell\kappa, \ell'\kappa'} \vec{u}(\ell\kappa) \cdot \overleftrightarrow{\Phi}(\ell\kappa, \ell'\kappa') \cdot \vec{u}(\ell'\kappa') \qquad (2.11)$$

This is called the <u>harmonic approximation</u>, and leads to linear equations of motion for the displacements,

$$M_{\ell\kappa} \frac{d^2}{dt^2} \vec{u}(\ell\kappa, t) + \sum_{\ell'\kappa'} \overleftrightarrow{\Phi}(\ell\kappa, \ell'\kappa') \cdot \vec{u}(\ell'\kappa', t) = 0 \qquad (2.12)$$

There are several general properties that the force constants $\Phi_{\alpha\beta}(\ell\kappa, \ell'\kappa')$ must possess[26]. The invariance of the potential energy φ under rigid-body translations and rotations imposes two conditions for a general lattice:

$$\sum_{\ell'\kappa'} \Phi_{\alpha\beta}(\ell\kappa, \ell'\kappa') = 0 \qquad (2.13)$$

---

† Dyadic quantities will be denoted by a wiggly line; e.g. $\overleftrightarrow{S}$ represents a dyad (or second rank tensor) with (cartesian) components $S_{\alpha\beta}$.

$$\sum_{\ell''\kappa''} \Phi_{\alpha\beta}(\ell\kappa, \ell''\kappa'') R_\gamma(\ell''\kappa'') = \sum_{\ell'\kappa'} \Phi_{\alpha\gamma}(\ell\kappa, \ell'\kappa') R_\beta(\ell'\kappa') \quad (2.14)$$

It follows immediately from the formal expression (2.10) for the coefficients $\Phi_{\alpha\beta}(\ell\kappa, \ell'\kappa')$ that there is a symmetry under interchange of sites:

$$\Phi_{\alpha\beta}(\ell\kappa, \ell'\kappa') = \Phi_{\beta\alpha}(\ell'\kappa', \ell\kappa) \quad (2.15)$$

It is convenient to introduce a matrix notation; the quantities $u_\alpha(\ell\kappa)$, $M_{\ell\kappa}$, $\Phi_{\alpha\beta}(\ell\kappa, \ell'\kappa')$ can be regarded as the matrix elements of matrices u, M, and Φ in a <u>crystal lattice-site representation</u>, with "basis vectors" $|\ell\kappa\alpha\rangle$:

$$M = \sum_{\ell\kappa\alpha} |\ell\kappa\alpha\rangle M_{\ell\kappa} \langle \ell\kappa\alpha| \quad (2.16)$$

$$\Phi = \sum_{\substack{\ell\kappa\alpha \\ \ell'\kappa'\beta}} |\ell\kappa\alpha\rangle \Phi_{\alpha\beta}(\ell\kappa, \ell'\kappa') \langle \ell'\kappa'\beta| \quad (2.17)$$

$$u = \sum_{\ell\kappa\alpha} u_\alpha(\ell\kappa) |\ell\kappa\alpha\rangle \quad (2.18)$$

The basis vectors $|\ell\kappa\alpha\rangle$ for this matrix representation satisfy

$$\langle \ell\kappa\alpha | \ell'\kappa'\beta \rangle = \delta_{\ell\ell'}\delta_{\kappa\kappa'}\delta_{\alpha\beta} \quad (2.19a)$$

$$\sum_{\ell\kappa\alpha} |\ell\kappa\alpha\rangle\langle\ell\kappa\alpha| = 1 \quad (2.19b)$$

The Hamiltonian (2.11) becomes

$$\mathcal{H} = \frac{1}{2}\dot{u}^T M \dot{u} + \frac{1}{2} u^T \Phi u \quad (2.20)$$

and the equation of motion (2.12),

$$M\ddot{u} + \Phi u = 0 \tag{2.21}$$

This equation characterizes a system of harmonic oscillators, and a trial solution of the form $\vec{u}(t) \sim \vec{u}_o e^{-i\omega t}$ will lead to an eigenvalue problem that defines the normal modes of the system. The eigenfrequencies are determined from a secular equation,

$$\det \left| M\omega^2 - \Phi \right| = 0 \tag{2.22}$$

which can be written in terms of the "dynamical matrix", $D = M^{-\frac{1}{2}} \Phi M^{-\frac{1}{2}}$ as

$$\det \left| \omega^2 - D \right| = 0 \tag{2.23}$$

In terms of the dynamical matrix $D^o = M_o^{-\frac{1}{2}} \Phi_o M_o^{-\frac{1}{2}}$ and a column vector, $Q = M_o^{\frac{1}{2}} u$, the unperturbed Hamiltonian (2.11) for a perfect lattice can be written in matrix form as

$$\mathcal{H}_o = \frac{1}{2} \dot{Q}^T \dot{Q} + \frac{1}{2} Q^T D^o Q \tag{2.24}$$

and the equation of motion,

$$\ddot{Q} + D^o Q = 0 \tag{2.25}$$

For a perfect lattice, there are several further restrictions on the $\Phi^o_{\alpha\beta}(\ell\kappa, \ell'\kappa')$ that are imposed by the invariance of the lattice under operations of the crystal space group. Invariance under primitive translations implies that $\Phi^o_{\alpha\beta}(\ell\kappa, \ell'\kappa')$ can be a function only of the differ-

ence $(\vec{R}_\ell - \vec{R}_{\ell'})$:

$$\Phi^{\circ}_{\alpha\beta}(\ell\kappa, \ell'\kappa') = \Phi^{\circ}_{\alpha\beta}(\ell-\ell'; \kappa\kappa') \qquad (2.26)$$

There are also restrictions on $\Phi^{\circ}_{\alpha\beta}(\ell\kappa, \ell'\kappa')$ imposed by the more general rotation operations $(S \mid \vec{t})$ of the space group. Under such an operation, every lattice site $(\ell\kappa)$ is taken into some similar site $(L\kappa)$:

$$R_\alpha(L\kappa) = \sum_\beta S_{\alpha\beta} R_\beta(\ell\kappa) + t_\alpha .$$

The operation $(S \mid \vec{t})$ induces a transformation of the displacements,

$$u \longrightarrow \mathcal{S} u ,$$

where $\mathcal{S}$ is a large (3rN x 3rN) matrix that describes the permutation of sites and rotation of vectors produced by $(S \mid \vec{t})$. If $\mathcal{S}$ is pictured as partitioned into boxes, then 3 x 3 orthogonal rotation matrices S will occur once, and only once, in every row and column labeled by the site indices $(\ell\kappa)$. That is, if site $(\ell\kappa)$ is taken into site $(L\kappa)$ under the operation $(S \mid \vec{t})$, then $\langle L\kappa\alpha \mid \mathcal{S} \mid \ell\kappa\beta \rangle = S_{\alpha\beta}$, but is zero otherwise.

The transformation properties that the matrix elements $\Phi^{\circ}_{\alpha\beta}(\ell\kappa, \ell'\kappa')$ have under an operation $(S \mid \vec{t})$ are derived from the requirement that the potential energy must be invariant, both as to value and form, under such operations. The potential energy in the harmonic approximation is a quadratic form, $\frac{1}{2} u^T \cdot \Phi^{\circ} \cdot u$, and its invariance under the space group of transformations $(S \mid \vec{t})$ implies that the coefficients $\Phi^{\circ}_{\alpha\beta}(\ell\kappa, \ell'\kappa')$ must transform like a second rank tensor. Under $(S \mid \vec{t})$,

$$\frac{1}{2} u^T \Phi^{\circ} u \longrightarrow \frac{1}{2} u^T \mathcal{S}^T \Phi^{\circ} \mathcal{S} u ,$$

and since the displacement column vector u can be regarded as arbitrary,

$$\mathcal{S}^{T}\,\Phi^{\circ}\,\mathcal{S} \;=\; \Phi^{\circ}.$$

Thus, if sites $(\ell_1 \kappa_1)$ and $(\ell_2 \kappa_2)$ are taken into $(L_1 K_1)$ and $(L_2 K_2)$, then

$$\Phi^{\circ}_{\alpha\beta}(L_1 K_1,\, L_2 K_2) = \sum_{\mu\nu} S_{\alpha\mu}\, \Phi^{\circ}_{\mu\nu}(\ell_1 \kappa_1,\, \ell_2 \kappa_2)\, S_{\beta\nu}. \qquad (2.28)$$

In order to carry out the reduction of a specific force constant tensor, it is necessary to consider the subgroup $\mathcal{G}$ of operations that (1) leave the crystal invariant, and (2) leave a pair of sites $(\ell_1 \kappa_1)$ and $(\ell_2 \kappa_2)$ invariant For operations $(S \mid \vec{t}) \in \mathcal{G}$, the following interrelation among the elements $\Phi^{\circ}_{\alpha\beta}(\ell_1 \kappa_1, \ell_2 \kappa_2)$ is obtained

$$\Phi^{\circ}_{\alpha\beta}(\ell_1 \kappa_1,\, \ell_2 \kappa_2) = \sum S_{\alpha\mu}\, S_{\beta\nu}\, \Phi^{\circ}_{\mu\nu}(\ell_1 \kappa_1,\, \ell_2 \kappa_2). \qquad (2.29)$$

These conditions are useful later, when they are invoked to simplify the general form that certain force constant matrices are required to assume for a rigid-ion model of CaF_2. In some cases, other physical considerations that are independent of the symmetry group $\mathcal{G}$ might lead to further simplifications.

The determination of the eigenfrequencies from the secular equation,

$$\det \left| \omega^2 - D^{\circ} \right| = 0 \qquad (2.30)$$

involves the diagonalization of the 3rN x 3rN matrix D°, but the exploitation of group theory can provide a considerable reduction in complexity. The total number of solutions to (2.30) is equal to the total number of

degrees of freedom, 3rN, but a significant simplification results from the fact that the eigenstates of a physical system must transform according to the irreducible representations of the symmetry group for that system. For a perfect lattice, the symmetry group is the crystal space group, which contains an invariant subgroup of pure translations through the lattice vectors $\vec{R}_\ell$.

For the present, we shall restrict our attention to the consequences of translational periodicity alone. As is well known[27-30], the representations of the (abelian) group of pure lattice vector translations $(1 \mid \vec{R}_\ell)$ are one-dimensional phase factors, $\exp(i\vec{k}\cdot\vec{R}_\ell)$, where the wave-vectors $\vec{k}$ are defined by (2.7) over the reciprocal lattice. A reflection of this fact is the general rule that the eigenstates of a translationally invariant system consist of <u>wave-like</u> excitations. In the present case, these eigenstates are the phonons, and the parameter $\vec{k}$ has the physical significance of representing the phonon momentum. The mathematical operation of Fourier transformation can be regarded, group-theoretically, as constituting a <u>projection</u> onto the representations characterized by the wave vector $\vec{k}$. The operation of Fourier transformation will have the effect of partially diagonalizing the Hamiltonian $\mathcal{H}_o$ for the perfect crystal, and it will reduce the secular equation (2.30) to a <u>block form</u> in which <u>orthogonal subspaces</u> labeled by different values of $\vec{k}$ are separated. The reduction to block form greatly simplifies the eigenvalue problem, since it is then only necessary to diagonalize a 3r x 3r matrix in each of the subspaces labeled by the N distinct $\vec{k}$-vectors in the first Brillouin zone. Define a projection operator,

$$P_{\vec{k}} = \frac{1}{N} \sum_{L} e^{i\vec{k}\cdot\vec{R}_L} T_L \tag{2.31}$$

where T_L is a unitary operator which translates the lattice sites through the vector $\vec{R}_L$. In the crystal lattice site representation, T_L can be defined by the relations

$$\begin{aligned} T_L \,|\, \ell\kappa\alpha\rangle &= |\, \ell+L, \kappa\alpha\rangle \\ T_L = T_L \sum_{\ell\kappa\alpha} |\, \ell\kappa\alpha\rangle\langle \ell\kappa\alpha\,| &= \sum_{\ell\kappa\alpha} |\, \ell+L, \kappa\alpha\rangle\langle \ell\kappa\alpha\,| \\ T_{L_1}\, T_{L_2} &= T_{L_1+L_2} \\ T_L^{-1} = T_L^{\dagger} &= T_{-L} \end{aligned} \tag{2.32}$$

It is easy to verify that the operators $P_{\vec{k}}$ satisfy the usual rules for projection operators,

$$P_{\vec{k}}\, P_{\vec{k}'} = \delta_{\vec{k},\vec{k}'}\, P_{\vec{k}} \tag{2.33a}$$

$$\sum_{\vec{k}} P_{\vec{k}} = 1 \tag{2.33b}$$

$$P_{\vec{k}}^{\dagger} = P_{\vec{k}} \tag{2.33c}$$

The relation (2.31) can be inverted, using (2.8a),

$$T_L = \sum_{\vec{k}} e^{-i\vec{k}\cdot\vec{R}_L} P_{\vec{k}} \tag{2.34}$$

and expresses the decomposition of the unitary operator T_L into a sum of projections onto the orthogonal subspaces labeled by $\vec{k}$. The eigenvalue

of T_L in the subspace $\vec{k}$ is $\exp(-i\vec{k}\cdot\vec{R}_L)$, and this can be expressed as $T_L P_k = \exp(-i\vec{k}\cdot\vec{R}_L)\, P_{\vec{k}}$. In the crystal lattice-site representation,

$$P_{\vec{k}} = \frac{1}{N} \sum_{\substack{\ell\kappa\alpha \\ L}} |\ell+L, \kappa\alpha\rangle\, e^{i\vec{k}\cdot\vec{R}_L} \langle \ell\kappa\alpha| \tag{2.35}$$

which can be written

$$P_{\vec{k}} = \sum_{\kappa\alpha} |\vec{k}, \kappa\alpha\rangle\langle \vec{k}, \kappa\alpha|, \tag{2.36}$$

where we have defined a set of vectors

$$|\vec{k}, \kappa\alpha\rangle = \frac{1}{\sqrt{N}} e^{i\vec{k}\cdot\vec{R}_\kappa} \sum_{\ell} e^{i\vec{k}\cdot\vec{R}_\ell} |\ell\kappa\alpha\rangle \tag{2.37a}$$

$$= \sqrt{N}\, e^{i\vec{k}\cdot R}\, P_{\vec{k}} |0\kappa\alpha\rangle \tag{2.37b}$$

These vectors satisfy an orthonormality condition,

$$\langle \vec{k}, \kappa\alpha | \vec{k}', \kappa'\beta\rangle = \delta_{\vec{k}\vec{k}'} \delta_{\kappa\kappa'} \delta_{\alpha\beta} \tag{2.38}$$

Thus, each of the orthogonal 3r-dimensional subspaces labeled by $\vec{k}$ can be spanned by the orthonormal set of vectors $|\vec{k}, \kappa\alpha\rangle$. The phase factor $\exp(i\vec{k}\cdot\vec{R}_\kappa)$ was included arbitrarily in the definition (2.37) to conform with usage in the literature. The statement of dynamical invariance of the lattice under a translation $(1 \mid \vec{R}_L)$ can be expressed mathematically as

$$T_L\, D^0\, T_L^{-1} = D^0 \tag{2.39}$$

This is just the condition $D^0_{\alpha\beta}(\ell\kappa, \ell'\kappa') = D^0_{\alpha\beta}(\ell+L, \kappa; \ell'+L, \kappa')$. Thus, the dynamical matrix D^0 commutes with the operators T_L:

$$T_L \, D^0 = D^0 \, T_L \tag{2.40}$$

By multiplying (2.40) by $\exp(i\vec{k}\cdot\vec{R}_L)$ and summing over all lattice sites $\vec{R}_L$, we obtain

$$P_{\vec{k}} \, D^0 = D^0 \, P_{\vec{k}} \tag{2.41}$$

and it follows from (2.33a) and (2.33b) that

$$D^0 = \sum_{\vec{k}} P_{\vec{k}} \, D^0 \, P_{\vec{k}} \tag{2.42}$$

Thus, D^0 can also be decomposed into a sum of projections onto the N distinct, orthogonal, 3r x 3r subspaces labeled by the wave-vector $\vec{k}$. Eq. (2.42) becomes

$$D^0 = \sum_{\vec{k}} \sum_{\substack{\kappa\alpha \\ \kappa'\beta}} |\vec{k}, \kappa\alpha\rangle \, D^0_{\alpha\beta}(\vec{k} \mid \kappa\kappa') \langle \vec{k}, \kappa'\beta| \tag{2.43}$$

where we have defined

$$D^0_{\alpha\beta}(\vec{k} \mid \kappa\kappa') = \langle \vec{k}, \kappa\alpha \mid D^0 \mid \vec{k}, \kappa'\beta \rangle \tag{2.44}$$

$D^0_{\alpha\beta}(\vec{k} \mid \kappa\kappa')$ is just the Fourier-transformed dynamical matrix,

$$D^0_{\alpha\beta}(\vec{k} \mid \kappa\kappa') = \sum_{\ell'} e^{-i\vec{k}\cdot(\vec{R}_{\ell\kappa} - \vec{R}_{\ell'\kappa'})} D^0_{\alpha\beta}(\ell\kappa, \ell'\kappa') \tag{2.45}$$

These equations have shown that D^0 has eigenstates $|\vec{k}, \ldots\rangle$ which can be partially labeled by the momentum $\vec{k}$. The reduction of D^0 to block form (2.42) makes it possible to factor the secular equation,

$$\det\left[1 - \frac{D^{\circ}}{\omega^2}\right] = \prod_{\vec{k}} \det\left[1 - \frac{P_{\vec{k}}\, D^{\circ} P_{\vec{k}}}{\omega^2}\right] = 0 \qquad (2.46)$$

There are also rotational symmetry operations for D°, and a further characterization of the states $|\vec{k},\ldots\rangle$ could be discussed in terms of the representations of the full space group. This would involve a consideration of the group of the k-vector, $\mathcal{G}_{\vec{k}}$, which consists of all operations which keep $\vec{k}$ invariant. The task of constructing the representations of the space group is equivalent to the problem of finding, for each wave-vector $\vec{k}$, all of the irreducible representations of the factor group, $\mathcal{G}_{\vec{k}}/\mathcal{T}_{\vec{k}}$, where $\mathcal{T}_{\vec{k}}$ is the group of all translations $(1\,|\,\vec{t})$ for which $\vec{k}\cdot\vec{t}$ is a multiple of 2π [31,32]. When $\vec{k} = 0$, this factor group becomes the point group of the crystal class, and it will be shown later how group theory is used to classify the symmetry of the $\vec{k} = 0$ modes for CaF_2.

For CaF_2, the space group is O_h^5-Fm3m, and the properties of the general representations throughout the Brillouin zone have been worked out in detail by Chen, Berenson, and Birman [33,34], using techniques developed earlier by Birman [35] for symmorphic space groups. We need not go into the involved subject of these representations here; it suffices to notice that, for every wave-vector $\vec{k}$, the subspace of $\vec{k}$ is 3r-dimensional, and the eigenstates of D° can be denoted by $|\vec{k},\sigma\rangle$, $\sigma = 1, 2, \ldots, 3r$. The additional knowledge that these modes must transform according to specific space group irreducible representations has no further usefulness for the general discussion at this point.

For a more complete discussion of space groups and their representations, reference can be made to an excellent review article by Koster [32]. A very thorough treatment of the symmetry properties of the normal vibra-

tions of a perfect crystal has recently appeared in review articles by Maradudin and Vosko[36], and by Warren[37]. The present discussion is limited to basic results that are directly relevant for this work.

Thus, the basis vectors in each of the N distinct and orthogonal $\vec{k}$-subspaces are chosen to be those which diagonalize the dynamical matrix in those subspaces:

$$\begin{aligned} D^\circ |\vec{k}\sigma\rangle &= \omega^2_{\vec{k}\sigma} |\vec{k}\sigma\rangle \\ \langle\vec{k}\sigma| D^\circ &= \omega^2_{\vec{k}\sigma} \langle\vec{k}\sigma| \end{aligned} \tag{2.47}$$

This equation defines the phonon eigenmodes, which are characterized by a momentum $\vec{k}$ and a branch index $\sigma = 1, 2, 3, \ldots, 3r$. In terms of the states $|\vec{k}\sigma\rangle$, we can write

$$P_{\vec{k}} = \sum_\sigma |\vec{k}\sigma\rangle\langle\vec{k}\sigma| \tag{2.48}$$

$$D^\circ = \sum_{\vec{k}\sigma} |\vec{k}\sigma\rangle\, \omega^2_{\vec{k}\sigma}\, \langle\vec{k}\sigma| \tag{2.49}$$

and

$$\langle\vec{k}\sigma\,|\,\vec{k}'\sigma'\rangle = \delta_{\vec{k}\vec{k}'}\,\delta_{\sigma\sigma'} \tag{2.50}$$

Let us define the relationship between the set of eigenvectors $|\vec{k}\sigma\rangle$ and the set of vectors $|\vec{k},\kappa\alpha\rangle$ encountered earlier (and which also span the subspace $\vec{k}$). If we use (2.36),

$$|\vec{k}\sigma\rangle = P_{\vec{k}}\,|\vec{k}\sigma\rangle = \sum_{\kappa\alpha} |\vec{k},\kappa\alpha\rangle\langle\vec{k},\kappa\alpha|\,\vec{k}\sigma\rangle = \sum_{\kappa\alpha} w_\alpha(\kappa|\vec{k}\sigma)\,|\vec{k},\kappa\alpha\rangle \tag{2.51}$$

where we define

$$w_\alpha(\kappa \mid \vec{k}\sigma) = \langle \vec{k}, \kappa\alpha \mid \vec{k}\sigma \rangle \tag{2.52}$$

The quantities $w_\alpha(\kappa \mid \vec{k}\sigma)$ represent the coefficients that allow the eigenstates $|\vec{k}\sigma\rangle$ to be constructed as a linear combination of $|\vec{k}, \kappa\alpha\rangle$ in the subspace $\vec{k}$. From (2.51),

$$D^\circ |\vec{k}\sigma\rangle = \sum_{\kappa'\beta} D^\circ |\vec{k}, \kappa'\beta\rangle\, w_\beta(\kappa' \mid \vec{k}\sigma) = \omega^2_{\vec{k}\sigma} |\vec{k}\sigma\rangle \tag{2.53}$$

Multiply by $\langle \vec{k}, \kappa\alpha|$ on the left, and use the definitions (2.44) and (2.52) to obtain

$$\sum_{\kappa'\beta} D^\circ_{\alpha\beta}(\vec{k} \mid \kappa\kappa')\, w_\beta(\kappa' \mid \vec{k}\sigma) = \omega^2_{\vec{k}\sigma}\, w_\alpha(\kappa \mid \vec{k}\sigma) \tag{2.54}$$

Equations (2.36), (2.48), and (2.49) can be used to give

$$\sum_\kappa \hat{w}^*(\kappa \mid \vec{k}\sigma) \cdot \hat{w}(\kappa \mid \vec{k}\sigma') = \delta_{\sigma\sigma'} \tag{2.55}$$

$$\sum_\sigma \hat{w}^*(\kappa \mid \vec{k}\sigma)\, \hat{w}(\kappa' \mid \vec{k}\sigma) = \tilde{1}\, \delta_{\kappa\kappa'} \tag{2.56}$$

$$D^\circ_{\alpha\beta}(\vec{k} \mid \kappa\kappa') = \sum_\sigma w_\alpha(\kappa \mid \vec{k}\sigma)\, \omega^2_{\vec{k}\sigma}\, w^*_\beta(\kappa' \mid \vec{k}\sigma) \tag{2.57}$$

All that remains is to determine the transformation properties between the basis vectors $|\ell\kappa\alpha\rangle$ of the crystal lattice site representation, and the basis vectors $|\vec{k}\sigma\rangle$ of the momentum space representation:

$$|\vec{k}\sigma\rangle = \sum_{\ell\kappa\alpha} |\ell\kappa\alpha\rangle \langle \ell\kappa\alpha \mid \vec{k}\sigma\rangle \tag{2.58}$$

The transformation function $\langle \ell\kappa\alpha | \vec{k}\sigma \rangle$ depends upon $\vec{R}_\ell$ only through a phase factor:

$$\langle \ell\kappa\alpha | \vec{k}\sigma \rangle = \langle 0\kappa\alpha | T_\ell^\dagger | \vec{k}\sigma \rangle = e^{i\vec{k}\cdot\vec{R}_\ell} \langle 0\kappa\alpha | \vec{k}\sigma \rangle \qquad (2.59)$$

and (2.37b) can be used to give

$$\langle \vec{k}, \kappa\alpha | \vec{k}\sigma \rangle = \sqrt{N}\, e^{-i\vec{k}\cdot\vec{R}_\kappa} \langle 0\kappa\alpha | \vec{k}\sigma \rangle \qquad (2.60)$$

By definition, the left hand side of (2.60) is equal to $w_\alpha(\kappa | \vec{k}\sigma)$, so the transformation function $\langle \ell\kappa\alpha | \vec{k}\sigma \rangle$ becomes

$$\langle \ell\kappa\alpha | \vec{k}\sigma \rangle = \frac{1}{\sqrt{N}} e^{i\vec{k}\cdot\vec{R}_{\ell\kappa}} w_\alpha(\kappa | \vec{k}\sigma) \qquad (2.61)$$

Formally, the relationship between the two choices of matrix representation can be summarized by a set of equations that define the linear transformation between the basis vectors:

$$| \ell\kappa\alpha \rangle = \frac{1}{\sqrt{N}} \sum_{\vec{k}\sigma} e^{-i\vec{k}\cdot\vec{R}_{\ell\kappa}} w_\alpha^*(\kappa | \vec{k}\sigma) | \vec{k}\sigma \rangle \qquad (2.62a)$$

$$| \vec{k}\sigma \rangle = \frac{1}{\sqrt{N}} \sum_{\ell\kappa\alpha} e^{i\vec{k}\cdot\vec{R}_{\ell\kappa}} w_\alpha(\kappa | \vec{k}\sigma) | \ell\kappa\alpha \rangle \qquad (2.62b)$$

In effect, we have carried out a linear, unitary transformation of the basis vectors $| \ell\kappa\alpha \rangle$ of the "crystal lattice site" representation, to a set of basis vectors $| \vec{k}\sigma \rangle$ that diagonalize the dynamical matrix D^o and define the "momentum space" representation. The Hamiltonian (2.25) for the perfect crystal can be written

$$\mathcal{H}_0 = \frac{1}{2}\sum_{\vec{k}\sigma}\left[\dot{Q}^\dagger(\vec{k}\sigma)\dot{Q}(\vec{k}\sigma) + \omega^2_{\vec{k}\sigma}\, Q^\dagger(\vec{k}\sigma)Q(\vec{k}\sigma)\right] \tag{2.63}$$

where we have defined $Q(\vec{k}\sigma)$ to be the matrix element $\langle \vec{k}\sigma | Q$ of the (column) matrix Q in the momentum space representation,

$$Q(\vec{k}\sigma) = \langle \vec{k}\sigma | Q = \frac{1}{\sqrt{N}}\sum_{\ell\kappa\alpha} e^{-i\vec{k}\cdot\vec{R}_{\ell\kappa}}\, w^*_\alpha(\kappa|\vec{k}\sigma)\langle \ell\kappa\alpha | Q \tag{2.64}$$

Recall that we defined $Q = M_0^{\frac{1}{2}}\, u$, so that $\langle \ell\kappa\alpha | Q = M_\kappa^{\frac{1}{2}}\, u_\alpha(\ell\kappa)$. By making use of the inverse relation, (2.62a), it is possible to express the displacements $u_\alpha(\ell\kappa)$ in terms of the phonon normal mode coordinates, $Q(\vec{k}\sigma)$:

$$u_\alpha(\ell\kappa) = \frac{1}{(NM_\kappa)^{\frac{1}{2}}}\sum_{\vec{k}\sigma} e^{i\vec{k}\cdot\vec{R}_{\ell\kappa}}\, w_\alpha(\kappa|\vec{k}\sigma)\, Q(\vec{k}\sigma) \tag{2.65}$$

If we take the matrix element $\langle \vec{k}\sigma |$ of the matrix equation of motion (2.26), we obtain immediately the familiar harmonic oscillator equations for the phonon normal mode coordinates,

$$\ddot{Q}(\vec{k}\sigma) + \omega^2_{\vec{k}\sigma}\, Q(\vec{k}\sigma) = 0 \tag{2.66}$$

Equations (2.61) and (2.62) will be very useful throughout this work for facilitating the transformation to momentum space.

Since it is the long-wavelength optic modes of a crystal that are important for light scattering, we shall discuss here the determination of the <u>symmetries</u> of the $\vec{k} = 0$ modes, with CaF_2 as an illustration. At

$\vec{k} = 0$, all of the primitive cells of a perfect crystal lattice vibrate in phase, so any two atoms which are equivalent (i.e., separated by some lattice vector $\vec{R}_\ell$) must have the same instantaneous displacements in those modes. Thus, the most general $\vec{k} = 0$ displacement can be completely described by r vector displacements, $\vec{v}_1$, $\vec{v}_2$, $\vec{v}_3$, ..., $\vec{v}_r$, corresponding to the r basis indices for a primitive cell. These displacements will be periodically repeated throughout the crystal. The 3r-dimensional column vector,

$$\vec{v} = \begin{pmatrix} \vec{v}_1 \\ \vec{v}_2 \\ \cdot \\ \cdot \\ \cdot \\ \vec{v}_r \end{pmatrix}$$

can be used as a basis function for the 3r x 3r reducible representation that determines the most general form that the $\vec{k} = 0$ modes can have under the point group symmetry of the crystal.

This representation is easily constructed. For every operation of the point group, similar atoms are transformed into each other, but the set of basis indices $\kappa = 1, 2, 3, \ldots, r$ can, in general, undergo a permutation. (For example, there are two inequivalent fluorines in the primitive cell of CaF_2, and under some operations of the O_h point group, the fluorine basis indices can be permuted.) Furthermore, all of the displacements will be rotated by a three-dimensional, orthogonal matrix S. Thus, for every operation of the point group, a 3r x 3r matrix $\mathcal{S}$ is constructed by placing 3 x 3 matrices S in boxes that are defined by the permutation induces on the basis indices. For example, under any one of the

six C_4 rotations for CaF_2, $Ca \rightarrow Ca$, $F_1 \rightarrow F_2$, $F_2 \rightarrow F_1$, and the matrix that represents this operation is

$$\mathcal{S} = \left(\begin{array}{c|c|c} S(C_4) & 0 & 0 \\ \hline 0 & 0 & S(C_4) \\ \hline 0 & S(C_4) & 0 \end{array}\right) \qquad (2.67)$$

The set of matrices $\mathcal{S}$ form a 3r-dimensional reducible representation that defines the transformation properties of a general displacement $\vec{v}$ with $\vec{k} = 0$. The <u>character</u> of some operation S in this representation Γ will be determined by the number of times a 3 x 3 rotation matrix S appears as a diagonal block. I.e., if n_b is the number of basis atoms that remain invariant under the point group operation S, then the character of the representation Γ will be given by

$$\chi^{\Gamma}(S) = \mathrm{Tr}\,\mathcal{S} = n_b \,\mathrm{Tr}\, S = \pm\, n_b\,(1 + 2\cos\theta) \qquad (2.68)$$

where θ is the rotation angle of S, and $\pm$ is used according to whether the rotation is proper or improper. This character can be decomposed by the standard methods of group theory[27-30]; the number of times an irreducible representation α occurs is given by

$$n_\alpha = \frac{1}{h} \sum_S \chi^{\Gamma}(S)\, \chi^{\alpha}(S)^* \qquad (2.69)$$

where h is the order of the group. (The method described here is based

on an original work of Wigner[38], who first discussed the normal modes of symmetrical systems.)

Fig 2.3 summarizes the character of the $\vec{k} = 0$ displacements for CaF_2; its decomposition into the irreducible representations of the O_h group leads to

$$\Gamma = 2 F_{1u} + F_{2g} \tag{2.70}$$

	E	$8C_3$	$3C_2$	$6C_2$	$6C_4$	I	$8S_3$	3σ	$6\sigma'$	$6S_4$
n_b	3	3	3	1	1	1	1	1	3	3
Tr(S)	3	0	-1	-1	1	-3	0	1	1	-1
$\chi(S)$	9	0	-3	-1	1	-3	0	1	3	-3

Fig. 2.3: Character table for $\vec{k} = 0$ modes in CaF_2

One of the F_{1u} representations corresponds to the acoustic phonon branches; the other six degrees of freedom correspond to optic modes. Under inversion, $Ca \rightarrow Ca$, $F_1 \rightarrow F_2$, and $F_2 \rightarrow F_1$. Hence, for the even F_{2g} mode, the calciums remain stationary, while the two fluorine sublattices vibrate against each other. For the odd F_{1u} optic mode, the fluorines all have the same displacement, and that of the calcium can be obtained by requiring the center of mass to be stationary in such a mode. The (unnormalized) mode vectors at $\vec{k} = 0$ are

$$\vec{w} = \left[\begin{array}{ccc|ccc|ccc}
0 & 0 & 0 & \frac{-2}{\sqrt{m_{Ca}}} & 0 & 0 & \sqrt{m_{Ca}} & 0 & 0 \\
0 & 0 & 0 & 0 & \frac{-2}{\sqrt{m_{Ce}}} & 0 & 0 & \sqrt{m_{Ca}} & 0 \\
0 & 0 & 0 & 0 & 0 & \frac{-2}{\sqrt{m_{Ca}}} & 0 & 0 & \sqrt{m_{Ca}} \\
\hline
1 & 0 & 0 & \frac{1}{\sqrt{M_F}} & 0 & 0 & \sqrt{m_F} & 0 & 0 \\
0 & 1 & 0 & 0 & \frac{1}{\sqrt{m_F}} & 0 & 0 & \sqrt{m_F} & 0 \\
0 & 0 & 1 & 0 & 0 & \frac{1}{\sqrt{m_F}} & 0 & 0 & \sqrt{m_F} \\
\hline
-1 & 0 & 0 & \frac{1}{\sqrt{m_F}} & 0 & 0 & \sqrt{m_F} & 0 & 0 \\
0 & -1 & 0 & 0 & \frac{1}{\sqrt{m_F}} & 0 & 0 & \sqrt{m_F} & 0 \\
0 & 0 & -1 & 0 & 0 & \frac{1}{\sqrt{m_F}} & 0 & 0 & \sqrt{m_F}
\end{array}\right] \qquad (2.71)$$

F_{2g} $\qquad$ F_{1u} OPTIC MODE $\qquad$ F_{1u} ACOUSTIC MODE

Although selection rules will not be discussed until later, we mention here that the (triply degenerate) F_{2g} mode is Raman-active, and the transverse optic F_{1u} mode is infrared-active. The infrared F_{1u} mode is split at $\vec{k} = 0$ into longitudinal and transverse branches, due to the effects of long-range electrostatic forces[25,39,119]. This phenomenon is connected with the macroscopic polarization field which accompanies a polar vibrational mode, and will be the subject of further remarks in Chapter VI, where the problem of constructing a model to describe the phonon spectrum of CaF_2 is discussed.

2.3 Anharmonic Effects

It is possible that the harmonic approximation will not be a good description for a perfect crystal, although it shall be used throughout this work and for the calculations to be carried out later for the mixed fluorite systems. The phonon normal modes have been obtained from the assumption that the potential energy is strictly quadratic in the displacements from equilibrium of the atoms; they are thus exact states of the Hamiltonian in the harmonic approximation, and are therefore independent and non-interacting. As was shown above, this approximation leads to well-defined dispersion relations between the frequency and momentum of the normal modes of vibration. For a given wave-vector $\vec{k}$, the frequency ω of an excitation is infinitely precise, and is given by one of the phonon branch frequencies $\omega_{\vec{k}\sigma}$; that is, the spectral content $A(\vec{k},\omega)$ of an excitation with momentum $\vec{k}$ is a delta-function, $\delta(\omega - \omega_{\vec{k}\sigma})$. For the harmonic crystal, a normal mode which is excited could never decay, and would thus have an infinite lifetime.

If anharmonic interactions are present, these phonon normal modes no longer represent the exact eigenstates of the vibrational system. However, if the anharmonic forces are small, it is still meaningful to describe the lattice in terms of these modes, although they become coupled by the anharmonic interactions and are no longer independent. Anharmonic coupling can thus provide a mechanism by which energy can be exchanged between the modes of the harmonic lattice--i.e., modes can decay into each other, and thus acquire a finite lifetime. The creation of an excitation with precise wave-vector $\vec{k}$ in such a system will contain contributions from all of the exact eigenstates of the system, and

will be distributed over a spectrum of frequencies. Thus, in an anharmonic crystal, there is no longer a precise and well-defined dispersion relation that relates frequency to momentum. Even with anharmonic interactions, the perfect crystal possesses translational periodicity, so it remains possible to characterize the excitations with a wave-vector $\vec{k}$. However, the frequency of a "phonon mode" with momentum $\vec{k}$ becomes "fuzzy," and in situations where anharmonic forces are very large, the concept of phonon modes may even become meaningless. In that case, the problem would have to be formulated in terms of a spectral density function $A(\vec{k},\omega)$ for each wave-vector $\vec{k}$. Loosely speaking, if the spectral amplitude of an excitation with momentum $\vec{k}$ is peaked at some frequency $\omega_{\vec{k}}$ with a well-defined (full) width $\Gamma_{\vec{k}}$, it is possible to retain the concept of "phonon" as developed above, by incorporating the width $\Gamma_{\vec{k}}/2$ with $\omega_{\vec{k}}$ to form a complex frequency $\omega_{\vec{k}} \pm i\,\Gamma_{\vec{k}}/2$.

In general, the most elegant mathematical description of the excitations of a many-body system makes use of quantum mechanical Green's function techniques, and Gillis, Werthamer, and Fredkin[40] have attempted to formulate a quantum many-body theory of lattice dynamics in that way. A simple discussion of how the spectral amplitude $A(\vec{k},\omega)$ of the excitations of a system can be related to the Fourier transforms of certain Green's functions is given by Nozieres[41]. In the simple case of a harmonic lattice that we shall use here, the phonon modes of frequency $\omega_{\vec{k}\sigma}$ and momentum $\vec{k}$ are non-interacting, and can be characterized as the singularities of the $(\vec{k},\omega)$ Fourier transform of a classical Green's function. In general, the methods of Green's functions span a wide range of sophistication, and in many applications, can become quite formal[40-46].

To include anharmonic forces in the treatment of lattice dynamics is a difficult task for realistic physical problems, and generally represents a difficult many-body calculation. Although it can provide no information about the broadening of the modes, the harmonic approximation can usually give a reasonably good description of the vibrational frequencies of typical crystal lattices. Some of the simpler aspects of the Green's function method that are useful for a discussion of the optical properties of mixed crystals will be developed in subsequent chapters.

There are many properties of a perfect crystal which are not explained by the harmonic approximation at all--e.g., lifetimes of modes, thermal expansion and conductivity, temperature dependence of some physical quantities, etc. On the other hand, some effects may depend for their existence upon the assumption of anharmonic forces, but in fact reflect properties of the crystal which are well described by the harmonic approximation--e.g., the phonon sidebands on the local modes induced by U-centers in crystals. (Of course, the latter effect can also arise from a higher order coupling between light and the electronic structure--e.g., the second-order electric moment.[1,47-50,59])

Cowley[51,52] has discussed the effects of anharmonic interactions on the lattice dynamics of a crystal; in these review articles, the mathematical techniques are developed and applied to a variety of optical, thermal, electrical, and mechanical properties. Maradudin[53] has discussed the anharmonic broadening of a local mode induced by a defect. Other references to work on defects in anharmonic crystals can be found in the review articles by Maradudin[1] and Elliott[59].

III. THE METHOD OF GREEN'S FUNCTIONS

3.1 Introduction

In this chapter, we shall develop the basic theory of classical phonon Green's functions (and their relation to the quantum mechanical, double-time Green's functions) for the lattice vibrational problem. There are numerous excellent review articles on the Green's function method[1, 54-60] for impurity problems. Although most of these[1,55-60] are restricted to the vibrational problem, Izyumov[54] has discussed the impurity problem with the more general objective of showing the unity that these techniques provide for vibrational, electronic, and magnetic systems. There is an extensive literature on the application of Green's function methods to electronic[61-82] and magnetic[83-89] impurity problems.

The formulation of the phonon problem in the harmonic approximation in terms of classical or quantum mechanical Green's functions is equivalent, because the equations of motion for a harmonic oscillator are the same in classical or quantum mechanics. The classical Green's function approach for the phonon problem is limited to the harmonic approximation, since the classical Green's function methods are typically formulated for systems which satisfy linear equations of motion. For calculations that involve anharmonic effects, the quantum mechanical formalism is more readily applied. The quantum mechanical formalism is also especially convenient, for it provides a relation between thermally-averaged correlation functions and Green's functions. In processes such as Raman scattering or neutron scattering, the physically observable scattering intensity or cross section can be related directly to such correlation functions.

As we shall see later, an essential condition that is necessary for the practical application of the Green's function method to impurity problems is that the perturbation caused by the defect is spatially localized. When the theory of phonon optical properties is formulated in terms of specific Green's functions, it will become clear that there are often two separate aspects to such an assumption.

For vibrational properties, the assumption of only a simple mass change for the defect is often inadequate to correctly explain experimental results, and changes in force constants must also be included. For an isolated point defect, the totality of sites that are affected by mass and force constant changes shall be called the impurity subspace. The difficulty of carrying out quantitative calculations for an actual crystal lattice increases rapidly as the size of the impurity subspace increases, so it is often desireable and usually necessary to restrict the assumptions on force constant changes. In order to make a problem manageable, compromises have to be made that will provide a physically realistic model of the impurity and host lattice, and simultaneously keep the defect space as small as possible. The exploitation of symmetry by the techniques of group theory can often provide great simplifications, but even then, the inclusion of more than nearest-neighbor force constant changes generally makes the computational problems incredibly difficult. Thus, only a small number of force constant changes are admitted.

A further assumption on localizability is involved when physically observable quantities are expanded in terms of Green's functions--e.g., by means of coefficients that couple light to the lattice. It is often necessary to make the assumption that these coefficients do not change,

or change only locally with the introduction of an impurity. This will be discussed further in Chapter IV, where the theory for Raman scattering and infrared absorption is given.

3.2 General Theory

In the harmonic approximation, the free vibrations of a crystal lattice not driven by external fields satisfies an equation of motion given by (2.12). It is convenient to introduce a classical Green's function G, which is defined by the equation of motion

$$\sum_{l''\kappa''\gamma} \left[M_{l\kappa}\delta_{ll''}\delta_{\kappa\kappa''}\delta_{\alpha\gamma}\frac{d^2}{dt^2} + \Phi_{\alpha\gamma}(l\kappa, l''\kappa'') \right] G_{\gamma\beta}(l''\kappa'', l'\kappa'; t) = -\delta(t)\delta_{\alpha\beta}\delta_{ll'}\delta_{\kappa\kappa'} \qquad (3.1)$$

In matrix notation,

$$\left[M\frac{d^2}{dt^2} + \Phi \right] G = -\delta(t)\,1 \qquad (3.2)$$

Where it exists, the Fourier transform

$$G(\omega) = \int_{-\infty}^{\infty} dt\, e^{i\omega t} G(t) \qquad (3.3)$$

is given by

$$G(\omega)^{-1} = M\omega^2 - \Phi \qquad (3.4)$$

The eigenfrequencies ω_s for the normal modes of vibration are determined from a secular equation,

$$\det\left[\omega^2 - D\right] = \det G^{-1}(\omega) / \det M = 0 \qquad (3.5)$$

and for a finite crystal, appear as simple poles of G along the real axis in the (complex) frequency plane.

So far, no boundary conditions have been imposed on this Green's function. A retarded (or causal) Green's function $G_r(t)$ is defined to satisfy the equation of motion (3.1) subject to the boundary conditions,

$$G_r(t) = \frac{d}{dt} G_r(t) = 0, \quad t < 0 \tag{3.6}$$

Likewise, it is possible to define an advanced Green's function with boundary conditions analogous to (3.6) for $t > 0$. For a system with time-reversal invariance, $G_r(t) = G_a(-t)$.

Formally, the inversion of the Fourier transform (3.4) is given by

$$G(t) = \frac{1}{2\pi} \int_{-\infty}^{\infty} d\omega \; e^{-i\omega t} \left(M\omega^2 - \Phi \right)^{-1} \tag{3.7}$$

However, $G(\omega)$ has simple poles on the real axis, and in order to carry out this inversion, it is necessary to make some prescription for integration around these singularities. The choice of integration contour that is made is related to the boundary conditions imposed on G(t). For a description of the system in terms of retarded Green's functions, $G_r(t)$ vanishes for $t < 0$, and for advanced Green's functions, $G_a(t)$ vanishes for $t > 0$. For the former description, it is necessary to integrate above the poles of $G(\omega)$, and for the latter, below the poles. Thus, for example,

$$G_r(t) = \frac{1}{2\pi} \int_{\Gamma} d\omega \, e^{-i\omega t} G(\omega) = \lim_{\epsilon \to 0^+} \frac{1}{2\pi} \int_{-\infty}^{\infty} d\omega \, e^{-i\omega t} G(\omega + i\epsilon) \tag{3.8}$$

where the contour Γ is shown in Fig. 3.1 below.

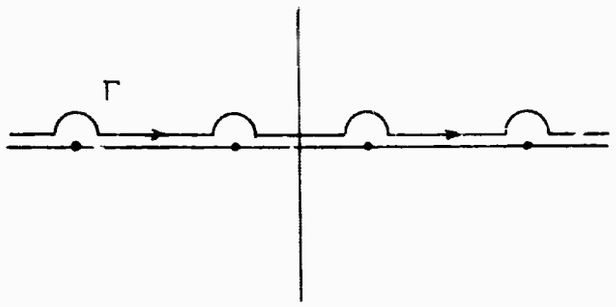

Fig. 3.1: Integration contour for $G_r(t)$

A similar result holds for the advanced Green's function $G_a(t)$, for which $G(\omega - i\varepsilon)$ appears. These rules are conveniently summarized: $G(\omega \mp i\varepsilon)$ is used for $G_{r,a}(t)$, respectively, when the transform (3.4) is formally inverted. It is, of course, always tacitly understood that the limit $\varepsilon \to 0^+$ is to be taken in all of the final results.

For a lattice driven by an external force, $F_\alpha(\ell\kappa,t)$, the equation of motion is

$$\left[M \frac{d^2}{dt^2} + \Phi \right] \cdot u(t) = F(t) \tag{3.9}$$

The response of the lattice can be expressed directly in terms of the Green's function:

$$u(t) = -\int_{-\infty}^{\infty} dt' \, G(t-t') F(t') \tag{3.10}$$

The use of the retarded Green's function is, perhaps, the most natural, since this description preserves the cause-and-effect order of stimulus

and response: no excitation occurs at times before a driving force is applied. In that case, the lattice response is given by

$$u(t) = -\int_{-\infty}^{\infty} dt'\, G_r(t-t')\, F(t') \tag{3.11}$$

The causal Green's function $G_r(t)$ shall be used in most of the subsequent development. No consequence of physical importance can depend upon this completely arbitrary choice of description. For a coherent driving force of the form

$$F(t) = \int_{-\infty}^{\infty} d\omega\, e^{-i\omega t}\, F(\omega) \tag{3.12}$$

the lattice response is, from the rule suggested above,

$$u(t) = -\lim_{\epsilon \to 0^+} \int_{-\infty}^{\infty} d\omega\, e^{-i\omega t}\, G(\omega+i\epsilon)\cdot F(\omega) \tag{3.13}$$

The $i\epsilon$ artifice in Eq. (3.13) is, of course, just a symbolic way of stating that the ω-integration is to be carried out along a contour slightly above the real axis. Note that, along such a contour, $F(t) \to 0$ as $t \to -\infty$, so that the causal description is consistent with an "adiabatic" (i.e., slow) switching-on of the interaction in the distant past.

For the harmonic lattice (to which we shall limit the present work), it was possible to obtain a simple, explicit form (3.4) for $G(\omega)$ that was analytic everywhere except for poles on the real axis. The significance of that statement can be made more precise, if we define, for complex z,

$$G_{r,a}(z) = \int_{-\infty}^{\infty} dt\, e^{izt} G_{r,a}(t) \tag{3.14}$$

If we assume that the inverse transform $G_{r,a}(\omega)$ exists--i.e., that $G_{r,a}(z)$ exists for all z on a contour (above or below) and infinitesimally close to the real axis--then we are led to the general property that $G_r(z)$ is analytic in the upper half-plane, and $G_a(z)$ in the lower half-plane. In general, if G(t) is defined as

$$G(t) = \begin{cases} G_r(t), & t > 0 \\ G_a(t), & t < 0 \end{cases} \tag{3.15}$$

then the Fourier transform,

$$G(z) = \begin{cases} G_r(z), & \text{Im } z > 0 \\ G_a(z), & \text{Im } z < 0 \end{cases} \tag{3.16}$$

is analytic throughout the entire complex frequency plane, except for the real axis. In more complicated problems involving anharmonic forces, Eq. (3.4) no longer holds, although these general analyticity properties continue to be valid. If the modes becomed damped by anharmonic forces, the singularities for $G_r(z)$ will be moved off of the real axis into the lower half-plane, and those for $G_a(z)$ to the upper half-plane.

There are some useful relations that exist for $G_{r,a}(z)$. First of all, the rule developed earlier for specifying the contour of integration can be expressed symbolically as

$$G_{r,a}(\omega) = \lim_{\epsilon \to 0^+} G(\omega \pm i\epsilon) \tag{3.17}$$

For a general system,

$$G_{r,s}(z) = G_{r,a}(-z^*)^* \tag{3.18}$$

and for a system invariant under time-reversal,

$$G_{r,a}(z) = G_{a,r}(-z) \tag{3.19}$$

The latter relation and the definition (3.16) lead to $G(z) = G(-z)$ for systems that are invariant under time-reversal. Notice that the result (3.4) for the harmonic lattice obeyed this requirement. For real ω, (3.18) and (3.19) can be specialized using (3.17) to give

$$G(\omega+i\varepsilon) = G(-\omega+i\varepsilon)^* \tag{3.20}$$

$$G(\omega+i\varepsilon) = G(-\omega+i\varepsilon) \tag{3.21}$$

which are the forms encountered most frequently in the subsequent work.

As a simple example that will motivate the use of Green's functions for later discussions of phonon optical properties, consider a classical linear system driven by a random, fluctuating force F(t). The average power absorbed in such a system can be expressed as

$$P = \langle F(t)\cdot \dot{u}(t)\rangle = -\int_{-\infty}^{\infty} dt' \langle F(t)\,F(t')\rangle \cdot \frac{d}{dt} G(t-t') \tag{3.22}$$

where the brackets $\langle\ \rangle$ represent an average over a statistical ensemble of systems. For the variables F(t), u(t) it is not meaningful to introduce the Fourier transform, but it is possible to define the Fourier transform of the correlation function $R(t',t) = \langle F(t')F(t)\rangle$ for stationary random processes. In that situation, the correlation function R depends

only upon $(t' - t)$, and if we define

$$R(\omega) = \int_{-\infty}^{\infty} d\tau\, e^{i\omega\tau} \langle F(\tau) F(0) \rangle \tag{3.23}$$

the power can be written

$$\frac{1}{2\pi} \int_{-\infty}^{\infty} d\omega\, (i\omega) \int_{-\infty}^{\infty} dt'\, e^{i\omega(t'-t)} \langle F(t') F(t) \rangle \cdot G(\omega + i\varepsilon)$$

$$= \frac{i}{2\pi} \int_{-\infty}^{\infty} d\omega\, (\omega)\, R(\omega) \cdot G(\omega + i\varepsilon)$$

Since $R(-\omega) = R(\omega)$, $G(-\omega+i\varepsilon) = G^*(\omega+i\varepsilon)$,

$$P = -\frac{1}{\pi} \int_{0}^{\infty} d\omega\, \omega\, R(\omega)\, \mathrm{Im}\, G(\omega + i\varepsilon) \tag{3.24}$$

and the <u>spectral power density</u> becomes

$$P(\omega) = -\frac{\omega}{\pi} \lim_{\epsilon \to 0^+} R(\omega)\, \mathrm{Im}\, G(\omega + i\varepsilon) \tag{3.25}$$

This simple classical example is an illustration of the usefulness that Green's functions have for the calculation of power absorption spectra in physical systems.

Another simple example is provided by the phonon density of states, which can also be expressed in terms of the imaginary part of a Green's function evaluated as ω approaches the real axis. It is easy to verify that, if a new (Green's) function $H(t)$ is defined as $H(t) = M\, dG/dt$, and thus,

$$H(\omega) = -i\omega M G(\omega) = -i M^{1/2} \frac{\omega}{\omega^2 - D} M^{-1/2} \tag{3.26}$$

the density of phonon states will be given by

$$\rho(\omega) = \frac{1}{3rN}\sum_s \delta(\omega-\omega_s) = \frac{2\omega}{3\pi r N} \mathrm{Tr}\left\{ M\, \mathrm{Im}\, G(\omega+i\varepsilon)\right\}$$
$$= -\frac{2}{3\pi r N}\, \mathrm{Re}\, \mathrm{Tr}\, H(\omega+i\varepsilon). \quad (3.27)$$

When a more general approach is introduced later to develop the Green's function formalism quantum mechanically, the "conjugate" Green's function H will achieve more significance.

For a perfect lattice with translational invariance, the Fourier transformed Green's function is

$$G^\circ(\omega)^{-1} = M_\circ \omega^2 - \Phi^\circ. \quad (3.28)$$

In terms of the dynamical matrix $D^\circ = M_\circ^{-\frac{1}{2}} \Phi^\circ M_\circ^{-\frac{1}{2}}$, defined in the earlier discussion of the phonon modes of the perfect lattice,

$$G^\circ(\omega) = M_\circ^{-1/2} \frac{1}{\omega^2 - D^\circ} M_\circ^{-1/2} \quad (3.29)$$

If we make use of (2.33b) and (2.48), the unperturbed Green's function G° can be written in spectral form,

$$G^\circ(\omega) = M_\circ^{-1/2} \sum_{\vec{k}\sigma} \frac{|\vec{k}\sigma\rangle\langle\vec{k}\sigma|}{\omega^2 - \omega_{\vec{k}\sigma}^2} M_\circ^{-1/2} \quad (3.30)$$

Then

$$\langle \ell\kappa\alpha | G^\circ(\omega) | \ell'\kappa'\beta\rangle = M_\kappa^{-1/2} \sum_{\vec{k}\sigma} \frac{\langle \ell\kappa\alpha|\vec{k}\sigma\rangle\langle\vec{k}\sigma|\ell'\kappa'\beta\rangle}{\omega^2 - \omega_{\vec{k}\sigma}^2} M_{\kappa'}^{-1/2} \quad (3.31)$$

which becomes, after inserting the expression (2.61) for the transformation functions $\langle \ell\kappa\alpha | \vec{k}\sigma\rangle$,

$$G^{\circ}_{\alpha\beta}(\ell\kappa, \ell'\kappa'; \omega) =$$

$$\frac{1}{N M_{\kappa}^{1/2}} \sum_{\vec{k}\sigma} e^{i\vec{k}\cdot(\vec{R}_{\ell\kappa} - \vec{R}_{\ell'\kappa'})} \frac{w_{\alpha}(\kappa|\vec{k}\sigma)\, w^{*}_{\beta}(\kappa'|\vec{k}\sigma)}{\omega^2 - \omega^2_{\vec{k}\sigma}} \frac{1}{M_{\kappa'}^{1/2}} \qquad (3.32)$$

For a finite lattice, the Green's function G° has poles along the real axis which become densely spaced as $N \to \infty$. In an infinite crystal, $G^{\circ}(\omega)$ will thus be analytic throughout the <u>entire</u> complex frequency plane except for <u>branch cuts</u> along the portions of the real axis corresponding to the (positive and negative) frequency band(s) of the crystal. This is illustrated in Fig. 3.2 below for a crystal that contains only one phonon band.

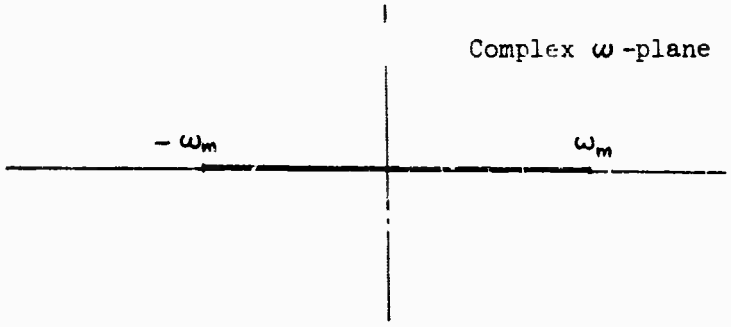

Fig. 3.2: Branch cut for $G^{\circ}(z)$ in an (infinite) crystal containing one phonon band.

Specifically, if $\omega\ (>0)$ is <u>in</u> one of the vibrational frequency bands of the lattice, then the Green's function $G^{\circ}(z)$ will exhibit a <u>jump discontinuity</u> as z crosses the real axis from $\omega+i\varepsilon$ to $\omega-i\varepsilon$:

$$G^{\circ}(\omega \pm i\varepsilon) = h^{(1)}(\omega) \mp i h^{(2)}(\omega) \qquad (3.33)$$

where the matrix $h^{(2)}(\omega)$ is given by

$$h^{(2)}(\omega) = \pi M_{\circ}^{-1/2} \delta(\omega^2 - D^{\circ}) M_{\circ}^{-1/2} \qquad (3.34)$$

with the matrix $\delta(\omega^2 - D^0)$ defined in terms of its spectral representation,

$$\delta(\omega^2 - D^0) = \sum_{\vec{k}\sigma} |\vec{k}\sigma\rangle \delta(\omega^2 - \omega^2_{\vec{k}\sigma}) \langle \vec{k}\sigma| \tag{3.35}$$

The real part, $h^{(1)}(\omega)$, is given by a Hilbert transform,

$$h^{(1)}(\omega) = \frac{1}{\pi} P \int_{\text{BANDS}} d\omega'^2 \frac{h^{(2)}(\omega')}{\omega^2 - \omega'^2} \tag{3.36}$$

The matrices $h^{(1)}(\omega)$ and $h^{(2)}(\omega)$ can also be expressed in the crystal lattice site representation $|\ell\kappa\alpha\rangle$, by the rule (2.61) given earlier. Thus, for example,

$$h^{(2)}_{\alpha\beta}(\ell\kappa, \ell'\kappa'; \omega) = \langle \ell\kappa\alpha | h^{(2)}(\omega) | \ell'\kappa'\beta \rangle$$

$$= \frac{\pi}{N(M_\kappa M_{\kappa'})^{1/2}} \sum_{\vec{k}\sigma} \delta(\omega^2 - \omega^2_{\vec{k}\sigma}) e^{i\vec{k}\cdot(\vec{R}_{\ell\kappa} - \vec{R}_{\ell'\kappa'})} w_\alpha(\kappa|\vec{k}\sigma) w^*_\beta(\kappa'|\vec{k}\sigma) \tag{3.37}$$

Clearly, if ω lies outside of the phonon frequency bands, the imaginary part $h^{(2)}(\omega)$ of the Green's function will vanish, since the delta-functions can only make a contribution when ω is in a band of phonon frequencies. Eq. (3.33) shows that the imaginary part of $G^0(z)$ changes sign as the branch cut on the real axis is crossed.

So far, all that has been emphasized is the usefulness that Green's functions have for describing the response of a lattice to an external force. However, the Green's function formalism also arises naturally as the most convenient mathematical framework for studying the perturbation on the lattice dynamics of a crystal containing defects. Their usefulness

for expressing concisely the coupling of an impurity site with the rest of the lattice will become apparent shortly. These techniques are, therefore, ideally suited to the study of optical properties of defects, since Green's functions contain, implicitly, the complete information about the perturbed eigenfrequency spectrum, and represent the response of the lattice to external electromagnetic fields as well. In principle, the determination of the normal modes of the perturbed lattice would provide a complete solution to the impurity problem, although such detailed information (even if it could be obtained) would not usually be of direct usefulness for discussing the physically observable properties. As the simple examples above have suggested, many quantities of physical interest (such as Raman and infrared spectra, phonon density of states, etc.) can be related directly to certain Green's functions. In the next section, it will be shown how Green's function methods can be used (in the harmonic approximation) for the vibrational impurity problem.

3.3 Lattice Dynamics of Defects

The Green's function $G(\omega)$ for a general lattice containing an arbitrary configuration of substitutional impurities was given by (3.4), and this can be related to the Green's function $G^{o}(\omega)$ for the unperturbed, perfect lattice, Eq. (3.28), by

$$G(\omega)^{-1} = G^{\circ}(\omega)^{-1} + V \tag{3.38}$$

where the defect matrix V is defined by

$$V = (M - M_{o})\omega^{2} - (\Phi - \Phi^{\circ}) \tag{3.39}$$

Thus

$$G(\omega) = G^{\circ}(\omega) - G^{\circ}(\omega)\,V\,G(\omega) \tag{3.40}$$

$$G(\omega) = \left[1 + G^{\circ}(\omega)V\right]^{-1} G^{\circ}(\omega)$$

$$= G^{\circ}(\omega) - G^{\circ}(\omega)V\left[1 + G^{\circ}(\omega)V\right]^{-1} G^{\circ}(\omega) \tag{3.41}$$

Klein[94] and Benedek and Nardelli[95] have discussed the defect problem from the point of view of phonon scattering and the T-matrix (the T-matrix in (3.41) is $V(1+G^{\circ}V)^{-1}$). In principle, Eq. (3.41) represents the solution of the problem of an arbitrary configuration of impurities, although for a general defect matrix V, it has little practical usefulness for providing any explicit knowledge of the nature of the perturbed modes, or for changes in actual physical quantities. However, if we restrict our attention to the problem of a single isolated substitutional defect in an otherwise perfect lattice, it is possible to obtain several useful results from this formalism. Since the use of Green's functions for impurity effects on lattice dynamics has been thoroughly discussed in the literature, particularly in several excellent review articles[1,54-60], only a brief account will be given here.

For the vibrational problem, the introduction of a substitutional point defect will involve changes in the mass and force constants. The situation is, of course, more complicated for defects such as molecular impurities, or interstitial impurities, since extra degrees of freedom are added to the problem[57,96,97]. The translational symmetry of the perfect lattice is destroyed, and the normal modes can no longer be labeled by a wave vector $\vec{k}$. The great simplifications that translational

invariance provided for the reduction of the secular equation to the 3r x 3r form (2.54) no longer obtain, and all that remains at our disposal is the point group symmetry that characterizes the impurity site and the surrounding lattice. For the problem of a single substitutional impurity, the exploitation of defect site symmetry and the use of matrix partition techniques[57,95,98] makes it possible to obtain several useful, quantitative results from the basic equation (3.41), provided that the space affected by the defect is not large. Define

$$G = \left|\begin{array}{c|c} g & G_{12} \\ \hline G_{21} & G_{22} \end{array}\right|, \quad V = \left|\begin{array}{c|c} V_o & 0 \\ \hline 0 & 0 \end{array}\right|, \quad G^o = \left|\begin{array}{c|c} g^o & G^o_{12} \\ \hline G^o_{21} & G^o_{22} \end{array}\right| \tag{3.42}$$

where the first set of rows or columns in each partition refers to the impurity subspace. If there are a total of n sites affected by the introduction of an impurity, then the matrices g, g^o, and V_o will be 3n x 3n. From (3.40), (3.41), one can show that

$$g(\omega) = \left[1 + g^o(\omega) V_o\right]^{-1} g^o(\omega) \tag{3.43}$$

The frequencies of the perturbed spectrum, which are the discrete poles of G for a finite lattice, are given by the secular equation, (3.5). Since

$$\det\left[1 + g^o(\omega) V_o\right] = \frac{\det G(\omega)^{-1}}{\det G^o(\omega)^{-1}} = \frac{\det M}{\det M_o} \frac{\prod_s (\omega^2 - \omega_s^2)}{\prod_{\vec{k}\sigma} (\omega^2 - \omega_{\vec{k}\sigma}^2)}$$

it follows from (3.5), (3.42) that the solutions to the equation

$$\det\left[1 + g^o(\omega) V_o\right] = 0 \tag{3.44}$$

will give the frequencies of those modes which are perturbed by the introduction of the impurity. Thus, for a localized defect described by V_0, the problem can be reduced to a form in which only those Green's functions defined for the (small) impurity subspace are involved. The way in which a defect is coupled to a pure lattice is thus expressed concisely in terms of the Green's function formalism. There is an extensive literature on the nature of the solutions for (3.44), and no attempt will be made here to duplicate the excellent accounts elsewhere, except for a few brief remarks.

It has been well known, since the early work of Lifshitz[99], Montroll and Potts[100], and others[1,101,102] that one striking consequence of equation (3.44) is the possibility of obtaining "local mode" (or "gap mode") solutions that have frequencies outside of the band(s) of frequencies allowed for the perfect lattice. When a defect atom of different mass, and perhaps characterized by different "spring constants," is introduced substitutionally into a perfect lattice, it may have vibrational properties considerably different from those of the host atom it replaces. As a simple example, when a light defect mass replaces a heavy mass in a one-dimensional chain, a mode can split off of the top of the vibrational continuum to produce a local mode. Because modes with frequencies outside of the band(s) are not propagated by the perfect crystal, these so-called "local modes" are actually characterized by a high degree of spatial localization around the defect, and the vibrations of the atoms in such a mode fall off rapidly with distance away from the defect site. Similar effects result from changes in the force constants. In three dimensions, there is generally a critical value for the mass or force con-

stant change tha must be exceeded in order to produce these effects. The in-band modes will be perturbed only slightly, with frequency shifts of order 1/N in the quasi-continuum. As $\varepsilon \to \infty$, the change in the band frequencies will approach zero, and in that limit, $g^o(\omega)$ will become a principle part integral (which is just Re $g^c(\omega+i\varepsilon)$). Since its solutions describe only the perturbed modes, Eq. (3.44) will have a solution only at the local mode frequency in that limit.

In addition to local modes outside of the band, there are also interesting resonance phenomena[1,103-110] that can occur inside of the band. The expression for many physical quantities (that can be related to the Green's function G) will contain an inverse, $(1 + g^o(\omega+i\varepsilon)v_o)^{-1}$. Inside the band, the imaginary part of $g^o(\omega+i\varepsilon)$ is, in general, non-zero, and if there is some frequency ω_o inside the band for which the real part of $\det[1 + g^o(\omega_o+i\varepsilon)v_o]$ vanishes, this can lead to a resonant behavior at that frequency with a "width" related to the imaginary part of $g^o(\omega_o+i\varepsilon)v_o$.

For example, if a sufficiently heavy defect is introduced into a perfect lattice, it will prefer to vibrate at a lower frequency than the typical host atoms, and this can result in a low-frequency, in-band resonance. Such "resonance modes" have often been loosely characterized as being at frequencies where a local mode would like to exist, but cannot, since the phonon density of states for the pure crystal is non-vanishing there. Such a ("quasi-local", or "virtual") mode would be able to decay into the continuum of neighboring band modes, and this mechanism would make the lifetime finite (or equivalently, give a "width" to the resonance). In contrast, of course, a true local mode that lies in a gap or above the maximum frequency of the unperturbed lattice is all by itself, and is un-

able (in the harmonic approximation) to decay into any of the other modes of the lattice.

Similar phenomena, such as local and resonance mode behavior, have been discussed by Wolfram and Callaway[83], Wang and Callen[86], Hone[88], and others for single impurities in magnetic systems. If impurities are introduced into ferro- or antiferromagnets described by a Heisenberg hamiltonian, the situation is analogous, in many respects, to the lattice vibrational problem in the harmonic approximation. At low temperatures, the system is described by non-interacting spin waves (magnons) which play the part of phonons. The magnons represent wave-like spin-deviation states from the ground state, just as we can consider phonons to represent wave-like displacements of atoms from an equilibrium configuration. (Spin waves are discussed in Kittel[39] and in a review article by Krankendonk and Van Vleck[111].) The ferro- or antiferromagnet consists of a system of spins localized at fixed lattice sites, and coupled by pairwise exchange interactions. For the perfect system (just as for the phonon problem) the normal modes are a set of magnon states described by dispersion curves giving energy versus $\vec{k}$. Once again, defects are considered in the approximation that the perturbation they produce is spatially localized. In the lattice site representation, this means that the change induced by the impurity on the exchange coupling constants (which are analogous to "force constants") must be localized near the impurity site. Furthermore, a general substitutional impurity can also involve a change in the spin. Although the formulation of the spin problem requires the quantum mechanical Green's function formalism, all of the results discussed above for the lattice dynamics of defects have their counterpart in magne-

tic systems. As would be expected, it is possible to obtain, for appropriate defect parameters, localized modes outside of the (magnon) bands of the perfect lattice; it is also possible to observe "virtual" or "resonance" modes, with finite lifetimes, within the band(s)[90-93].

The electronic impurity problem for a substitutional defect was first treated by Koster and Slater[61], and it has also been discussed by Wolff[62], Clogston[63], Friedel[65] and others. For this type of problem, we are interested in the effects of a highly localized impurity potential on the wave function of an electron in an otherwise perfect, translationally periodic, crystal field. By expanding wave functions and operators in terms of Wannier functions (states which are highly localized about atomic sites) it is also possible to treat the electronic impurity problem by Green's function methods analogous to those for lattice vibrations. If the perturbation is sufficiently large, electronic bound states analogous to local modes can appear outside of the energy band(s) for the pure crystal. Elliott[59] has given a good simple example to illustrate the electron impurity problem: suppose a single defect is introduced at the origin of an "empty lattice", described by a single band of free electrons with energies $E(\vec{k}) = \hbar^2\vec{k}^2/2m$. The single impurity problem then consists only of the defect potential at the origin, and all that is required are the solutions for the electron wave function in a potential well. Consider an impurity potential such as that illustrated in Fig. 3.3 below. The positive energy solutions correspond, by analogy, to the continuum band modes of the vibrational problem, and except for an asymptotic phase shift at large distances, their wave functions are not appreciably altered from the free, plane-wave solutions, except in the vicinity of the defect.

If the well is sufficiently complex that it attempts to form a bound state at an energy of one of the continuum states outside of the well, then a virtual or resonance state will form which can decay, with finite probability, through the barrier and into the potential-free region. The probability density of a state with energy E_1 will be resonantly enhanced in the region of the defect well. Likewise, if the well is deep enough, it can form true bound states, with an energy E_o outside of the continuum energy band; such a state is analogous to the vibrational local mode.

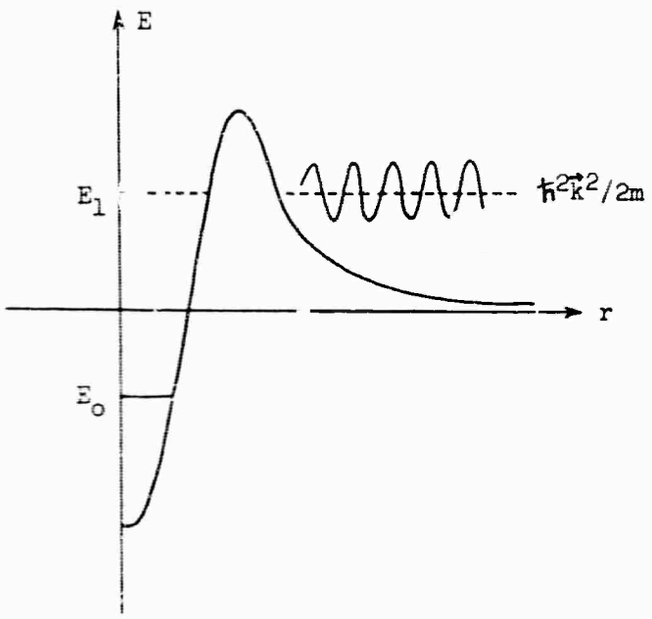

Fig. 3.3: One-electron impurity potential for the "empty lattice" with a single, substitutional defect at the origin. E_o represents a true bound state, and E_1 a virtual state.

For further details concerning the electronic and magnetic impurity problems, reference can be made to the literature, and especially to the

review article by Izyumov[54].

Let us now return to the lattice vibration problem. The introduction of a single isolated defect can, under favorable conditions, cause one of the modes of the perfect lattice to split off from the continuum and form a localized vibrational mode. When many impurities are present, they can interact (even if only indirectly through the intermediate coupling with other host atoms) and it is possible to produce a more complicated local mode spectrum. For small concentrations, the defects will be far apart, and the results for the isolated impurity problem will be adequate for many purposes. However, depending upon the configuration of the impurities, the multiple impurity problem can, in general, become very complex. For example, the localized mode structure may contain many components from "islands" of adjacent defects, and these localized cluster effects can become important for some problems if the concentration of defects is not small. Many authors have studied the local mode structure for the multiple-impurity problem exactly for simple models in conjunction with the random crystal problem. This topic is, therefore, properly postponed until Chapter V, where we will discuss disordered lattices.

3.4 Quantum Mechanical Double-Time Green's Functions

Zubarev[46] has given an excellent review of the theory of quantum mechanical double-time Green's functions, which have recently been used in a variety of statistical mechanical, impurity, and many-body problems. As we shall see, one of the basic, simplifying features of the harmonic approximation makes it possible to use, equivalently, either a classical or quantum mechanical formulation for the lattice vibration problem. However, the quantum mechanical framework is far more versatile, in general,

and it is necessary for extending Green's function methods to magnetic and electronic systems, which cannot be described by classical equations. Even for the lattice vibration problem, where a classical description could suffice, the quantum mechanical formulation has many advantages, for it expresses results as thermally averaged correlation functions.

In the harmonic approximation, a certain quantum mechanical Green's function will turn out to obey the same equation of motion as the classical function G, introduced earlier in Eq. (3.2). When anharmonic interactions are included, the classical differential equations of motion for the lattice displacements becomes non-linear, and a description of the system in terms of the classical Green's function G(t) is not available. It then becomes necessary to resort to the more general quantum mechanical formulation of Green's functions.

Within the harmonic approximation, a simple, linear, second-order differential equation, in closed form, describes the time evolution of the classical Green's function G(t). This led to a simple, explicit form for the Fourier transform $G(\omega)$, given by (3.4). The presence of anharmonic interactions, which requires the quantum mechanical formalism, leads to the necessity of defining an infinite heirarchy of Green's functions, coupled by an infinite sequence of equations of motion. For the quantum mechanical Green's function G(t) that is analogous to the classical one in the harmonic approximation, there would no longer be a simple equation of motion in closed form, and it would no longer be possible to obtain, simply, the Fourier transform $G(\omega)$. Further remarks shall be made at the appropriate places below.

The retarded and advanced Green's functions (at some finite temperature T) for two Heisenberg operators A(t) and B(t') are defined by

$$G_r^{AB}(t-t') = \frac{1}{i}\theta(t-t')\left\langle \left[A(t), B(t')\right]\right\rangle_T \tag{3.45a}$$

$$G_a^{AB}(t-t') = \frac{-1}{i}\theta(t'-t)\left\langle \left[A(t), B(t')\right]\right\rangle_T \tag{3.45b}$$

and

$$G^{AB}(t) = \begin{cases} G_r^{AB}(t), & t > 0 \\ G_a^{AB}(t), & t < 0 \end{cases} \tag{3.45c}$$

where $\theta(t)$ is the unit step-function, defined by $\theta(t) = 0$ for $t < 0$, and $\theta(t) = 1$ for $t > 0$. The brackets $\langle\ \rangle_T$ represent an average over a thermodynamic ensemble defined by a density matrix $\rho_o = e^{-\beta\mathcal{H}}$, where T is the temperature and $\beta = 1/kT$. I.e., for an operator A(t),

$$\langle A(t)\rangle_T = \frac{Tr\left(\rho_o A(t)\right)}{Tr\,\rho_o} = \frac{Tr\left[e^{-\beta\mathcal{H}}A(t)\right]}{Tr\left(e^{-\beta\mathcal{H}}\right)}$$

In order to motivate the quantum mechanical definition for the Green's function given above, it is instructive to show it arises naturally in expressing, to lowest order, the driven response of a system, in thermodynamic equilibrium at temperature T, to an externally applied field. Let the unperturbed system be defined by the hamiltonian $\mathcal{H}$, and suppose that an external perturbation is applied, which couples a driving force F(t) to some operator B. In the Schrödinger picture,

$$H = \mathcal{H} + B\cdot F(t)$$

In the Schrödinger picture, the state of the system (in this case, e.g., described by a density matrix ρ) evolves in time, whereas in the Heisenberg picture, the state is regarded as remaining constant (i.e. ρ_o), and the dynamics is described by time evolution of the operators. The evolution in time for an operator A(t) is described by a unitary transformation,

$$A(t) = U(t)^{\dagger} A U(t) \tag{3.46}$$

where

$$U(t) = \exp(-i\mathcal{H}t)\left(\exp -i\int_{-\infty}^{t} dt' B(t') F(t')\right)_{+} \tag{3.47}$$

The expression on the right contains a time-ordered exponential, $(\exp\ldots)_{+}$, which is defined formally in terms of its expansion by a rule that states that all operator products are to be ordered in such a way that later times occur on the left[112]. The operator B(t) is given by

$$B(t) = \exp(i\mathcal{H}t)\, B \exp(-i\mathcal{H}t) \tag{3.48}$$

which defines the <u>interaction representation</u> for the complete system (including the perturbation). Note that B(t) is just the Heisenberg operator for the system without the perturbation.

Then, if it is assumed that there is no static contribution from $\mathrm{Tr}(\rho_o A)$, the <u>response</u> in the operator A due to the coupling of B with an external driving force F(t) is, to <u>lowest order</u> in F,

$$\langle A(t)\rangle_{\tau} = -i\int_{-\infty}^{t} dt' \left\langle \left[A(t), B(t')\right]\right\rangle_{\tau} F(t')$$

$$= \int_{-\infty}^{\infty} dt' G_r^{AB}(t-t') F(t') \tag{3.49}$$

If the time-ordered exponential in (3.47) had been expanded further, higher order terms which are non-linear in the driving force F would result. Such terms would be useful, for example, in obtaining quantum mechanical expressions for the non-linear susceptibilities in optics[113].

For the case of an external field of frequency ω that is switched on "adiabatically" (i.e., slowly) in the distant past, given by the real part of

$$F_\omega(t) = F_o \exp(-i\omega t + \varepsilon t),$$

the response becomes

$$\langle A(t)\rangle_T = \chi^{AB}(\omega) \cdot F_\omega(t) \tag{3.50}$$

where

$$\chi^{AB}(\omega) = G^{AB}(\omega + i\varepsilon) \tag{3.51}$$

The linear susceptibility is, therefore, just the Fourier transform of a double-time Green's function.

The equation of motion for the Green's function $G^{AB}(t)$ can be obtained by invoking the equations of motion for the operators A(t), B(t) which, by definition, evolve in time as Heisenberg operators of the unperturbed system, viz.,

$$A(t) = e^{i\mathcal{H}t} A e^{-i\mathcal{H}t}. \tag{3.52}$$

Then

$$i\, d/dt\, A(t) = \left[A(t), \mathcal{H}\right], \tag{3.53}$$

which is the familiar Heisenberg equation of motion for the unperturbed

system (i.e., with no external driving fields). The equation of motion for $G_r^{AB}(t)$ becomes

$$i\frac{d}{dt}G_r^{AB}(t) = \delta(t)\langle[A(t), B(0)]\rangle_T + \frac{1}{i}\theta(t)\langle[[A(t), \mathcal{H}], B(0)]\rangle_T \quad (3.54)$$

The presence of the $\delta(t)$ allows the first term in (3.54) to be written as an equal-time commutator, $\delta(t)\langle[A(0), B(0)]\rangle_T$. The second term on the right is a new Green's function, and this is a general characteristic of the quantum mechanical theory: successive differentiations will continue to generate new Green's functions on the RHS, leading to an infinite heirarchy of coupled equations.

By specializing the operators A, B, the quantum mechanical formalism could be applied to vibrational, magnetic, electronic, or other systems. (For the electronic Green's functions, anti-commutators must be used.) In the present case, we wish to discuss the vibrational problem. For an arbitrary crystal lattice, we can define a (retarded) displacement-displacement Green's function G, and a momentum-displacement Green's function H as

$$G_{\alpha\beta}(\ell\kappa, \ell'\kappa'; t) = \frac{1}{i}\theta(t)\langle[u_\alpha(\ell\kappa, t), u_\beta(\ell'\kappa', 0)]\rangle_T \quad (3.55a)$$

$$H_{\alpha\beta}(\ell\kappa, \ell'\kappa'; t) = \frac{1}{i}\theta(t)\langle[p_\alpha(\ell\kappa, t), u_\beta(\ell'\kappa', 0)]\rangle_T \quad (3.55b)$$

where $p_\alpha(\ell\kappa, t) = M_{\ell\kappa}\,du_\alpha(\ell\kappa, t)/dt$ is the conjugate momentum operator. By differentiating once,

$$\frac{d}{dt} M_{\ell\kappa} G_{\alpha\beta}(\ell\kappa, \ell'\kappa'; t) = H_{\alpha\beta}(\ell\kappa, \ell'\kappa'; t) \tag{3.56}$$

and

$$\frac{d}{dt} H_{\alpha\beta}(\ell\kappa, \ell'\kappa'; t) = \frac{1}{i}\delta(t)\left\langle \left[p_\alpha(\ell\kappa, 0),\ u_\beta(\ell'\kappa', 0)\right]\right\rangle_T$$

$$- \theta(t)\left\langle \left[\left[p_\alpha(\ell\kappa, t), \mathcal{H}\right],\ u_\beta(\ell'\kappa', 0)\right]\right\rangle_T \tag{3.57}$$

The right hand side of (3.56) contained a term with $\delta(t)$ which vanishes because it included a $[u,u]$ commutator. In the harmonic approximation, the right hand side of (3.57) does not generate any new Green's function; in fact, it reproduces the original Green's function G. By invoking the equal-time commutator relations,

$$\left[p_\alpha(\ell\kappa, t),\ u_\beta(\ell'\kappa', t)\right] = \frac{1}{i}\delta_{\alpha\beta}\delta_{\kappa\kappa'}\delta_{\ell\ell'} \tag{3.58}$$

it follows, in the harmonic approximation, that

$$\left[p_\alpha(\ell\kappa, t), \mathcal{H}\right] = \frac{1}{i}\sum_{\ell'\kappa'\gamma} \Phi_{\alpha\gamma}(\ell\kappa, \ell'\kappa')\, u_\gamma(\ell'\kappa', t) \tag{3.59}$$

Eq. (3.58) and (3.59) can be used to simplify (3.57), which becomes

$$\frac{d}{dt} H_{\alpha\beta}(\ell\kappa, \ell'\kappa'; t) = -\delta(t)\delta_{\alpha\beta}\delta_{\kappa\kappa'}\delta_{\ell\ell'}$$

$$- \sum_{\ell''\kappa''\gamma} \Phi_{\alpha\gamma}(\ell\kappa, \ell''\kappa'')\frac{1}{i}\theta(t)\left\langle \left[u_\gamma(\ell''\kappa'', t), u_\beta(\ell'\kappa', 0)\right]\right\rangle_T \tag{3.60}$$

The original Green's function G has reappeared on the right hand side. In matrix notation, (3.56) and (3.60) become

$$M\frac{d}{dt}G = H \tag{3.61}$$

$$\frac{d}{dt}H = -\Phi G - \delta(t)1 \tag{3.62}$$

By differentiating (3.61) and using (3.62), we obtain finally

$$\left(M\frac{d^2}{dt^2} + \Phi\right)G = -\delta(t)1 \tag{3.63}$$

which is identical to the equation of motion (3.2) for the classical Green's function G introduced earlier. Recall that H(t), the "conjugate" Green's function, occurred earlier in connection with the phonon density of states (cf. Eq. (3.26), (3.27)).

With the inclusion of anharmonic forces, the simple form (3.59), (3.62), and (3.63) no longer hold. The presence of anharmonic terms is the hamiltonian,

$$V_A = \frac{1}{6}\sum_{\substack{l_1\kappa_1\alpha_1\\ l_2\kappa_2\alpha_2\\ l_3\kappa_3\alpha_3}} \Phi_{\alpha_1\alpha_2\alpha_3}(l_1\kappa_1, l_2\kappa_2, l_3\kappa_3)\, u_{\alpha_1}(l_1\kappa_1)u_{\alpha_2}(l_2\kappa_2)u_{\alpha_3}(l_3\kappa_3) + \frac{1}{24}\sum_{1,2,3,4}\Phi(1,2,3,4)u(1)u(2)u(3)u(4) + \dots \tag{3.64}$$

will modify the commutation relation (3.59):

$$\left[P_\alpha(l\kappa,t),\mathcal{H}\right] = \frac{1}{i}\sum_{l_1\kappa_1\alpha_1}\Phi_{\alpha\alpha_1}(l\kappa, l_1\kappa_1)\,u_{\alpha_1}(l_1\kappa_1,t) + \frac{1}{2i}\sum_{\substack{l_1\kappa_1\alpha_1\\ l_2\kappa_2\alpha_2}}\Phi_{\alpha\alpha_1\alpha_2}(l\kappa, l_1\kappa_1, l_2\kappa_2)u_{\alpha_1}(l_1\kappa_1,t)u_{\alpha_2}(l_2\kappa_2,t) + \dots \tag{3.65}$$

The equation of motion (3.63) is now replaced by

$$\sum_{\ell_1\kappa_1\alpha_1}\Big[\, M_{\ell\kappa}\,\delta_{\ell\ell_1}\,\delta_{\kappa\kappa_1}\,\delta_{\alpha\alpha_1}\,\frac{d^2}{dt^2} + \Phi_{\alpha\alpha_1}(\ell\kappa,\ell_1\kappa_1)\Big] G_{\alpha_1\beta}(\ell_1\kappa_1,\ell'\kappa';t) =$$

$$-\delta(t)\,\delta_{\alpha\beta}\,\delta_{\ell\ell'}\,\delta_{\kappa\kappa'} - \frac{1}{2}\sum_{\substack{\ell_1\kappa_1\alpha_1\\ \ell_2\kappa_2\alpha_2}} \Phi_{\alpha\alpha_1\alpha_2}(\ell\kappa,\ell_1\kappa_1,\ell_2\kappa_2)\ \times$$

$$\frac{1}{i}\,\theta(t)\Big\langle\Big[\,u_{\alpha_1}(\ell_1\kappa_1,t)\,u_{\alpha_2}(\ell_2\kappa_2,t),\ u_\beta(\ell'\kappa',0)\Big]\Big\rangle_T + \ldots \qquad (3.66)$$

and <u>new</u> Green's functions occur on the RHS. The calculation has immediately become a more complicated many-body problem, and requires some sort of truncation approximation to terminate the equations. Since the simple closed form (3.63) for G(t) is no longer valid, it is no longer possible to use the simple form (3.4) for $G(\omega)$ if the harmonic approximation is abandoned.

Frequently, the Fourier transform of certain thermally averaged correlation functions of the form $R^{AB}(t - t') = \langle A(t)B(t')\rangle_T$ appear in the treatment of physically observable quantities. The spectral density function,

$$J^{AB}(\omega) = \int_{-\infty}^{\infty} dt\, e^{i\omega t}\,\langle A(t)\,B(0)\rangle_T \qquad (3.67)$$

can be expressed in terms of the Green's functions $G^{AB}(\omega)$ in a relatively simple way. Since $A(t) = \exp(i\mathcal{H}t)\,A(0)\exp(-i\mathcal{H}t)$, it is possible to exploit the formal similarity between time and temperature dependence in the thermal average,

$$\langle B(0)A(t)\rangle_T = \frac{1}{Z} Tr\left\{ e^{-\beta\mathcal{H}} B(0) e^{i\mathcal{H}t} A(0) e^{-i\mathcal{H}t} \right\} \qquad (3.68)$$

where $Z = Tr(e^{-\beta\mathcal{H}})$ is the partition function. Simple rearrangement, using the cyclic property of the trace, leads to

$$\langle B(0)A(t)\rangle_T = \langle A(t-i\beta)\, B(0)\rangle_T \qquad (3.69)$$

so that

$$\int_{-\infty}^{\infty} dt\, e^{i\omega t}\langle [A(t), B(0)]\rangle_T = (1 - e^{-\quad}, J^{AB}(\omega) \qquad (3.70)$$

Again, the $i\varepsilon$ artifice can be used to express

$$G^{AB}(\omega \pm i\varepsilon) = \int_{-\infty}^{\infty} dt\, e^{i\omega t} G^{AB}_{r,a}(t) \qquad (3.71)$$

Subtraction of the (two) equations (3.71) gives

$$i\left[G^{AB}(\omega+i\varepsilon) - G^{AB}(\omega-i\varepsilon)\right] = \int_{-\infty}^{\infty} dt\, e^{i\omega t}\langle [A(t), B(0)]\rangle_T \qquad (3.72)$$

where the relation $[\theta(t) + \theta(-t)] = 1$ has been used. Combination of (3.70) and (3.72) leads to a final result which is a useful relation[46] expressing the spectral density of the correlation function $\langle A(t)B(0)\rangle_T$ in terms of the Green's function $G^{AB}(\omega)$:

$$J^{AB}(\omega) = i\left[1 + n(\omega)\right] \lim_{\varepsilon\to 0^+} \left[G^{AB}(\omega+i\varepsilon) - G^{AB}(\omega-i\varepsilon)\right] \qquad (3.73)$$

where $n(\omega) = \left[e^{\beta\omega} - 1\right]^{-1}$ is the Bose distribution function. It is pos-

sible to express each of the Green's functions $G_{r,a}^{AB}(\omega)$ separately in terms of the spectral distribution $J^{AB}(\omega)$ by making use of a convenient representation of the $\theta(t)$ step-function,

$$\theta(t) = \frac{i}{2\pi}\int_{-\infty}^{\infty} d\omega' \frac{e^{-i\omega' t}}{\omega' + i\varepsilon} \tag{3.74}$$

Then

$$G_{r,a}^{AB}(\omega) = \pm \frac{1}{2\pi}\int_{-\infty}^{\infty} \frac{d\omega'}{\omega' + i\varepsilon}\int_{-\infty}^{\infty} dt\, e^{i(\omega \mp \omega')t}\left\langle [A(t), B(0)]\right\rangle_T \tag{3.75}$$

which can be reduced, by means of (3.70), to yield

$$G_{r,a}^{AB}(\omega) = \frac{1}{2\pi}\int_{-\infty}^{\infty} d\omega' \left(1 - e^{-\beta\omega'}\right)\frac{J^{AB}(\omega')}{\omega - \omega' \pm i\varepsilon} \tag{3.76}$$

The formal rule

$$\frac{1}{x \pm i\varepsilon} = P\left(\frac{1}{x}\right) \mp i\pi\delta(x) \tag{3.77}$$

can be invoked to express (3.76) explicitly:

$$G_{r,a}^{AB}(\omega) = \frac{1}{2\pi} P\int_{-\infty}^{\infty} d\omega' \left(1 - e^{-\beta\omega'}\right)\frac{J^{AB}(\omega')}{\omega - \omega'} \mp \frac{i}{2}\left(1 - e^{-\beta\omega}\right)J^{AB}(\omega) \tag{3.78}$$

The displacement-displacement Green's function G defined in (3.55) can be used to evaluate the Fourier transform of a certain correlation function that will occur later in the theory of first-order Raman scattering from phonons:

$$\int_{-\infty}^{\infty} dt\, e^{i\omega t}\left\langle u_\alpha(\ell\kappa, t) u_\beta(\ell'\kappa', 0)\right\rangle_T = -2\left[1 - e^{-\beta\omega}\right]^{-1} \operatorname{Im} G_{\alpha\beta}(\ell\kappa, \ell'\kappa'; \omega + i\varepsilon) \tag{3.79}$$

IV. THE PHONON OPTICAL PROPERTIES

4.1 Raman Scattering

The Raman effect is an inelastic scattering process in which light, interacting with matter, can transfer energy to (or receive energy from) the material system. In the present case, we shall be concerned with Raman scattering from lattice vibrations, which involves the creation or destruction of phonons when light interacts with a crystal. Raman scattering from other excitations--e.g., spin waves[114,115], electronic states[116,117], and perhaps plasmons[118], etc.--is also possible.

An electromagnetic wave can be coupled to the phonon modes in a crystal by means of the electronic polarizability, and the scattering mechanism is the fluctuations in the polarizability that are induced by the lattice vibrations. Classically, the effect can be pictured as radiation from an electric dipole that was induced by an incident light wave, and which is modulated in time because of the coupling of the electronic motion to the lattice mode oscillators. If we neglect the effects of resonant enhancement that can result when the incident frequency ω_i is near an electronic absorption band of the crystal, then the Raman effect is not sensitive to the frequency ω_i. Loudon[119] has recently given a comprehensive review of Raman scattering, and several other authors have treated[120-123] specific aspects of the theory of RS from phonons. Except for some of the more basic details, it will not be our purpose here to develop the theory of RS. It will be shown how the scattering intensity from lattice vibrations can be related to certain phonon Green's functions.

Since energy must be conserved for the total system of radiation and matter in the scattering process, the frequency of the scattered light

is either decreased (Stokes component) or increased (anti-Stokes component) by an amount ω_o,

$$\omega_f = \omega_i \mp \omega_o$$

where $\hbar\omega_o$ is the energy gained or lost by the lattice. The present work shall be restricted to the first-order Raman effect, in which a single phonon is created or destroyed in the scattering process.

The wavelength of light is very long compared with typical lattice spacings, and the conservation of momentum implies that the phonons excited in the first-order Raman effect will have a very small wave-vector $\vec{k}$ relative to the allowed momenta of the first Brillouin zone. The approximation can be made that $\vec{k} \approx 0$, and the first-order Raman spectrum will exhibit a series of lines that correspond to certain optical phonon frequencies at the center of the Brillouin zone. There are also selection rules involved, and only lattice vibrations having certain types of symmetry can give rise to first-order Raman scattering.

Group theory[29] provides the selection rules by which one decides which modes are Raman-active, infrared-active, or neither ("silent modes"). Raman-active modes must transform, under the operations of the crystal point group, like a second rank tensor (i.e., according to representations with x^2, y^2, xy, etc. basis functions). For Raman scattering from phonons, one can usually assume the second rank tensor to be symmetric. IR-active modes must transform according to the representations for a polar vector (x, y, z basis functions). If every atom of the lattice is at a site of inversion symmetry, all $\vec{k} = 0$ phonons will have odd parity, and there can be no first-order Raman-active modes. If the point group

does not contain inversion symmetry (at any site), modes can be simultaneously Raman- and IR-active, and special complications arise because of the long-range electric polarization field[25,39,119]. These complications do not occur in crystals with a center of inversion symmetry, for which Raman- and IR-active modes are complementary and have definite parity. Finally, there can be situations where it is possible to have modes which are silent--i.e., neither Raman- nor IR-active. Loudon[119] has listed the forms of the polarization tensors for phonons of given symmetries that can be used to determine the effect of geometry on scattering intensity.

For the O_h point group, the components of a symmetric, second rank tensor transform according to $(A_{1g} + E_g + F_{2g})$, and those of a polar vector according to F_{1u}. Thus, the F_{2g} and F_{1u} optic modes, found in Sec. 2.2 for CaF_2 at $\vec{k} = 0$, are respectively Raman and infrared active. A rigorous quantum mechanical treatment of the combined system of radiation, electronic, and vibrational degrees of freedom is difficult, and not always very fruitful for obtaining practical results. Loudon[119] and Lax and Burstein[124] have discussed Raman scattering from crystal lattices in terms of the coupled system of photons, phonons, and excitons, but since explicit knowledge of the electronic states is impossible, most of these treatments are only useful for a formal understanding of the problem. For the first-order Raman effect, involving the creation (or destruction) of one phonon, there are several combinations of intermediate interactions between these three coupled systems that can contribute to the scattering; it is only of academic interest to examine the elementary processes individually. For most purposes (including the present work) it is possible to adopt a semi-classical approach in which the incident

light field is regarded as a classical source, and the details of the electronic states of the system are lumped into certain phenomenological constants that characterize the polarizability. The description of Raman scattering in terms of the polarizability is based on the early work of Born and Bradburn[125], and has been expanded into a very useful formalism by Xinh[47].

An incident light field of frequency ω_i will induce a polarization,

$$M_\alpha(t) = \sum_\beta P_{\alpha\beta}\left(\{\vec{u}_i(t)\};\ \omega_i\right) E_\beta(\omega_i) e^{-i\omega_i t} \qquad (4.1)$$

where the electronic polarizability tensor $P_{\alpha\beta}$ depends upon the positions of the ions $\vec{u}_i(t)$, and upon the frequency ω_i. It is tacitly assumed that the frequency of the exciting light ω_i is much less than the electronic transition frequencies, so that $P_{\alpha\beta}$ will be approximately independent of ω_i[25,47]. (E.g., a 6328 Å helium-neon laser corresponds to an exciting frequency of $\omega_i \sim 1.96$ ev., compared to about 6 ev. for the band gap in CaF_2). Furthermore, since the frequencies of electronic motion are so high, it is possible to regard the polarizability as a parametric function of the instantaneous positions of the nuclei. This "adiabatic approximation" is reasonable, because the vibrational frequencies are so low that the electronic system always sees, effectively, a static lattice with the ions in their instantaneous positions. Classically, it can be seen that the lattice vibrations will induce a frequency-mixing in the polarization $\vec{M}$ (Eq. (4.1)) when $P_{\alpha\beta}$ is expanded in terms of the displacements $\vec{u}(\ell\kappa,t)$, which were given by (2.65) in terms of the normal mode oscillators. In the treatment to be presented below, the vibrational part of the system shall be treated quantum mechanically.

The intensity per unit solid angle of the scattered radiation is given by[25,47],

$$I(\omega) = \frac{\omega_i^4}{2\pi c^3} \sum_{\alpha\beta\gamma\delta} n_\alpha n_\beta \, i_{\alpha\gamma,\beta\delta}(\omega) E_\gamma E_\delta^* \qquad (4.2)$$

where $\hat{n}$ is a unit polarization vector of the scattered radiation, and $\vec{E}$ is the (complex) amplitude of the electric field for the incident radiation. The scattering tensor $i_{\alpha\gamma,\beta\delta}(\omega)$ can be expressed as a Fourier transform of a correlation function of the electronic polarizability,

$$i_{\alpha\gamma,\beta\delta}(\omega) = \frac{1}{2\pi} \int_{-\infty}^{\infty} dt \, e^{i\omega t} \left\langle P_{\beta\delta}(t) P_{\alpha\gamma}(0) \right\rangle_T \qquad (4.3)$$

where $P_{\beta\delta}(t)$ is a Heisenberg operator. If $P_{\alpha\beta}(t)$ is expanded in terms of the nuclear displacements,

$$P_{\alpha\beta}(t) = P_{\alpha\beta} + \sum_{\ell\kappa\mu} P_{\alpha\beta,\mu}(\ell\kappa) \, u_\mu(\ell\kappa, t) + \ldots \qquad (4.4)$$

and substituted into (4.3), the first term of (4.4) will contribute to Rayleigh scattering, the second term to one-phonon Raman scattering, the next to second-order Raman scattering, and so on. For first-order RS,

$$i_{\alpha\gamma,\beta\delta}(\omega) = \sum_{\substack{\ell\kappa\mu \\ \ell'\kappa'\nu}} P_{\alpha\gamma,\mu}(\ell\kappa) \, I_{\mu\nu}(\ell\kappa, \ell'\kappa'; \omega) \, P_{\beta\delta,\nu}(\ell'\kappa') \qquad (4.5)$$

where

$$I_{\mu\nu}(\ell\kappa, \ell'\kappa'; \omega) = \frac{1}{2\pi} \int_{-\infty}^{\infty} dt \, e^{i\omega t} \left\langle u_\mu(\ell\kappa, t) \, u_\nu(\ell'\kappa', 0) \right\rangle_T \qquad (4.6)$$

and has been evaluated earlier (cf. Eq. (3.79)). Thus, the Raman scattering intensity $I(\omega)$ can be related, by means of the coupling coefficients $P_{\alpha\beta,\mu}(\ell\kappa)$, to the phonon displacement-displacement Green's function G, discussed earlier:

$$I(\omega) \sim [n(\omega)+1] \sum_{\substack{\ell\kappa\mu\,\ell'\kappa'\nu \\ \alpha\beta\gamma\delta}} P_{\alpha\gamma,\mu}(\ell\kappa)\, \mathrm{Im}\, G_{\mu\nu}(\ell\kappa,\ell'\kappa';\omega+i\varepsilon)\, P_{\beta\delta,\nu}(\ell'\kappa') \times n_\alpha n_\beta E_\gamma E_\delta^* \qquad (4.7)$$

Eq. (4.7) is a general result, valid for an arbitrary lattice, and if we define a column vector $p_\mu(\ell\kappa) = n_\alpha P_{\alpha\beta,\mu}(\ell\kappa) E_\beta$, it can be expressed in matrix notation as

$$I(\omega) \sim p\ \mathrm{Im}\, G(\omega+i\varepsilon)\, p \qquad (4.8)$$

For a <u>perfect</u> crystal, the coupling coefficients $P^{\circ}_{\alpha\beta,\mu}(\ell\kappa)$ are independent of the cell index ℓ, and will have certain symmetry properties determined by the group of operations that leave the crystal and the site κ invariant. The symmetry of each site κ determines the <u>form</u> of the tensors $P^{\circ}_{\alpha\beta,\mu}(\kappa)$, and provides one point of view for obtaining the selection rules for the first-order Raman effect. Since $P^{\circ}_{\alpha\beta,\mu}(\kappa)$ is a third-rank tensor, it follows that $P^{\circ}_{\alpha\beta,\mu}(\kappa)$ will vanish if κ is at a site with inversion symmetry. In particular, if <u>every</u> atom of a perfect crystal is a site of inversion symmetry, then all of the first-order coupling coefficients $P^{\circ}_{\alpha\beta,\mu}(\kappa)$ must vanish, and there can be no first-order allowed Raman spectra.

For a perfect crystal, the sum over all cell indices ℓ, ℓ', in (4.7) will serve to <u>project onto the $\vec{k} = 0$ modes</u>. Furthermore, it is only the

Raman-active modes that are selected, because of the structure of the coefficients $P^{o}_{\alpha\beta,\mu}(\kappa)$. To see this, we shall elaborate somewhat.

In order to treat a slightly more general situation, suppose that impurities are introduced into the crystal that do not significantly change the P^{o}-coefficients, but which do perturb the lattice dynamics; the phonon spectral density will then be characterized by a Green's function G. Then

$$I(\omega) \sim p^{\circ}\, \mathrm{Im}\, G(\omega+i\varepsilon)\, p^{\circ} = \mathrm{Im}\; p^{\circ} 1\, G(\omega+i\varepsilon)\, p^{\circ} \qquad (4.9)$$

where we have inserted the unit operator, 1, between p° and G. If we use the identity

$$1 = \frac{1}{\sqrt{N}} \sum_{\substack{\ell\kappa\mu \\ \vec{k}\sigma}} |\ell\kappa\mu\rangle\, e^{i\vec{k}\cdot\vec{R}_{\ell\kappa}}\, w_{\mu}(\kappa|\vec{k}\sigma)\langle\vec{k}\sigma| \qquad (4.10)$$

then we obtain

$$I(\omega) \sim \sum_{\substack{\ell\kappa\mu \\ \vec{k}\sigma}} e^{i\vec{k}\cdot\vec{R}_{\ell\kappa}}\, w_{\mu}(\kappa|\vec{k}\sigma)\; p^{\circ}|\ell\kappa\mu\rangle\langle\vec{k}\sigma|\, \mathrm{Im}\, G(\omega+i\varepsilon)\, p^{\circ} \qquad (4.11)$$

Since the coefficients $p^{\circ}|\ell\kappa\mu\rangle = p^{\circ}_{\mu}(\kappa)$ characteristic of a perfect lattice are independent of the cell index, the sum over ℓ in (4.11) can be carried out to produce $\delta_{\vec{k},0}$, which confirms the above assertion that there is a projection onto $\vec{k} = 0$. (Of course, the same thing happens on the RHS of G if a similar expression is inserted between G and p°.) Hence,

$$I(\omega) \sim \sum_{\kappa\mu\sigma} \left\{ p^{\circ}_{\mu}(\kappa)\, w_{\mu}(\kappa|\vec{k}=0,\sigma) \right\} \langle\vec{k}=0,\sigma|\, \mathrm{Im}\, G(\omega+i\varepsilon)\, p^{\circ} \qquad (4.12)$$

When the sum over κ is taken, the quantity in brackets will vanish for all but the Raman-active modes. We shall illustrate this for CaF_2, which has only the one Raman-active F_{2g} mode. Since Ca→Ca, F_1→F_2, and F_2→F_1 under inversion (about a Ca site), it follows that

$$P^{o}_{\alpha\beta,\mu}(Ca) = 0$$
$$P^{o}_{\alpha\beta,\mu}(F_1) = -P^{o}_{\alpha\beta,\mu}(F_2) \qquad (4.13)$$

For the $\vec{k} = 0$ F_{1u} modes in CaF_2, the fluorines all have the same displacements; for the F_{2g} Raman-active mode, the two fluorine sublattices have equal and opposite displacements. The κ-sum in (4.12) will therefore project only onto the $\vec{k} = 0$ F_{2g} Raman mode. In a crystal such as CaF_2, for which there is only one first-order Raman-active mode,

$$I(\omega) \sim \langle \vec{k}=0,\sigma_R \mid \mathrm{Im}\, G(\omega+i\varepsilon) \mid \vec{k}=0,\sigma_R \rangle \qquad (4.14)$$

This equation applies to situations where the impurities do not change the P-coefficients. For an imperfect crystal containing defects that differ considerably (in electronic structure) from the host atoms the replace, the coefficients $P_{\alpha\beta,\mu}(\ell\kappa)$ will not, in general, be the same as those for the pure lattice. In particular, they need no longer be independent of the cell index ℓ. Because translational symmetry is destroyed, it becomes possible to <u>induce</u> scattering from modes other than those at $\vec{k} = 0$. For example, this will be possible when impurities are added to a pure host which has no first-order allowed Raman effect. In the alkali halides, crystal symmetry demands that all $P^{o}_{\alpha\beta,\mu}(\kappa)$ vanish, because

every atom κ is at a center of inversion--there is thus no first-order RS allowed. The introduction of a defect--e.g., a U-center--will lead to a new set of quantities $P_{\alpha\beta,\mu}(\ell\kappa)$ which depend upon ℓ, since translational symmetry has been destroyed for every site except for that of the impurity center.

To calculate the RS intensity from a single defect by means of (4.7) would require knowledge of the perturbed Green's function $G(\omega+i\varepsilon)$ for <u>every</u> pair of lattice sites in the crystal. For a general defect problem, it would do little good to assume that the defect matrix v_o is highly localized if no restrictive assumptions are made for the polarizability coefficients $P_{\alpha\beta,\mu}(\ell\kappa)$. Xinh[47] has treated the problem of RS from U-centers in alkali halides by assuming that the defect induced P-coefficients are non-zero only in the localized subspace of the impurity, so that the sums over $(\ell\kappa)$ and $(\ell'\kappa')$ in (4.7) extend only over sites affected by v_o. Then, all that is required is $g(\omega+i\varepsilon)$, given by (3.43). For a perfect lattice containing only a small number of such impurities, there will be approximate local symmetry about a defect site. It is then possible to simplify the $P_{\alpha\beta,\mu}(\ell\kappa)$ to some extent by applying a reduced symmetry group of operations that leave the crystal, the defect, and the (nearby) site $(\ell\kappa)$ invariant. For a good discussion of the simplification of $i_{\alpha\gamma,\beta\delta}(\omega)$, $P_{\alpha\beta,\mu}(\ell\kappa)$, and other analogous quantities by symmetry considerations, reference can be made to the work of Xinh[47].

For a host in which there is a first-order allowed Raman line, the coefficients $P^{o}_{\alpha\beta,\mu}(\kappa)$ will not vanish, but will have a structure which projects onto the $\vec{k} = 0$ Raman mode. The introduction of impurities into such a crystal again may alter the structure of the P's in the vicinity of a defect, but the strongest part of the spectrum will continue to be

a central $\vec{k} \sim 0$ line. If we define $p = p^o + \delta p$, then in addition to the contribution (4.9) that results in a $\vec{k} = 0$ projection due to p^o, there may also be induced scattering from the fluctuation term δp:

$$I(\omega) \sim \mathrm{Im}\left[p^o G(\omega+i\varepsilon)p^o + p^o G(\omega+i\varepsilon)\delta p \right.$$
$$\left. \delta p\, G(\omega+i\varepsilon)p^o + \delta p\, G(\omega+i\varepsilon)\delta p \right] \qquad (4.15)$$

The important thing to be emphasized is that the spectrum of Raman scattering from phonons depends upon a combination of effects--lattice vibrational characteristics, and electronic polarizability. If the impurities differ mainly in mass or "spring constant" characteristics, but are not very different in electronic structure, it is reasonable to assume that the polarizability coefficients will not change, or will change only slightly. In any case, some assumptions about the electronic coupling of defects (in addition to those about the mechanical vibrational characteristics) must always be made if the Raman effect is to be used as a probe of the lattice dynamics of crystals containing impurities.

4.2 Infrared Absorption

There are several excellent references that treat the dielectric properties of matter. Stern[126] has given a review that covers the general field in great detail, and Martin[127] has discussed, in particular, the study of lattice vibrations by far infrared spectroscopy. Kubo[128], Cowley[51,52], Maradudin[1], Bilz[129], and many others[18,130,131] have used the Green's function point of view to treat the complex dielectric constant $\varepsilon(\omega)$, from which the absorption, reflectivity, and other quanti-

ties may be calculated. The review article by Maradudin[1] can be consulted for many references to work on impurity-induced infrared lattice absorption in crystals.

In the present situation, we are interested only in the infrared absorption from optical phonons, and shall not be concerned with electronic or other effects. We shall show how it is possible to express the frequency-dependent dielectric constant $\varepsilon(\omega)$ in terms of the phonon Green's function discussed earlier, just as was done for the Raman scattering intensity in the previous section. The reflectivity at normal incidence is usually the experimentally measured quantity, unless very thin samples are available for absorption measurements. The reflectivity can be obtained from

$$R(\omega) = \left| \frac{\sqrt{\varepsilon(\omega)} - 1}{\sqrt{\varepsilon(\omega)} + 1} \right|^2 \tag{4.16}$$

When far infrared radiation impinges on a crystal, it interacts strongly with only those transverse optical phonon modes near $\vec{k} = 0$ which possess an electric dipole moment. Although an accurate treatment of the interaction requires a redefinition of the normal modes of the total system of vibrations and radiation (cf. discussion in Sec. 6.2, §3) we can begin to discuss the problem in the limit that the electric dipole moment for these modes is vanishingly small. In such a process, energy is conserved, and the absorption of light energy is accompanied by the excitation of a phonon, but with no change in the electronic state of the system. The $\vec{k} \sim 0$ selection rule will be relaxed if impurities

are introduced into the crystal, and then light will be able to interact with other polar modes of the (imperfect) lattice. For a perfect crystal without phonon damping processes (i.e., in the harmonic approximation) the so-called reststrahlen bands are δ-function absorption peaks at the $\vec{k} = 0$ TO modes which have vector-like symmetry.

Assume that a (long-wavelength) light field, turned on adiabatically, interacts with the electric dipole moment $\vec{M}$ of a crystal lattice:

$$H' = - \vec{M} \cdot \vec{E} \exp(-i\omega t + \varepsilon t). \tag{4.17}$$

This perturbation is of the same form as that considered in Sec. 3.4, and leads to a response function $\chi_{\alpha\beta}(\omega)$ for $< M_\alpha(t) >$ which can be expressed (cf. Eq. (3.50), (3.51)) as the Fourier transform of the Green's function $G_r^{MM}(t)$ between two $\vec{M}$-operators:

$$< M_\alpha(t) >_T = \sum_\beta \chi_{\alpha\beta}(\omega)\, E_\beta \exp(-i\omega t + \varepsilon t),$$

where

$$\chi_{\alpha\beta}(\omega) = i \int_0^\infty dt \, \langle [M_\alpha(t), M_\beta(0)] \rangle_T \exp[i(\omega + i\varepsilon)t] \tag{4.18}$$

The electric dipole moment $\vec{M}$ can be expanded in terms of the ionic displacements,

$$M_\alpha(t) = \sum_{\ell\kappa\mu} \mathcal{M}_{\alpha,\mu}(\ell\kappa)\, u_\mu(\ell\kappa, t) + \frac{1}{2} \sum_{\substack{\ell\kappa\mu \\ \ell'\kappa'\nu}} \mathcal{M}_{\alpha,\mu\nu}(\ell\kappa, \ell'\kappa')\, u_\mu(\ell\kappa, t) u_\nu(\ell'\kappa', t) + \ldots \tag{4.19}$$

The first order coefficient (for the linear term) has the significance of representing an effective charge tensor, and for one-phonon absorption processes, this is the important term. Just as for the force constants $\Phi_{\alpha\beta}(\ell\kappa,\ell'\kappa')$ and the electronic polarizability coefficients $P_{\alpha\beta,\mu}(\ell\kappa)$, the coefficients $\mathcal{M}_{\alpha,\mu}(\ell\kappa)$ for the first order electric moment induced by lattice displacements will satisfy various symmetry conditions[47]. There will be the rigid-body conditions analogous to (2.13) and (2.14) for an arbitrary lattice, and the more stringent tensor transformation relations analogous to (2.28) for a perfect lattice. In some cases, it is also possible to invoke site symmetry about a defect, just as for the P-coefficients. If only the first order electric moment is retained, then insertion of (4.19) into (4.18) gives the one-phonon contribution to the far-infrared dielectric constant. The susceptibility $\chi_{\alpha\beta}(\omega)$ becomes

$$\chi_{\alpha\beta}(\omega) = \sum_{\substack{\ell\kappa\mu \\ \ell'\kappa'\nu}} \mathcal{M}_{\alpha,\mu}(\ell\kappa)\langle \ell\kappa\mu \,|\, G(\omega+i\varepsilon) \,|\, \ell'\kappa'\nu\rangle \mathcal{M}_{\beta,\nu}(\ell'\kappa') \quad (4.20)$$

For the perfect crystal, the coefficients $\mathcal{M}_{\alpha,\mu}(\kappa)$ are independent of the cell index ℓ, and because we have again summed over ℓ, ℓ' (just as in Eq. (4.7) and following discussion) the expression (4.20) will lead to a projection onto the $\vec{k} \to 0$ modes. However, the limit as $\vec{k} \to 0$ of the phonon Green's function is not uniquely defined for modes that have an electric moment (this is related to the fact that $D^{o}(\vec{k})$ has a term that looks like $(3\,\frac{\vec{k}\vec{k}}{k^2} - 1)$ as $\vec{k} \to 0$, which will be discussed in Sec. 6.2, §3). There will be a dependence upon the direction of approach, but only insofar as this direction fixes the definition of "longitudinal" and "transverse." The limiting <u>singularities</u> of G are well-defined, of course, but they are split

into transverse and longitudinal branches because of the macroscopic electric field that is associated with the longitudinal wave (this phenomenon is discussed in more detail in Sec. 6.2, §3). The susceptibility $\chi_{\alpha\beta}(\vec{k}\to 0,\omega)$ can, in fact, be expressed as[1]

$$\chi_{\alpha\beta}(\vec{k}\to 0,\omega) = \hat{k}_\alpha \hat{k}_\beta \, \chi^L(\omega) + \left[\delta_{\alpha\beta} - \hat{k}_\alpha \hat{k}_\beta\right] \chi^T(\omega) \qquad (4.21)$$

There are, therefore, two scalar susceptibilities, $\chi^T(\omega)$ and $\chi^L(\omega)$, which measure the response of the lattice to transverse and longitudinal electromagnetic fields, respectively. It is the former quantity that is of interest for the optical properties, since the electric moment vector $\vec{M}$ is coupled to a transverse electric (radiation) field in (4.17). It is only the <u>transverse</u> optic phonon modes that can contribute to the lattice absorption,

$$\frac{1}{2} < \vec{E}\cdot\dot{\vec{M}} > = \omega \, \mathrm{Im}\, \chi^T(\omega) \; |\vec{E}(\omega)|^2$$

and it will, moreover, be only the transverse lattice susceptibility $\chi^T(\omega)$ that contributes to the optical dielectric constant $\epsilon(\omega)$, which is used in (4.16) to calculate the reflectivity. In matrix notation, (4.20) would be written as $\chi_{\alpha\beta}(\omega) = \mathcal{M}_\alpha G(\omega+i\varepsilon)\mathcal{M}_\beta$, where the first order coefficients have been made into a column matrix $\mathcal{M}_\alpha$, with $< \ell\kappa\mu|\mathcal{M}_\alpha = \mathcal{M}_{\alpha,\mu}(\ell\kappa)$. For the situation where the coefficients $\mathcal{M}^0_{\alpha,\mu}(\kappa)$ are those of the perfect lattice, it will be only the transverse <u>IR modes</u> (as we would expect) that are selected by the sum in (4.19); we can insert a (matrix) factor $M_0^{-\frac{1}{2}}\cdot 1\cdot M_0^{\frac{1}{2}}$ between $\mathcal{M}^0_\alpha$ and G,

$$\chi_{\alpha\beta}(\omega) = \mathcal{M}^{\circ}_{\alpha}\, M_o^{-\frac{1}{2}} \cdot 1 \cdot M_o^{\frac{1}{2}}\, G(\omega+i\varepsilon)\mathcal{M}^{\circ}_{\beta}$$

and again use the identity (4.10) to obtain

$$\chi_{\alpha\beta}(\omega) \sim \sum_{\substack{\ell\kappa\mu \\ \vec{k}\sigma}} \mathcal{M}^{\circ}_{\alpha}\, M_o^{-1/2} |\ell\kappa\mu\rangle\, e^{i\vec{k}\cdot\vec{R}_{\ell\kappa}}\, w_{\mu}(\kappa|\vec{k}\sigma) \langle \vec{k}\sigma |\, M_o^{1/2} G(\omega+i\varepsilon)\mathcal{M}^{\circ}_{\beta}.$$

Because $\mathcal{M}^{\circ}_{\alpha}\, M_o^{-\frac{1}{2}} |\ell\kappa\mu\rangle = \mathcal{M}^{\circ}_{\alpha,\mu}(\kappa)/M_{\kappa}^{\frac{1}{2}}$ is independent of the cell index, we can again sum over ℓ to obtain a $\delta_{\vec{k},0}$, which accounts for the (LHS) projection onto $\vec{k} = 0$:

$$\chi_{\alpha\beta}(\omega) \sim \sum_{\kappa\mu\sigma} \left\{ \frac{1}{\sqrt{M_{\kappa}}}\, w_{\mu}(\kappa|\vec{k}=0,\sigma)\mathcal{M}^{\circ}_{\alpha,\mu}(\kappa) \right\} \langle \vec{k}=0,\sigma |\, M_o^{1/2} G(\omega+i\varepsilon)\mathcal{M}^{\circ}_{\beta}. \tag{4.22}$$

When the sum over ℓ is taken, the structure of the coefficients $\mathcal{M}^{\circ}_{\alpha,\mu}(\kappa)$ will have the effect of cancelling all but the optic modes with polar symmetry, since the expression in brackets is just the dipole moment of a unit cell generated in mode σ. The situation is, therefore, completely analogous to that for Raman scattering, where the sum (4.12) led to a projection onto the $\vec{k} = 0$ Raman mode. We shall again illustrate for CaF_2. Under inversion (about a Ca site), Ca → Ca, F_1 → F_2, and F_2 → F_1, and since $\mathcal{M}^{\circ}_{\alpha,\mu}(\kappa)$ is a second rank tensor, it will be even under inversion. Thus,

$$\mathcal{M}^{\circ}_{\alpha,\mu}(F_1) = \mathcal{M}^{\circ}_{\alpha,\mu}(F_2) \tag{4.23a}$$

and the tensor for Ca can be obtained from a relation that is the counterpart of the translation condition (2.13),

$$\mathcal{M}^{o}_{\alpha,\mu}(Ca) + 2\,\mathcal{M}^{o}_{\alpha,\mu}(F) = 0 \qquad (4.23b)$$

Eq. (4.23) is easily seen to hold if the effective charge tensors are assumed to be scalars--e.g., 2Ze for Ca, and -Ze for each F. (This is, in fact, what we shall assume in a rigid ion model to be discussed later for CaF_2.) In any case, Eq. (4.23a) demonstrates that the F_{2g} Raman mode does not contribute to (4.22), since for that mode (Ca stationary, and F_1 and F_2 with equal and opposite displacements), the expression in brackets in (4.22) vanishes. Likewise, (4.23b) shows that the acoustic mode (all displacements equal) cannot contribute either. (Cf. Eq. (2.71))

Notice that an extra (matrix) factor $M_o^{\frac{1}{2}}$ had to be included for the IR results--this is a consequence of the fact that the <u>displacements</u> in the $\vec{k} = 0$ modes are related to the vectors $\hat{w}(\kappa|\vec{k}\sigma)$ by an extra factor of $M_\kappa^{-\frac{1}{2}}$. It is actually the vector $M_o^{-\frac{1}{2}}\mathcal{M}^o$ (and not just $\mathcal{M}^o$) that projects onto the appropriate $\vec{k} = 0$ IR mode. Strictly speaking, for the same reason it would be necessary to include such a factor in the discussion of the Raman effect; however, it was omitted there because of our tacit intent to apply the formalism to the fluorites, for which $M_o^{\frac{1}{2}}|\vec{k}=0,\sigma_R\rangle = m_F^{\frac{1}{2}}|\vec{k}=0,\sigma_R\rangle$. (This relation is a consequence of the fact that only the fluorine masses are involved in the Raman mode for CaF_2.) For a more complicated structure, a factor $M_o^{\frac{1}{2}}$ would have to be included for the Raman result as well.

Eq. (4.20) is general, and holds for the phonon susceptibility for an arbitrary lattice. Much of the discussion that was given for the P-coefficients in Sec. 4.1 for RS applies here also. For example, if impurities are added to a perfect crystal lattice which has no one-phonon

absorption allowed, the relaxation of the $\vec{k} = 0$ selection rule by the defects can lead to induced infrared lattice absorption, if the defects have significantly different effective charge characteristics. To treat such problems, assumptions of localizability must again be made on the M-coefficients as well as on the mass and force constant characteristics.

In addition to the TO optical phonon contributions to the dielectric constant $\varepsilon(\omega)$, there will also be contributions from ultraviolet (electronic) absorption processes. In the far-infrared region, the frequency ω is so low that the latter processes contribute only a constant value, $\chi^e \sim (\varepsilon_\infty - 1)/4\pi$ to the total susceptibility (χ^e is the electronic susceptibility, and ε_∞ the high frequency dielectric constant). Thus, for crystals with only one IR-active mode, if we assume that the first order electric moment coefficients do not change,

$$\varepsilon(\omega) - \varepsilon_\infty \sim \langle \vec{k}=0,TO | \; M_o^{-\frac{1}{2}} \, G(\omega+i\varepsilon) \, M_o^{-\frac{1}{2}} \; | \vec{k}=0,TO \rangle \qquad (4.24)$$

We can verify that the result (4.24) holds for the perfect crystal if we insert the unperturbed Green's function, $G^o(\omega+i\varepsilon)$, which gives

$$\varepsilon(\omega) - \varepsilon_\infty = K \left\langle \vec{k}=0,TO \left| \frac{1}{(\omega+i\varepsilon)^2 - D^o} \right| \vec{k}=0,TO \right\rangle = \frac{K}{\omega^2 - \omega_{TO}^2 + i\varepsilon}$$

The constant K can be expressed as $K = -\omega_{TO}^2(\varepsilon_o - \varepsilon_\infty)$, where $\varepsilon(0) = \varepsilon_o$ is the static dielectric constant. Thus, we obtain

$$\varepsilon(\omega) = \varepsilon_\infty - \frac{\varepsilon_o - \varepsilon_\infty}{\omega^2 - \omega_{TO}^2 + i\varepsilon} \cdot \omega_{TO}^2$$

which is in agreement with the well-known result[25,179] for the disper-

sion of a (harmonic) lattice with one IR mode. Eq. (4.24) becomes, finally,

$$\varepsilon(\omega)/\varepsilon_\infty - 1 =$$

$$\left(1 - \frac{\epsilon_o}{\epsilon_\infty}\right) \cdot \omega_{TO}^2 \left\langle \vec{k} = 0, TO \,\middle|\, M_o^{1/2} G(\omega + i\varepsilon) M_o^{1/2} \,\middle|\, \vec{k} = 0, TO \right\rangle \quad (4.25)$$

V. DISORDERED SYSTEMS

5.1 Introduction

When a pure crystal lattice is altered by the introduction of a single substitutional impurity, many qualitative and quantitative results can be established with the Green's function techniques, provided that the "defect matrix" v_o for the impurity is localized. For many purposes, those effects which are induced by a small concentration c of point defects (e.g., impurity-induced RS or IR absorption) can be interpreted in the context of the isolated impurity problem. Xinh[47], Martin[130], and many others (cf. Maradudin[1]) have treated such problems by multiplying the results obtained for a single defect calculation by cN, the number of impurities present. For properties which exist originally in the perfect crystal, but which are modified by the addition of impurities, the situation is generally more complicated. For example, the effects of frequency shift or broadening of (existing) Raman or IR modes that results when a small finite concentration of impurities is introduced, cannot be explained so easily.

In many cases--e.g., the systems[2-22] that were discussed in Chapter I--two similar isomorphs which are mutually soluble and able to form homogeneous mixtures at large concentrations have been studied experimentally. In other cases, particular impurities may have electronic or chemical properties significantly different from those of the host atoms they replace, and it may not be possible to grow crystals with more than a trace amount of such impurities. For a situation where the concentration of impurities can be increased to finite amounts to form disordered crystals, the theoretical problems become more difficult. Many of the

properties of such mixed crystal systems will display features which cannot be simply explained by extrapolation from results for the single impurity problem.

When a finite concentration c of impurities is added to a host crystal, they will be distributed in some unknown way over cN sites throughout the lattice. The easiest mathematical assumption to make for the mixed crystal problem is that a random, disordered lattice is formed--i.e., that the probability that a given site contains an impurity atom is c, and a host atom, (1 - c). The impurities are regarded as replacing hosts in a perfectly random way, with the probability for the occurrence of an impurity (on any given site) that is uncorrelated with the presence of specific atoms on the neighboring sites. This assumption has been made in almost all of the theoretical work that has been done in this field.

Since Raman scattering and IR absorption can be related directly to certain Green's functions, the most logical approach to a theory of these effects in mixed crystals would be to extend the previous results to an average Green's function formalism. The average Green's function <G> for concentration c can be defined as a statistical ensemble average of the Green's function G (for cN impurity sites, given by (3.41)), over all possible configurations of a host lattice containing cN impurities. We shall pursue the average Green's function formalism further, after we give a brief survey of some of the other work in this field. For the study of the frequency spectrum (i.e., density of states) of a disordered lattice, there have been numerous other theoretical approaches, some of which have been quite different in their direction of attack. Maradudin[1] has reviewed many of these other methods in some detail. There has also been

much work on the application of the average Green's function method to electronic[68-82] and magnetic[83-89] systems, although we shall not discuss these topics here.

The earliest work on the frequency distribution of a disordered lattice was done by Dyson[132], who obtained a result (for a simple linear chain) in the form of a functional integral equation. His work was extended and simplified by Bellman[133], des Cloiseaux[134], and Englman[135], but these methods are formidable to apply, and unsuitable for numerical calculations. Schmidt[136] originated another method which also led to a solution in the form of a functional equation, but was unable to solve it except for certain limiting cases. Agacy[137], Hori and Asahi[138] Hori[139], and Mahanty[140] have also used Schmidt's method, and results have been obtained for a simple linear chain that agree with spectra computed by numerical methods. However, Schmidt's technique has not been extended beyond one dimension, and it has little usefulness for realistic problems. A "moment-trace" method has been developed by Maradudin et al[141], and by Domb et al[142], but because it is based on the assumption of a smooth spectrum, it is unable to account for some of the complicated effects that can occur at high frequencies.

Dean[143-5], Bacon[145,147], Martin[144,146], Rosenstock and McGill [148], and Payton and Visscher[149] have carried out exact (machine) calculations for simple models of 1-, 2-, and 3-dimensional lattices that were generated in a random manner. Their work has provided much useful information, both qualitative and quantitative, about certain striking features in the frequency spectrum of a disordered lattice. This work is valuable, because it can be used for a comparison of the exact results

(for a particular lattice) with those obtained by the average Green's function calculations. The latter are often limited in their validity because of the necessity of certain approximations, and the possibility of comparison with exact results in simple examples gives some general indications of where these approximations may be inadequate. The approach of these authors to the calculation of frequency spectra uses theorems about the roots of polynomials in a Sturm sequence; the resulting spectra are exact, and often reveal complicated structure at the high frequency ends. An example of this behavior (taken from P. Dean, Proc. Roy. Soc. A254, 507 (1960)) is shown in Fig. 5.1 for a 50-50 mixture of atoms, with a mass ratio of two, on a linear chain (of 64,000 atoms) with nearest-neighbor forces. The fine-structure can be interpreted as impurity bands corresponding to localized mode frequencies that characterize various types of clusters of the lighter atoms[143-5]. This figure also shows a comparison between the exact spectrum, and the results of a moment-trace calculation for the same system using the methods of Domb et al[142]. Dean[143] has shown how short-range or long-range order can be incorporated into the machine calculations for the simple linear chain; although the high frequency local mode region of the spectrum can be sensitive to a degree of order (compare the solid and dotted lines in Fig. 5.1), the low frequency end and the middle of the band are appreciably less sensitive, and depend mostly on the percentage composition. Rosenstock and McGill[148] and Dean and Bacon[145] have studied the form of all the exact normal modes of a short, randomly generated, linear chain, and have confirmed that the lower frequency modes are wave-like, and the higher frequency modes highly localized in

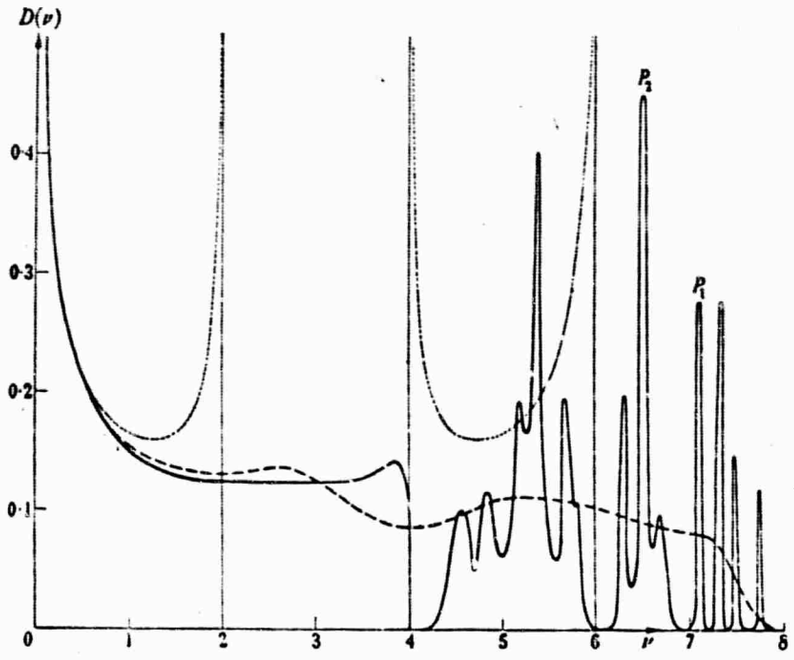

Fig. 5.1: Frequency distribution for isotopic, two-component linear chains (with mass ratio 2, and 50-50 mixture). The solid curve is for a completely disordered chain (generated for 64,000 atoms in a completely random manner), and was obtained by the machine calculations of Dean. The dashed curve represents a moment-trace calculation for the same system; the dotted curve is the distribution for an ordered linear chain. (This figure was taken from the work of P. Dean, Proc. Roy. Soc. A254, 507 (1960), Ref. 143.)

spatial character. Although all of these alternate approaches to the disorder problem have been involved only with the frequency distribution, they do suggest, if only qualitatively, the situations where caution may be necessary in the application of the average Green's function method, which will be described in more detail below.

The formulation of the theory of average Green's functions shall, in principle, be applicable for any concentration. In practice, however, the calculation of the proper self-energy function which arises presents a formidable obstacle, and except for rather simple, idealized problems, the best efforts to date have produced numerical results only to lowest order in the concentration c. Many authors have discussed problems of this kind using diagrammatic methods that are analogous to those used in field theory or in many-body problems. Langer[150], Poon and Bienenstock[151], Leath and Goodman[152], Takeno[153], Yonezawa and Matsubara [76], and others have approached the problem by expanding G in terms of G^{o} and V (cf. Eq. (3.41)); they obtain $\langle G \rangle$ as an expansion of "configuration averages" of the form $\langle G^{o}VG^{o}VG^{o}...VG^{o} \rangle$, and represent the terms in these summations pictorially by diagrams. The method of calculating the configurational averages is based on the cumulant expansion methods of Kubo[154], and involves the so-called "multiple occupancy" polynomials $F_n(c)$, discussed in detail by some of these authors[76,152]. These diagrammatic techniques are often cumbersome, usually requiring a degree of "bookkeeping" skill, and have been applied only to simple lattice models. The average Green's function $\langle G \rangle$ can, however, be obtained without recourse to diagrammatic methods[55,155,82]; in practice, it is much more straightforward to make use of the general expressions for $\langle G \rangle$. These approaches clearly demonstrate the relation between the random impurity problem and the isolated impurity problem. A number of results for simple models, which were obtained by previous authors using diagrammatic sums, have been obtained more easily[155].

Except for methods that attempt to introduce "self-consistency," the tacit assumption in all of the numerical calculations that have been done is that it is possible to expand the proper self-energy for the average Green's function in a power series in the concentration c. Because of the mathematical difficulties involved, even for non-"self-consistent" approaches, it is generally very tedious (even for simple models) to carry out calculations beyond first order in c. There have been some attempts to develop self-consistent theories that would be valid for treating problems with large concentrations of impurities. Yonezawa and Matsubara[76] have developed a self-consistent approximation suggested by diagrammatic considerations (replacing an unperturbed propagator by the actual propagator in a certain class of diagram sums). This method leads to an integral equation involving complicated matrix exponentials. Davies and Langer[156] appeal to general analyticity properties, and modify the original first order results of Langer[150] in an ad hoc way, again by replacing an unperturbed propagator by the actual propagator. Taylor[157] has recently developed a method, based on the multiple-scattering formalism of Lax[68], that leads to an infinite heirarchy of "conditional average" equations that must be terminated by an approximation. The average Green's function is expressed in terms of the propagator of an "effective field", rather than G^{o}; after an approximation is made to terminate the set of equations, the scattering matrix is set equal to zero as the criterion for the "best" approximation to the proper self-energy function. Velicky, Kirkpatrick, and Ehrenreich[82] have adopted a similar approach for a self-consistent theory for the electronic problem. All of the self-consistent theories for the vibrational problem

share the common disadvantage that their usefulness is limited to the simplest possible systems with mass changes only. When force constant changes must be included to adequately describe the defects, it becomes questionable whether it would be practical to develop the theory beyond first order in the concentration. Even to first order in c, calculations for the (relatively simple) $Ca_{1-c}Sr_cF_2$ system present a cumbersome computational task.

Taylor's calculations for the frequency spectrum of isotopically disordered three-dimensional systems at large concentrations are in good agreement with the results of machine calculations by Payton and Visscher. However, for small concentrations of light impurities, Taylor's method is not able to produce the spike structure at high frequencies that are attributable to local modes of defect clusters. As the concentration increases beyond certain finite amounts (the "critical percolation concentration"), one no longer has "isolated defect clusters." The spike structure displayed by the machine calculations tends to smooth out in the region of larger concentrations, and Taylor's results achieve better agreement. For low concentrations of heavy defects, Taylor's results agree well; the modes of defects and defect clusters are not isolated, and there is no complicated high frequency spike structure. His method is also somewhat better than that of Davies and Langer, for it is able to predict an impurity band (for light defects) that lies astride the local-mode frequency of a single mass defect. Although it is by no means obvious, some of the various self-consistent theories are related or equivalent. The connection between Taylor's method and that of Davies and Langer has been discussed recently by Leath[158]. He shows how these two methods can be viewed in terms of diagrams, and that although the two

methods sum the same diagrams, the latter authors' treatment does not properly compensate against multiple occupancy of sites by defects. A general discussion of these complications has also been given by Elliott et al[159]. Velicky et al[82] compare some of the self-consistent methods that have been applied to electronic properties of mixed crystals. Since we shall not be concerned with self-consistent methods in this work, we shall not discuss these topics further.

5.2 The Average Green's Function

We turn now to a discussion of the average Green's function formalism[155]. For a lattice with an arbitrary configuration of impurities, the Green's function G was expressed by (3.41) in terms of G^o and the defect matrix V,

$$G(\omega) = G^o(\omega) - G^o(\omega)V\left[1 + G^o(\omega)V\right]^{-1} G^o(\omega) \qquad (3.41)$$

and for a single isolated defect located at some site $i = (\ell_o, \kappa_o)$, this becomes

$$G_1 = G^o - G^o v_i \left[1 + G^o v_i\right]^{-1} G^o$$

where

$$v_i = \begin{pmatrix} \ddots & & \\ & \boxed{v_o} & \\ & & \ddots \end{pmatrix}$$

represents the defect matrix for the i^{th} impurity subspace, and has the form v_o that characterizes a single isolated defect.

Consider now the case where a single impurity is added not to a perfect lattice, but to one which already contains n = cN defects, all of the same type. If the Green's function for that particular distribution of cN impurities is denoted by $G(c,\gamma)$, where "γ" specifies the particular configuration of impurities, then

$$G(c,\gamma)^{-1} = (G^{o})^{-1} + V(\gamma) \tag{5.1}$$

If another impurity is added at a new site i, consistent with γ, then the Green's function for the lattice with cN + 1 = (c + 1/N)N defects becomes

$$G(c+1/N,\ \gamma')^{-1} = (G^{o})^{-1} + V(\gamma') = G(c,\gamma)^{-1} + \delta V(\gamma,i) \tag{5.2}$$

where γ' is the new configuration that results by adding a defect at site i to the existing configuration γ, and $\delta V(\gamma,i)$ is the change produced in the defect matrix. This equation can be written

$$G(c+1/N,\ \gamma')^{-1} =$$

$$G(c,\gamma) - G(c,\gamma)\delta V(\gamma,i)\left[1 + G(c,\gamma)\delta V(\gamma,i)\right]^{-1} G(c,\gamma)$$

If a "configuration average" is taken over all γ and i which are consistent with each other,

$$\langle G(c+\tfrac{1}{N})\rangle = \langle G(c)\rangle - \frac{1}{N}\langle G(c)\rangle f(c)\langle G(c)\rangle \qquad (5.3)$$

where

$$f(c) \equiv N\langle G(c)\rangle^{-1}\langle G(c,\gamma)\delta V(\gamma,i)\left[1+G(c,\gamma)\delta V(\gamma,i)\right]^{-1}G(c,\gamma)\rangle\langle G(c)\rangle^{-1} \qquad (5.4)$$

This average can, in principle, be carried out, although it has no usefulness for actual computation. As $N \to \infty$, (5.3) becomes

$$\frac{d}{dc}\langle G(c)\rangle = -\langle G(c)\rangle f(c)\langle G(c)\rangle \qquad (5.5)$$

which can be immediately integrated to cast the result for $< G(c) >$ into a standard form,

$$\langle G(c)\rangle^{-1} = (G^{\circ})^{-1} + F(c) \qquad (5.6)$$

where

$$F(c) = \int_{o}^{c} dc\, f(c) \qquad (5.7)$$

is called the "proper self-energy." This is the quantity that arises formally in many-body theory from a Dyson equation, which relates the actual propagator to the unperturbed propagator. Note that all of these quantities are a function of ω, but this dependence has been suppressed to simplify the notation.

The tacit assumptions have been made that $< G(c) >$ is differentiable, and that $f(c)$ is integrable. These assumptions are also inherent in the

(equivalent) iterative technique of diagram summation, since all the results for $< G >$ obtained by that method are also expressed as power series in c. The assumption is generally made that F(c) has a power series expansion about c = 0. (This need not necessarily be true--perhaps $F(c) \sim \sqrt{c(1-c)}$, for example.) Assuming that F(c) is analytic at c = 0, and using the fact that F(0) = 0, we can expand

$$F(c) = cf(0) + \frac{1}{2}c^2 f'(0) + \ldots \tag{5.8}$$

Eq. (5.5) can be used to express successive derivatives of f(c) in terms of the derivatives of $< G(c) >$. Since $< G(0) > = G^0$,

$$\begin{aligned} f(0) &= -(G^0)^{-1} \frac{d}{dc}\langle G(c)\rangle\Big|_{c=0} (G^0)^{-1} \\ f'(0) &= -(G^0)^{-1} \frac{d^2}{dc^2}\langle G(c)\rangle\Big|_{c=0} (G^0)^{-1} \\ &\quad + 2(G^0)^{-1} \frac{d}{dc}\langle G(c)\rangle\Big|_0 (G^0)^{-1} \frac{d}{dc}\langle G(c)\rangle\Big|_0 (G^0)^{-1} \end{aligned} \tag{5.9}$$

etc. The relationship between the multiple-impurity problem and the random disorder problem becomes apparent when the derivatives of $< G(c) >$ are automatically defined through the following heirarchy of expressions:

$$\begin{aligned} \frac{d}{dc}\langle G(c)\rangle\Big|_0 &= \lim_{N\to\infty} N\left[\langle G_1\rangle - G^0\right] \\ \frac{d^2}{dc^2}\langle G(c)\rangle\Big| &= \lim_{N\to\infty} N^2\left[\langle G_2\rangle - 2\langle G_1\rangle + G^0\right] \end{aligned} \tag{5.10}$$

etc., where $< G_n >$ is the multiple-impurity Green's function of (3.41) averaged over all possible configurations in which n impurities are present. Thus, for example,

$$\langle G_1 \rangle - G^\circ = - G^\circ \left\{ \frac{1}{N} \sum_i v_i (1 + G^\circ v_i)^{-1} \right\} G^\circ$$

$$\langle G_2 \rangle - G^\circ = - G^\circ \left\{ \frac{2}{N(N-1)} \sum_{i,j}{}' v_{ij} (1 + G^\circ v_{ij})^{-1} \right\} G^\circ \qquad (5.11)$$

etc. To lowest order in the concentration, the proper self-energy for $< G(c) >$ becomes $F(c) = cF^{(1)}(c)$, where

$$F^{(1)}(c) = \sum_i v_i \left[1 + G^\circ v_i \right]^{-1} \qquad (5.12)$$

Note that the sum over <u>sites</u> i is usually just a sum over the cell index ℓ with a fixed basis index κ_o. Of course, if some particular type of defect replaces an atom which can have several different basis indices (e.g., if an H^- replaces an F^- in CaF_2), a sum over κ_o will also be required. The equations to be developed are thus easily modified for that case.

There is an analogous equation for the proper self-energy associated with the average conjugate Green's function, $< H(c) >$, and in general, these proper self-energies are <u>not</u> the same. The corresponding "defect matrix" for H is given by $w_o = (i/\omega)(\Phi^\circ M_o^{-1} - \Phi M^{-1})$, and does not always have an "impurity subspace" that coincides with that for v_o. This will become apparent when a simple example is considered later.

The average Green's function $< G(c,\omega) >$ can be written

$$\langle G(c,\omega)\rangle^{-1} = G^{\circ}(\omega)^{-1} + F(c) = M_{\circ}\omega^2 - \Phi^{\circ} + F(c)$$

$$= M_{\circ}^{1/2}\left[\omega^2 - D^{\circ} + M_{\circ}^{-1/2} F(c) M_{\circ}^{-1/2}\right] M_{\circ}^{1/2} \qquad (5.13)$$

so that

$$M_{\circ}^{1/2}\langle G(c,\omega)\rangle M_{\circ}^{1/2} = \left[\omega^2 - D^{\circ} + M_{\circ}^{-1/2} F(c) M_{\circ}^{-1/2}\right]^{-1} \qquad (5.14)$$

We shall be interested in the function

$$\mathcal{F}(c) = M_{\circ}^{-1/2} F(c) M_{\circ}^{-1/2} \qquad (5.15)$$

which can be expressed in momentum space using the relation (2.62ℓ) given earlier. The sum over all sites ℓ in the expression (5.12) makes it immediately obvious that the first order term in the proper self-energy will be diagonal in $\vec{k}$. Denote the defect matrix v_i by $v_{\circ}(\ell,\kappa_{\circ})$, and assume that the substitutional impurities under consideration correspond to one (fixed) value of $\kappa_{\circ}$. Then the first order result $\mathcal{F}^{(1)}(\omega)$ is given by

$$\mathcal{F}^{(1)}(\omega)_{\vec{k}\sigma,\vec{k}'\sigma'} = \langle \vec{k}\sigma \,|\, M_{\circ}^{-1/2} F^{(1)}(\omega) M_{\circ}^{-1/2} \,|\, \vec{k}'\sigma'\rangle$$

$$= -\frac{1}{N}\sum_{\substack{\ell,\kappa_1,\alpha \\ \ell_2\kappa_2\beta}}{}' e^{-i\vec{k}\cdot\vec{R}_{\ell,\kappa_1}} \frac{1}{\sqrt{M_{\kappa_1}}} w_{\alpha}^{*}(\kappa_1|\vec{k}\sigma)\, e^{i\vec{k}'\cdot\vec{R}_{\ell_2\kappa_2}} w_{\beta}(\kappa_2|\vec{k}'\sigma') \frac{1}{\sqrt{M_{\kappa_2}}}$$

$$\times \sum_{\substack{\ell \\ (\kappa_{\circ}\ \text{fixed})}} \langle \ell,\kappa,\alpha \,|\, v_{\circ}(\ell,\kappa_{\circ})\left[1 + G^{\circ}(\omega) v_{\circ}(\ell,\kappa_{\circ})\right]^{-1} \,|\, \ell_2\kappa_2\beta\rangle \qquad (5.16)$$

The matrix element on the right is, of course, unaltered by a uniform translation of the site indices ℓ_1, ℓ_2, and ℓ by a lattice vector $\vec{R}_L$; in particular, we can translate by $-\vec{R}_\ell$ to obtain

$$< \ell_1\kappa_1\alpha|\ v_o(\ell,\kappa_o)\left[1 + G^o v_o(\ell,\kappa_o)\right]^{-1}\ |\ell_2\kappa_2\beta >$$

$$< \ell_1-\ell,\kappa_1\alpha|\ v_o(\kappa_o)\left[1 + G^o v_o(\kappa_c)\right]^{-1}\ |\ell_2-\ell,\kappa_2\beta >.$$

$v_o(\kappa_o)$ is just the defect matrix for an impurity in the $\ell = 0$ cell, and we shall abbreviate it as v_o. It then follows, from a uniform translation of the ℓ_1 and ℓ_2 summation indices in (5.16) by $-\vec{R}_\ell$, that

$$\langle \vec{k}\sigma\,|\,\mathcal{F}^{(1)}(\omega)\,|\,\vec{k}'\sigma'\rangle = e^{-i(\vec{k}-\vec{k}')\cdot\vec{R}_\ell}\langle \vec{k}\sigma\,|\,\mathcal{F}^{(1)}(\omega)\,|\,\vec{k}'\sigma'\rangle$$

which implies that $< \vec{k}\sigma|\,\mathcal{F}^{(1)}(\omega)|\vec{k}'\sigma' > = 0$, unless $\vec{k} = \vec{k}'$. Hence, $\mathcal{F}^{(1)}$ is diagonal in $\vec{k}$, and we can write $< \vec{k}\sigma|\,\mathcal{F}^{(1)}(\omega)|\vec{k}'\sigma' > = \delta_{\vec{k}\vec{k}'}\,\mathcal{F}^{(1)}(\vec{k},\omega)_{\sigma\sigma'}$. The sum over ℓ, which has not yet been taken, just cancels the factor N, since the translation of the ℓ_1 and ℓ_2 summation indices removed all of the ℓ-dependence. Hence,

$$\mathcal{F}^{(1)}(\vec{k},\omega)_{\sigma\sigma'} = \sum_{\substack{\ell\kappa\alpha \\ \ell'\kappa'\beta}} e^{-i\vec{k}\cdot(\vec{R}_{\ell\kappa}-\vec{R}_{\ell'\kappa'})}\, w^*_\alpha(\kappa|\vec{k}\sigma)\, w_\beta(\kappa'|\vec{k}\sigma') \times \frac{1}{\sqrt{M_\kappa}}\left\langle \ell\kappa\alpha\,\middle|\, v_o\left[1 + g^o(\omega)v_o\right]^{-1}\,\middle|\,\ell'\kappa'\beta\right\rangle \frac{1}{\sqrt{M_{\kappa'}}} \tag{5.17}$$

Inspection of the expressions (5.9)-(5.11) shows that the proper self-energy is diagonal in $\vec{k}$ to all orders in the concentration c, and since

G^o is diagonal in $\vec{k}$, the average Green's function $< G(c,\omega) >$ will also be diagonal. The mathematical process of averaging over all configurations has the important effect of restoring $\vec{k}$ as a good "quantum number," in a certain sense. The fact that $< G(c,\omega) >$ is diagonal in $\vec{k}$ is an expression of the translational invariance that an "average crystal" would be expected to possess; in fact, $< G(c,\omega) >$ will have all of the space group symmetry of the empty lattice. This is not to say that there are eigenmodes of the perturbed system with well-defined momentum $\vec{k}$; the random disordered crystal is defined by a configuration average over a large ensemble of systems, each of which is not periodic. An experiment which probes the crystal by exciting a disturbance of well-defined momentum $\vec{k}$ will, therefore, yield a spread in frequencies. Mathematically, this will be described by the imaginary part of the proper self-energy.

To illustrate the equivalence of the results of the differential and the diagrammatic techniques, and to demonstrate the relative ease with which (5.17) can be applied, we shall consider a simple example. Langer [150] has treated (using diagrams) the problem of a random, disordered chain of atoms with isotopic mass defects, bound by nearest-neighbor force constants. For the average Green's function $< G >$, the defect matrix is a simple scalar, $v_o = (m' - m)\omega^2$. The (one-dimensional) impurity subspace thus involves only one unperturbed Green's function,

$$g^o = \frac{1}{mN} \sum_k \frac{1}{\omega^2 - \omega_k^2}$$

and the first order proper self-energy can be immediately calculated from (5.17) to give

$$\mathcal{F}^{(1)}(k,\omega) = \frac{1}{m} v_o \left\{ 1 + g^o(\omega) v_o \right\}^{-1}$$

$$= \left(\frac{m'}{m} - 1 \right) \omega^2 \left\{ 1 + \left(1 - \frac{m'}{m} \right) \frac{\omega^2}{N} \sum_k \frac{1}{\omega_k^2 - \omega^2} \right\}^{-1}$$

which is independent of k. Langer, however, calculates the proper self-energy associated with the average conjugate Green's function < H(c) >. In that case, the form of the "defect matrix" is

$$w_o = (i/\omega)\, \Phi^o \left[M_o^{-1} - M^{-1} \right]$$

and even though only a simple mass change is involved, w_o is not a simple scalar, since the force-constant matrix Φ^o that appears on the left couples the nearest-neighbor sites. The impurity subspace for w_o is thus three-dimensional. However, $(M_o^{-1} - M^{-1}) = (1/m - 1/m')|0\rangle\langle 0|$ projects only onto the impurity site "0", and

$$w_o \left[1 + H^o w_o \right]^{-1} = \frac{i}{\omega} \Phi^o |0\rangle\langle 0| \left\{ \frac{\left(\frac{1}{m} - \frac{1}{m'} \right)}{1 + \left(\frac{1}{m} - \frac{1}{m'} \right) \langle 0 | M_o G^o(\omega) \Phi^o | 0 \rangle} \right\}$$

where we have used $(i/\omega)H^o(\omega) = M_o G^o(\omega)$. The proper self-energy for < H > becomes

$$\frac{\omega}{i} F^{(1)}(k,\omega) = \left\{ \frac{\left(\frac{1}{m} - \frac{1}{m'} \right)}{1 + \left(\frac{1}{m} - \frac{1}{m'} \right) \langle 0 | M_o G^o \Phi^o | 0 \rangle} \right\} \sum_\ell e^{-ik\ell} \langle \ell | \Phi^o | 0 \rangle$$

The matrix element $\langle 0|M_o G^o \Phi^o|0\rangle$ is obtained by multiplying

$$\Phi^{\circ} = \begin{pmatrix} 2\alpha & -\alpha & 0 \\ -\alpha & 2\alpha & -\alpha \\ 0 & -\alpha & 2\alpha \end{pmatrix} \quad \text{and} \quad G^{\circ} = \begin{pmatrix} g_0 & g_1 & g_2 \\ g_1 & g_0 & g_1 \\ g_2 & g_1 & g_0 \end{pmatrix},$$

where α is the spring constant (for nearest neighbors), and

$$g_0 = \frac{1}{mN} \sum_{k'} \frac{1}{\omega^2 - \omega_{k'}^2}$$

$$g_1 = \frac{1}{mN} \sum_{k'} \frac{\cos k'a}{\omega^2 - \omega_{k'}^2}$$

The dispersion relation for the unperturbed chain is given by

$$\omega_k^2 = \frac{2\alpha}{m}\left(1 - \cos ka\right) = \frac{4\alpha}{m} \sin^2 \frac{ka}{2}$$

and can be used to obtain

$$\sum_{\ell} e^{-ik\ell} \langle \ell | \Phi^{\circ} | o \rangle = m\omega_k^2$$

$$\frac{1}{m}\langle o | M_o G^{\circ} \Phi^{\circ} | o \rangle = \frac{1}{N} \omega^2 \sum_{k'} \frac{1}{\omega^2 - \omega_{k'}^2} - 1$$

After minor manipulations, the PSE associated with $\langle H \rangle$ becomes

$$- \frac{c\omega_k^2\left(1 - \frac{m'}{m}\right)}{1 - \left(1 - \frac{m'}{m}\right)\frac{\omega^2}{N} \sum \frac{1}{\omega_{k'}^2 - \omega^2}}$$

and agrees with the result of Langer's calculation. It is also possible to demonstrate that the second order calculation to order c^2 (using (5.11b)) agrees with that of Langer; since it involves slightly more algebra, it

will be omitted here. It is also possible to use this method to obtain (155) the one- and two-dimensional results of Poon and Bienenstock(151) for random spring constants.

Except for some of the self-consistent techniques, the numerical application of these average Green's function methods have been confined, even for the simplest models, to the approximation that the PSE can be expanded to the lowest order in the concentration c. For the frequency distribution function, comparisons can be made with the exact results obtained by Dean and others(143-149) in order to obtain some criteria for where the average Green's function approximations are valid. However, the complete spectral function $< G(c;\vec{k},\omega) >$ obviously contains much more information than the density of states, $<\rho(\omega^2)> \sim \text{Im Tr}\{<MG(\omega+i\varepsilon)>\} \sim \text{Im} \sum_{\vec{k}\sigma} <\vec{k}\sigma|<MG(\omega+i\varepsilon)>|\vec{k}\sigma>$. Since there have been no exact machine calculations (even for simple models) of the more <u>detailed</u> information contained in $< G(c;\vec{k},\omega) >$, no comparisons with exact results are possible in that case. Thus, the validity of many of the approximations that are required in practice to evaluate the average Green's function $< G(c;\vec{k},\omega) >$ are speculative, and there remain many open questions. However, it is possible to proceed with caution in order to avoid applying these approximations to situations where they are known to be inadequate for the calculation of the density of states. For example, an expansion of the PSE to first order in the concentration c would probably be a bad approximation in the vicinity of band edges, or in regions where there are localized mode impurity bands. Since the results to order c are related to the single impurity problem, those to order c^2 to the two-impurity problem, etc., it is possible that the exotic behavior that is known to characterize the density of states (and presumably, also the complete Green's

function $< G(c;\vec{k},\omega) >$) could be properly described if it were possible to carry out the PSE sum to all orders in c However, it is also possible (and indeed, more likely) that there may be a non-analytic dependence on c in these frequency regions, and that expansion in powers of c is not possible at all. There has recently been some work by Domb[142c] and Lifshitz[80,160] for certain artificial limiting cases in simple models (and again, only for the frequency distribution function) that suggests a non-analytic dependence on c.

The first order approximation in c is probably the most reliable for small concentrations of impurities that do not give rise to local modes. For defects that can produce these complicated impurity bands, the machine solutions show that an expansion in powers of c may be adequate to describe the behavior in low and intermediate frequency regions. Nevertheless, the validity of the expansion of the PSE to lowest order in c has often been assumed to apply for the entire frequency region. For disordered systems that do not involve changes in the P- or M-coefficients, Raman scattering and IR absorption are related to certain projections onto the average Green's function $< G(\vec{k} = 0,\omega+i\varepsilon) >$, according to the results of Chapter IV. (Cf. Eq. (4.14) and (4.24).) Thus, we can discuss both effects in a parallel way, and the general semi-qualitative remarks that follow could apply equally well to RS or IR. The evaluation of the average Green's function requires the PSE, which (to lowest order in c) will involve (according to (5.17)) certain projections onto $cv_o\left[1 + g^o(\omega+i\varepsilon)v_o\right]^{-1}$. If the first order PSE (different for RS and IR, of course) is denoted by $c\left[P_1(\omega) + iP_2(\omega)\right]$, then the denominator of the relevant $< G(\vec{k} = 0) >$ Green's function will have a structure of the form $\left[\ \omega^2 - \Omega_o^2 + c\{P_1(\omega) + iP_2(\omega)\}\ \right]$, where Ω_o

represents the $\vec{k} = 0$ Raman or IR mode frequency for the pure crystal. Thus, there will be a singularity at a frequency Ω_1, given by

$$\Omega_1^2 \sim \Omega_o^2 - cP_1(\Omega_o)$$

and Ω_1 will be shifted from Ω_o by $\sim \frac{1}{2}cP_1(\Omega_o)/\Omega_o$, and broadened by $\sim cP_2(\Omega_o)/\Omega_o$. In addition, $< G(c;\vec{k}=0,\omega+i\varepsilon) >$ may also exhibit a singularity near any local mode (or resonance mode) frequency ω_o produced by the $_o\left[1 + g^o(\omega+i\varepsilon)v_o\right]^{-1}$ structure of the first order PSE function. Fig. 5.2 shows a schematic example of a situation where the real part P_1 of the PSE becomes infinite at a local mode frequency ω_o; if it is assumed that the expansion of the PSE to first order in c is valid for all frequencies (in the low concentration limit), then the local mode frequency that shows up for the single impurity problem will also occur (slightly shifted) as a singularity in $< G(c;\vec{k}=0,\omega+i\varepsilon) >$ at ω_1. For very small concentrations ($c \ll 1$), this singularity at ω_1 (cf. Fig. 5.2) is approximately the local mode frequency, as would be expected. However, such a theory cannot predict a width to the

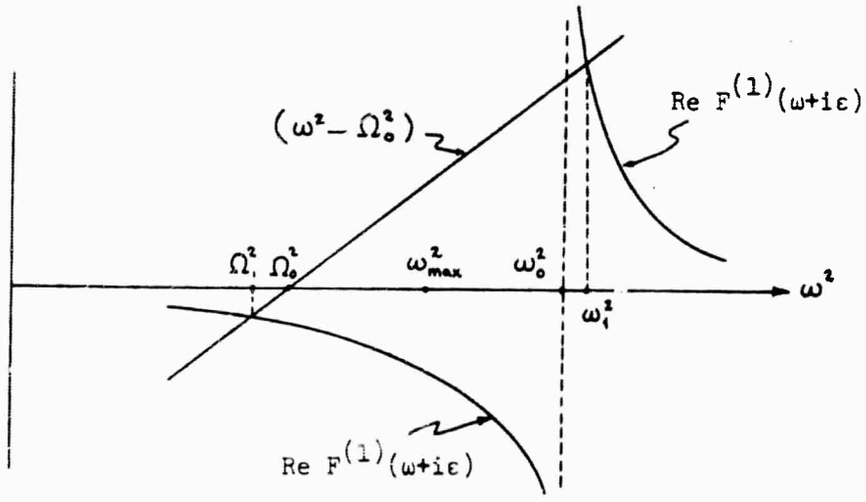

Fig. 5.2

mode at ω_1, since the imaginary part of the PSE, $P_2(\omega)$, vanishes outside of the unperturbed band of frequencies. In a self-consistent treatment, this would not be the case; self-consistency is able to provide the correct analyticity properties for the PSE--viz., a branch cut along the perturbed band, and along the impurity bands that form outside of the unperturbed band[156-8]. Xinh[47] and Maradudin[1] have done calculations on RS and IR absorption using a first order PSE that they assume to be valid in the local mode region, and also obtain singularities of the ω_1-type. This type of spectral behavior would thus seem to apply to the two-mode behavior observed in some mixed crystal systems[11-20], although the mathematical justification for assuming the validity of the first order approximation to the PSE in the high-frequency local mode region is unsubstantial.

For situations where local modes do not occur, and where $g^o v_o$ can be neglected compared to unity, there will be only the Ω_1 singularity for $< G(c;\vec{k}=0,\omega+i\varepsilon) >$. In that case, we obtain the "virtual crystal approximation" which accounts for the one-mode behavior[2-10] in which a single optic frequency shifts linearly with concentration.

VI. THE MIXED-FLUORITE SYSTEMS

6.1 Introduction

For many years since 1928, when Raman scattering was first reported by C. V. Raman[161], experimental work in this field has been carried out using mercury discharge lamps for the exciting radiation, with photographic detection of the spectra. Because Raman scattering intensities are typically very low, intense light sources are required, and long exposure times necessary. The numerous experimental difficulties involved made this type of work somewhat unappealing, and placed some limitations on the type of effects that could be studied. The development of laser light sources, which have the advantages of monochromaticity, high intensity, high collimation, and plane polarization, provided exactly what Raman spectroscopy badly needed and has led to a rebirth of interest in this field in recent years. The use of lasers makes it possible to study low-temperature effects and polarization effects easily. A further impetus for the renewed experimental interest in Raman scattering has been provided by modern electronic developments that have made it possible to streamline the detection system; we shall presently describe what we believe to be a relatively sophisticated photon-counting technique (using a multi-channel analyzer) that we have used to measure the spectra. When this work was originally reported[2], it was the first time that such a detection system had been used for Raman spectroscopy, although others have most likely used similar methods in allied fields.

We have studied experimentally[2] the Raman scattering from the mixed crystal systems $Ca_{1-x}Sr_xF_2$ and $Ba_{1-x}Sr_xF_2$ for a variety of concentrations

from x = 0 to x = 1. These crystals, which have long been known to form continuous solid solutions[162-4], were obtained from Optovac, Inc. A block diagram of the basic setup which we used to measure right angle scattering in these systems is shown in Fig. 6.1. All of the major equipment, except for a low-temperature He-dewar and an electronic control device that was used to regulate the spectrometer scan (described below), was obtained commercially. The light source used was a Spectra Physics Model 116 helium-neon gas laser, which we operated at 6328 Å, with a typical power output of ∿ 25 milliwatts. The laser light source was focused at the center of the crystal sample, and a dielectric-coated spherical mirror with high reflectivity at 6328 Å was used to reflect the emergent laser light back through the crystal. This forms an "external cavity" with the laser, and the purpose of this trick was to increase the effective light intensity in the sample by using multiple passes of the beam. In practice, this increased the output intensity of the scattered radiation by about a factor of two. The use of this method is not possible if it is desired to make high precision polarization measurements, since the several reflections would probably destroy the plane polarization characteristic of the exciting radiation into the sample. A double prism arrangement (cf. Inset, Fig. 6.1) produced a vertical line source, which is imaged onto the entrance slit of a 1-meter Jarrell Ash, Model 78-420 spectrometer. Because the systems that we studied exhibit first order Raman frequency shifts on the order of ∿ 300 cm^{-1}, the separation from the laser line is far enough that the problem of extraneous scattering in the spectrometer can be eliminated using a dielectric interference filter at the entrance slit to reject the laser light. We used a step-function filter that rejected 6328 Å

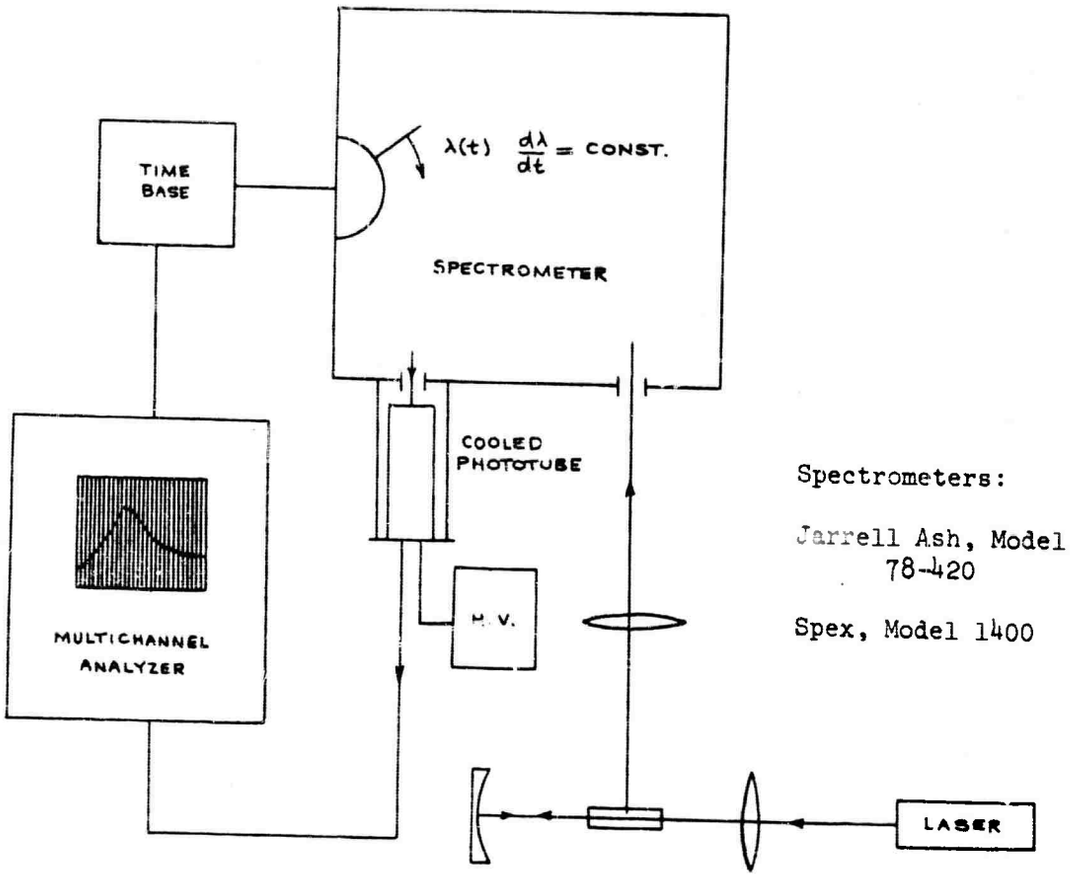

Spectrometers:

Jarrell Ash, Model 78-420

Spex, Model 1400

Nuclear Chicago RIDL, Model 34-12B 400-channel analyzer

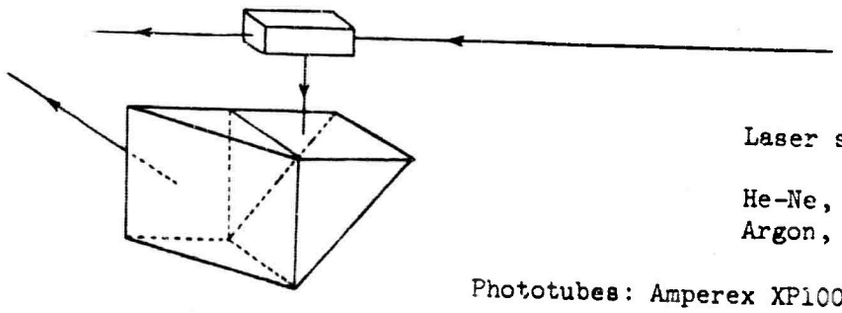

Laser sources:

He-Ne, 6328 Å
Argon, 4880 Å

Phototubes: Amperex XP1002; EMI 9558

Fig. 6.1: Block diagram showing experimental setup for measurement of right-angle Raman scattering.

light by $\sim 10^{-3}$, and passed at $\sim 80\%$, with essentially flat response, light shifted by $\gtrsim 250\ cm^{-1}$.

The method of detection involved photon counting; an Amperex XP1002 phototube (which has an S-20 response) was used at the exit slit of the Jarrell Ash. Signal pulses from the phototube were fed into a Nuclear Chicago RIDL Model 34-125 multi-channel analyzer. This instrument is used in the "time base" mode of operation: all of the pulses that arrive from the phototube, in a selected interval of time, are counted and stored sequentially in 400 channels. The spectrometer is equipped with a motor drive that is capable of scanning the spectrum at selected discrete speeds, and the RIDL channel width is also variable with discrete values (typically, we used a channel width of 1 or 2 seconds). The phototube was housed in an assembly that permitted it to be cooled to a low temperature by blowing cold N_2 gas, boiled off from a liquid nitrogen dewar, over the cathode. Operation of the tube at lower temperatures decreases the problems of dark current from thermionic emission.

In order to improve signal-to-noise characteristics, it is often desireable to scan the same spectral range over and over, and add up the results. This can be done easily with the RIDL, since it is capable of adding a new spectrum to one already stored in its memory. An electronic and mechanical control device (designed at Harvard) was used to regulate this multiple scan feature. The details of this mechanism are rather involved, and it is unnecessary to give more than this operational description of how it worked. With multiple scanning of a spectrum, it was possible to obtain very good signal-to-noise; Fig. 6.2 shows a typical Raman spectrum (in this case, taken for $Ca_{.4}Sr_{.6}F_2$) taken at room temperature. With ten

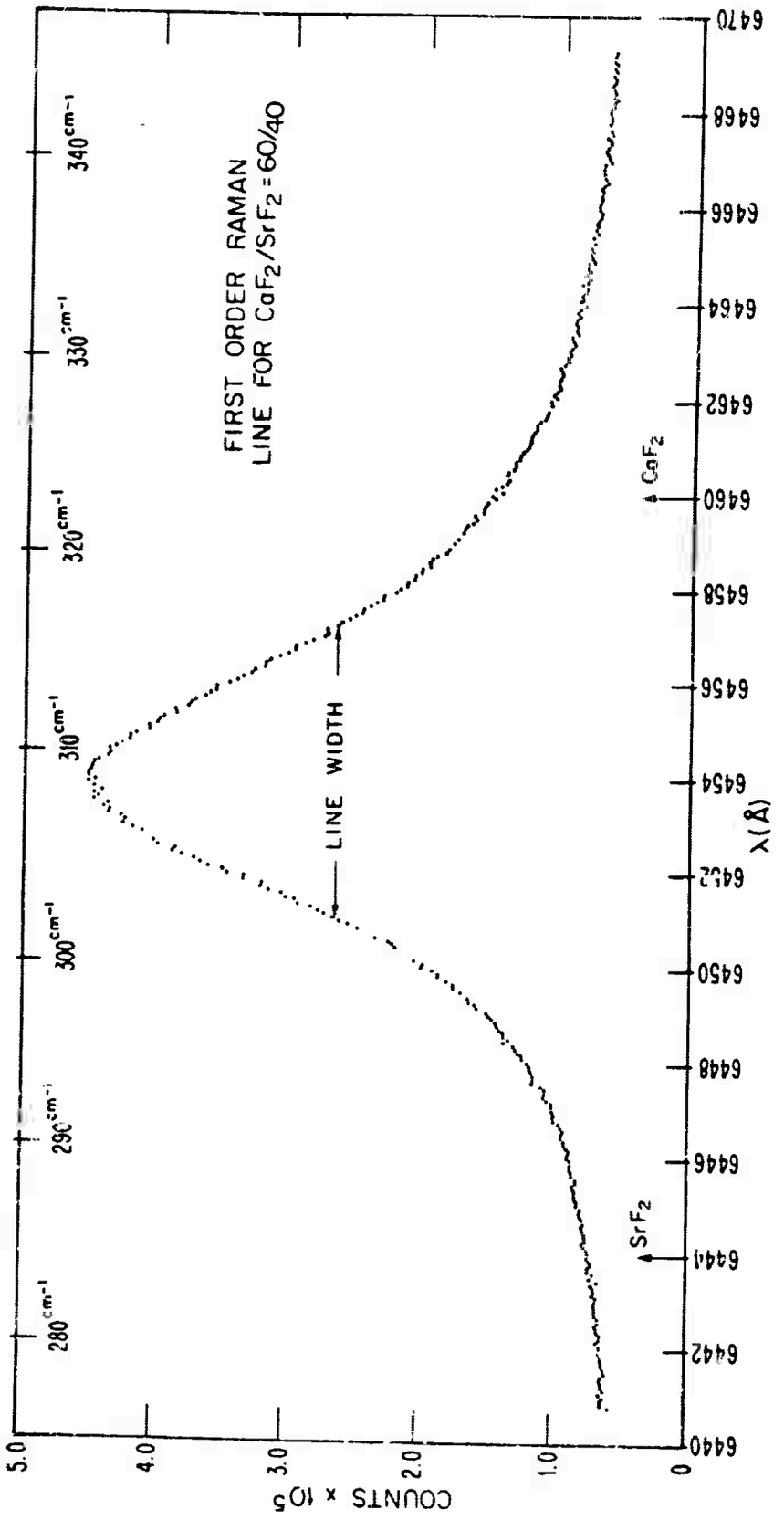

Fig. 6.2: A typical Raman spectrum (in this case, for Ca/Sr = 60/40, at room temperature) using the multichannel analyzer for detection (ten sweeps).

passes over the spectral range. The use of a multi-channel analyzer and the photon counting technique provides a method by which very clean data can be obtained. Furthermore, the time required to produce a spectrum such as that shown in Fig. 6.2 (with ten passes) would be only about two hours (assuming 2 second widths for the RIDL). Compared with the long exposure times required by photographic techniques, this is a definite advantage. However, the usefulness of this method is decreased if it is necessary to observe a spectrum over large wavelength intervals, for which correspondingly more time would be required. Fig. 6.2 covers a total range of ~ 30 Å or ~ 75 cm^{-1} (at 6328 Å). The low temperature measurements carried out at 6328 Å were obtained using a (Harvard built) cold-finger He dewar.

Later measurements were taken on a similar setup, which included a Spex model 1400 double monochrometer, an ionized argon laser (operated at 4880 Å with $\sim$ 200 mw.) built at Harvard, and a Janis Super Vari-Temp (Model 10DT) He gas-cool dewar. The phototube, which was again cooled, was an EMI 9558, with an S-20 response. The Spex double monochrometer significantly reduced the problem of extraneous scattering, so it was not necessary to use a dielectric filter for eliminating the laser line when this apparatus was used. Furthermore, the multiple-reflection cavity was not used in this case, since the argon laser intensity was significantly higher than that of the helium-neon laser.

The experimental results for the $Ca_{1-x}Sr_xF_2$ and $Sr_{1-x}Ba_xF_2$ mixed crystal systems are shown in Fig. 6.4 and Fig. 6.5; the first order $\vec{k} \sim 0$ Raman line shifts linearly with concentration, with an integrated intensity that remains approximately constant, and with a linewidth that in-

creases and peaks near the 50-50 mixture. Because Raman scattering is such a weak effect, it was necessary to use relatively large spectrometer slit openings for studying these systems. (For the Jarrell Ash spectrometer and 6328 Å laser, $\sim 3.9\ cm^{-1}$, and for the Spex spectrometer and the 4880 Å laser, $\sim 1.6\ cm^{-1}$.) In order to obtain linewidth results, it is then necessary to convolute the observed line profiles with the "slit function", which can be inferred from an observation of the laser line with the same slits. Theoretically (for curved slits, or for straight slits with small vertical aperture) the slit function should be a triangle. In practice, the slit function for the Jarrell Ash data had a small top, and that for the Spex (with straight slits) had a small tail on one side. Assuming that the slit function is approximately trapezoidal, as shown in Fig. 6.3 below, the convolution of the slit function $S(\omega)$ with a Lorentzian line,

$$\mathcal{L}(\omega) = \frac{\Gamma}{2\pi}\int_{-\infty}^{\infty} d\omega' \frac{S(\omega')}{(\omega'-\omega)^2+\Gamma^2/4}$$

becomes

$$\mathcal{L}(\omega) = g(\omega) + g(-\omega),$$

where

$$g(\omega) = \frac{1}{\pi}\left\{ \tan^{-1}\frac{2(A-\omega)}{\Gamma} + \tan^{-1}\frac{2\omega}{\Gamma} + \left(1-\frac{\omega-A}{B}\right)\left[\tan^{-1}\frac{2(A+B-\omega)}{\Gamma} + \tan^{-1}\frac{2(\omega-A)}{\Gamma}\right]\right\} - \frac{\Gamma}{4\pi B}\log\frac{(A+B-\omega)^2+\Gamma^2/4}{(A-\omega)^2+\Gamma^2/4}.$$

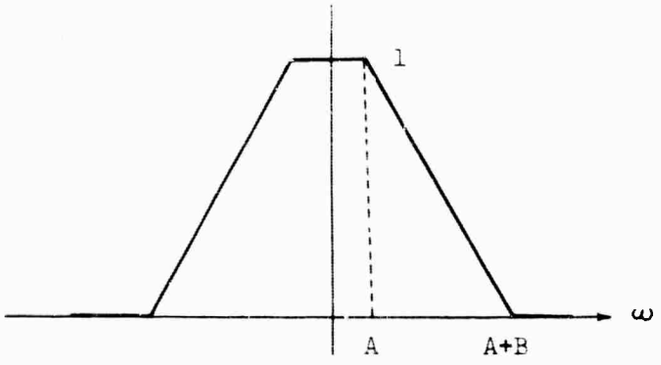

Fig. 6.3: Trapezoidal slit function, $S(\omega)$

For any selected values of A and B, one can compute, numerically, a table of observed full-widths versus Γ, which represents the "true width" for (an assumed Lorentzian) process. It is important to note that it is not possible to merely subtract the instrumental width from observed widths when the slits are opened wide.

The low temperature ($\sim 4^{\circ}$ K) linewidth data was taken using both the 6328 Å and 4880 Å lasers, and after the appropriate convolutions, the results of the two sets of measurements were reasonably consistent (cf. Fig. 6.5). Taking into account the experimental error involved in reading the date, as well as that for the convolution process, these values are probably accurate to about $\pm$ .3 cm^{-1}, with a systematic discrepancy of $\sim$ .3 cm^{-1} in the two sets of measurements. Taking into consideration the fact that the two sets of data were taken at different times and with completely different experimental equipment, a systematic error of that magnitude does not seem too large. However, the source of that systematic error is most likely in the assumptions made for the shape of the slit function, which could easily lead to a systematic error of that magnitude when the two sets of data are reduced by convolutions with different slit functions.

Although it is possible that excitation with 4880 Å or 6328 Å could produce different linewidth results, it is unlikely that this discrepancy is a real effect. H. Goldberg (private communication) has carried out the convolution for the 6328 Å measurement of $Ca_{.98}Sr_{.02}F_2$ by an independent procedure, and obtains $\sim 1.6\ cm^{-1}$, which is consistent with the present results. These considerations suggest that the origin of the systematic error is probably related to the convolution process.

Some data was also taken at liquid nitrogen temperature, and within the experimental error, the results for the shifts and linewidths were about the same at $\sim 4^{o}K$ and $\sim 77^{o}K$.

The theory of the $Ca_{1-x}Sr_xF_2$ mixed crystal that is discussed later in this work is only able to predict the contribution of disordering to the linewidth; since it is only the change in linewidth with concentration that concerns us here, the possible discrepancy of $\sim .3\ cm^{-1}$ between the two sets of data (at $4^{o}K$) is not relevant. The dashed line of Fig. 6.5 is the result of a numerical calculation to be described later.

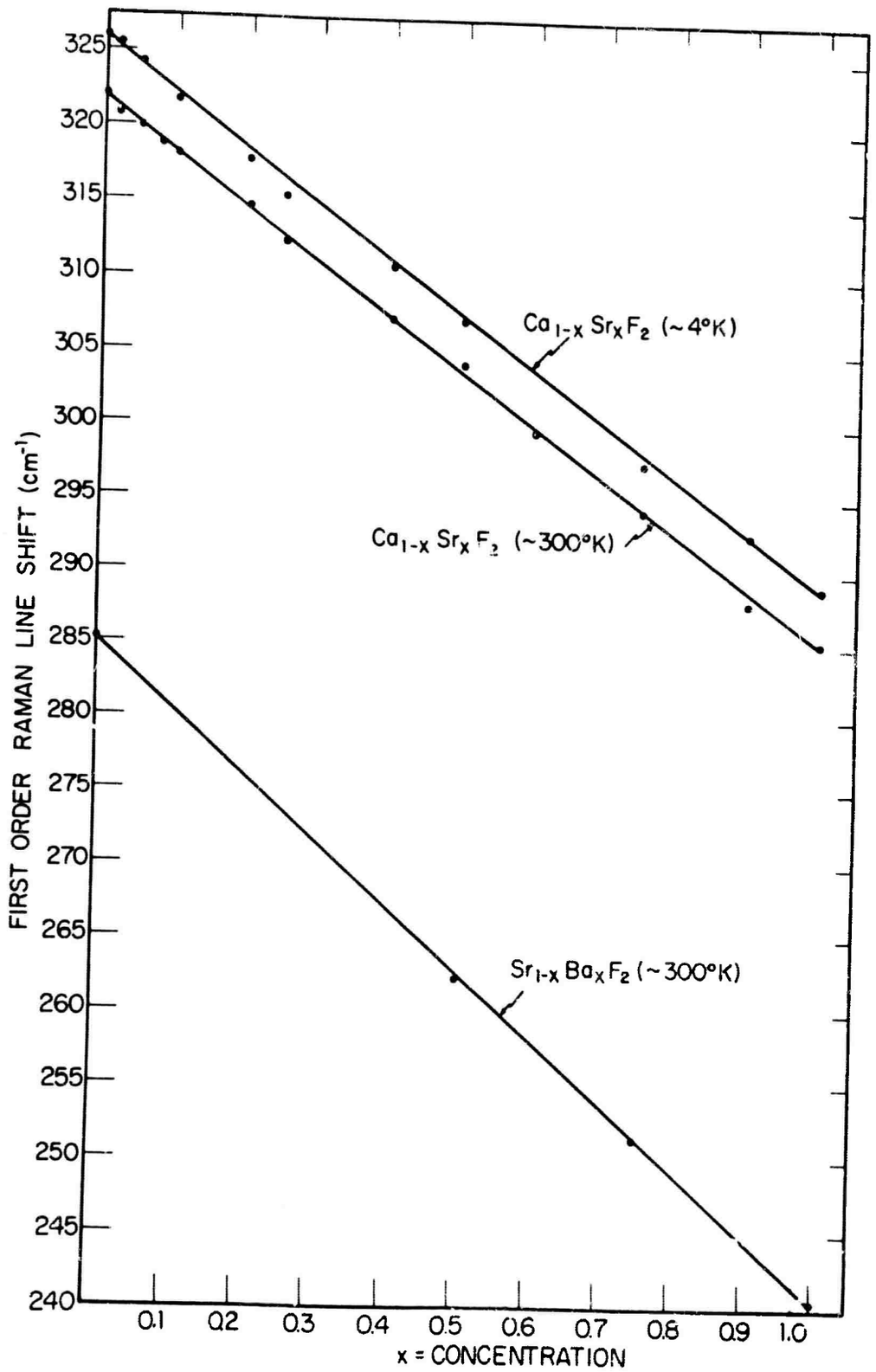

Fig. 6.4: First order Raman line shifts for $Ca_{1-x}Sr_xF_2$ and $Sr_{1-x}Ba_xF_2$

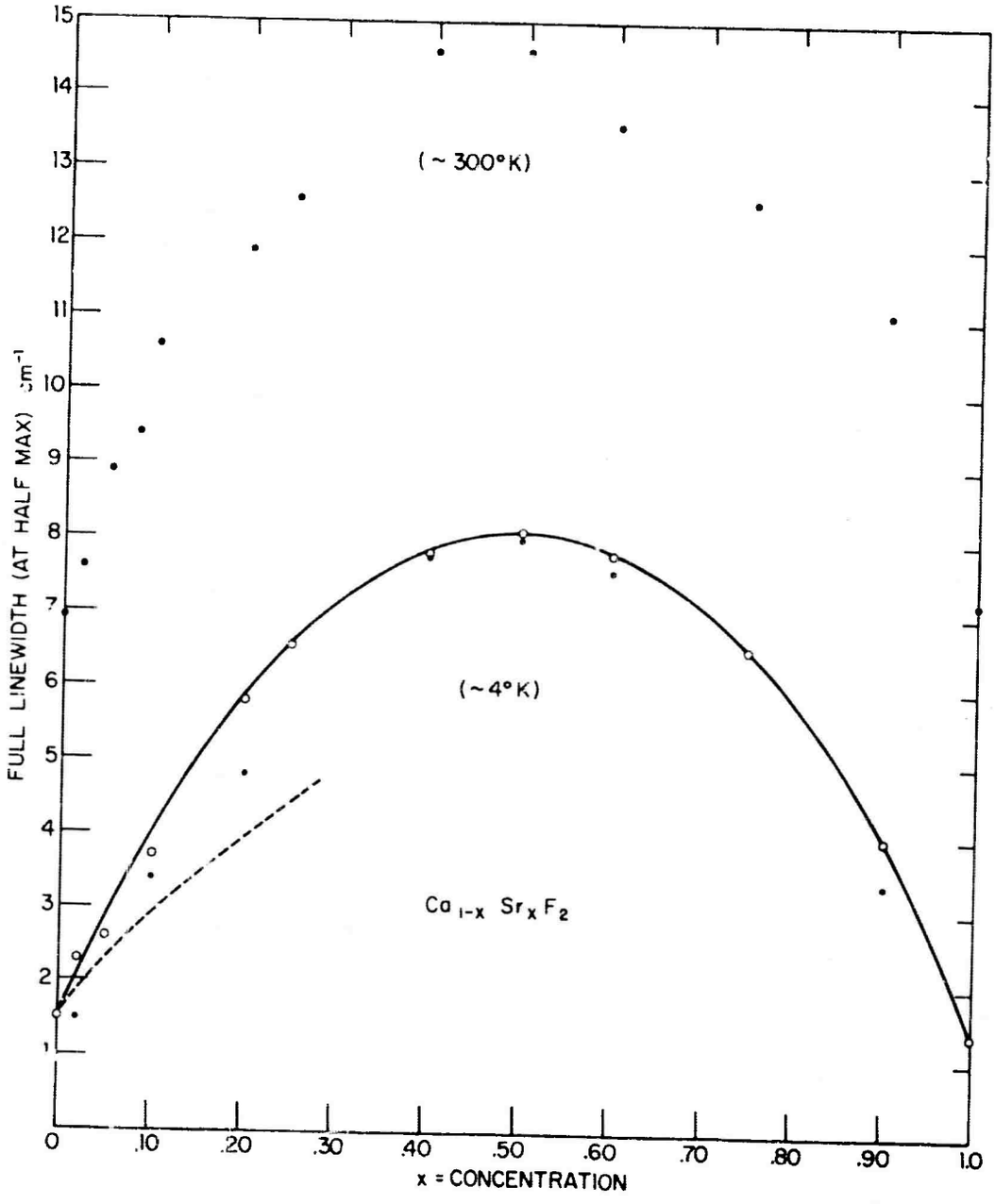

Fig. 6.5: Experimental and theoretical (full) linewidths (at half max) for the $Ca_{1-x}Sr_xF_2$ system. Experimental points are the actual widths after convolution; dashed line is theoretical. Open circles correspond to 4880 Å, Spex data, and closed to the 6328 Å, Jarrell Ash measurements.

6.2 The Rigid Ion Model for CaF_2

In order to calculate the phonon Green's functions that were involved in the preceding mathematical treatment of the isolated defect or random disorder problems, it is necessary to have knowledge of the phonon eigenfrequencies $\omega_{\vec{k}\sigma}$ and eigenvectors $\hat{w}(\kappa|\vec{k}\sigma)$ throughout the first Brillouin zone for the unperturbed (perfect) lattice. These quantities shall be evaluated using a "rigid ion" model, due to Ganesan and Srinivasan[165], for the fluorite lattice. In this idealized model, the (ionic) CaF_2 crystal is regarded as consisting of a lattice of rigid, non-polarizable ions which interact through long-range electrostatic and short-range repulsive forces. The short-range interaction terms, whose physical origin is a repulsion between overlapping electronic distributions, fall off rapidly with distance, and are included only for nearest neighbors in this model. The Coulomb forces between ions are assumed to be electrostatic interactions between rigidly spherical charge distributions (i.e., "point" charges) that are multiples of an effective electronic charge, Ze. The polarizability of the ions cannot be properly taken into account with this model, however.

It would, perhaps, be more sophisticated to use a "shell model"[169-72] for the calculations; in that case, the ions of the lattice would be assumed to consist of positively charged massive cores surrounded by massless and negatively charged spherical shells. In the simplest approximation, the cores and shells would be assumed to be coupled by a scalar, isotropic force constant. As the lattice vibrates, the shell and core would be assumed to retain their rigid spherical shapes, although it would be possible to generate a dipole moment on the ion when the shell and core

are relatively displaced. Two equations of motion would be necessary for the (coupled) system of cores and shells, and the computational labor would be increased. Alternatively, the rigid ion model would probably be improved by the inclusion of more than nearest-neighbor short-range forces. In addition to increasing the computational difficulties, both of these attempts to improve the model have one common disadvantage: they require an increase in the number of force constant parameters, and there is only a limited amount of experimental data available that can be used to fix these phenomenological constants. A more complete description of the physics of the rigid ion model, and the successes it has for predicting various experimental quantities, can be found in the original sources[165-8]. Many of the formal details that are relevant to the present calculation of phonon eigenfrequencies and eigenvectors are omitted in the work of Ganesan and Srinivasan[165], and shall be described in more detail here.

The ultimate aim--the numerical calculation of some of the phonon Green's functions $G^{o}_{\alpha\beta}(\ell\kappa,\ell'\kappa';\omega+i\varepsilon)$ given by (3.32) - (3.37), requires a good model for the pure CaF_2 lattice dynamics. The accuracy of these calculations <u>may</u> be impaired by one difficulty that cannot be simply remedied in either the rigid ion model or the shell model. Namely, the harmonic approximation itself may be inadequate to describe the unperturbed modes of pure CaF_2 no matter which of these models is used, or how detailed the force constant assumptions may be. It is possible that anharmonic interactions are not completely negligible, and that each of the modes of the pure lattice will have a broadened frequency. This could have the effect of smearing out some of the structure in $G^{o}(\omega+i\varepsilon)$, or perhaps even of altering the results more drastically. There are, in fact, indications from

the infrared reflectivity spectra of pure CaF_2 that the harmonic approximation is now completely adequate to describe the modes of CaF_2 accurately. The inclusion of the effects of anharmonic broadening would require that we abandon most of the simplifying features of the harmonic approximation, and would lead to a complicated many-body problem. To make this improvement in the formalism would not be a trivial matter; to include anharmonic effects properly, it is necessary to work with a coupled heirarchy of Green's function equations, as we mentioned earlier. Phenomenologically, we could, perhaps, extend Eq. (3.28) by including a damping term in the equation of motion (2.12) for the pure lattice dynamics. I.e.,

$$\sum_{\ell'\kappa'} \left[M_\kappa \delta_{\ell\ell'} \delta_{\kappa\kappa'} \overleftrightarrow{1} \frac{d^2}{dt^2} + \overleftrightarrow{\Gamma}_o(\ell\kappa, \ell'\kappa') \frac{d}{dt} + \overleftrightarrow{\Phi}^o(\ell\kappa, \ell'\kappa') \right] \cdot \vec{u}(\ell'\kappa', t) = 0 \tag{6.1}$$

which would lead to

$$G_r^o(\omega)^{-1} = (M_o \omega^2 - \Phi^o) + i\omega\Gamma_o \tag{6.2}$$

The resulting secular equation,

$$\det \left[(\omega^2 - \omega_{\vec{k}\sigma}^2) \delta_{\sigma\sigma'} + i\gamma_{\sigma\sigma'}(\vec{k})\, \omega \right] = 0, \tag{6.3}$$

where

$$\gamma_{\sigma\sigma'}(\vec{k}) = \langle \vec{k}\sigma \,|\, M_o^{-1/2} \Gamma_o M_o^{-1/2} \,|\, \vec{k}\sigma' \rangle \tag{6.4}$$

is a 9×9 matrix that would define the broadening of the phonon modes at any wave vector $\vec{k}$. There is, however, no obvious way of obtaining the form of γ from data available for the crystal; the experimentally available

parameters give very little detailed information about the broadening of phonon modes throughout the Brillouin zone. Without going into detail, it is instructive to make the observation here that a formal quantum mechanical treatment of the anharmonic crystal[52] could be represented by a Dyson equation that relates the actual Green's function (propagator) of the pure crystal to the harmonic Green's function and a proper self-energy function $\Pi(\omega)$:

$$G^{o}_{actual} = G^{o}_{harm} - G^{o}_{harm}\,\Pi(\omega)\,G^{o}_{actual} \tag{6.5}$$

or

$$G^{o}(\omega)^{-1} = (M_{o}\omega^{2} - \Phi^{o}) + \Pi(\omega) \tag{6.6}$$

This is completely analogous to the formal result obtained in the treatment of averaged Green's functions for the disorder problem (Eq. (5.6)), although the "proper self-energy" in the two cases are not the same. The proper self-energy $\Pi(\omega)$ will have both real and imaginary parts, and in addition to adding a damping to the modes, it will also renormalize the frequencies[52]. The renormalized frequencies are, of course, those that would be observed experimentally (e.g., in neutron scattering, optical spectroscopy, etc.). Note the similarity between (6.6) and the phenomenological form (6.2).

Because of the severe complications that would be involved, no attempt will be made to include broadening in the model for pure CaF_2. The harmonic approximation permits the calculation of the pure Green's functions from the spectral forms (3.32)-(3.37). The neglected effects of

anharmonic broadening probably represent a more serious limitation on the accuracy of the calculated Green's functions than the choice of model to be used here. At low temperatures, where the vibrations of the nuclei are small, the anharmonic interaction effects are reduced, and we can, therefore, hope to minimize those effects by carrying out the calculations for low temperatures ($\sim 4^{o}K$).

Later, when the averaged Green's function methods are applied to the optical properties of the mixed fluorites, it will be necessary to include (in a somewhat sloppy way) an intrinsic width for certain $\vec{k} = 0$ optic modes in pure CaF_2. This can be done, as remarked above, by including an imaginary part $\gamma/2$ with the phonon frequency ω_o. The earlier discussion of analyticity properties specifies that this phenomenological damping should be represented by a pole in the lower half-plane for the retarded Green's function description; i.e., the broadened mode should be represented by the complex frequency $(\omega_o - i\gamma/2)$.

1) Short-Range, Non-Coulombic Contributions

The present model includes short-range forces between nearest-neighbor fluorines, nearest-neighbor calciums, and between a given calcium and its nearest-neighbor fluorines. Symmetry techniques can be used to determine the general forms of the nearest-neighbor force constant matrices. The reduction is carried out by examining the interrelation between the elements $\Phi^{o}_{\alpha\beta}(\ell\kappa,\ell'\kappa')$ expressed by (2.29) for the group $\mathcal{G}$ of elements that: 1) leave the crystal invariant, and 2) leave the pair of sites $(\ell\kappa)$ and $(\ell'\kappa')$ invariant. For the following discussion, we shall label the arguments of the force constant matrices Φ^{o} as $\Phi^{o}_{\alpha\beta}(\vec{R}_{\ell'\kappa}-\vec{R}_{\ell\kappa};\kappa,\kappa')$, and

shall express the components of the vector $(\vec{R}_{\ell'\kappa'} - \vec{R}_{\ell\kappa})$ in dimensionless units for which r_o, the F-F separation, is taken to be unity (cf. Fig.2.1).

The group $\mathcal{G}$ of symmetry operations for the nearest-neighbor calcium-fluorine interaction is C_{3v}, consisting of E, $2C_3$, and 3σ. The two C_3 operations are the $\pm 120^\circ$ rotations about a (111)-axis joining Ca and F, and the three reflection planes are the (110)-planes. From these operations, it can be shown that $\phi^o_{\alpha\beta}(\frac{1}{2},\frac{1}{2},\frac{1}{2};Ca,F)$ contains only two independent constants, and all of the other force constant tensors pertaining to the nearest-neighbor Ca-F short-range interaction can then be obtained from $\bar{\Phi}^o(\frac{1}{2},\frac{1}{2},\frac{1}{2};Ca,F)$ by using (2.28) with appropriate rotation operations:

$$
\begin{aligned}
\bar{\Phi}^o(-\tfrac{1}{2},-\tfrac{1}{2},\tfrac{1}{2};Ca,F) &= -\begin{vmatrix} \alpha_1 & \beta_1 & -\beta_1 \\ \beta_1 & \alpha_1 & -\beta_1 \\ -\beta_1 & -\beta_1 & \alpha_1 \end{vmatrix} = \bar{\Phi}^o(\tfrac{1}{2},\tfrac{1}{2},-\tfrac{1}{2};Ca,F) \\
\bar{\Phi}^o(-\tfrac{1}{2},\tfrac{1}{2},\tfrac{1}{2};Ca,F) &= -\begin{vmatrix} \alpha_1 & -\beta_1 & -\beta_1 \\ -\beta_1 & \alpha_1 & \beta_1 \\ -\beta_1 & \beta_1 & \alpha_1 \end{vmatrix} = \bar{\Phi}^o(\tfrac{1}{2},-\tfrac{1}{2},-\tfrac{1}{2};Ca,F) \\
\bar{\Phi}^o(\tfrac{1}{2},\tfrac{1}{2},\tfrac{1}{2};Ca,F) &= -\begin{vmatrix} \alpha_1 & \beta_1 & \beta_1 \\ \beta_1 & \alpha_1 & \beta_1 \\ \beta_1 & \beta_1 & \alpha_1 \end{vmatrix} = \bar{\Phi}^o(-\tfrac{1}{2},-\tfrac{1}{2},-\tfrac{1}{2};Ca,F) \\
\bar{\Phi}^o(\tfrac{1}{2},-\tfrac{1}{2},\tfrac{1}{2};Ca,F) &= -\begin{vmatrix} \alpha_1 & -\beta_1 & \beta_1 \\ -\beta_1 & \alpha_1 & -\beta_1 \\ \beta_1 & -\beta_1 & \alpha_1 \end{vmatrix} = \bar{\Phi}^o(-\tfrac{1}{2},\tfrac{1}{2},-\tfrac{1}{2};Ca,F)
\end{aligned}
\qquad (6.7)
$$

For the nearest-neighbor calcium ions along the (110)-directions, the symmetry group is C_{2v}, with the operations E, C_2, σ_1, σ_2. The resulting force constant matrices are

$$\tilde{\Phi}^o(1,1,0;Ca,Ca) = -\begin{vmatrix} \beta_2 & \gamma_2 & 0 \\ \gamma_2 & \beta_2 & 0 \\ 0 & 0 & \alpha_2 \end{vmatrix} = \tilde{\Phi}^o(-1,-1,0;Ca,Ca)$$

$$\tilde{\Phi}^o(1,0,1;Ca,Ca) = -\begin{vmatrix} \beta_2 & 0 & \gamma_2 \\ 0 & \alpha_2 & 0 \\ \gamma_2 & 0 & \beta_2 \end{vmatrix} = \tilde{\Phi}^o(-1,0,-1;Ca,Ca)$$

$$\tilde{\Phi}^o(0,1,1;Ca,Ca) = -\begin{vmatrix} \alpha_2 & 0 & 0 \\ 0 & \beta_2 & \gamma_2 \\ 0 & \gamma_2 & \beta_2 \end{vmatrix} = \tilde{\Phi}^o(0,-1,-1;Ca,Ca)$$

$$\tilde{\Phi}^o(0,-1,1;Ca,Ca) = -\begin{vmatrix} \alpha_2 & 0 & 0 \\ 0 & \beta_2 & -\gamma_2 \\ 0 & -\gamma_2 & \beta_2 \end{vmatrix} = \tilde{\Phi}^o(0,1,-1;Ca,Ca) \qquad (6.8)$$

$$\tilde{\Phi}^o(1,0,-1;Ca,Ca) = -\begin{vmatrix} \beta_2 & 0 & -\gamma_2 \\ 0 & \alpha_2 & 0 \\ -\gamma_2 & 0 & \beta_2 \end{vmatrix} = \tilde{\Phi}^o(-1,0,1;Ca,Ca)$$

$$\tilde{\Phi}^o(1,-1,0;Ca,Ca) = -\begin{vmatrix} \beta_2 & -\gamma_2 & 0 \\ -\gamma_2 & \beta_2 & 0 \\ 0 & 0 & \alpha_2 \end{vmatrix} = \tilde{\Phi}^o(-1,1,0;Ca,Ca)$$

Finally, for the nearest-neighbor fluorines the symmetry group is C_{2v}, and leads to the following forms:

$$\tilde{\Phi}^{o}(1,0,0;F,F) = -\begin{vmatrix} \alpha_3 & 0 & 0 \\ 0 & \beta_3 & 0 \\ 0 & 0 & \beta_3 \end{vmatrix} = \tilde{\Phi}^{o}(-1,0,0;F,F)$$

$$\tilde{\Phi}^{o}(0,1,0;F,F) = -\begin{vmatrix} \beta_3 & 0 & 0 \\ 0 & \alpha_3 & 0 \\ 0 & 0 & \beta_3 \end{vmatrix} = \tilde{\Phi}^{o}(0,-1,0;F,F) \qquad (6.9)$$

$$\tilde{\Phi}^{o}(0,0,1;F,F) = -\begin{vmatrix} \beta_3 & 0 & 0 \\ 0 & \beta_3 & 0 \\ 0 & 0 & \alpha_3 \end{vmatrix} = \tilde{\Phi}^{o}(0,0,-1;F,F)$$

The "self" force constant matrices $\tilde{\Phi}^{o}(0,0,0;Ca,Ca)$ and $\tilde{\Phi}^{o}(0,0,0;F,F)$ can be calculated from the condition (2.13) that resulted from invariance under rigid-body translation:

$$\tilde{\Phi}^{o}(0,0,0;Ca,Ca) = 4(\alpha_1 + 2\beta_2 + \alpha_2)\cdot\tilde{1}$$

$$\tilde{\Phi}^{o}(0,0,0;F,F) = 2(2\alpha_1 + 2\beta_3 + \alpha_3)\cdot\tilde{1} \qquad (6.10)$$

They are multiples of the unit matrix, which we would expect, since the vector (0,0,0) has the full O_h symmetry. The short-range force contributions to the Fourier-transformed dynamical matrix, Eq. (2.45), become

$$D_{xx}^{sr}(\vec{k}|1,1) = \frac{4}{m_{Ca}}\Big[2\alpha_1 + \beta_2(2 - \cos k_x \cos k_y - \cos k_x \cos k_z) + \alpha_2(1 - \cos k_y \cos k_z)\Big]$$

$$D_{xy}^{sr}(\vec{k}|1,1) = \frac{4}{m_{Ca}}\gamma_2 \sin k_x \sin k_y$$

$$D_{xx}^{sr}(\vec{k}|1,2) = -\frac{4\alpha_1}{\sqrt{m_{Ca}m_F}}\Big[\cos \tfrac{1}{2}k_x \cos \tfrac{1}{2}k_y \cos \tfrac{1}{2}k_z + i \sin \tfrac{1}{2}k_x \sin \tfrac{1}{2}k_y \sin \tfrac{1}{2}k_z\Big]$$

$$D_{xy}^{sr}(\vec{k}|1,2) = \frac{4\beta_1}{\sqrt{m_{Ca}m_F}}\Big[\sin \tfrac{1}{2}k_x \sin \tfrac{1}{2}k_y \cos \tfrac{1}{2}k_z + i \sin \tfrac{1}{2}k_z \cos \tfrac{1}{2}k_x \cos \tfrac{1}{2}k_y\Big]$$

$$D_{xx}^{sr}(\vec{k}|2,3) = -\frac{2}{m_F}\Big[\alpha_3 \cos k_x + \beta_3(\cos k_y + \cos k_z)\Big]$$

$$D_{xy}^{sr}(\vec{k}|2,3) = 0 \qquad (6.11)$$

$$D_{\alpha\beta}^{sr}(\vec{k}|1,3) = D_{\alpha\beta}^{sr}(\vec{k}|1,2)^*$$

$$D_{\alpha\beta}^{sr}(\vec{k}|2,2) = D_{\alpha\beta}^{sr}(\vec{k}|3,3) = \frac{2}{m_F}(\alpha_3 + 2\beta_3 + 2\alpha_1)$$

with all other elements determined by cyclic permutation of x, y, and z. The components of the $\vec{k}$-vector appearing in (6.11) are expressed in the dimensionless units for which r_o (the F-F separation) is chosen to be unity.

2) Long-Range Coulomb Contributions

In the harmonic approximation the quadratic truncation of the (1/r) Coulomb forces leads to a sum of dipole-dipole interactions distributed over the entire lattice. In the present model, the charges on the rigid, non-polarizable ions are assumed to be +2Ze for the calciums, and -Ze for the fluorines, where Ze is an effective charge which(along with the other constants α_1, β_1, α_2, β_2, γ_2, α_3, and β_3) will later be determined from experimentally observed parameters. Since the ions are assumed to be rigid and non-polarizable, the dipole moments arise purely from mechanical displacements from equilibrium. From the expansion

$$\frac{1}{|\vec{r}+\vec{u}|} = \frac{1}{r} - \frac{\vec{r}}{r^3}\cdot\vec{u} + \vec{u}\cdot\frac{1}{2}\left\{3\frac{\vec{r}\vec{r}}{r^2} - 1\right\}\frac{1}{r^3}\cdot\vec{u} + \cdots$$

it is possible to express the total Coulomb potential energy

$$\varphi^{coul} = \frac{1}{2}\sum_{\substack{i,j \\ i\neq j}}{}' \frac{Q_i Q_j}{|\vec{r}_i - \vec{r}_j|}, \quad \vec{r}_i = \vec{R}_i + \vec{u}_i$$

as

$$\varphi^{coul} = \varphi_0 + \frac{1}{2}\sum_{\substack{i,j \\ i\neq j}}{}' Q_i Q_j (\vec{u}_i - \vec{u}_j)\cdot \frac{1}{2|\vec{R}_i - \vec{R}_j|^3}\left\{3\frac{(\vec{R}_i-\vec{R}_j)(\vec{R}_i-\vec{R}_j)}{|\vec{R}_i-\vec{R}_j|^2} - 1\right\}\cdot(\vec{u}_i - \vec{u}_j) \tag{6.12}$$

in the harmonic approximation. Here, i and j refer to ion sites, and $\vec{u}_i$ and $\vec{u}_j$ represent displacements from the equilibrium positions $\vec{R}_i$ and $\vec{R}_j$.

The Coulomb energy must be expressed as a quadratic form in the displacements,

$$\varphi^{coul} = \frac{1}{2} \sum_{i,j} \vec{u}_i \cdot \overleftrightarrow{\Phi}^{coul}(i,j) \cdot \vec{u}_j$$

and comparison with the expansion (6.12) yields

$$\overleftrightarrow{\Phi}^{coul}(i,j) = - \frac{Q_i Q_j}{|\vec{R}_i - \vec{R}_j|^3} \left\{ 3 \frac{(\vec{R}_i - \vec{R}_j)(\vec{R}_i - \vec{R}_j)}{|\vec{R}_i - \vec{R}_j|^2} - 1 \right\} \quad (i \neq j)$$

$$\overleftrightarrow{\Phi}^{coul}(i,i) = 0 \tag{6.13}$$

Thus, the Coulomb energy in the harmonic approximation is formally equivalent to a sum of dipole-dipole interactions between dipoles $Q_i\vec{u}_i$ and $Q_j\vec{u}_j$ at sites i and j:

$$\varphi^{coul} = - \frac{1}{2} \sum_{i,j}{}' (Q_i \vec{u}_i) \cdot \frac{1}{R_{ij}^3} \left\{ 3 \frac{\vec{R}_{ij}\vec{R}_{ij}}{R_{ij}^2} - 1 \right\} \cdot (Q_j \vec{u}_j) \tag{6.14}$$

The Coulomb contribution to the Fourier-transformed dynamical matrix (Eq. (2.45)) becomes

$$\overleftrightarrow{D}^{coul}(\vec{k} \mid \kappa,\kappa') = - \frac{Q_\kappa Q_{\kappa'}}{(M_\kappa M_{\kappa'})^{1/2}} \sum_{\ell}{}' \frac{e^{-i\vec{k}\cdot(\vec{R}_\ell + \vec{r}_{\kappa\kappa'})}}{|\vec{R}_\ell + \vec{r}_{\kappa\kappa'}|^3} \times$$

$$\left\{ 3 \frac{(\vec{R}_\ell + \vec{r}_{\kappa\kappa'})(\vec{R}_\ell + \vec{r}_{\kappa\kappa'})}{|\vec{R}_\ell + \vec{r}_{\kappa\kappa'}|^2} - 1 \right\} \tag{6.15}$$

where $\vec{r}_{\kappa\kappa'} = (\vec{R}_\kappa - \vec{R}_{\kappa'})$, and where the ' on the sum means that terms for which $|\vec{R}_\ell + \vec{r}_{\kappa\kappa'}| = 0$ are to be omitted. The summand falls off as $1/R_\ell^3$ at large distances, but since the area of a spherical shell goes as R_ℓ^2,

the sum falls off only $\sim 1/R_\ell$. However, the convergence is assisted by the phase factor, $\exp\left[-i\vec{k}\cdot(\vec{R}_\ell + \vec{r}_{\kappa\kappa'})\right]$, which oscillates rapidly as $\vec{R}_\ell$ increases, and by the dyadic expression in curly brackets (an angular factor which has $Y_{2,m}$ symmetry) and whose contribution over a large sphere tends to average to zero. The convergence of (6.15) is extremely slow, and as $\vec{k} \to 0$, the sum is only conditionally convergent and depends, in a limiting way, on the direction of approach to the origin. We shall return to this point later, when we discuss the splitting of the F_{1u} $\vec{k} = 0$ modes of CaF_2 into longitudinal and transverse branches.

In order to evaluate the Coulomb contribution (6.15) to the dynamical matrix $\tilde{\tilde{D}}^0(\vec{k}|\kappa\kappa')$, it is convenient to use techniques formulated by Nijboer and De Wette[173] for a general class of lattice sums. These are, essentially, the Ewald sum methods, and are necessary for converting the slowly converging series (6.15) into a form suitable for numerical computation.

No attempt will be made here to elaborate on the generality of the techniques, nor to provide complete motivation for all of the steps in the derivation, since excellent discussion is available in the original source[173]. The development below will contain only those steps that are relevant for an evaluation of the specific type of lattice sum that arises in the expression (6.15) for $\tilde{\tilde{D}}^{coul}(\vec{k}|\kappa\kappa')$. Consider the sum

$$\tilde{\tilde{S}}(\vec{k}, \vec{r}_{\kappa\kappa'}) = \sum_\ell{}' \frac{e^{-i\vec{k}\cdot(\vec{R}_\ell + \vec{r}_{\kappa\kappa'})}}{|\vec{R}_\ell + \vec{r}_{\kappa\kappa'}|^3} \left\{ 3 \frac{(\vec{R}_\ell + \vec{r}_{\kappa\kappa'})(\vec{R}_\ell + \vec{r}_{\kappa\kappa'})}{|\vec{R}_\ell + \vec{r}_{\kappa\kappa'}|^2} - 1 \right\} \quad (6.16)$$

which can be written

$$\overleftrightarrow{S}(\vec{k}, \vec{r}_{\kappa\kappa'}) = \int d\vec{r} \; \frac{w(\vec{r}, \vec{k})}{|\vec{r}|^3} \left\{ 3 \; \frac{\vec{r}\,\vec{r}}{|\vec{r}|^2} - 1 \right\} \qquad (6.17)$$

where

$$w(\vec{r}, \vec{k}) = \sum_{\ell}{}' e^{-i\vec{k}\cdot\vec{r}} \, \delta(\vec{r} - \vec{R}_\ell - \vec{r}_{\kappa\kappa'}) \qquad (6.18)$$

with the primes on the sums again indicating that a term is to be omitted if $(\vec{R}_\ell + \vec{r}_{\kappa\kappa'}) = 0$. Since the vector $\vec{r}_{\kappa\kappa'}$ has the physical meaning of a relative displacement of two ions κ, κ' within a unit cell, it is clear that no primitive translation vector $\vec{R}_\ell$ can make $(\vec{R}_\ell + \vec{r}_{\kappa\kappa'}) = 0$ unless $\vec{r}_{\kappa\kappa'} = 0$ (i.e., $\kappa = \kappa'$). The primes on the sum thus refer only to that case. (Note that the function $\overleftrightarrow{S}(\vec{k},\vec{r}_{\kappa\kappa'})$ is a dyadic quantity.)

Introduce an auxiliary function $\mathcal{H}(\vec{r})$, and split the sum $\overleftrightarrow{S}(\vec{k},\vec{r}_{\kappa\kappa'})$ into two terms:

$$\overleftrightarrow{S}(\vec{k}, \vec{r}_{\kappa\kappa'}) = \int d\vec{r} \; \frac{w(\vec{r}, \vec{k})}{|\vec{r}|^3} \left\{ 3 \; \frac{\vec{r}\,\vec{r}}{|\vec{r}|^2} - 1 \right\} \mathcal{H}(\vec{r})$$

$$\int d\vec{r} \; \frac{w(\vec{r}, \vec{k})}{|\vec{r}|^3} \left\{ 3 \; \frac{\vec{r}\,\vec{r}}{|\vec{r}|^2} - 1 \right\} \left[1 - \mathcal{H}(\vec{r}) \right] \qquad (6.19)$$

The function $\mathcal{H}(\vec{r})$ shall be chosen to have the following properties, and the necessity for these should become apparent as the derivation progresses:

i) $\mathcal{H}(\vec{r})$ is a rapidly decreasing function of $|\vec{r}|$,

ii) $\mathcal{H}(\vec{r})$ is finite at the origin,

iii) $(1 - \mathcal{H}(\vec{r}))/r^3$ is slowly varying at the origin,

iv) $\mathcal{H}(\vec{r})$ is otherwise arbitrary.

Further considerations discussed subsequently will lead to a convenient

ultimate choice for the function $\mathcal{H}(\vec{r})$. In the separation of $\tilde{\tilde{S}}(\vec{k},\vec{r}_{KK'})$ above, the first term in (6.19)

$$\tilde{\tilde{S}}_1 = \sum_{\ell}{}' \frac{e^{-i\vec{k}\cdot(\vec{R}_\ell+\vec{r}_{KK'})}}{|\vec{R}_\ell+\vec{r}_{KK'}|^3}\left\{3\frac{(\vec{R}_\ell+\vec{r}_{KK'})(\vec{R}_\ell+\vec{r}_{KK'})}{|\vec{R}_\ell+\vec{r}_{KK'}|^2}-1\right\}\mathcal{H}(\vec{R}_\ell+\vec{r}_{KK'}) \tag{6.20}$$

will converge rapidly, because of the factor $\mathcal{H}(\vec{r})$, while the second term,

$$\tilde{\tilde{S}}_2 = \sum_{\ell}{}' \frac{e^{-i\vec{k}\cdot(\vec{R}_\ell+\vec{r}_{KK'})}}{|\vec{R}_\ell+\vec{r}_{KK'}|^3}\left\{3\frac{(\vec{R}_\ell+\vec{r}_{KK'})(\vec{R}_\ell+\vec{r}_{KK'})}{|\vec{R}_\ell+\vec{r}_{KK'}|^2}-1\right\}\left[1-\mathcal{H}(\vec{R}_\ell+\vec{r}_{KK'})\right] \tag{6.21}$$

will converge no faster than the original expression for $\tilde{\tilde{S}}(\vec{k},\vec{r}_{KK'})$. However, we can exploit Parseval's theorem (for a discrete lattice) to transform the sum $\tilde{\tilde{S}}_2$, which is slowly convergent over the real lattice, to a form which converges rapidly over the reciprocal lattice. The general philosophy of this technique is based on the property that the Fourier transform of a smooth, slowly-varying function will decay rapidly in "momentum space". The ultimate choice for the function $\mathcal{H}(\vec{r})$ will thus be based on the objective of making the Fourier transform of

$$\frac{1}{|\vec{R}_\ell+\vec{r}_{KK'}|^3}\left\{3\frac{(\vec{R}_\ell+\vec{r}_{KK'})(\vec{R}_\ell+\vec{r}_{KK'})}{|\vec{R}_\ell+\vec{r}_{KK'}|^2}-1\right\}\left[1-\mathcal{H}(\vec{R}_\ell+\vec{r}_{KK'})\right]$$

decrease as rapidly over the reciprocal lattice as the summand of $\tilde{\tilde{S}}_1$ decreases over the real lattice. The second term

$$\tilde{\tilde{S}}_2 = \int d\vec{r}\;\frac{w(\vec{r},\vec{k})}{|\vec{r}|^3}\left\{3\frac{\vec{r}\vec{r}}{|\vec{r}|^2}-1\right\}\left[1-\mathcal{H}(\vec{r})\right] \tag{6.22}$$

can be written as an integral over momentum space by using Parseval's theorem. If we define

$$w(\vec{h},\vec{k}) = \frac{1}{(2\pi)^3}\int d\vec{r}\; e^{-i\vec{h}\cdot\vec{r}}\, w(\vec{r},\vec{k}) \tag{6.23}$$

$$\tilde{g}(\vec{h}) = \int d\vec{r}\; e^{-i\vec{h}\cdot\vec{r}}\, \frac{1}{r^3}\left\{ 3\,\frac{\vec{r}\vec{r}}{r^2} - 1 \right\}\left[1 - \mathcal{H}(\vec{r})\right] \tag{6.24}$$

then Parseval's theorem states that

$$\tilde{\tilde{S}}_2 = \int d\vec{h}\; w(\vec{h},\vec{k})\,\tilde{g}(\vec{h}) \tag{6.25}$$

The form of the Fourier transform of $w(\vec{r},\vec{k})$, which will be derived below, makes explicit the connection between Parseval's theorem and the duality that allows a sum over a discrete lattice to be transformed into a sum over its reciprocal lattice. It is convenient to define a new functic. $\tilde{w}(\vec{r},\vec{k})$ by

$$\tilde{w}(\vec{r},\vec{k}) = e^{-i\vec{k}\cdot\vec{r}} \sum_{\ell} \delta(\vec{r} - \vec{R}_\ell - \vec{r}_{\kappa\kappa'}) = w(\vec{r},\vec{k}) + \delta_{\kappa\kappa'}\delta(\vec{r}) \tag{6.26}$$

Note that (6.26) here contains no ' on the sum, as (6.18) did. Then, since

$$e^{i\vec{k}\cdot\vec{r}}\,\tilde{w}(\vec{r},\vec{k}) = \sum_{\ell} \delta(\vec{r} - \vec{R}_\ell - \vec{r}_{\kappa\kappa'}) \tag{6.27}$$

is a periodic function of $\vec{r}$ over the lattice, it can be expanded in a Fourier series as

$$e^{i\vec{k}\cdot\vec{r}}\,\tilde{w}(\vec{r},\vec{k}) = \sum_{\mu} A_\mu(\vec{k},\vec{r}_{\kappa\kappa'})\, e^{i\vec{h}_\mu\cdot\vec{r}} \tag{6.28}$$

where the vectors $\vec{h}_\mu$ are the reciprocal lattice vectors, defined by (2.6). If this expression is multiplied by $\exp(-i\vec{h}_\lambda \cdot \vec{r})$ and integrated over the total volume of the crystal,

$$\sum_\mu A_\mu(\vec{k}, \vec{r}_{kk'}) \int_{\text{crystal}} d\vec{r}\; e^{-i(\vec{h}_\lambda - \vec{h}_\mu)\cdot\vec{r}} = \sum_\ell \int_{\text{crystal}} d\vec{r}\; e^{-i\vec{h}_\lambda \cdot \vec{r}} \delta(\vec{r} - \vec{R}_\ell - \vec{r}_{kk'})$$

then by using the relation

$$\int_{\text{crystal}} d\vec{r}\; e^{-i(\vec{h}_\lambda - \vec{h}_\mu)\cdot\vec{r}} = \Omega\, \delta_{\lambda\mu}$$

we obtain

$$A_\lambda(\vec{k}, \vec{r}_{kk'}) = \frac{1}{\Omega} \sum_\ell \int_{\text{crystal}} d\vec{r}\; e^{-i\vec{h}_\lambda \cdot \vec{r}}\, \delta(\vec{r} - \vec{R}_\ell - \vec{r}_{kk'}) \qquad (6.29)$$

where Ω is the volume of the crystal. The coefficients $A_\lambda(\vec{k}, \vec{r}_{kk'})$ reduce to

$$A_\lambda(\vec{k}, \vec{r}_{kk'}) = \frac{1}{\Omega} \sum_\ell e^{-i\vec{h}_\lambda \cdot (\vec{R}_\ell + \vec{r}_{kk'})} = \frac{N}{\Omega} e^{-i\vec{h}_\lambda \cdot \vec{r}_{kk'}}$$

$$= \frac{1}{v_a} \exp\left(-i\vec{h}_\lambda \cdot \vec{r}_{kk'}\right) \qquad (6.30)$$

Thus, the function $\tilde{w}(\vec{r},\vec{k})$ can be expressed as a sum over the reciprocal lattice,

$$\tilde{w}(\vec{r}, \vec{k}) = \frac{1}{v_a} e^{-i\vec{k}\cdot\vec{r}} \sum_\lambda \exp\left[i\vec{h}_\lambda \cdot (\vec{r} - \vec{r}_{kk'})\right] \qquad (6.31)$$

and the Fourier transform, $\tilde{w}(\vec{h},\vec{k})$, can also be expressed as a sum over the reciprocal lattice,

$$\tilde{w}(\vec{h},\vec{k}) = \frac{1}{v_a} \sum_{\lambda} \delta(\vec{h}+\vec{k}-\vec{h}_\lambda)\, e^{-i\vec{h}_\lambda \cdot \vec{r}_{nk}} \tag{6.32}$$

From this expression for $\tilde{w}(\vec{h},\vec{k})$, it is apparent from (6.25) that the term $\tilde{\tilde{S}}_2$ can be transformed into a sum over the reciprocal lattice of the crystal. If the function $\mathcal{F}(\vec{r})$ is chosen to be a function of $|\vec{r}|$ only, then the transform function $\tilde{g}(\vec{h})$ defined by (6.24) can be further simplified by carrying out the angular part of the integration with the aid of the addition theorem for spherical harmonics. The separation of the integrations,

$$\tilde{\tilde{g}}(\vec{h}) = \int dr\, r^2\, \frac{1}{r^3}\left[1-\mathcal{F}(r)\right] \int d\Omega_{\vec{r}}\, e^{-i\vec{h}\cdot\vec{r}} \left\{ 3\frac{\vec{r}\vec{r}}{r^2} - 1 \right\} \tag{6.33}$$

involves the evaluation of an "angular part",

$$\tilde{\tilde{I}}(\vec{h},\vec{r}) = \frac{1}{r^3} \int d\Omega_{\vec{r}}\; e^{-i\vec{h}\cdot\vec{r}} \left(3\frac{\vec{r}\vec{r}}{r^2} - 1 \right) \tag{6.34}$$

which can be expressed in the form

$$\tilde{\tilde{I}}(\vec{h},\vec{r}) = \frac{\partial^2}{\partial\vec{\rho}\,\partial\vec{\rho}} \int d\Omega_{\vec{r}}\; \frac{e^{-i\vec{h}\cdot\vec{r}}}{|\vec{r}+\vec{\rho}|} \Bigg|_{\vec{\rho}=0} \tag{6.35}$$

Expand

$$e^{-i\vec{h}\cdot\vec{r}} = \sum_{\ell} i^{\ell}\,(2\ell+1)\, j_\ell(hr)\, P_\ell(\hat{h}\cdot\hat{r})$$

and

$$\frac{1}{|\vec{r}+\vec{\rho}|} = \sum_{\ell'} (-1)^{\ell'} \frac{\rho^{\ell'}}{r^{\ell'+1}} P_{\ell'}(\hat{r}\cdot\hat{\rho})$$

for $|\vec{\rho}| < r$. Then

$$\int d\Omega_{\vec{r}} \frac{e^{-i\vec{h}\cdot\vec{r}}}{|\vec{r}+\vec{\rho}|} =$$

$$\sum_{\ell\ell'} (-1)^{\ell'} i^{\ell} (2\ell+1) \frac{\rho^{\ell'}}{r^{\ell'+1}} j_{\ell}(hr) \cdot P_{\ell}(\hat{h}\cdot\hat{r}) P_{\ell'}(\hat{r}\cdot\hat{\rho})$$

which can be simplified, with the aid of the orthonormality relation

$$\int d\Omega_{\vec{r}} P_{\ell}(\hat{h}\cdot\hat{r}) P_{\ell'}(\hat{r}\cdot\hat{\rho}) = \frac{4\pi}{2\ell+1} \delta_{\ell\ell'} P_{\ell}(\hat{h}\cdot\hat{\rho}) \qquad (6.36)$$

to give

$$\frac{1}{4\pi} \int d\Omega_{\vec{r}} \frac{e^{-i\vec{h}\cdot\vec{r}}}{|\vec{r}+\vec{\rho}|} = \sum_{\ell} (-i)^{\ell} \frac{\rho^{\ell}}{r^{\ell+1}} j_{\ell}(hr) P_{\ell}(\hat{h}\cdot\hat{\rho})$$

Expansion to $O(\rho^2)$ yields

$$\frac{1}{4\pi} \int d\Omega_{\vec{r}} \frac{e^{-i\vec{h}\cdot\vec{r}}}{|\vec{r}+\vec{\rho}|} = \frac{1}{r} j_0(hr) - \frac{i}{r^2} j_1(hr) \vec{\rho}\cdot\frac{\vec{h}}{h}$$

$$- \frac{1}{2r^3} j_2(hr) \vec{\rho}\cdot\left(3\frac{\vec{h}\vec{h}}{h^2} - 1\right)\cdot\vec{\rho} + \ldots$$

and with (6.35), leads to the result that

$$\overline{\overline{I}}(\vec{h},\vec{r}) = -\frac{4\pi}{r^3} j_2(hr)\left[3\frac{\vec{h}\vec{h}}{h^2} - \overline{\overline{1}}\right] \tag{6.37}$$

Hence,

$$\overline{\overline{g}}(\vec{h}) = -4\pi\left(3\frac{\vec{h}\vec{h}}{h^2} - \overline{\overline{1}}\right)\int_0^\infty dr\,\frac{1}{r} j_2(hr)\left[1 - \mathcal{F}(r)\right] \tag{6.38}$$

A judicious choice for $\mathcal{F}(\vec{r}) = \mathcal{F}(r)$ is the "incomplete gamma function,"

$$\mathcal{F}(\vec{r}) = \Gamma(5/2\,;\alpha r^2)/\Gamma(5/2) \tag{6.39}$$

where

$$\Gamma(n\,;x) = \int_x^\infty dt\, e^{-t} t^{n-1}$$

This form for $\mathcal{F}(r)$ will be shown to have the desirable properties that both $\mathcal{F}(r)$ and the integral arising in (6.38) are rapidly decreasing functions of their arguments. The constant α is completely arbitrary, and can be conveniently chosen to make convergence in the two sums $\overline{\overline{S}}_1$ and $\overline{\overline{S}}_2$ equally rapid. The integral in (6.38),

$$\int_0^\infty \frac{dr}{r} j_2(hr)\left[1 - \mathcal{F}(r)\right] = \int_0^\infty \frac{dr}{r} j_2(hr)\,\frac{1}{\Gamma(5/2)}\int_0^{\alpha r^2} dt\, e^{-t} t^{3/2}$$

can be rewritten with a change of variables, $\rho = hr$ and $t = \alpha r^2 u^2$, as

$$\frac{8\alpha^{5/2}}{3h^5\sqrt{\pi}}\int_0^\infty d\rho \int_0^1 du\; \rho^4 u^4\, e^{-\alpha\rho^2 u^2/h^2}\, j_2(\rho)$$

Use

$$\int_0^\infty du\ u^4 j_2(u) e^{-bu^2} = \frac{e^{-1/4b}}{16\, b^3}\sqrt{\frac{\pi}{b}}$$

to obtain, finally,

$$\tilde{\tilde{g}}(\vec{h}) = -\frac{4\pi}{3} e^{-h^2/4u}\left(3\frac{\vec{h}\vec{h}}{h^2} - 1\right) \qquad (6.40)$$

The sum $\tilde{\tilde{S}}_2$ becomes

$$\tilde{\tilde{S}}_2 = \int d\vec{h}\ \tilde{w}(\vec{h},\vec{k})\tilde{\tilde{g}}(\vec{h}) + \delta_{KK'}\int d\vec{r}\ \delta(\vec{r})\frac{1}{r^3}\left[1 - \mathcal{F}(r)\right]\left(3\frac{\vec{r}\vec{r}}{r^2} - 1\right)$$

Since

$$\frac{1}{r^3}\left[1 - \mathcal{F}(r)\right] \sim r^2,$$

as $\vec{r} \to 0$, the second term with $\delta_{KK'}$ vanishes, and $\tilde{\tilde{S}}_2$ becomes, upon substitution of (6.32) and (6.40),

$$\tilde{\tilde{S}}_2 = -\frac{4\pi}{3v_a}\sum_\lambda e^{-i\vec{h}_\lambda\cdot\vec{r}_{KK'}} e^{-|\vec{h}_\lambda - \vec{k}|^2/4\alpha}\left\{3\frac{(\vec{h}_\lambda - \vec{k})(\vec{h}_\lambda - \vec{k})}{|\vec{h}_\lambda - \vec{k}|^2} - 1\right\} \qquad (6.41)$$

$\mathcal{F}(r)$ can be expressed in terms of the "complementary error function,"

$$\mathcal{F}(r) = \mathrm{Erfc}\left(r\sqrt{\alpha}\right) + 2r\, e^{-\alpha r^2}\sqrt{\frac{\alpha}{\pi}}\left(1 + \frac{2}{3}\alpha r^2\right) \qquad (6.42)$$

and we obtain, finally,

$$\tilde{\tilde{S}}(\vec{k},\vec{r}_{\kappa\kappa'}) = \sum_{\ell} \frac{e^{-i\vec{k}\cdot(\vec{R}_\ell+\vec{r}_{\kappa\kappa'})}}{|\vec{R}_\ell+\vec{r}_{\kappa\kappa'}|^3}\left\{3\frac{(\vec{R}_\ell+\vec{r}_{\kappa\kappa'})(\vec{R}_\ell+\vec{r}_{\kappa\kappa'})}{|\vec{R}_\ell+\vec{r}_{\kappa\kappa'}|^2}-1\right\}\times$$

$$\left[\mathrm{Erfc}\left(\sqrt{\alpha}\,|\vec{R}_\ell+\vec{r}_{\kappa\kappa'}|\right)+2|\vec{R}_\ell+\vec{r}_{\kappa\kappa'}|\sqrt{\frac{\alpha}{\pi}}\,e^{-\alpha|\vec{R}_\ell+\vec{r}_{\kappa\kappa'}|^2}\left(1+\frac{2\alpha}{3}|\vec{R}_\ell+\vec{r}_{\kappa\kappa'}|^2\right)\right]$$

$$-\frac{4\pi}{3V_a}\sum_{\lambda} e^{-i\vec{h}_\lambda\cdot\vec{r}_{\kappa\kappa'}-|\vec{h}_\lambda-\vec{k}|^2/4\alpha}\left\{3\frac{(\vec{h}_\lambda-\vec{k})(\vec{h}_\lambda-\vec{k})}{|\vec{h}_\lambda-\vec{k}|^2}-1\right\} \qquad (6.43)$$

The sum $\tilde{\tilde{S}}(\vec{k},\vec{r}_{\kappa\kappa'})$ is thus expressed as two sums, one over the real lattice, and the other over the reciprocal lattice, and both sums are rapidly converging. In order to make the two series converge about equally rapidly, a value of $\alpha = \pi/2$ was chosen for actual computer calculations (the details of which can be found in an appendix).

The Coulomb contribution to the dynamical matrix involves only three lattice sum functions $\tilde{\tilde{S}}(\vec{k},\vec{r}_{\kappa\kappa'})$:

$$\begin{aligned}
\tilde{\tilde{D}}^{\mathrm{coul}}(\vec{k}|1,1) &= -\frac{4Z^2e^2}{m_{Ca}}\,\tilde{\tilde{S}}(\vec{k},\{000\}) \\
\tilde{\tilde{D}}^{\mathrm{coul}}(\vec{k}|2,2) &= -\frac{Z^2e^2}{m_F}\,\tilde{\tilde{S}}(\vec{k},\{000\}) = \tilde{\tilde{D}}^{\mathrm{coul}}(\vec{k}|3,3) \\
\tilde{\tilde{D}}^{\mathrm{coul}}(\vec{k}|1,2) &= 2\frac{Z^2e^2}{\sqrt{m_{Ca}m_F}}\,\tilde{\tilde{S}}(\vec{k},\{\tfrac{1}{2}\tfrac{1}{2}\tfrac{1}{2}\}) = \tilde{\tilde{D}}^{\mathrm{coul}}(\vec{k}|2,1)^* \qquad (6.44) \\
\tilde{\tilde{D}}^{\mathrm{coul}}(\vec{k}|1,3) &= \tilde{\tilde{D}}^{\mathrm{coul}}(\vec{k}|3,1)^* = \tilde{\tilde{D}}^{\mathrm{coul}}(\vec{k}|2,1) \\
\tilde{\tilde{D}}^{\mathrm{coul}}(\vec{k}|3,2) &= -\frac{Z^2e^2}{m_F}\,\tilde{\tilde{S}}(\vec{k},\{100\}) = \tilde{\tilde{D}}^{\mathrm{coul}}(\vec{k}|2,3)^*
\end{aligned}$$

We have, by means of (6.11) and (6.44), obtained the complete expression for the Fourier transformed dynamical matrix $\tilde{D}^{o}(\vec{k}|\kappa\kappa')$. The phonon eigenfrequencies $\omega_{\vec{k}\sigma}$ and eigenvectors $\hat{w}(\kappa|\vec{k}\sigma)$ can be obtained for any wave vector $\vec{k}$ by means of (2.54). All that remains is the determination of the model parameters.

3) Long-Wavelength Optic Modes

At this point, it is instructive to examine the form of the $\vec{k} = 0$ modes in more detail, in order to illustrate the remarks made earlier about the splitting of the degeneracy of the optic F_{1u} modes into transverse and longitudinal branches by the long-range Coulomb field. If we split off the term for which $\lambda = (0,0,0)$ in expression (6.43), then as $\vec{k} \to 0$, we will be left with two absolutely (and rapidly) convergent sums that each approach zero. (This is a consequence of the fact that both sums contain an angular factor of $Y_{2,m}$ symmetry, and there exists no linear combination of the spherical harmonics $Y_{2,m}$ that has cubic symmetry.) Thus, as $\vec{k} \to 0$, only the $\lambda = (0,0,0)$ term remains, and (6.43) becomes

$$\lim_{\vec{k}\to 0} \tilde{\Im}(\vec{k},\vec{r}_{\kappa\kappa'}) = -(4\pi/3v_a)\left[3\,\frac{\vec{k}\vec{k}}{k^2} - 1\right] \qquad (6.45)$$

and this dyad clearly depends upon the direction of approach as we take the limit $\vec{k} \to 0$. Therefore, the Coulomb contribution to the dynamical matrix $D^{o}(\vec{k}\to 0|\kappa\kappa')$ will also display this property as $\vec{k}$ becomes small. However, the eigenvalues $\omega^2_{\vec{k}\sigma}$ do not depend upon the direction of approach (it would be shocking if they did!). The dyad $(3\,\frac{\vec{k}\vec{k}}{k^2} - 1)$ can be taken to

define a set of axes with one longitudinal vector parallel to $\vec{k}$, and two (arbitrarily selected) transverse, orthogonal vectors that are perpendicular to $\vec{k}$. In that cartesian system, the dyad is diagonal, with eigenvalues respectively 2, -1, -1. The dynamical matrix $\tilde{D}^{0}(\vec{k}\to 0|\kappa\kappa')$ splits into three independent blocks, when it is partitioned into boxes according to the longitudinal and transverse vectors defined in the above way:

$$\lim_{\vec{k}\to 0} D^{0}(\vec{k}) = \begin{array}{c|ccc} & \text{LO} & \text{TO}_1 & \text{TO}_2 \\ \hline \text{LO} & d_1 & & \\ \text{TO}_1 & & d_2 & \\ \text{TO}_2 & & & d_3 \end{array} \qquad (6.46)$$

The matrices $d_\nu(\kappa\kappa')$, $\nu = 1, 2, 3$, are all 3 x 3, with rows and columns labeled by the basis indices $\kappa, \kappa' = 1, 2, 3$. They are given by

$$M_\kappa^{1/2}\, d_\nu(\kappa,\kappa')\, M_{\kappa'}^{1/2} = \begin{pmatrix} 4\zeta_\nu & -2\zeta_\nu & -2\zeta_\nu \\ -2\zeta_\nu & \xi+\zeta_\nu & \zeta_\nu-\xi \\ -2\zeta_\nu & \zeta_\nu-\xi & \xi+\zeta_\nu \end{pmatrix} \qquad (6.47)$$

where

$$\begin{aligned} \zeta_\nu &= \left(2\alpha_1 + \lambda(\nu)\,\frac{4\pi}{3v_a}\,Z^2e^2\right) \\ \xi &= 2(\alpha_1 + \alpha_3 + 2\beta_3) \end{aligned} \qquad (6.48)$$

and where $\lambda(\nu) = 2, -1, -1$ for $\nu = 1, 2, 3$ are the eigenvalues of the dyad $\left(3\,\frac{\vec{k}\vec{k}}{k^2} - 1\right)$. Because the dynamical matrix has split into three inde-

pendent blocks, it can be diagonalized separately for each of the three "subspaces." Clearly, since the matrices d_2 and d_3 are identical, the eigenfrequencies for the two transverse polarizations will be the same. It is straightforward to obtain the secular equation,

$$\omega^2\left(\omega^2 - \frac{2}{m_F}\xi\right)\left(\omega^2 - 2\left[\frac{1}{m_F} + \frac{2}{m_{Ca}}\right]\zeta_\nu\right) = 0 \qquad (6.49)$$

from which we can obtain the eigenfrequencies of the optic modes:

$$\omega_R^2 = \frac{4}{m_F}(\alpha_1 + \alpha_3 + 2\beta_3) \qquad (6.50a)$$

$$\omega_{TO}^2 = 2\left[\frac{1}{m_F} + \frac{2}{m_{Ca}}\right]\left(2\alpha_1 - \frac{4\pi}{3V_a}Z^2e^2\right) \qquad (6.50b)$$

$$\omega_{LO}^2 = 2\left[\frac{1}{m_F} + \frac{2}{m_{Ca}}\right]\left(2\alpha_1 + \frac{8\pi}{3V_a}Z^2e^2\right) \qquad (6.50c)$$

ω_R is the frequency of the triply degenerate, Raman-active, F_{2g} mode; ω_{TO} is the frequency of the double degenerate, IR-active, transverse F_{1u} mode; and ω_{LO} is the frequency of the longitudinal F_{1u} mode, split from ω_{TO}. These expressions could have been obtained from (6.47) directly by using the vectors $\vec{w}(\vec{k}=0,\sigma)$ for the $\vec{k} = 0$ modes given earlier by (2.71). Eq. (6.50) for these three frequencies supplies three relations that can be used later to help determine the parameters of the rigid ion model. The above demonstration has been somewhat formal, and does not really illustrate the physics involved, which we shall discuss below.

The (harmonic oscillator) equations of motion for the ions are coupled to the Maxwell equations for the electromagnetic field, whenever there is a macroscopic polarization field induced by the lattice vibrations. Even in the electrostatic approximation, for which the Coulomb

interaction is treated as instantaneous, the existence of an induced polarization for any mode will lead to a splitting of the degeneracy between the longitudinal and transverse branches of that mode. It is the existence of such an accompanying polarization field that is responsible for the splitting of the $\vec{k} = 0$ F_{1u} optic mode in CaF_2 which was described earlier. For the Raman-active F_{2g} mode, for which no polarization is established, no extra complication of this kind arises. One of the conveniences of studying first order Raman scattering from crystals with inversion symmetry is that the Raman-active modes in such substances are not complicated by the presence of such an electric polarization field. Let us show how the splitting of the degeneracy as $\vec{k} \to 0$ arises in the electrostatic approximation, for which only part of the Maxwell equations are retained, viz.,

$$\begin{aligned} \nabla\cdot(\vec{E} + 4\pi\vec{P}) &= 0 \\ \nabla \times \vec{E} &= 0 \end{aligned} \qquad (6.51)$$

These two equations imply, respectively, that $\hat{k}\cdot(\vec{E} + 4\pi\vec{P}) = 0$, and $\hat{k} \times \vec{E} = 0$, for wavelike solutions (in the present case, we are interested in the long-wavelength solutions, $\vec{k} \to 0$). Thus,

$$\begin{aligned} \vec{E} &= 0 \qquad \text{(transverse waves)} \\ \vec{E} &= -4\pi\vec{P} \qquad \text{(longitudinal waves)} \end{aligned} \qquad (6.52)$$

For an F_{1u} mode in CaF_2, the equation of motion for the ions can be written as

$$m_{Ca}\ddot{\vec{u}}_{Ca} + 8\alpha_1(\vec{u}_{Ca} - \vec{u}_F) = 2Ze\vec{E}_i$$
$$m_F\ddot{\vec{u}}_F + 4\alpha_1(\vec{u}_F - \vec{u}_{Ca}) = -Ze\vec{E}_i \qquad (6.53)$$

where we have invoked the fact that the two fluorine sublattices have the same displacement ($\vec{u}_F$) in such a mode, and where $\vec{E}_i$ is the internal electric field developed by the deformation. In the rigid ion model which we are using, the ions are non-polarizable, so electronic effects are neglected. The polarization will be given by

$$\vec{P} = \frac{2Ze}{V_a}(\vec{u}_{Ca} - \vec{u}_F) \qquad (6.54)$$

and for systems with cubic (or higher) symmetry, the internal field is

$$\vec{E}_i = \vec{E} + (4\pi/3)\vec{P} \qquad (6.55)$$

Thus, from (6.52),

$$\vec{E}_i = (4\pi/3)\vec{P} \quad \text{(transverse wave)}$$
$$\vec{E}_i = -(8\pi/3)\vec{P} \quad \text{(longitudinal wave)} \qquad (6.56)$$

If we define $\vec{v} = (\vec{u}_{Ca} - \vec{u}_F)$, the two equations (6.53) can be manipulated to give

$$\ddot{\vec{v}}_T + 2\left[\frac{2}{m_{Ca}} + \frac{1}{m_F}\right]\left(2\alpha_1 - \frac{4\pi}{3V_a}Z^2e^2\right)\vec{v}_T = 0$$
$$\ddot{\vec{v}}_L + 2\left[\frac{2}{m_{Ca}} + \frac{1}{m_F}\right]\left(2\alpha_1 + \frac{8\pi}{3V_a}Z^2e^2\right)\vec{v}_L = 0 \qquad (6.57)$$

We can immediately identify the LO and TO frequencies from this equation,

and these agree with the earlier result (6.50). This derivation shows more clearly that the splitting is an electrostatic effect, and that the origin of the frequency difference for the LO and TO branch is the non-vanishing electric field (cf. Eq. (6.52)) associated with a longitudinal mode.

Actually, the preceding remarks about the long-wavelength optic modes have not been completely accurate, for the discussion up to this point has been based, essentially, only upon the equations of electrostatics. Although the lattice vibrations have been treated in a dynamical way, all of the time dependent equations of the electromagnetic field have been suppressed, and these must be included in a rigorous treatment. The tacit assumption in the development has been that there is an instantaneous static Coulomb interaction between the vibrating ions, and only lattice equations of motion were considered. In reality, of course, the Coulomb field does not act instantaneously, and a more complete description of the lattice modes in an ionic crystal requires that all of the equations of the electromagnetic field be included on an equal basis, in order to describe the effects of retardation. These considerations lead to some important phenomena for $\vec{k} \to 0$ in ionic solids, and we shall summarize some of the important aspects here.

In addition to a splitting of frequencies for vector-like modes, the situation near $\vec{k} = 0$ is further complicated because of retardation effects. The two electrostatic equations really describe only the longitudinal part of the electromagnetic field, which is derived from the instantaneous charge sources (i.e., the instantaneous Coulomb field). The remaining Maxwell equations, which must be reinstated in order to describe important phenomena near $\vec{k} = 0$ that electrostatics is incapable of explaining,

constitute dynamical equations for the transverse radiation field (i.e., the photon field) which has been neglected so far. In a region near $\vec{k} = 0$, when the dispersion relation of photons and phonons brings the frequencies of these two systems near resonance with each other, there can be a strong interaction between transverse mechanical waves and radiation. The exact solutions to the equations of motion for the coupled system of vibrations and the electromagnetic field are a complicated mixture of photon and phonon ("polaritons") in that region of $\vec{k}$-space. A simplified sketch of the situation for a diatomic lattice is shown in Fig. 6.6. This behavior is discussed in much more detail by Born and Huang[25] and others[39,119,174-7], and leads to the famous Lyddane-Sachs-Teller[176] formula,

$$\omega_{LO} = \omega_{TO} (\varepsilon_o / \varepsilon_\infty)^{1/2} \qquad (6.58)$$

where ε_o and ε_∞ are the static and high-frequency dielectric constants. It is shown by Cochran and Cowley[177] and by Loudon[119] how these results can be extended to more complicated crystals--e.g., many infrared-active branches, uniaxial crystal structure, etc.

For Raman scattering in crystals lacking inversion symmetry, the first order Raman-active modes will display these complications as $\vec{k} \to 0$. However, typical light sources used in Raman scattering have $\vec{k} \sim 20{,}000$ cm^{-1}. The phonons involved in right angle Raman scattering will have a momentum $\vec{k} \sim 0$ relative to the Brillouin zone edge ($\sim 10^8$ cm^{-1}), but it will be far to the right of the polariton mixing region shown in Fig. 6.6.

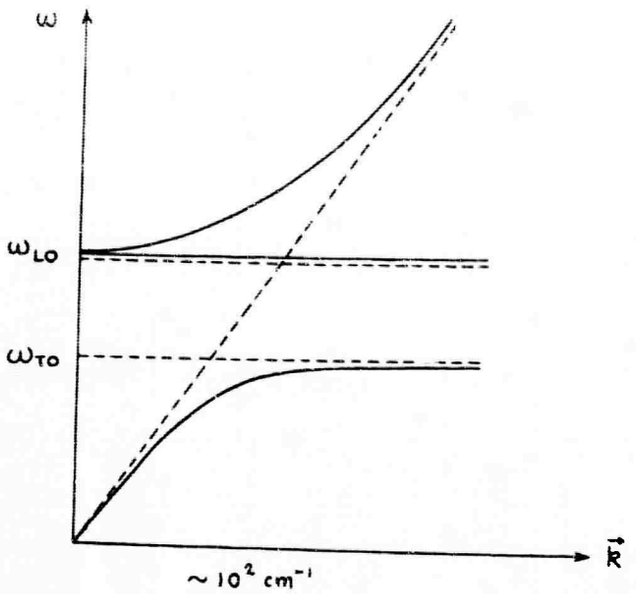

Fig. 6.6: Dispersion curves for optical waves in a diatomic lattice near $\vec{k} = 0$. The dashed lines represent phonons and photons without interaction; the solid lines describe the coupled system of lattice vibrations and radiation.

4) Determination of the Model Parameters

The rigid ion model adopted in this work contains eight constants, Z, α_1, β_1, α_2, β_2, γ_2, α_3, and β_3. In order to determine these parameters, it is necessary to relate them to experimentally measured quantities. Eq. (6.50) for the $\vec{k} = 0$ optic frequencies provides three relations, and three others are supplied by the expression for the elastic constants[165]:

$$C_{11} = \frac{1}{r_o}\left[\alpha_1 + 2\beta_2 + \alpha_3 + 3\frac{Z^2e^2}{V_a}\right] \tag{6.59a}$$

$$C_{12} = \frac{1}{r_o}\left[2\beta_1 - 2\gamma_2 - \alpha_1 - 2\alpha_2 - \beta_2 - \beta_3 - \frac{11}{2}\frac{Z^2e^2}{V_a}\right. \tag{6.59b}$$

$$C_{44} = \frac{1}{r_o}\left[\alpha_1 + 2\alpha_2 + \beta_2 + \beta_3 - 3\frac{Z^2e^2}{V_a} - \frac{(-\beta_1 + 5Z^2e^2/V_a)^2}{\alpha_1 + \alpha_3 + 2\beta_3}\right] \tag{6.59c}$$

Following Ganesan and Srinivasan[165], we can reduce the number of parameters from eight to six by making the assumptions that α_2 and β_3, the force constants for displacement of two calciums or two fluorines perpendicular to the line joining them, is zero. The six remaining constants, Z, α_1, β_1, β_2, γ_2, and α_3, can then be obtained from experimental knowledge of ω_R, ω_{TO}, ω_{LO}, C_{11}, C_{12}, and C_{44}. The Lyddane-Sachs-Teller formula (6.58) is usually used to obtain the LO frequency from the experimentally measured TO frequency. There are several references to experimental work on the optical[178-182] and elastic[183-185] constants of the fluorites in the literature. The table below gives the values of certain parameters for CaF_2 at low temperature ($\sim 4^oK$), with the resulting force constants α_1, β_1, β_2, γ_2, and α_3 (in units of e^2/r_o^3, where r_o = F-F separation, as shown in Fig. 2.1) and effective charge Z.

ω_R (cm^{-1})	326	Z^2	.609
ω_{TO} (cm^{-1})	267[a]	α_1	1.537
ω_{LO} (cm^{-1})	472[a]	β_1	2.707
ε_o	6.38[a]	β_2	.315
ε_∞	2.047[a]	γ_2	.274
C_{11} (dyne/cm^2)	17.4×10^{11} [b]	α_3	1.079
C_{12} (dyne/cm^2)	5.6×10^{11} [b]		
C_{44} (dyne/cm^2)	3.59×10^{11} [b]		
r_o (Å)	2.725		

([a]) Reference 179; ([b]) Reference 183

6.3 Theoretical Calculations: $Ca_{1-x}Sr_xF_2$

In addition to a physically realistic model for the pure CaF_2 lattice, a good model is needed to describe the effects of a substitutional Sr^{++} impurity. The calculation of the proper self-energy, to lowest order in the concentration x, can be carried out for the mixed-fluorite system $Ca_{1-x}Sr_xF_2$ by using Eq. (5.12). However, in order to make the computational aspect of the problem manageable, assumptions have to be made on the force constant changes (induced by a Sr^{++} impurity) that will keep the defect subspace as small as possible.

In the model of the defect to be adopted here, we shall assume that the long-range Coulomb forces are not affected, and that there are no force constant changes associated with the short-range interaction between the ++ ions. The defect matrix, $v_o = (M - M_o)\omega^2 - (\Phi - \Phi^o)$, shall be constructed from the following assumptions:

1) The mass of the ++ metal ion changes (Sr^{++} replaces Ca^{++}),
2) The effective charge Z does not change,
3) All nearest-neighbor short-range interactions (except for that between ++ ions) may change.

These requirements lead to a defect space that contains nine atoms: it is an XY_8 complex, consisting of the ++ impurity and its eight nearest fluorines, as shown in Fig. 6.7. The calculation of the proper self-energy requires the evaluation of

$$v_o\left[1 + g^o(\omega+i\varepsilon)v_o\right]^{-1},$$

which is of order 27 x 27. Even with the present simple assumptions, the

dimensionality of the impurity subspace is quite large. Clearly, without the simplifications that point symmetry can provide, the calculation would be a formidable task.

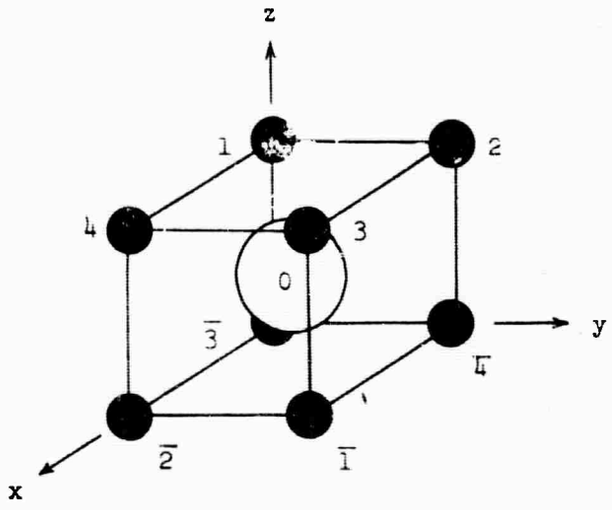

Fig. 6.7: Impurity subspace.

The matrix g^o is the Green's function (imbedded) in that subspace, for the unperturbed lattice. Even though it is here confined to the defect subspace, g^o has the full symmetry of the perfect lattice--i.e., O_h point group symmetry, and also, translation symmetry. The simplifications that group theory provides are tremendous: instead of the 378 independent elements that a general (symmetric) 27 x 27 matrix possesses, g^o can be shown to have only 13 independent elements. The transformation properties for $g^o_{\alpha\beta}(\ell\kappa,\ell'\kappa';\omega+i\varepsilon)$ are the same as those expressed by (2.28) for Φ^o, and the reduction of the 27 x 27 matrix g^o is a laborious manipulation of rotation operations. The details are omitted; the final result is displayed in Fig. 6.8, which shows the most general form that g^o can have in

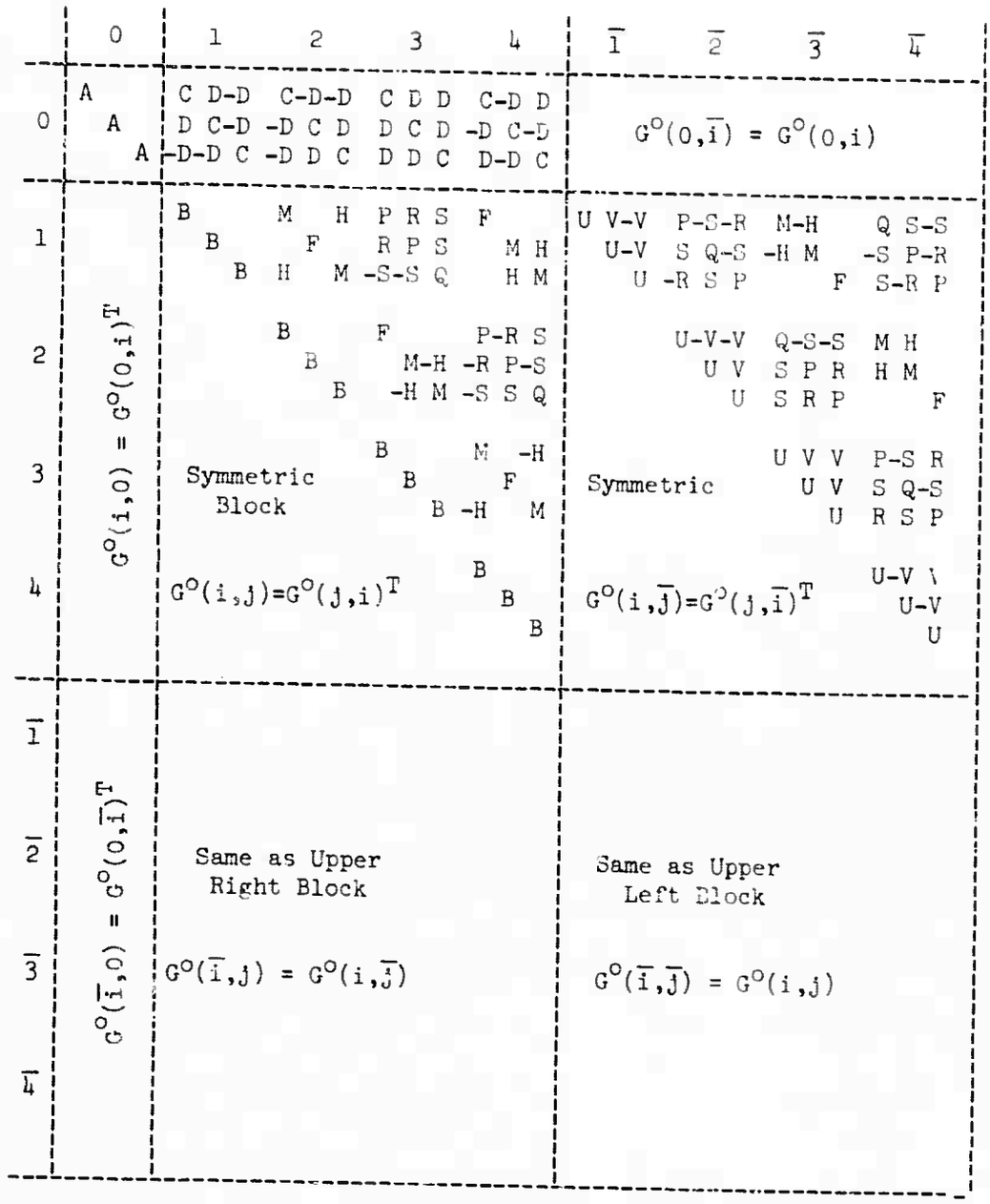

Fig. 6.8: The unperturbed phonon Green's function matrix, containing 13 independent functions A, B, ..., U, V, for the XY_8 impurity subspace shown in Fig. 6.7. The site labels i,j = 0, 1, 2, ..., etc. refer to the notation in Fig. 6.7.

the impurity subspace. The notation 0, 1, 2, ..., $\bar{1}$, $\bar{2}$, ... etc. refers to the site labels introduced in Fig. 6.7. The numerical calculation of the 13 Green's functions A, B, ..., U, V is described in the appendix, and the real and imaginary parts of these functions are displayed graphically there.

The defect matrix v_o, and also $v_o[1 + g^o(\omega+i\varepsilon)v_o]^{-1}$, has the site symmetry of the XY_8 complex, i.e., the 48 operations of the O_h point group. There will be one mass change, $(m_{Sr} - m_{Ca})$, and three force constant changes, $\delta\alpha_1$, $\delta\beta_1$, and $\delta\alpha_3$ involved in the defect matrix v_o (refer to the notation used for the rigid ion model). The change in α_1 is calculated from (6.50) using the (assumed unchanged) value of $Z^2 = .609$ and the value[.79] of $\omega_{TO} = 225$ cm^{-1} for SrF_2 (at $\sim 4^oK$); the change in β_1 is obtained from (6.59b) using the experimental value[184] of $C_{12} = 4.75 \times 10^{11}$ dynes/cm^2 for SrF_2 (at $\sim 4^oK$); and the change in α_3 comes from (6.50a) using the experimental value of $\omega_R = 290$ cm^{-1} for SrF_2 (at $\sim 4^oK$). The masses of Ca and Sr (relative to the fluorine mass) are, respectively, 2.109 and 4.612; the change is thus $\delta m = 2.503$. Since every nearest-neighbor F-F pair shares the subspace for two possible impurity sites, the average α_3 force constant is used for two F ions located between a Sr^{++} defect and a Ca^{++} host atom. This is equivalent to associating a change of $\frac{1}{2}\delta\alpha_3$ in the F-F matrix elements for the defect matrix v_o that describes a single Sr^{++} impurity. The complete form of the matrix v_o over the 27 x 27 dimensional impurity subspace is displayed in Fig. 6.9. The "self" force constant changes in Fig. 6.9 were determined from the translation condition (2.13), which is valid for an arbitrary lattice.

Under each of the 48 operations of the O_h group, a matrix X defined

	0	1	2	3	4	$\bar{1}$	$\bar{2}$	$\bar{3}$	$\bar{4}$
0	X_o	X_1	X_2	X_3	X_4	X_1	X_2	X_3	X_4
1	X_1	$-X_1-\frac{1}{2}\delta\alpha_3$	$\begin{matrix}0\\ \frac{1}{2}\delta\alpha_3\\ 0\end{matrix}$		$\begin{matrix}\frac{1}{2}\delta\alpha_3\\ 0\\ 0\end{matrix}$			$\begin{matrix}0\\ 0\\ \frac{1}{2}\delta\alpha_3\end{matrix}$	
2	X_2	$\begin{matrix}0\\ \frac{1}{2}\delta\alpha_3\\ 0\end{matrix}$	$X_2-\frac{1}{2}\delta\alpha_3$	$\begin{matrix}\frac{1}{2}\delta\alpha_3\\ 0\\ 0\end{matrix}$					$\begin{matrix}0\\ 0\\ \frac{1}{2}\delta\alpha_3\end{matrix}$
3	X_3		$\begin{matrix}\frac{1}{2}\delta\alpha_3\\ 0\\ 0\end{matrix}$	$X_3-\frac{1}{2}\delta\alpha_3$	$\begin{matrix}0\\ \frac{1}{2}\delta\alpha_3\\ 0\end{matrix}$	$\begin{matrix}0\\ 0\\ \frac{1}{2}\delta\alpha_3\end{matrix}$			
4	X_4	$\begin{matrix}\frac{1}{2}\delta\alpha_3\\ 0\\ 0\end{matrix}$		$\begin{matrix}0\\ \frac{1}{2}\delta\alpha_3\\ 0\end{matrix}$	$X_4-\frac{1}{2}\delta\alpha_3$		$\begin{matrix}0\\ 0\\ \frac{1}{2}\delta\alpha_3\end{matrix}$		
$\bar{1}$	X_1								
$\bar{2}$	X_2	Same as Upper Right Block				Same as Upper Left Block			
$\bar{3}$	X_3	$v_o(\bar{i},j) = v_o(i,\bar{j})$				$v_o(\bar{i},\bar{j}) = v_o(i,j)$			
$\bar{4}$	X_4								

$$X_1 = \begin{vmatrix} \delta\alpha_1 & \delta\beta_1-\delta\beta_1 \\ \delta\beta_1 & \delta\alpha_1-\delta\beta_1 \\ -\delta\beta_1-\delta\beta_1 & \delta\alpha_1 \end{vmatrix} \quad X_2 = \begin{vmatrix} \delta\alpha_1-\delta\beta_1-\delta\beta_1 \\ -\delta\beta_1 & \delta\alpha_1 & \delta\beta_1 \\ -\delta\beta_1 & \delta\beta_1 & \delta\alpha_1 \end{vmatrix} \quad X_3 = \begin{vmatrix} \delta\alpha_1 & \delta\beta_1 & \delta\beta_1 \\ \delta\beta_1 & \delta\alpha_1 & \delta\beta_1 \\ \delta\beta_1 & \delta\beta_1 & \delta\alpha_1 \end{vmatrix} \quad X_4 = \begin{vmatrix} \delta\alpha_1-\delta\beta_1 & \delta\beta_1 \\ -\delta\beta_1 & \delta\alpha_1-\delta\beta_1 \\ \delta\beta_1-\delta\beta_1 & \delta\alpha_1 \end{vmatrix}$$

$$X_o = (M_{Sr}-M_{Ca})\omega^2 - 8\delta\alpha_1$$

Fig. 6.9: The defect matrix v_o in the XY_8 impurity subspace; the site labels 0, 1, 2,..., etc. refer to the notation in Fig. 6.7.

over the sites of the XY_8 impurity subspace will be subjected to a 27-dimensional similarity transformation $\mathcal{S}$: $X \rightarrow \mathcal{S} X \mathcal{S}^{-1}$. If X has the symmetry of the XY_8 "defect molecule", then it will be invariant under all of these similarity transformations, and X will commute with each of the 48 27-dimensional matrices $\mathcal{S}$. The 27-dimensional (reducible) representation formed by these similarity transformations can be shown to reduce to

$$\Gamma(XY_8) = A_{1g} + E_g + F_{1g} + 2F_{2g} + A_{2u} + E_u + 3F_{1u} + F_{2u} \qquad (6.60)$$

With some intuition, it is possible to construct 27-dimensional column vectors with the appropriate symmetries that can be used as "basis vectors" to reduce the matrix X into block form, corresponding to the decomposition (6.60) into orthogonal subspaces with A_{1g}, E_g, F_{1g}, ..., etc. symmetry. These (unnormalized) basis vectors are displayed in Fig. 6.10, and are, of course, not unique; all that is claimed for them is that they have the symmetry stated. They have been constructed so that the equivalent polarizations (e.g., in a 3-dimensional representation such as F_{2g}) are orthogonal. However, since they were obtained purely by geometrical intuition, it will be only accidental if they diagonalize a given matrix X <u>completely</u>. All of the simplification that group theory can provide is contained in the decomposition (6.60), and since some representations (e.g., F_{2g} and F_{1u}) occur more than once, complete diagonalization in those subspaces cannot be accomplished by (O_h) symmetry considerations alone. Aside from the fact that there are three equivalent polarizations, the reduction of a matrix X with the symmetry of the XY_8 "defect molecule"

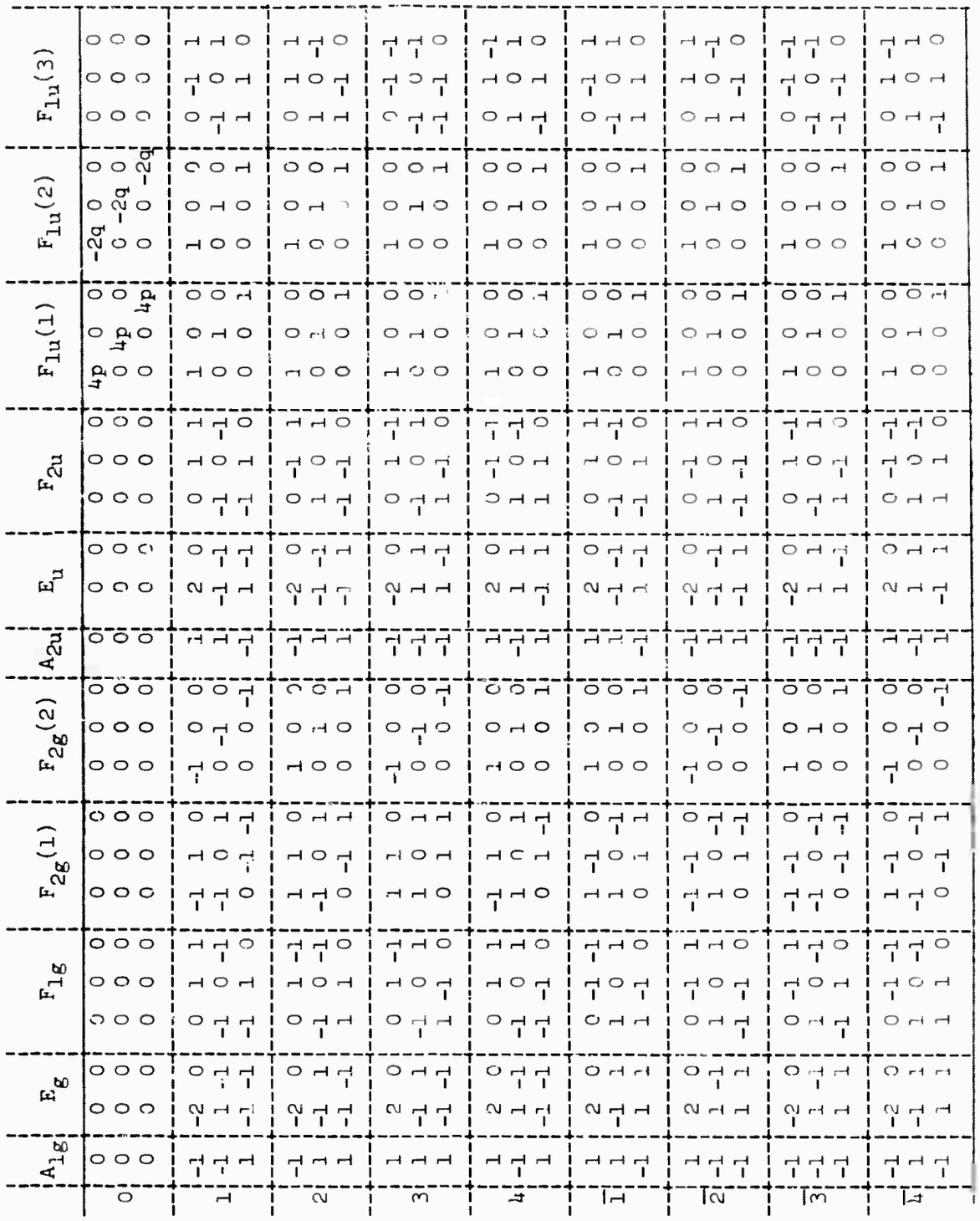

Fig. 6.10: (Unnormalized) mode vectors for an XY_8 complex in the symmetry subspaces given by the decomposition of Eq. (6.60).

		F_{2g} 1	F_{2g} 2	F_{1u} 1	F_{1u} 2	F_{1u} 3
F_{2g}	1	B-H+F-U -V-R-Q+2S	$(V-R-H)\sqrt{2}$			
	2	$(V-R-H)\sqrt{2}$	B-U-2M-F +2P+Q			
F_{1u}	1			$8(B+U+2M+F+2P+Q+2p^2A+8pC)/u^2$	$8(B+U+2M+F+2P+Q-A+2C(2p-q))/uv$	$4(H-R-V-4pD)/u$
	2			$8(B+U+2M+F+2P+Q-A+2(2p-q)C)/uv$	$4(2(B+U+2M+F+2P+Q)+q^2A-8qC)/v^2$	$4(H-R-V+2qD)/v$
	3			$4(H-R-V-4pD)/u$	$4(H-R-V+2qD)/v$	$B+H-F+U+V-R-Q+2S$

		1	2	1	2	3
F_{2g}	1	$-(\delta\alpha_1+\delta\beta_1)$	$\delta\beta_1\sqrt{2}$			
	2	$\delta\beta_1\sqrt{2}$	$-(\delta\alpha_1+\delta\alpha_3)$			
F_{1u}	1			$8(2p^2\delta m\omega^2-\delta\alpha_1(4p-1)^2)/u^2$	$(8/uv)(-\omega^2\delta m+\delta\alpha_1(4p-2q+7))$	$-(4/u)\delta\beta_1(4p-1))$
	2			$(8/uv)(-\omega^2\delta m+\delta\alpha_1(4p-2q+7))$	$(4/v^2)(q^2\omega^2\delta m-2\delta\alpha_1(2q+1)^2)$	$(4/v)\delta\beta_1(1+2q)$
	3			$-(4/u)\delta\beta_1(4p-1)$	$(4/v)\delta\beta_1(1+2q)$	$-(\delta\alpha_1+\delta\beta_1+\delta\alpha_3)$

$$p = m_{Ca}/m_F = 1/q, \quad \delta m = m_{Sr}-m_{Ca}, \quad u^2 = 8(1+2p^2), \quad v^2 = 4(2+q^2)$$

Fig. 6.11: The unperturbed Green's function matrix G^o and the defect matrix v_o in the F_{2g} and F_{1u} symmetry subspaces as determined by the mode vectors of Fig. 6.10.

will lead to (three) 2 x 2 F_{2g} blocks, and (three) 3 x 3 F_{1u} blocks. The diagonalization of these blocks will determine the linear combinations of F_{2g} and F_{1u} vectors (given in Fig. 6.10) that diagonalize a particular matrix X completely. The elements of the unperturbed Green's function matrix g^o and of the defect matrix v_o can be calculated for each of the symmetry subspaces by using Fig. 6.8, 6.9, and 6.10. These calculations are rather tedious, and have been carried out for the F_{2g} and F_{1u} subspaces, with the results shown in Fig. 6.11. These matrices are necessary later for the evaluation of $v_o\left[1 + g^o(\omega+i\varepsilon)v_o\right]^{-1}$ (which occurs in the first order proper self-energy) as a function of frequency in the F_{2g} and F_{1u} subspaces. (The constants p, q in Fig. 6.8, 6.9, 6.10, and 6.11 are related by $p = 1/q$, but are otherwise arbitrary; it shall prove convenient for the later infrared calculations to choose $p = m_{Ca}/m_F$.)

1) Raman Scattering

It may be reasonable to assume that the formation of a mixed crystal from two similar isomorphs, such as $Ca_{1-c}Sr_cF_2$ or $Ba_{1-c}Sr_cF_2$, will not involve any appreciable changes in the $P^o_{\alpha\beta,\mu}(\kappa)$ coefficients that characterize the electronic polarizability structure. Evidence for this assumption could be taken to be the fact that significant changes in these quantities would most likely lead to induced scattering from impurity modes, other than the $\vec{k} \sim 0$ excitation. Since this is contrary to our observations of a single peak which shifts linearly, and broadens with concentration, we shall assume that the dominant scattering mechanism comes from the first term in (4.15), which was expressed by (4.14). Using that result, we can write the scattering intensity as

$$I(\omega) \sim \mathrm{Im}\left[\omega^2 - \left(\omega_R - i\frac{\gamma_R}{2}\right)^2 + i\varepsilon + c\,\langle\sigma_R|\, M_o^{-1/2}\, F^{(1)}(\vec{k}=0,\ \omega+i\varepsilon)\, M_o^{-1/2}\,|\sigma_R\rangle\right]^{-1} \tag{6.61}$$

where the proper self-energy has been expanded only to the lowest order in c. We have also included, phenomenologically, a broadening to the $\vec{k} = 0$ mode of pure CaF_2 by adding a term $-i\gamma_R/2$ to ω_R, where γ_R represents a full width. From (5.17), it is evident that, as $\vec{k} \to 0$, the proper self-energy term in the denominator of (6.61) is just the projection of $v_o\left[1 + g^o(\omega+i\varepsilon)v_o\right]^{-1}$ onto the mode defined by the second set of F_{2g} vectors listed in Fig. 6.10. Calculations have been carried out for the first order PSE that occurs in expression (6.61) for the RS intensity, and the results are shown in Fig. 6.12 (with details in the appendix). These calculations have verified the validity of the conjecture that $g^o v_o$ is negligible compared to unity for the Raman mode. This leads (according to the discussion in Sec. 5.2) to the "virtual crystal approximation" for the first order Raman line, as observed; this behavior is related to the real part of the PSE. The linewidth, on the other hand, is related to the imaginary part of the PSE, according to (6.61). One of the necessary assumptions that this formalism makes is that the contribution of disordering to the linewidth of mixed crystals is additive with other effects, which are included only phenomenologically by the addition of the term $-i\gamma_R/2$ which characterizes the pure crystal (c=0). The results of the linewidth calculations that were carried out using (6.61) and the PSE function of Fig. 6.12 are shown by the dashed line in Fig. 6.5, which

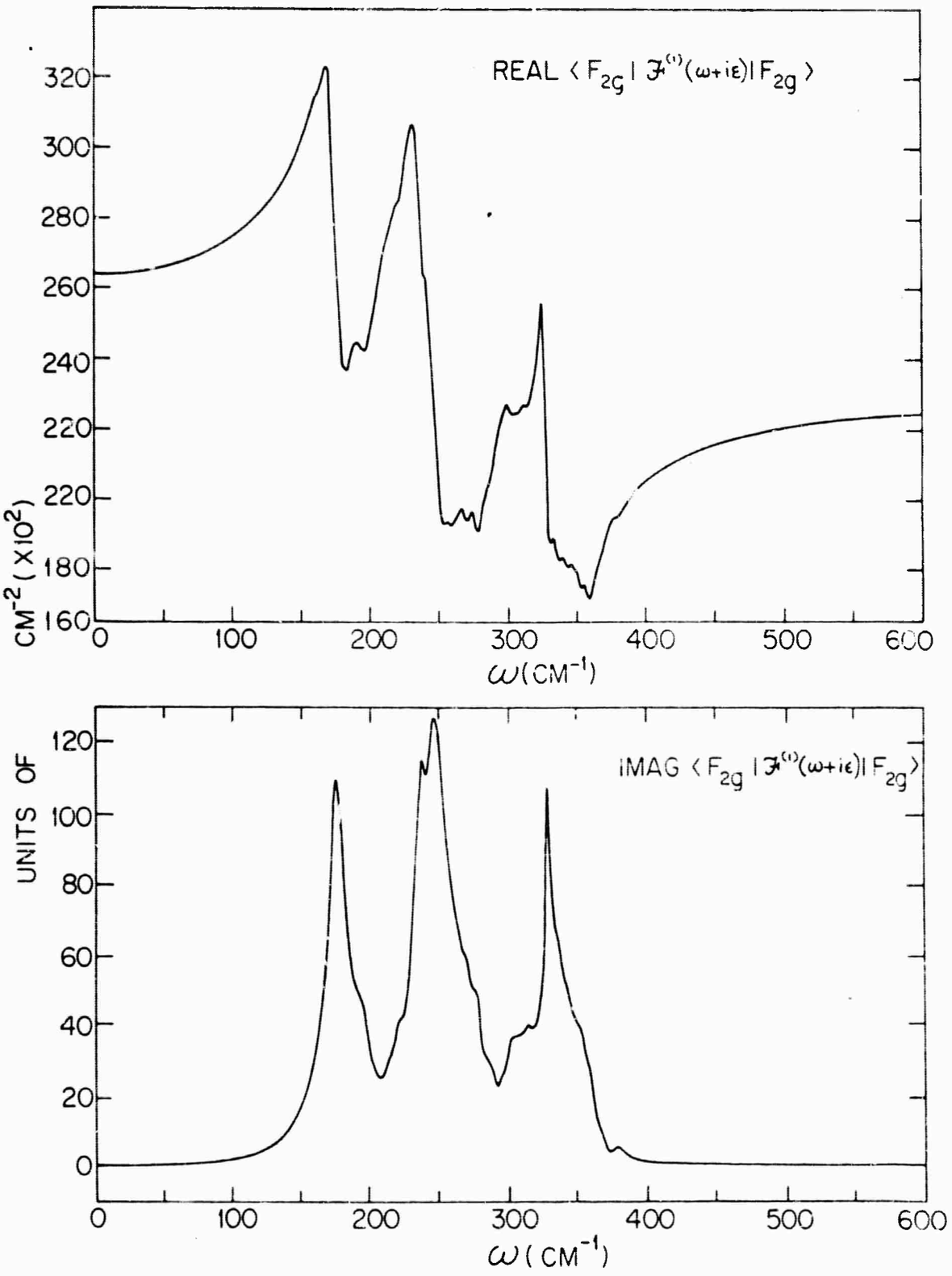

Fig. 6.12: The ($\vec{k}$ = 0) proper self-energy function $\langle \sigma_R | M_o^{-\frac{1}{2}} \mathcal{F}^{(1)}(\vec{k}=0, \omega+i\epsilon) M_o^{-\frac{1}{2}} | \sigma_R \rangle$ that occurs in Eq. (6.61) for the Raman scattering intensity.

also contains the experimental data. The results of these calculations agree reasonably well with the experimental observations.

2) Infrared Reflectivity

A similar procedure was followed in an attempt to explain the infrared reflectivity data obtained for the $Ca_{1-c}Sr_cF_2$ systems by Verleur and Barker[3]. It was assumed that, with the introduction of a Sr^{++} impurity, the first order electric moment coefficients do not change appreciably from the values $\mathcal{M}^o_{\alpha,\mu}(\kappa)$ that characterize the pure CaF_2 host. Thus, we shall again assume that the dominant contribution to the mixed crystal behavior (in this case, the far-infrared dielectric function $\varepsilon(\omega)$) comes from the (transverse, TO) $\vec{k} \sim 0$ excitations. Then, to lowest order in c for the PSE, the expression (4.25) for $\varepsilon(\omega)$ becomes

$$\varepsilon(\omega)/\varepsilon_\infty = 1 + (\omega_{TO}^2 - \omega_{LO}^2)\Big[\omega^2 - \omega_{TO}^2 + i\Gamma\omega\omega_{TO} + c\,\langle\sigma_{TO}|\, M_o^{-1/2}\, F^{(1)}(\vec{k}=0, \omega+i\varepsilon)\, M_o^{-1/2}\,|\sigma_{TO}\rangle\Big]^{-1} \qquad (6.62)$$

where we have, once again, included a phenomenological term $i\Gamma\omega\omega_{TO}$ (conforming to the notation in Verleur and Barker[3]) to account for the damping of the TO frequency of the pure CaF_2 lattice. Thus, we take[3] Γ = .025. The value of ε_∞ for pure SrF_2 is[179] 2.07, compared to 2.047 for CaF_2, so it is a good approximation to regard ε_∞ as a constant in (6.62). Again, if we appeal to (5.17) and (2.71), it is possible to show that, as $\vec{k} \to 0$, the proper self-energy in the denominator of (6.62) will be the projection of $v_o\big[1 + g^o(\omega+i\varepsilon)v_o\big]^{-1}$ onto the mode defined by the second

set of F_{1u} vectors listed in Fig. 6.10. (This is a consequence of the $M_o^{-\frac{1}{2}}$ factors, and our convenient choice of $p = m_{Ca}/m_F = 1/q$.) The results of the calculation for the PSE that occurs in (6.62) are shown in Fig. 6.13. (Details of the calculation can be found in the appendix.) Eq. (6.62) was used in conjunction with (4.16) to calculate the far-infrared reflectivity for pure CaF_2 and for $Ca_{.75}Sr_{.25}F_2$, since these cases can be compared with the experimental observations of Verleur and Barker[3]. These results are displayed in Fig. 6.14, and although the quantitative agreement is not perfect, there are many qualitative similarities between the theoretical and experimental reflectivities. The inability of a single (damped) mode to adequately describe the pure CaF_2 crystal is an indication of the fact that the crystal may not be well-approximated by a purely harmonic solid. The effect of anharmonic processes has also been discussed briefly by Bosomworth[179], who also observes departure from a harmonic lattice in his study of IR absorption in pure CaF_2. The theoretical curve for the mixed crystal $Ca_{.75}Sr_{.25}F_2$ does describe the general decrease of the reflectivity, as compared with the pure crystal, and the rounding off of the edge at ~ 280 cm^{-1}. It also displays a bump near 350 cm^{-1}, as observed. However, there is an anomolous structure at ~ 210 cm^{-1} which corresponds to the sharp peak in the PSE, shown in Fig. 6.13. This coincides with a minimum in the density of states for pure CaF_2 (cf. Fig. A-14 in the appendix) and is probably an accidental anomoly of the host model. In addition to the fact that anharmonic effects are completely neglected (which is probably the most serious deficiency), it is also possible that the models of the defect or the host are not sufficiently sophisticated. Finally, the assumption that the $\mathcal{M}^o$-coefficients do not change may be inaccurate, and in that case, there could be a complicated absorption structure throughout the band.

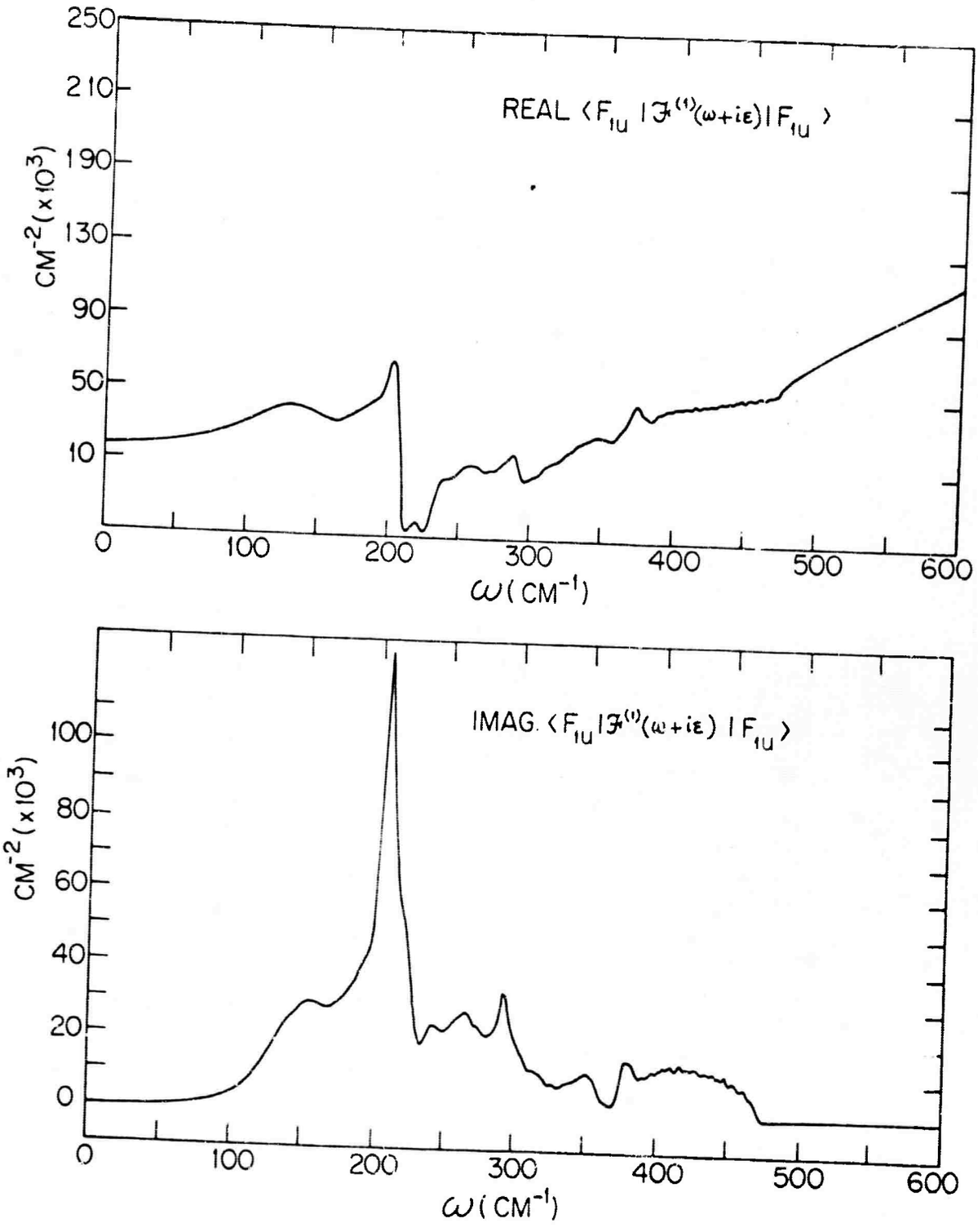

Fig. 6.13: The proper self energy function $\langle \sigma_{TO} | M_O^{-\frac{1}{2}} F^{(1)}(\vec{k}=0, \omega+i\varepsilon) M_O^{-\frac{1}{2}} | \sigma_{TO} \rangle$ that occurs in Eq. (6.62) for the far infrared dielectric function $\varepsilon(\omega)$.

(a)

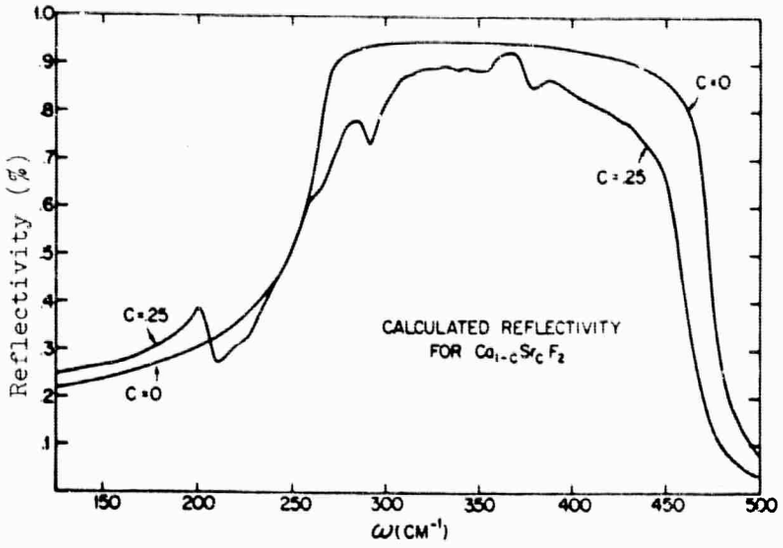

(b)

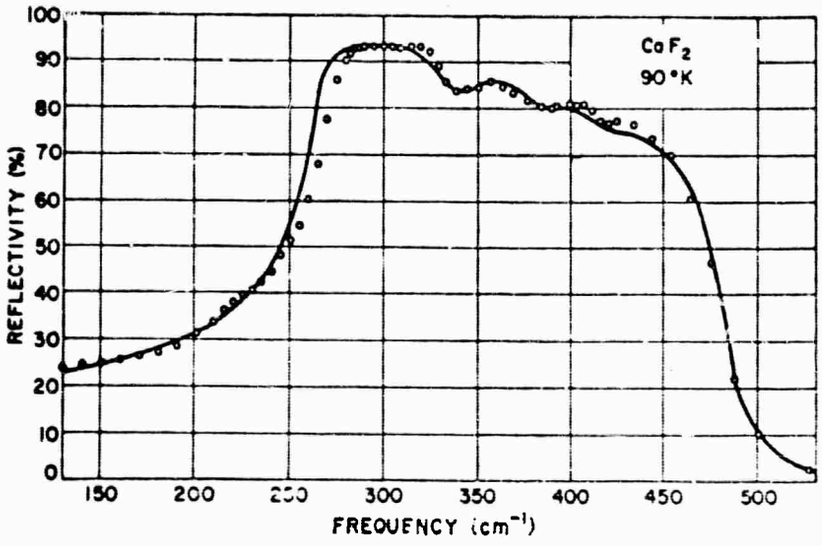

(c)

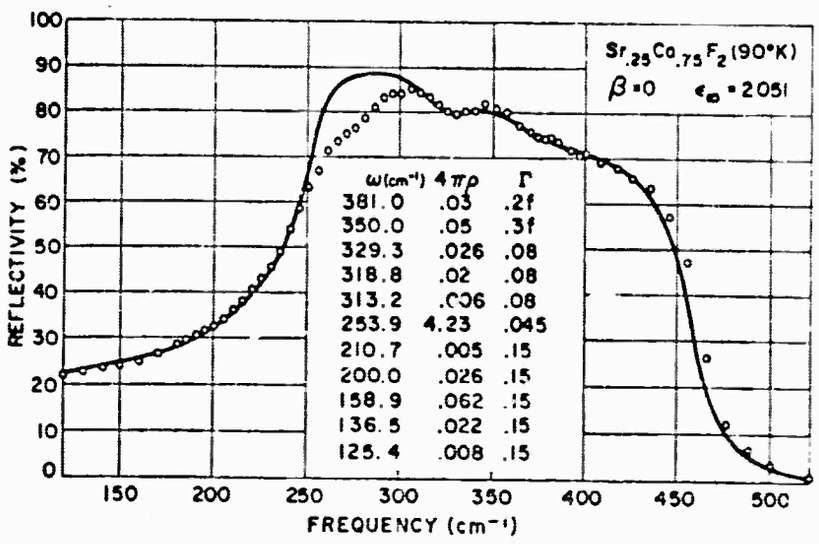

Fig. 6.14: (a) Theoretical calculations for the reflectivity; (b) and (c) are experimental results, taken from the work of Verleur and Barker, Phys. Rev. 164, 1169 (1967), Ref. 3. (The open circles are the experimental points.)

APPENDIX

In this appendix, we shall briefly describe some of the computational techniques that have been used in this work. Listings of some of the main (FORTRAN IV) programs will be included, as well as some graphical results for the density of states, dispersion curves, and certain Green's functions for pure CaF_2. The computer programs have been written in a manner that is general enough to permit their use for any of the fluorites; they are based only upon the assumption of a harmonic rigid ion lattice, and require knowledge only of ω_R, ω_{TO}, ω_{LO}, C_{11}, C_{12}, C_{44}, a (= $2r_o$), and m_{Ca}/m_F. Because these programs would be useful for a wide variety of phonon defect problems that involve fluorite host lattices, it was considered worthwhile to include them in this appendix. For example, the phonon Green's functions that are calculated by these programs could also be applied to problems of defect-induced RS or IR absorption, to vibrational sidebands[186] in fluorescence spectra, neutron scattering from impurities[187], etc.

1) General Remarks

The calculation of the phonon eigenfrequencies $\omega_{\vec{k}\sigma}$ and eigenvectors $w_\alpha(\kappa|\vec{k}\sigma)$, using the rigid ion model for the harmonic fluorite lattice, can be carried out by diagonalizing the (total) Fourier transformed dynamical matrix $D^o_{\alpha\beta}(\vec{k}|\kappa\kappa')$, given by (6.11) and (6.44). These quantities can be determined, for any given wave vector $\vec{k}$ in the first BZ, by using subroutine "KSPACE", which is included in this appendix. We shall first discuss some general symmetry conditions that $D^o_{\alpha\beta}(\vec{k}|\kappa\kappa')$ possesses which are useful for simplifying unperturbed Green's function calculations, which involve sums over all $\vec{k}$ in the first BZ (cf. Eq. (3.32)). The eigenvectors and eigen-

values for the phonon branches have the point group symmetry of the crystal (O_h in the present case), and the meaning of this statement shall become more precise below. If $(\ell\kappa) \to (LK)$ and $(\ell'\kappa') \to (L'K')$ under an operation $(S|\vec{t})$ of the crystal space group, then from (2.45),

$$S\,\tilde{\tilde{D}}^{o}(\vec{k}|\kappa\kappa')\,S^{-1} = \sum_{\ell'} e^{-i\vec{k}\cdot(\vec{R}_{\ell\kappa} - \vec{R}_{\ell'\kappa'})}\,\tilde{\tilde{D}}^{o}(LK,L'K') \qquad (A.1)$$

and since $(\vec{R}_{\ell\kappa} - \vec{R}_{\ell'\kappa'}) = S^{-1}\cdot(\vec{R}_{LK} - \vec{R}_{L'K'})$, this can be written

$$S\,\tilde{\tilde{D}}^{o}(\vec{k}|\kappa\kappa')\,S^{-1} = \sum_{\ell'} e^{-i\vec{k}\cdot S^{-1}\cdot(\vec{R}_{LK} - \vec{R}_{L'K'})}\,\tilde{\tilde{D}}^{o}(LK,L'K') \qquad (A.2)$$

Thus, finally,

$$S\,\tilde{\tilde{D}}^{o}(\vec{k}|\kappa\kappa')\,S^{-1} = \tilde{\tilde{D}}^{o}(S\vec{k}|KK') \qquad (A.3)$$

If we set

$$\mathcal{S}_{K\kappa} = \begin{cases} S & \text{if } \kappa \to K \text{ under operation } (S|\vec{t}) \\ 0 & \text{if } \kappa \not\to K \text{ under operation } (S|\vec{t}) \end{cases} \qquad (A.4)$$

then

$$\mathcal{S}\,D^{o}(\vec{k})\,\mathcal{S}^{-1} = D^{o}(S\vec{k}) \qquad (A.5)$$

Since $\mathcal{S}$ represents a similarity transformation, it follows that $D^{o}(S\vec{k})$ and $D^{o}(\vec{k})$ will have the same eigenvalues. If we write

$$\mathcal{S}\,D^{o}(\vec{k})\,\mathcal{S}^{-1}\cdot\mathcal{S}\,w(\vec{k}\sigma) = \omega^{2}_{\vec{k}\sigma}\,\mathcal{S}\,w(\vec{k}\sigma) \qquad (A.6)$$

we see from (A.5) and (A.6) that $w(\vec{k}\sigma)$ is an eigenvector of $D^0(S\vec{k})$ with eigenvalue $\omega^2_{\vec{k}\sigma}$. Thus, if we denote the eigenvectors of $D^0(S\vec{k})$ by $w(S\vec{k},\sigma)$, we can write $w_\alpha(K|S\vec{k},\sigma) = \sum_\beta S_{\alpha\beta} w_\beta(\kappa|\vec{k}\sigma)$, where κ is the basis index that is transformed into K under rotation S. Thus, knowledge of the phonon eigenfrequencies and eigenvectors for a given wave vector $\vec{k}$ can be used to calculate these quantities for all of the momenta in the "star of $\vec{k}$." Thus, for a general value of $\vec{k}$, there will be 48 vectors $S\vec{k}$ in the star of $\vec{k}$, but only one matrix diagonalization is required to obtain complete information about all of them. Since numerical diagonalization of the 3r x 3r matrix $D^0_{\alpha\beta}(\vec{k}|\kappa\kappa')$ is a time-consuming process, this exploitation of crystal symmetry can be a valuable simplification when sums over $\vec{k}$, involving the $\omega_{\vec{k}\sigma}$ and $w_\alpha(\kappa|\vec{k}\sigma)$, must be carried out. Furthermore, since $D^0_{\alpha\beta}(\ell\kappa,\ell'\kappa')$ is real, it is easy to show from Eq. (2.45) that $D^0(-\vec{k}) = D^0(\vec{k})^*$; this implies that $w_\alpha(\kappa|\vec{k}\sigma)^*$ is the eigenvector associated with the eigenvalue $\omega^2_{\vec{k}\sigma}$ for the matrix $D^0(-\vec{k})$.

2) Unperturbed Green's Functions

The 13 independent Green's functions $g^0_{\alpha\beta}(\ell\kappa,\ell'\kappa';\omega+i\varepsilon)$ that arise in the XY_8 defect subspace (and which have been denoted by A,B,...U,V in Fig. 6.8) can be calculated by a "histogram" method, using Eq. (3.33), (3.36), and (3.37). The band of (normalized) squared frequencies $(\omega/\omega_{max})^2$ is divided into a number (e.g., 200) of equally spaced intervals, or "bins." It is convenient to calculate the imaginary part of $g^0(\omega+i\varepsilon)$ first, using the spectral representation (3.37), which contains a sum over all $\vec{k}$ in the first BZ. The δ-functions can be regarded as contributing only to the "bin" in which the frequency $\omega_{\vec{k}\sigma}$ lies. After choosing a suitable mesh size G for the grid of momentum vectors, the $N = G^3$ vectors $\vec{k}$ in the first BZ are defined by Eq. (2.9) (for an fcc lattice). However, because of the considerations

above regarding the point group symmetry of the quantities $\omega_{\vec{k}\sigma}$ and $w_\alpha(\kappa|\vec{k}\sigma)$, the summation in (3.37) can be reduced to a sum over a restricted set of $\vec{k}$-vectors that lie in only 1/48 of the first BZ: all of the <u>other</u> $\vec{k}$-vectors will lie in the "stars" of these vectors. (This 1/48 region of $\vec{k}$-space is shown in Fig. 2.2, and shall be called the "fundamental wedge.") Furthermore, since inversion takes $\vec{k} \to -\vec{k}$, and since $D^o(-\vec{k}) = D^o(\vec{k})^*$, it is easy to show that Eq. (3.37) can be written

$$h^{(a)}_{\alpha\beta}(\ell\kappa, \ell'\kappa'; \omega) =$$

$$\frac{\pi}{N(M_\kappa M_{\kappa'})^{1/2}} \sum_{\vec{k} \text{ in } 1/48} m(\vec{k}) \sum_{\vec{k}_i = S_i\vec{k}} \delta(\omega^2 - \omega^2_{\vec{k}\sigma}) 2\,\mathrm{Re}\left\{ e^{i\vec{k}_i\cdot(\vec{R}_{\ell\kappa} - \vec{R}_{\ell'\kappa'})} w_\alpha(\kappa|\vec{k}_i\sigma)\, w^*_\beta(\kappa'|\vec{k}_i\sigma) \right\} \tag{A.7}$$

where the sum over S_i is a sum over <u>proper</u> rotations only. (For every rotation S_i, the improper rotation IS_i produces a result which is just the complex conjugate; hence, the "2 Re".) The quantity $m(\vec{k})$ in A.7 is a multiplicity factor that represents the fraction of the point $\vec{k}$ which lies in the "fundamental wedge": if $\vec{k}$ lies on points or lines of high symmetry, some of the proper rotations S_i will not yield <u>new</u> $\vec{k}$-vectors, and in such a case, some $\vec{k}$-vectors would be accidentally included more than once in the sum. The factor $m(\vec{k})$ prevents this; e.g., for $\vec{k} = (0,0,0)$, $m(\vec{k}) = 1/48$. The multiplicity factor is just related to the "group of the $\vec{k}$-vector," $\mathcal{G}(\vec{k})$, and a summary is given in Table A.1. A convenient method for determining $m(\vec{k})$ for any $\vec{k}$-point in the "fundamental wedge" is described in the listing of program I given later. Since the imaginary parts of the phonon Green's functions are volume integrals (in $\vec{k}$-space) of δ-functions, they are really equivalent to surface integrals; arithmetically, they behave more like derivatives than integrals, and it is necessary to use a fine mesh for the

$\vec{k}$	$\mathcal{G}(\vec{k})$	$m(\vec{k})$
Γ	O_h	1/48
Δ	D_{4h}	1/16
L	D_{3d}	1/12
W	D_{2d}	1/8
Δ	C_{4v}	1/8
Λ	C_{3v}	1/6
Z	C_{2v}	1/4
Σ	C_{2v}	1/4
Q	C_2	1/2
S	C_{2v}	1/4
U	C_{2v}	1/4
K	C_{2v}	1/4
$z = 0$	C_s	1/2
$x = \pi$	C_s	1/2

Table A.1: Points of high symmetry in the first BZ for a fcc lattice; $\mathcal{G}(\vec{k})$ is the group of the $\vec{k}$-vector, and $m(\vec{k})$ represents the fraction of $\vec{k}$ that lies in the fundamental 1/48 wedge.

Brillouin zone if good resolution is desired. Table A.2 gives the total number of distinct $\vec{k}$-vectors involved in the sum (A.7) over the fundamental wedge for a given grid size, G (which corresponds to using a total of $N = G^3$ points for the entire first BZ). The calculation of the imaginary part of a given Green's function is carried out with (A.7) by determining, for each $\vec{k}$ in the fundamental wedge, the 9 "bins" that correspond to

$(\omega_{\vec{k}\sigma}/\omega_{max})^2$, $\sigma = 1,2,\ldots,9$; a contribution

$$\sim m(\vec{k}) \sum_{S_i} e^{i(S_i\vec{k}).(\vec{R}_{\ell\kappa} - \vec{R}_{\ell'\kappa'})} \, \mathrm{Re}\left\{ w_\alpha(\kappa|S_i\vec{k},\sigma) w^*_\beta(\kappa'|S_i\vec{k},\sigma) \right\} \quad (A.8)$$

then results for $\mathrm{Im}\ {}^{\circ}_{\alpha\beta}(\ell\kappa,\ell'\kappa';\ \omega+i\varepsilon)$ at the frequency $\omega = \omega_{\vec{k}\sigma}$, and is dropped into that "bin." In practice, we used a mesh size of G = 40 for carrying out the sums over the 1/48 wedge of $\vec{k}$-vectors, and this required a calculation of the $\omega_{\vec{k}\sigma}$ and $w_\alpha(\kappa|\vec{k}\sigma)$ at 1686 distinct $\vec{k}$ points (cf. Table

G	n_o	G	n_o
2	3	52	3514
4	8	54	3906
6	16	56	4334
8	30	58	4784
10	48	60	5272
12	74	62	5784
14	106	64	6337
16	149	66	6915
18	199	68	7536
20	262	70	8184
22	334	72	8878
24	422	74	9600
26	520	76	10370
28	636	78	11170
30	764	80	12021
32	913	82	12903
34	1075	84	13838
36	1260	86	14806
38	1460	88	15830
40	1686	90	16888
42	1928	92	18004
44	2198	94	19156
46	2486	96	20369
48	2805	98	21619
50	3143	100	22932

Table A.2: For a mesh size G, there are $N = G^3$ $\vec{k}$-vectors (defined by (2.9)) in the entire first BZ; n_o gives the number of distinct $\vec{k}$-vectors in the fundamental 1/48 wedge.

A.2). This corresponds to a grid of $N = 40^3 = 64{,}000$ points for the entire first BZ, and required approximately 4 hours on the IBM 7094. After the imaginary parts of the Green's functions $g^{o}_{\alpha\beta}(\ell\kappa,\ell'\kappa';\omega+i\varepsilon)$ have been calculated by this histogram technique, the real parts can be obtained using the Hilbert transform relation, (3.36). The real and imaginary parts of the 13 independent Green's functions $g^{o}_{\alpha\beta}(\ell\kappa,\ell'\kappa';\omega+i\varepsilon)$ for CaF_2 that occur in the XY_8 subspace of Fig. 6.7, and which have been labeled A, B, ... U, V in Fig. 6.8, are displayed graphically in Fig. A-1 to A-13. They have been included in this appendix because it is quite conceivable that they would be useful for the study of other phonon effects in CaF_2.

3) Computer Programs

Because the listings of the computer programs are liberally sprinkled with "COMMENT" cards which describe most of the minor details (and which leave almost nothing to the imagination) it is unnecessary to elaborate further on these calculations here. Some of the programs make use of Share Library Subroutines, and where that is the case, it is always stated in the COMMENT cards. We have attempted to use names for FORTRAN variables which are consistent with the mathematical quantities appearing in this work; e.g., the force constant α_1 is called ALPHA1, etc. (To avoid confusion, the mesh size G for the grid of $\vec{k}$-vectors is called N in these programs, since G is often used to denote a Green's function.) To adapt these programs to any of the fluorites, it is only necessary to have knowledge of the following experimental constants:

1) ω_R, ω_{TO}, ω_{LO}, the $\vec{k} = 0$ optic frequencies in cm^{-1},

2) C_{11}, C_{12}, C_{44}, the elastic constants in units of 10^{11} dyne/cm^2,

3) a, m_{Ca}/m_F, lattice constant ($\mathring{A}$), and the ratio of masses.

In the order in which the listings appear later, these programs do the following:

Program I: Deck Name "CAF2". This program will calculate, as a function of $(\omega/\omega_{max})^2$ and in units of $1/(m_F\ \omega_{max}^2)$, the real and imaginary parts of

$$< \ell\kappa\alpha|\ g^o\ |\ell'\kappa'\beta > \ = \ M_\kappa^{-\frac{1}{2}} < \ell\kappa\alpha|\ \frac{1}{\omega^2 - i\varepsilon - D^o}\ |\ell'\kappa'\beta > M_{\kappa'}^{-\frac{1}{2}}$$

for the 13 independent functions that occur in the XY_8 complex of Fig. 6.7, and denoted in Fig. 6.8 by A, B, ..., U, V. The (complex) array GFCN(M,I), M = 1,...,13, and I = 1,...,501 represents these 13 Green's functions (see chart in program listing for exact identification) for 501 values of $(\omega/\omega_{max})^2 = (I - 1)/200$, corresponding to a range of 2.5 times the band of squared frequencies. The density of squared states, in units of $1/\omega_{max}^2$, is also calculated as a function of $(\omega/\omega_{max})^2$, and is represented by the (real) array RHO(I), I = 1,...,201. All that is required to use this program is a single DATA card (8F9.4) containing the values of a, ω_{TO}, ω_{LO}, ω_R, C_{11}, C_{12}, C_{44}, and m_{Ca}/m_F in the units specified earlier. The program makes the assumption (based on CaF_2) that $\omega_{max} = \omega_{LO}$; if that is not the case for some other fluorite, a minor modification (a change of one card) will be necessary. A tape on A5 is needed for writing the output (two records, GFCN and RHO) in binary. The deck setup is as follows:

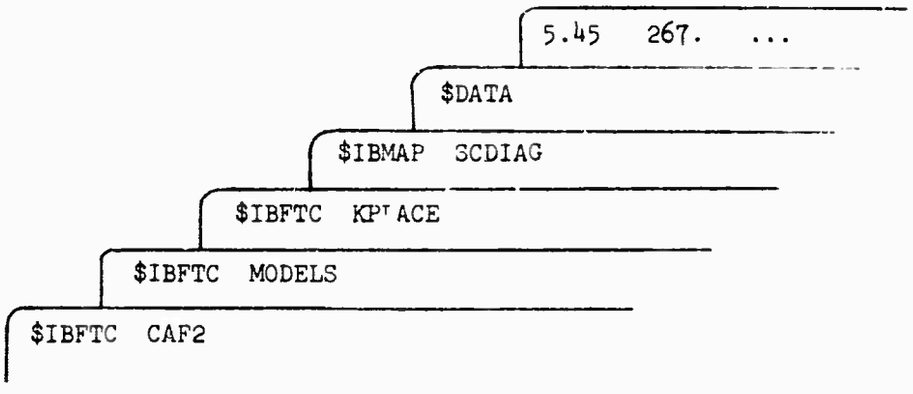

where the decks named "KPLACE" and "MODELS" are Programs II and III below, and where the deck "SCDIAG" is a Share Library Subroutine, SDA 3368, which diagonalizes hermitian matrices. SCDIAG actually occurs because it is a necessary part of the package associated with KPLACE, described next.

Program II: SUBROUTINE KSPACE, Deck Name "KPLACE". This subroutine will construct the Fourier transformed dynamical matrix $D^{o}_{\alpha\beta}(\vec{k}|\kappa\kappa')$ for a given wave vector $\vec{k}$ in the first BZ (using Eq. (6.11) and (6.44)), and then diagonalize it to produce the phonon eigenfrequencies $\omega_{\vec{k}\sigma}$ and eigenvectors $w(\vec{k}\sigma)$. The calling sequence is CALL KSPACE (KX, KY, KZ, OMEGA, W, MU), where

KX, KY, KZ — is a triplet of (floating point) numbers that specify the wave vector as

$$\vec{k} = \frac{\pi}{N} (KX, KY, KZ)$$

OMEGA — is a real 9-dimensional array that contains the final calculated values of $\omega_{\vec{k}\sigma}$, $\sigma = 1,2,\ldots,9$, in cm^{-1}

W — is a complex array, dimensioned W(3,3,9) corresponding to W(ALPHA, KAPPA, SIGMA), and containing the 9 eigenvectors $w_{\alpha}(\kappa|\vec{k}\sigma)$, $\sigma = 1,2,\ldots,9$.

MU — specifies a write-out option that is described more fully in the program listing.

This subroutine requires, as part of the package, a Share Library Subroutine "SCDIAG", SDA 3368. N (which corresponds to the mesh size G), ALPHA1, ALPHA2,..., etc. must be listed in COMMON with the main program. The main program must also contain dimensioned storage space for OMEGA and W. The following miscellaneous details should be noticed: 1) MCA is the mass of the ++ ion in units of the fluorine mass; 2) the force constants ALPHA1, ALPHA2, ..., GAM2 are assumed to be in units of e^2/r_o^3, where $e = 4.803 \times 10^{10}$ is the electronic charge in esu; 3) A is the lattice constant ($= 2r_o$) in $\mathring{A}$, and 4) $\kappa = 1, 2, 3$ correspond, respectively, to Ca, F_1, and F_2.

Program III: SUBROUTINE MODEL, Deck Name "MODELS". This subroutine will determine the parameters ALPHA1, ALPHA2, ..., GAM2, ZSQ of the rigid ion model from the experimental quantities discussed earlier. The calling sequence is CALL MODEL (T, A, WTO, WLO, WR, C11, C12, C44, MASS, ZSQ, ALPHA1, ALPHA2, ALPHA3, BETA1, BETA2, BETA3, GAM2), where

T	is the temperature in ^{o}K,
A	is the lattice constant in Å,
WTO, WLO, WR	are the $\vec{k} = 0$ optic frequencies in cm^{-1} at T ^{o}K,
C11, C12, C44	are the elastic constants, in units of 10^{11} dyne/cm2, at T ^{o}K,
MASS	is the ratio of the ++ mass to that of F,
ZSQ	is Z^2, the square of the effective charge (dimensionless),
ALPHA1,..., ...,GAM2	are the short range force constants in units of e^2/r_o^3, where e = 4.803 x 10^{10} is the electronic charge in esu, and r_o is the F-F separation in cm.

Program IV: Deck Name "GFCN". This program will calculate the symmetrized Green's functions in the F_{2g}, F_{1u}, A_{1g}, and E_g subspaces (refer to the charts in the program listing for complete details). It will also convert the Green's functions to functions of frequency ω, in cm^{-1}, and will calculate the ordinary phonon density of states, $\rho^{o}(\omega)$, in units of $1/\omega_{max}$. The symmetrized matrix elements for g^{o} in the F_{2g} and F_{1u} subspaces were given in Fig 6.11, based on the basis vectors of Fig. 6.10; in the A_{1g} and E_g subspaces, the Green's functions are given by

$$\begin{aligned} \langle A_{1g}|\, g^{o}\, |A_{1g}\rangle &= B + Q - U - F - 2(H + 2S + V + P + R - M) \\ \langle E_g|\, g^{o}\, |E_g\rangle &= B + Q - U - F + R + H + V + 2(S + M - P) \end{aligned} \qquad (A.9)$$

In order to use this program, a single DATA card containing the values of m_{Ca}/m_F and ω_{max} (2F9.4) must be provided. The tape with the (binary) Green's function data calculated from Program I is required on A5. On B5, a tape must be supplied to write the output in binary. 16 logical records will be written: 15 records containing complex arrays G(I), I = 1,...,IMAX, giving the symmetrized $g^o(\omega+i\varepsilon)$ matrix elements for the F_{2g}, A_{1g}, E_g, and F_{1u} subspaces, and one real array R(I), I = 1,...,IMAX, for the density of states $\rho^o(\omega)$. (Refer to the charts in the program listing for a precise specification of the Green's function matrix elements.) The subscript variable I = 1,...,IMAX for these arrays gives the frequency $\omega = (I - 1)$ in CM^{-1}; IMAX is determined by the largest integer that satisfies the condition $(IMAX/\omega_{max})^2 \leq 2.5$ (since the original calculations of "CAF2" were carried out for $0 \leq (\omega/\omega_{max})^2 \leq 2.5$).

Program V: Deck Name "DEFECT". This program will calculate matrix elements of the perturbed Green's function $g(\omega+i\varepsilon) = \left[1 + g^o(\omega+i\varepsilon)v_o\right]^{-1}g^o(\omega+i\varepsilon)$ in the A_{1g}, E_g, F_{2g}, and F_{1u} symmetry manifolds of the XY_8 defect space, for an impurity matrix v_o as discussed in Sec. 6.3. It will also calculate the (complex) eigenvalues $\lambda(\omega)$ of the matrix $g^o(\omega+i\varepsilon)v_o$ in those symmetry subspaces, and the proper self-energy functions that occur in Eq. (6.61) and (6.62), and displayed in Fig. 6.12 and 6.13 for CaF_2.

To use this program, it is necessary to have the tape of symmetrized Green's functions generated by Program IV, "GFCN". Various experimental quantities are entered in data statements (cf. program listing). A tape must be supplied on B5 for writing output data in binary, and the input tape from "GFCN" is required on A5. There will also be a standard printout that

gives the calculated data in tabular form. The binary output tape on B5 will contain 24 logical records, which are identified specifically in COMMENT cards in the program listing. The deck setup is as follows:

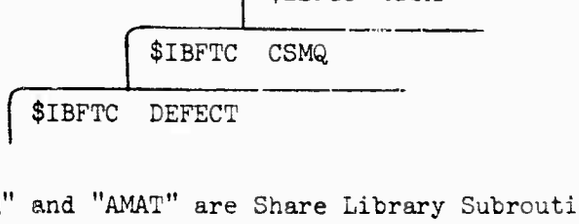

The decks "CSMQ" and "AMAT" are Share Library Subroutines:

1) Deck "CSMQ": SUBROUTINE CSIMEQ, SDA 3084, inverts complex matrices, and

2) Deck "AMAT": SUBROUTINE ALLMAT, SDA 3441, diagonalizes an arbitrary complex matrix.

Program VI: Deck Name "W VS K". This program will produce CALCOMP plots of the phonon dispersion curves for an arbitrary $\vec{k}$-direction in a fluorite lattice. To use the program, the following DATA cards are necessary:

1) Card 1: Contains the values of a, ω_{TO}, ω_{LO}, ..., etc.(8F9.4)

2) Card 2,3,...,n: Contains four integers, N1, N2, N3, and N (3I2, I3); the direction of the $\vec{k}$ is specified by (N1, N2, N3), and N is the number of intervals into which $\vec{k}$ is divided from (0,0,0) to the first BZ edge along that direction. ($N \leq 40$)

The output will be a standard printout giving $\omega_{\vec{k}\sigma}$ and $w_\alpha(\kappa|\vec{k}\sigma)$ in tabular form, and CALCOMP plots of all of the dispersion curves. A tape on A6 is necessary to generate the CALCOMP plots. Timing is about 5 seconds per $\vec{k}$ point. The deck setup is as follows:

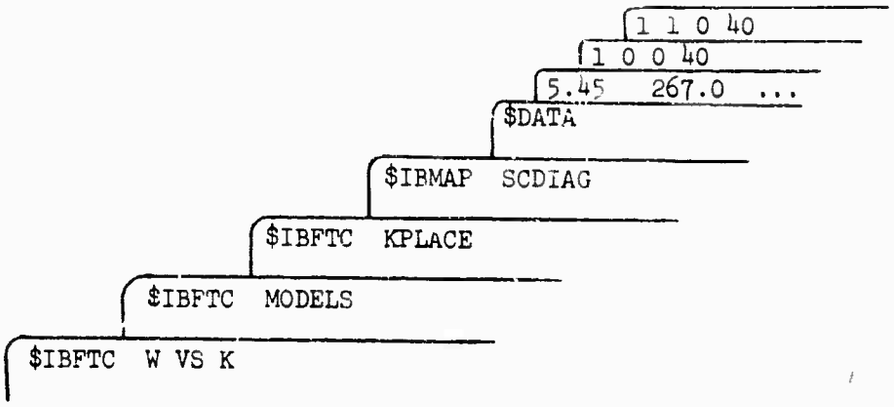

All of these subroutines have been encountered earlier; "KPLACE" and "MODELS" are Program II and III above, and SCDIAG is a part of KPLACE (Share SDA 3368). Fig. A-14 shows some dispersion curves calculated for the (100), (110), and (111) directions in CaF_2.

The card listings of these programs, I-VI, are given on the following pages.

I-1

```
      DIMENSION WKS(8,19), KAP1(13), KAP2(13), KPERM(24,3), S(24,3,3),
     1ROTR(3), G(S,13,501),RHOT2(1),SYMB(13),SUFF(,3), D1R(9), D(2)
     8,3) AA,BY,A2,KA,KB,KC,ROOTL,LL1(13),LL2(13),LL3(13),MASS(3),MCA
      REAL MPC2
      INTEGER ALPHA(11), BETA(15)
      COMPLEX WTS,S,9), Z, PHASE,H1,H2,GFCN(13,501)
      COMMON N,ALPHA1,ALPHA2,ALPHA3,BETA1,BETA2,BETA3,GAM2,ZSQ,MCA,A
      EQUIVALENCE (GFCN(1), E(1))
C
C-----------------------------------------------------------------------
C  THE FORCE CONSTANTS ALPHA1, ALPHA2, ...., GAM2 ARE LISTED IN UNITS OF
C  1E**2/R0**3), WHERE R0 = A*2.  A TAPE ON A5 IS NEEDED FOR OUTPUT .
      READ (5,105) A, WTO, WLF, WR, C11, C12, C44, MCA
      CALL MODEL (4., A, WTO, WLO, WR, C11, C12, C44, MCA, SSQ, ALPHA1,
     1ALPHA2, ALPHA3, BETA1, BETA2, BETA3, GAM3)
  102 FORMAT (8F9.4)
C-----------------------------------------------------------------------
C
C  THE FOLLOWING ARE THE 24 THREE-DIMENSIONAL ORTHOGONAL MATRICES THAT
C  REPRESENT THE 24 'PROPER' ROTATIONS OF THE O-H GROUP.  THESE MATRICES
C  ARE USEFUL, FOR SUMS OVER THE ENTIRE FIRST BRILLOUIN ZONE CAN BE
C  REDUCED TO A CONSIDERATION OF ONLY 1/48 OF THIS ZONE, CALLED THE
C  'FUNDAMENTAL WEDGE' BELOW. IT IS, THEREFORE, POSSIBLE TO GREATLY CON-
C  SERVE COMPUTATION TIME IN THE CALCULATION OF GREEN'S FUNCTIONS BY
C  EXPLOITING THE FACT THAT THE EIGENVECTORS AND EIGENVALUES FOR THE
C  PHONON BRANCHES WILL HAVE THE POINT-GROUP SYMMETRY OF THE CRYSTAL.
C
      DATA S(S(1,I,J),J=1,3),I=1,3)/
C
     1                          1.,  0.,  0.,
     2                          0.,  1.,  0.,
     3                          0.,  0.,  1./
C
C  THESE ARE THE 180 DEGREE ROTATIONS ABOUT X, Y, AND Z --
C
      DATA (((S(L,I,J),J=1,3),L=2,4),I=1,3)/
C
     1    1.,  0.,  0.,      -1.,  0.,  0.,      -1.,  0.,  0.,
     2    0., -1.,  0.,       0.,  1.,  0.,       0., -1.,  0.,
     3    0.,  0., -1.,       0.,  0., -1.,       0.,  0.,  1./
C
C  THESE ARE THE 120 DEGREE ROTATIONS--
C
      DATA (((S(L,I,J),J=1,3),L=5,7 ),I=1,3)/
C
     1    0.,  1.,  0.,       0.,  0.,  1.,       0., -1.,  0.,
     2    0.,  0.,  1.,       1.,  0.,  0.,       0.,  0., -1.,
     3    1.,  0.,  0.,       0.,  1.,  0.,       1.,  0.,  0./
C
      DATA (((S(L,I,J),J=1,3),L=8,10),I=1,3)/
C
     1    0.,  0.,  1.,       0.,  1.,  0.,       0.,  0., -1.,
     2   -1.,  0.,  0.,       0.,  0., -1.,       1.,  0.,  0.,
     3    0., -1.,  0.,      -1.,  0.,  0.,       0., -1.,  0./
```

I-2

```
      DATA (((S(L,I,J),J=1,3),L=11,12),I=1,3)/
C
     1    0., -1.,  0.,       0.,  0., -1.,
     2    0.,  0.,  1.,      -1.,  0.,  0.,
     3   -1.,  0.,  0.,       0.,  1.,  0./
C
C  THESE ARE THE 90 DEGREE ROTATIONS ABOUT X, Y, AND Z --
C
      DATA (((S(L,I,J),J=1,3),L=13,15),I=1,3)/
C
     1    1.,  0.,  0.,       1.,  0.,  0.,       0.,  0.,  1.,
     2    0.,  0.,  1.,       0.,  0., -1.,       0.,  1.,  0.,
     3    0., -1.,  0.,       0.,  1.,  0.,      -1.,  0.,  0./
C
      DATA (((S(L,I,J),J=1,3),L=16,18),I=1,3)/
C
     1    0.,  0., -1.,       0.,  1.,  0.,       0., -1.,  0.,
     2    0.,  1.,  0.,      -1.,  0.,  0.,       1.,  0.,  0.,
     3    1.,  0.,  0.,       0.,  0.,  1.,       0.,  0.,  1./
C
C  THESE ARE 180 DEGREE ROTATIONS ABOUT (110) AXES --
C
      DATA (((S(L,I,J),J=1,3),L=19,21),I=1,3)/
C
     1    0., -1.,  0.,       0.,  1.,  0.,      -1.,  0.,  0.,
     2   -1.,  0.,  0.,       1.,  0.,  0.,       0.,  0., -1.,
     3    0.,  0., -1.,       0.,  0., -1.,       0., -1.,  0./
C
      DATA (((S(L,I,J),J=1,3),L=22,24),I=1,3)/
C
     1   -1.,  0.,  0.,       0.,  0., -1.,       0.,  0.,  1.,
     2    0.,  0.,  1.,       0., -1.,  0.,       0., -1.,  0.,
     3    0.,  1.,  0.,      -1.,  0.,  0.,       1.,  0.,  0./
C
      DATA(KAP1(M),ALPHA(M),KAP2(M),BETA(M),LL1(M),LL2(M),LL3(M),M=1,13)
C
     1/1,1,1,1,0.,0.,0.,2,1,2,1,0.,0.,0.,3,1,2,1,0.,1.,0.,1,3,2,2,0.,1.,
     20.,3,1,2,1,0.,...,0.,2,1,2,1,1.,1.,0.,2,3,2,3,1.,1.,0.,2,1,2,2,1.,
     31.,0.,2,3,2,1,1.,1.,0.,2,1,1,1,.5,.5,.5,2,1,1,2,.5,.5,.5,2,1,1,1,
     41.,1.,1.,2,1,3,2,1.,1.,1./
C
C  THE FOLLOWING ALPHAMERIC DATA WILL BE USEFUL FOR WRITE-OUT FORMAT--
C
      DATA     D,SUFF,SYMB/4H REAL ,4H IMAG ,2H5T,2HND,2HRD,10H5HTH,1HA,
     11HB,1HP,1HF,1HH,1HP,1HQ,1HR,1HS,1HC,1HO,1HU,1HV/
C
C  UNDER EVERY ROTATION S(L), L = 1,24, THE BASIS ATOMS (CA, F1, F2) ARE
C  PERMUTED IN SUCH A WAY THAT CA'S STAY CA'S, AND F'S STAY F'S. HOWEVER
C  IT IS POSSIBLE FOR F1 TO BECOME F2 UNDER SUCH A ROTATION, AND KPERM
C  JUST DESCRIBES WHAT EACH BASIS INDEX BECOMES UNDER ROTATION S. NOTICE
C  THAT WE HAVE ARRANGED THE ROTATION MATRICES IN SUCH A WAY THAT THE
C  FIRST 12 OF THEM PRESERVE (CA,F1,F2), WHEREAS THE LAST 12 INTERCHANGE
C  THE FLUORINES.
C
      DATA ((KPERM(L,K),L=1,24),K=1,3)/24*1,12*2,12*3,12*3,12*2/
```

I-3

```
      N = 40
      EN = N
      EN3 = EN**3
      NN = N+1
      N1 = N/3 + 1
      N3 = 3*N/4 + 1
      PI = 3.14159265
      EPS = .005
C
C  WE SHALL CALCULATE GREEN'S FUNCTIONS WITH A SMALL NEG. IMAG. PART IN
C  THE COMPLEX OMEGA**2 PLANE.  THERE ARE 13 SUCH GREEN'S FUNCTIONS THAT
C  ARE NEEDED IF THE IMPURITY SUBSPACE IS DEFINED BY AN XY8 COMPLEX CON-
C  TAINING A ++ ION AND ITS EIGHT NEAREST-NEIGHBOR FLUORINES.  THESE 13
C  GREEN'S FUNCTIONS WILL BE LABELED BY AN INDEX M = 1, 2, 3, ...., 13.
C  THE FOLLOWING CHART GIVES THE INDICES THAT DEFINE WHAT THESE GREEN'S
C  FUNCTIONS ARE--I.E., IT GIVES THE VALUES OF KAP1, ALPHA, ...ETC. FOR
C  EACH OF THE 13 FUNCTIONS G(L1,KAP1,ALPHA, L2,KAP2,BETA, OMEGA**2-
C  I*ETA).  THE VECTOR (LL1, LL2, LL3) IS JUST R(L2,KAP2) - R(L1,KAP1),
C  IN DIMENSIONLESS UNITS FOR WHICH THE LATTICE CONSTANT (A) = 2.
C
C        M      G   KAP1   ALPHA KAP2   BETA    LL1    LL2    LL3
C-----------------------------------------------------------------------
C            .      .      .      .      .      .      .      .
C        1   .  A   .  1   .  1   .  3   .  1   .  0   .  0   .  0
C            .      .      .      .      .      .      .      .
C        2   .  B   .  2   .  1   .  3   .  1   .  0   .  0   .  0
C            .      .      .      .      .      .      .      .
C        3   .  H   .  3   .  1   .  2   .  1   .  0   .  1   .  0
C            .      .      .      .      .      .      .      .
C        4   .  F   .  3   .  3   .  2   .  3   .  0   .  1   .  0
C            .      .      .      .      .      .      .      .
C        5   .  H   .  3   .  1   .  3   .  3   .  0   .  1   .  0
C            .      .      .      .      .      .      .      .
C        6   .  P   .  2   .  1   .  2   .  1   .  1   .  1   .  0
C            .      .      .      .      .      .      .      .
C        7   .  Q   .  2   .  3   .  3   .  3   .  1   .  1   .  0
C            .      .      .      .      .      .      .      .
C        8   .  R   .  3   .  1   .  2   .  2   .  1   .  1   .  0
C            .      .      .      .      .      .      .      .
C        9   .  S   .  2   .  3   .  2   .  1   .  1   .  1   .  0
C            .      .      .      .      .      .      .      .
C       10   .  C   .  3   .  1   .  1   .  1   . .5   . .5   . .5
C            .      .      .      .      .      .      .      .
C       11   .  O   .  3   .  1   .  1   .  2   . .5   . .5   . .5
C            .      .      .      .      .      .      .      .
C       12   .  U   .  2   .  1   .  3   .  1   .  1   .  1   .  1
C            .      .      .      .      .      .      .      .
C       13   .  V   .  3   .  1   .  3   .  2   .  1   .  1   .  1
C            .      .      .      .      .      .      .      .
C-----------------------------------------------------------------------
C
C  THE 13 COMPLEX GREEN'S FUNCTIONS ARE SPECIFIED BY GFCN(M,I), WHERE
C  M RUNS FROM 1 TO 13, AND I (WHICH CORRESPONDS TO OMEGA**2, IN INCRE-
C  MENTS OF .005 X BANDWIDTH) RUNS FROM 1 TO 501 (2.5 TIMES THE BAND).
C  THE CMPLX ARRAY GFCN IS EQUIVALENT WITH G--WE SHALL USE G(1,M,I) AND
```

I-4

```
C  G(2,M,I) RESPECTIVELY FOR THE REAL AND IMAGINARY PART OF THE GREEN'S
C  FUNCTION G(M, OMEGA**2 - I*ETA).  THE FUNCTIONS G(2,M,I) WILL BE NON-
C  ZERO ONLY IN THE BAND (I.E., FOR I BETWEEN 1 AND 201).  THE REAL PART
C  OF THE COMPLEX GREEN'S FUNCTION, G(1,M,I), DOES NOT VANISH OUTSIDE
C  THE BAND, AND IS (1/PI) TIMES THE HILBERT TRANSFORM OF THE IMAG PART,
C  G(2,M,I).
C
C
C  THE METHOD OF CALCULATION OF THE DENSITY OF SQUARED STATES, AND OF
C  THE 13 GREEN'S FUNCTIONS A,B,H,F,...,U,V IS THE 'HISTOGRAM' TECHNIQUE.
C  EACH OF THESE FUNCTIONS INVOLVES A SUM OVER (K,SIGMA), WHERE K ARE
C  THE VECTORS IN THE 1ST BRILLOUIN ZONE, AND SIGMA ARE THE PHONON
C  BRANCH INDICES.  BECAUSE THE SUMS TO BE EVALUATED INVOLVE DELTA-
C  FUNCTIONS, THEY ARE ACTUALLY EQUIVALENT TO SURFACE INTEGRALS, AND
C  THUS BEHAVE (ARITHMETICALLY, ANYWAY) MORE LIKE DERIVATIVES THAN INTE-
C  GRALS.  THUS, IT IS NECESSARY TO USE A FINE MESH IN THE BRILLOUIN
C  ZONE.   THE METHOD OF COMPUTATION INVOLVES A SUMMATION OVER 1/48 OF
C  THE B.Z. (SEE BELOW).  AT EVERY POINT K, THE SQUARED FREQUENCIES
C  (NORMALIZED TO GO FROM 0 TO 1), AND THE (COMPLEX) COLUMN EIGENVECTORS
C  ARE CALCULATED BY SUBROUTINE 'ASPACE'.  EACH OMEGA**2 IS THEN MULTI-
C  PLIED BY 200, 1.5 IS ADDED, AND DECIMAL PART IS TRUNCATED, TO SORT
C  EVERY SQUARED FREQUENCY IN THE 9 BRANCHES INTO A 'BIN', LABELED FROM
C  1 TO 201.   THEN, FOR EACH GREEN'S FUNCTION, THE CONTRIBUTIONS CALCU-
C  LATED AT POINT K ARE DROPPED INTO THE APPROPRIATE BINS.  THE WIDTH
C  OF THE 'BINS' AND THE REPRESENTATION OF THE DELTA-FUNCTION SHOULD BE
C  COMPATIBLE.  FURTHERMORE, THE BINS SHOULD BE WIDE ENOUGH SO THAT
C  MANY CONTRIBUTIONS WILL BE DROPPED INTO EACH ONE, ON THE AVERAGE.
C
C---------------------- THE BRILLOUIN ZONE -----------------------------
C
C  THE FIRST BRILLOUIN ZONE IS THE FAMILIAR OCTAHEDRON, TRUNCATED BY SIX
C  PLANES--THIS LEAVES A GEOMETRICAL SOLID WITH 8 QUASI-HEXAGONAL FACES,
C  AND SIX SQUARE FACES.  THE VECTORS TO THE CENTERS OF THE 'HEXAGONAL'
C  FACES ARE OF THE FORM (PI/2)*(1,1,1), AND TO THE CENTERS OF THE
C  SQUARE FACES, OF THE FORM PI*(1,0,0).  WE ARE GOING TO CONSIDER A
C  REGION OF THE 1ST B.Z. DEFINED BY--
C
C         1)  KX, KY, KZ  ALL POSITIVE INTEGERS
C         2)  KX, KY, KZ ALL EVEN, OR ALL ODD
C         3)  KZ.LE.KY.LE.KX
C         4)  KX.LE.N,  KY.LE.N,  KZ.LE.N
C         5)  (KX + KY + KZ).LE.3N/2
C
C  THIS REGION OCCUPIES 1/48 OF THE 1ST B.Z.   FOR EVERY VECTOR K IN
C  THIS REGION, WE CAN FORM THE 'STAR OF K'--THIS WILL PRODUCE (EXCEPT
C  FOR POINTS, LINES, ETC. OF HIGH SYMMETRY) 48 DISTINCT VECTORS.  AT
C  EACH OF THESE 48 PTS. IN K-SPACE, THE EIGENFREQUENCIES ARE THE SAME.
C
C  FOR N = 40, THERE ARE 64,000 POINTS IN THE BRILLOUIN ZONE.  IN THE
C  FUNDAMENTAL 1/48 WEDGE, THERE ARE 1444 DISTINCT POINTS THAT MUST BE
C  CONSIDERED IN CARRYING OUT AN INTEGRATION OVER K.
C
C  SOME OF THESE 1444 POINTS LIE ON LINES OR FACES OF THE 'FUNDAMENTAL
C  WEDGE', AND THUS LIE ONLY FRACTIONALLY IN THAT 1/48 ZONE.  FOR A
C  GIVEN POINT K, WE MUST TEST TO SEE WHETHER IT LIES ON SUCH LINES OR
C  FACES TO DETERMINE ITS MULTIPLICITY--I.E., TO DETERMINE HOW MANY VEC-
```

I-5

```
C   TORS LIE IN THE 'STAR OF K'.  THE MULTIPLICITY OF A K-VECTOR IS, OF
C   COURSE, JUST A MEASURE OF THE ORDER OF THE 'GROUP OF THE K-VECTOR'.
C   THERE ARE 6 TESTS FOR POINTS, LINES, AND FACES OF HIGH SYMMETRY THAT
C   ARE SUFFICIENT TO DETERMINE THE MULTIPLICITY OF EVERY K-VECTOR IN THE
C   FUNDAMENTAL WEDGE.  EACH TEST HAS AN ASSOCIATED FRACTION--1/2 OR 1/6.
C   FOR ANY GIVEN POINT K, THOSE FRACTIONS FOR EACH 'TEST' WHICH THE
C   POINT K SATISFIES ARE MULTIPLIED TOGETHER TO YIELD A RESULT, Z1.
C   48*Z1 THEN GIVES THE MULTIPLICITY OF THAT POINT.  THE TESTS ARE--
C
C         1) (KZ=0)  FACTOR = 1/2
C         2) (KY=0)  FACTOR = 1/2
C         3) (KX=0, OR KX=KY)  FACTOR = 1/2
C         4) (KX=KZ)  FACTOR = 1/6
C         5) (KX=KY OR KY=KZ, BUT NOT KX=KZ)  FACTOR = 1/2
C         6) (K IS ON THE LINE LK)  FACTOR = 1/2
C
C-----------------------------------------------------------------------
C
      DO 4 M = 1,17
      DO 4 I = 1,301
    4 G(2,M,I) = 0.
C
      DO 16 I = 1,201
   16 RHO(I) = 0.
C
C   THIS PROGRAM ASSUMES THAT THE MAXIMUM FREQUENCY IS WMAX = WLO (BASED
C   ON CAF2).  IF THAT IS NOT THE CASE, A MINOR CHANGE IS NECESSARY HERE.
      WMAX = WLO
      WMAX2 = WMAX**2
C
C-----------------------------------------------------------------------
C
      DO 1 KZ1 = 1,N1
         KZ = KZ1 - 1
         AC = PI*KZ/EN
         Z1=1.0
         IF(KZ1.EQ.1)  Z1 = Z1/2.0
C
      DO 1      KY1 = KZ1,N2,2
                KY = KY1 - 1
                AB = PI*KY/EN
                Z2 = Z1
                IF(KY1.EQ.1)  Z2 = Z2/2.0
C
      DO 1            KX1 = KY1,NN,2
                      KX = KX1 - 1
                      AA = PI*KX/EN
                      Z3 = Z2
                      IF(KX1.EQ.1.OR.KX1.EQ.NN)  Z3 = Z3/2.0
C
C   WE ARE ALREADY IN THE 1/48 REGION OF K-SPACE BECAUSE KZ.LE.KY.LE.KX.
C   FURTHERMORE, BECAUSE KY1 AND KX1 SKIP IN UNITS OF 2, THE TRIPLET KX,
C   KY, KZ ARE ALL EVEN OR ALL ODD.  WE CAN NOW TEST THE TRIPLET TO SEE
C   IF IT SATISFIES THE REMAINING CONDITION FOR BEING A K-POINT IN THE
C   FIRST BRILLOUIN ZONE --
C
```

I-6

```
                 IA = KX1 + KY1 + KZ1 - 3
                 IN = 3*N/2
                 IF(IA.GT.IN)  GO TO 1
C
C   THIS CHECKS TO SEE THAT THE HEXAGONAL FACE BOUNDARY HAS NOT BEEN
C   PASSED.  THE REMAINING MULTIPLICITY FACTORS ARE--
C
                 IF (KZ1.EQ.KX1)  GO TO 22
                 IF (KZ1.EQ.KY1.OR.KY1.EQ.KX1)  Z3 = Z3/2.0
                 GO TO 23
   22            Z3 = Z3/6.0
   23            IF((IA.EQ.IN).AND.(KY1.EQ.N1))  Z3 = Z3/2.0
C
C
C                    ********************************
C
C                    CALL KSPACE(KX,KY,KZ,WSIG,N,D)
C
C                    ********************************
C
C
      DO 45 J = 1,6
      A = WSIG(J)**2/WMAX2
      IF (A.GT.1.)  A = 1.
      BIN(J) = 200.*A + 1.5
      I = BIN(J)
      RHO(I) = RHO(I) + Z3
C
C   WE HAVE APPROXIMATED A DELTA FCN, DELTA(A), AS BEING A RECTANGULAR
C   SPIKE OF HEIGHT 1/EPS, AND EXTENDING FROM A - EPS/2 TO A + EPS/2.
C   THUS, EACH FREQUENCY CONTRIBUTES TO ONLY ONE POINT.
C
   45 CONTINUE
C
C   THE SQUARED FREQUENCIES IN THE NINE BANDS HAVE BEEN NORMALIZED TO GO
C   FROM 0.0 TO .99949949.  THE DENSITY OF SQUARED STATES WILL BE A SPEC-
C   TRUM THAT EXTENDS FROM 0 TO 1 IN OMEGA**2 SPACE.
C
C-----------------------------------------------------------------------
C
C   WE DESIRE TO CALCULATE 17 GREEN'S FUNCTIONS, M = 1,15 -- THESE ARE
C   SPECIFIED BY G(K1,J1,K2,J2) WITH K1,J1,K2,J2 DEFINED FOR M = 1,15.
C
      DO 2 T = 1,24
C
C   L = 1,24 (L,T) PERFORM A SUM OVER ALL 24 ROTATIONS OF THE GROUP 'O'
C   THE ROTATED K-VECTOR WILL HAVE COMPONENTS GIVEN BY ROTK(J).
C
            DO 5 L = 1,3
    5       ROTK(L) = S(L,1,I)*KA + T(L,2)*KB + S(L,3,I)*KC
C
            DO E M = E,1E
                 K1 = KAP1(M)
                 K2 = KAP2(M)
                 JE = ALPHA(M)
                 J2 = BETA(M)
C
```

I-7

```
               RDOTL = ROTK(1)*LL(1,M) + ROTK(2)*LL(2,M) + ROTK(3)*LL(3,M)
               Z = CMPLX(0., -RDOTL)
               PHASE = CEXP(Z)
C
               K11 = KPERM(T,K1)
               K22 = KPERM(T,K2)
C
               DO 6 J = 1,9
                    I = BIN(J)
C
      W1=S(L,J1,1)*W(1,K11,J)+S(L,J1,2)*W(2,K11,J)+S(L,J1,3)*W(3,K11,J)
      W2=S(L,J2,1)*W(1,K22,J)+S(L,J2,2)*W(2,K22,J)+S(L,J2,3)*W(3,K22,J)
C
                    X = Z3*REAL(PHASE*W1*CONJG(W2))
C
                    G(2,M,I) = G(2,M,I) + X
C
C   THE CONTRIBUTION FROM K AND -K PRODUCES A REAL NUMBER X.  BECAUSE
C   THE INVERSION OPERATION MERELY PRODUCES A COMPLEX CONJUGATE RESULT,
C   THE REALITY OF THE FUNCTION G(2,M,I) IS IMMEDIATELY APPARENT, AND IT
C   IS ONLY NECESSARY TO CONSIDER THE 'PROPER ROTATIONS' OF THE GROUP 'O'
C
C
    6          CONTINUE
C
    E     CONTINUE
C
    2 CONTINUE
C
    1 CONTINUE
C
C-----------------------------------------------------------------------
C
C
C   FOR 200 BINS/BAND, EXPERIENCE HAS SHOWN THAT THE RESULTANT GREEN'S
C   FCTNS ARE SOMEWHAT 'RAGGED' IF N IS ONLY 40.  THUS, THE IMAGINARY
C   PARTS CALCULATED ABOVE WILL BE SMOOTHED BY EXTENDING THE EFFECTIVE
C   WIDTH OF THE BINS TO .01 X BAND (ALTHOUGH THE ARGUMENT OMEGA**2 WILL
C   STILL ADVANCE IN INCREMENTS OF .005 X BAND) --
C
      DO 24 M = 1,15
      B = G(2,M,1)
      G(2,M,1) = .5*(B + G(2,M,2))
      DO ES I = 2,200
            A = G(2,M,I)
            D = G(2,M,I+1)
            G(2,M,I) = .5*(.5*B + A + .5*D)
            B = A
   ES CONTINUE
   24 G(2,M,201) = .5*(B + G(2,M,201))
C
      MASS(1) = MCA
      MASS(2) = 1.
      MASS(3) = 1.
C
      DO A M = 1,15
```

I-8

```
      K1 = KAP1(M)
      K2 = KAP2(M)
      DENOM = EPS*ENE*SQRT(MASS(K1)*MASS(K2))/(2.*PI)
      DO A I = 1,201
    A G(2,M,I) = G(2,M,I)/DENOM
C
      B = RHO(1)
      RHO(1) = .5*(B + RHO(2))
      DO 20 I = 2,200
            C = RHO(I)
            D = RHO(I+1)
            RHO(I) = .5*(.5*B + C + .5*D)
            B = C
   20 CONTINUE
      RHO(201) = .5*(B + RHO(201))
C
      SUM = 0.
      DENOM = EPS*ENE*4.
      DO 21 I = 1,201
      RHO(I) = 48.*RHO(I)/DENOM
   21 SUM = SUM + RHO(I)
      SUM = SUM/200.
C
C   THE FUNCTION G(2,M,I) IS THE IMAGINARY PART OF THE GREEN'S FUNCTION
C   EVALUATED WITH A SMALL NEGATIVE IMAG. PART IN THE COMPLEX OMEGA**2
C   PLANE.  WE WILL HAVE TO DIVIDE BY PI WHEN WE TAKE THE HILBERT TRANS-
C   FORM THAT GIVES THE REAL PART OF THE GREEN'S FUNCTION.  RHO IS THE
C   DENSITY OF SQUARED STATES, EACH BAND NORMALIZED TO GO FROM
C   OMEGA**2 = 0. TO 1.0. THE FUNCTION RHO IS ALSO NORMALIZED TO UNIT
C   AREA AS A FUNCTION OF OMEGA**2.
C
C   THE GREEN'S FUNCTIONS CALCULATED BY THE PROGRAM ARE IN UNITS OF
C   1/(MASS PL * OMEGA MAX**2).
C
      WRITE (6,101) (I,RHO(I), I = 1,201), SUM
  101 FORMAT(1H1,45X,29HTHE DENSITY OF SQUARED STATES,S1/1,5E9,14,1H1,10
     1X,6HRHO,4X,//,201(5DX,I5,1PE11.5,/),//,5DX,7HAREA = ,E14.4)
C
      DO 50 M = 1,15
      D2 = D(2)
   50 WRITE (6,100) Q2,M,SUFF(M),KAP1(M),ALPHA(M),KAP2(M),BETA(M),LL(1,M)
     1,LL(2,M),LL(3,M),SYMB(M),Q2,D2,Q2,Q2,Q2,I1,G(2,M,I),I=1,205)
C
  100 FORMAT(1H1,//,55X,20HTHE FOLLOWING IS THE,A8,11HPART OF THE,15,A2,
     1EH GREEN'S FCN,/,28X,7HG(KAP1=,I1,7H,ALPHA=,I1,8H,KAP2=,I1,6H,BET
     2A=,I1,10H,(R2-R1)=(,F5.1,1H,,F5.1,1H,,F5.1,14H),OMEGA**2) = ,A1,
     3//,  8X,11HI(1H-1,/,4X,1H1,5I2X,1H1,5X,A8,5H1G1,5X,2H1 1,/,4X,11D(1
     44H-I,/,9X,1H1,5I20X,1H1,1X1,/,200(9X,1H1,9I14,1PE14.4,2X,2H1 1,/,
     59X,1H1,5I20X,1H1,1X1,/),4X,11D(1H-1))
C
C
C---------CALCULATION OF THE HILBERT TRANSFORM FUNCTIONS --------------
C
C   THE INTEGRATIONS INVOLVED IN THE CALCULATIONS OF THE HILBERT TRANS-
C   FORMS ARE CARRIED OUT WITH SIMPSON'S RULE.  THE CODE TERMS GIVE CON-
C   TRIBUTIONS TO THE INTEGRAL IN THE REGION (A-EPS, A+EPS) WHERE THE
```

I-9

```
C   INTEGRAND HAS A SINGULARITY CAUSED BY THE DENOMINATOR.  THIS CORREC-
C   TION FACTOR IS GIVEN BY  -2*EPS*G(2,M,1), AND THIS DERIVATIVE IS
C   CALCULATED AS THE AVERAGE VALUE FROM SUCCESSIVE, OVERLAPPING, PARA-
C   BOLIC FITS.
C
        DO 10 M = 1,11
C
        DO 10 I = 1,501
C
        G(1,M,I) = 0.
C
              IF(I.EQ.1)  CORR=G(2,M,1) - 4.*G(2,M,2)
              IF(I.EQ.2)  CORR = (7.*G(2,M,2)-5.*G(2,M,3)+G(2,M,4))/2.0
              IF(I.GT.2.AND.I.LT.200) CORR = (G(2,M,I+2) - G(2,M,I-2) +
     1                          5.*(G(2,M,I-1) - G(2,M,I+1)))/3.0
              IF(I.EQ.200) CORR = (5.*G(2,M,199) - G(2,M,198) - 5.*G(2,M,
     1                          200))/2.0
              IF(I.EQ.201) CORR = 4.*G(2,M,200) - G(2,M,199)
              IF (I.GT.201)  CORR = 0.
        X = I-1
        I1 = I-2
              IF (I1.GT.201) I1=200
        I2 = I+1
              IF (I-2) 12,12,13
C
     13 DO 11 J = 1,I1
        Y = J-1
     11 G(1,M,I) = G(1,M,I) + G(2,M,J)*(3.*(Y-X) + .5)/((Y-X)*(Y-X+.5))
     1               + G(2,M,J+1)*(3.*(Y-X) + 2.5)/((Y-X+1.)*(Y-X+.5))
C
     12       IF(I2-T) 15,14,16
C
     14 DO 17 J = I2,200
        Y = J-1
     17 G(1,M,I) = G(1,M,I) + G(2,M,J)*(3.*(Y-X) + .5)/((Y-X)*(Y-X+.5))
     1               + G(2,M,J+1)*(3.*(Y-X) + 2.5)/((Y-X+1.)*(Y-X+.5))
C
     15 G(1,M,I) = -(1./X.)*G(1,M,I) + CORR
        G(1,M,I) = G(1,M,I)/PI
C
     10 CONTINUE
C
C-------------------------------------------------------------------------
C
        WRITE (8)  GFCN
        WRITE (8)  RHO
        REWIND 8
C
        DO 80 M = 1,11
        Q1 = Q(I)
     80 WRITE (6,100) Q1,M,SUFF(M),KAP1(M),ALPHA(M),KAP2(M),BETA(M),LL1(M)
       1,LL2(M),LL3(M),SYMB(M),(Q1,Q1,Q1,Q1,Q1,(1,G(1,M,I),I=1,5CO)
C
C
         ETURN
        END
```

II-1

```
      SUBROUTINE KSPACE(RX,RY,RZ,OMEGN,N,NUT
C
C
C   THIS PROGRAM WILL CALCULATE THE FOURIER TRANSFORMED DYNAMICAL MATRIX
C   FOR THE FLUORITE LATTICE (E.G., CAF2) AND DIAGONALIZE IT, WITH THE
C   FOLLOWING OUTPUT OPTIONS--
C
C     1) NU=0     NO WRITTEN OUTPUT
C     2) NU=1     EIGENFREQUENCIES (IN CM-1)
C     3) NU=2     EIGENFREQ'S (CM-1), AND COLUMN EIGENVECTORS
C     4) NU=3     THE D(R) MATRIX BEFORE DIAGONALIZATION, CERTAIN
C                 MATRICES A(1), A(2), A(3) RELATED TO COULOMB SUMS,
C                 AND THE EIGENFREQUENCIES AND COLUMN EIGENVECTORS
C
C   THE K-VECTOR IS SPECIFIED BY GIVING THREE (FLOATING PT.) NUMBERS RX,
C   RY, AND RZ, AS--
C
C                    K-VECTOR = (PI/N)*(RX, RY, RZ)
C
C   IN UNITS OF (1/RO), WHERE RO = A/2 (I.E., RO IS THE FLUORINE-FLUORINE
C   SEPARATION, WHICH IS HALF THE LATTICE CONSTANT 'A').  OMEGA(9) IS AN
C   ARRAY CONTAINING THE FINAL EIGENFREQUENCIES (CM-1) FOR THE WAVE-VEC-
C   TOR K, AND THE (COMPLEX) ARRAY W(3,3,9) = W(ALPHA,KAPPA,SIGMA) GIVES
C   THE ORTHONORMALIZED COLUMN EIGENVECTORS.  OMEGA(9), AND W(3,3,9) MUST
C   BE ASSIGNED APPROPRIATE DIMENSION SPACE IN THE MAIN PROGRAM THAT
C   CALLS 'KSPACE'.  N REPRESENTS THE SIZE OF THE BRILLOUIN ZONE MESH,
C   AND MUST BE LISTED, ALONG WITH NUMEROUS FORCE CONSTANTS, IN A COMMON
C   STATEMENT WITH THE MAIN PROGRAM.
C
C   E (THE ELECTRONIC CHARGE), RO (THE FL-F DISTANCE), AND MFL (THE
C   FLUORINE MASS) ARE ALL TAKEN TO BE UNITY.  LATER, TO OBTAIN RESULTS
C   FOR THE PHONON EIGENFREQUENCIES IN CM-1, IT WILL BE NECESSARY TO MUL-
C   TIPLY VALUES OF OMEGA**2 BY A SCALE FACTOR, GIVEN BY
C
C                 SCALE = 2 E**2/(PI**2 FLMASS C**2 A**3).
C
C   THE 'PRIMITIVE VECTORS' FOR THE REAL AND RECIPROCAL LATTICES ARE,
C   RESPECTIVELY, (IN THE DIMENSIONLESS UNITS ADOPTED HERE)--
C
C        T1 = (0,1,1)          T2 = (1,0,1)          T3 = (1,1,0)
C
C        B1 = (-1,1,1)/2       B2 = (1,-1,1)/2       B3 = (1,1,-1)/2
C
C   'RECIPROCAL LATTICE VECTORS' ARE INTEGER COMBINATIONS OF THE VECTORS
C   B1, B2, AND B3.  THE MOST GENERAL RECIPROCAL LATTICE VECTOR IS OF THE
C   FORM  KLAMBDA = PI*(H1, H2, H3), WHERE H1, H2, H3 IS A TRIPLET OF IN-
C   TEGERS THAT ARE ALL EVEN, OR ALL ODD.  THE MOST GENERAL REAL LATTICE
C   VECTOR IS OF THE FORM  RLATTICE = (H1, H2, H3), WHERE H1+H2+H3 = EVEN
C
C-------------------------------------------------------------------------
C
      DIMENSION V(3), U(3), B(3), B(3,3), A(2,3), OMEGA2(V), OMEGA(V)
      REAL KX,KY,KZ,R(3),RSQ, MCA, MFC2
      COMPLEX PHASE, D(3,3,3,3), DK(V,V), A(9,3,3), Z, W(9,V),W(3,3,V)
      LOGICAL HTEST
```

II-2

```
      EQUIVALENCE (DK(1), D(1))
      COMMON N,ALPHA1,ALPHA2,ALPHA3,BETA1,BETA2,BETA3,GAM2,ZSQ,MCA,A
C
C-------------------------------------------------------------------------
C
C   THE 'BASIS VECTORS' ARE DENOTED BY B(3,3) = B(ALPHA,KAPPA), WHERE
C   KAPPA = 1, 2, 3 FOR CA, F1, AND F2 RESPECTIVELY.
C
      DATA B/ .5, .5, .5,      0., 0., 0.,      1., 0., 0./
C                CA               F1               F2
C     KAPPA =    1                2                3
C
C   THE SHORT RANGE CA-F NEAREST NEIGHBOR INTERACTION HAS THE FORM--
C
C                       .                            .
C                       . ALPHA1   BETA 1   BETA 1  .
C                       .                            .
C                       .                            .
C    PHI(CA,F2) = -     . BETA 1   ALPHA1   BETA 1  .    (FORCE CONSTANT MATRIX
C                       .                            .     FOR L = (1,1,1)/2.)
C                       .                            .
C                       . BETA 1   BETA 1   ALPHA1  .
C                       .                            .
C
C   THE SHORT RANGE CA-CA NEAREST NEIGHBOR INTERACTION HAS THE FORM--
C
C                       .                            .
C                       . BETA 2   GAMMA2     0.    .
C                       .                            .
C                       .                            .
C    PHI(CA,CA) = -     . GAMMA2   BETA 2     0.    .    (FORCE CONSTANT MATRIX
C                       .                            .     FOR L = (1,1,0).)
C                       .                            .
C                       .   0.       0.     ALPHA2  .
C                       .                            .
C
C   THE SHORT RANGE F1-F2 NEAREST NEIGHBOR INTERACTION HAS THE FORM--
C
C                       .                            .
C                       . ALPHA3     0.       0.    .
C                       .                            .
C                       .                            .
C    PHI(F1,F2) = -     .   0.     BETA 3     0.    .    (FORCE CONSTANT MATRIX
C                       .                            .     FOR L = (1,0,0).)
C                       .                            .
C                       .   0.       0.     BETA 3  .
C                       .                            .
C
C   ALPHA1, ALPHA2, ALPHA3, BETA1, ...ETC. ARE THE SHORT RANGE FORCE CON-
C   STANTS FOR THE CAF2  LATTICE AS DEFINED IN THE PAPER BY GANESAN AND
C   SRINIVASAN, CAN. JOURN. OF PHYSICS, 40,74-90. SOME OF THE CONSTANTS
C   ARE SET EQUAL TO ZERO IN THE MODELS OF GANESAN AND SRINIVASAN (BE-
C   CAUSE OF A LACK OF ENOUGH EXPERIMENTAL, PHYSICAL PARAMETERS).  HOW-
C   EVER, ALL OF THE NEAREST-NEIGHBOR FORCE CONSTANTS THAT RESULT FROM
C   GENERAL GROUP-THEORETICAL SYMMETRY ARGUMENTS HAVE BEEN RETAINED IN
C   WRITING THE PROGRAM, SINCE A LATER MODEL MIGHT BECOME AVAILABLE WITH
```

II-3

```
C  DIFFERENT VALUES FOR THE SHORT-RANGE FORCE-CONSTANTS.  FURTHERMORE,
C  THIS WILL MAKE THE PROGRAM MORE VERSATILE FOR POSSIBLE APPLICATION
C  TO OTHER FLUORITES.  ZSQ IS THE SQUARE OF THE 'EFFECTIVE CHARGE' Z.
C  THE FORCE CONSTANTS ARE MULTIPLES OF E**2/R0**3.
C
C  THE SELF FORCE-CONST MATRICES FOR L = (0,0,0) ARE OBTAINED FROM THE
C  CONDITION ON TRANSLATIONAL INVARIANCE, AND ARE ALL MULTIPLES OF THE
C  UNIT DYAD--
C
C                                                                : 1 0 0 :
C                                                                :       :
C     PHI(F1,F1) = PHI(F2,F2) = (2*ALPHA3+4*BETA3+4*ALPHA1)      : 0 1 0 :
C                                                                :       :
C                                                                : 0 0 1 :
C
C                                                            : 1 0 0 :
C                                                            :       :
C     PHI(CA,CA) = ( 8 ALPHA1 + 4 ALPHA2 + 8 BETA2 )         : 0 1 0 :
C                                                            :       :
C                                                            : 0 0 1 :
C
C  REFERRING TO PP. 85-88 IN GANESAN,SRINIVASAN, THE FORCE CONSTANT
C  BETA1 BECOMES DEPENDENT UPON THE SQUARE OF THE MOMENTUM--
C
      C = .5
      BET1 = BETA1*(1. - C*(KX**2 + KY**2 + KZ**2)/EN**2)
C
      MAX = 9
      PI = 3.1415927
      RADPI = 1.7724539
      EN = N
C
C
      K(1) = PI*KX/EN
      K(2) = PI*KY/EN
      K(3) = PI*KZ/EN
C
C
C-----------------------------------------------------------------------
C
C  THE INITIAL ENTRIES STORED IN D(J1,KAP1,J2,KAP2) WILL BE RELATED TO
C  THE NON COULOMB, SHORT-RANGE FORCE CONTRIBUTIONS.  KAPPA = 1,2,3 WILL
C  CORRESPOND TO CA, F1, F2, AND J1, J2, AND J3 ARE CARTESIAN INDICES.
C
      DO 1  J1 = 1,3
            J2 = J1 + 1 - (J1/3)*3
            J3 = J2 + 1 - (J2/3)*3
C
C  J1,J2,J3 FORM A CYCLIC SEQUENCE--I.E. 1,2,3 OR 2,3,1 OR 3,1,2.
C
            D(J1,1,J1,1) = 2.*ALPHA1 + BETA2*(2.-COS(K(J1))*(COS(K(J2))
     1                     + COS(K(J3)))) + ALPHA2*(1. - COS(K(J2))*
     2                     COS(K(J3)))
C
```

II-4

```
            D(J2,1,J1,1) = GAM2*SIN(K(J2))*SIN(K(J3))
            D(J3,1,J2,1) = D(J2,1,J3,1)
C
C
            D(J1,2,J1,2) = 2.*(ALPHA3 + 2.*BETA3 + 2.*ALPHA3)
            D(J2,2,J3,2) = (0.0, 0.0)
            D(J3,2,J2,2) = (0.0, 0.0)
C
C
C           D(I,3,J,3) IS EQUAL TO D(I,2,J,2)
C
C
            D(J1,1,J1,2) = 2.*ALPHA1*CMPLX(COS(.5*K(1))*COS(.5*K(2))*COS
     1                     (.5*K(3)), SIN(.5*K(1))*SIN(.5*K(2))*SIN(.5*
     2                     K(3)))
C
            D(J2,1,J3,2) = -2.*BET1 *CMPLX(COS(.5*K(J1))*SIN(.5*K(J2))
     1                     *SIN(.5*K(J3)), SIN(.5*K(J1))*COS(.5*K(J2))
     2                     *COS(.5*K(J3)))
C
            D(J3,1,J2,2) = D(J2,1,J3,2)
C
C
C           D(I,3,J,3) IS THE CMPLX CONJG OF D(I,1,J,2)
C
C
            D(J1,2,J1,3) = -2.*(ALPHA3*COS(K(J1))+BETA3*(COS(K(J2)) +
     1                     COS(K(J3))))
            D(J2,2,J3,3) = (0.,0.)
            D(J3,2,J2,3) = (0.,0.)
C
    1 CONTINUE
C
C  LATER, THESE QUANTITIES MUST BE MULTIPLIED BY FACTORS OF CHARGE AND
C  SQUARE ROOTS OF MASS.  CF. EQUATIONS THAT TERMINATE ON STATEMENT 54.
C
C-----------------------------------------------------------------------
C
C
      KSQ = KX**2 + KY**2 + KZ**2
      IF(KSQ.EQ.0.)  K(1) = 1.E-10
C
C  IF K = (0,0,0), THEN THE COULOMBIC CONTRIBUTION TO D IS NOT UNIQUELY
C  DEFINED--AS K APPROACHES THE ORIGIN, THE LIMIT OF THE COULOMBIC PART
C  OF D DEPENDS UPON THE DIRECTION OF APPROACH TO K = 0.  FOR VERY SMALL
C  K, WE GET A TENSOR THAT SHOWS CLEARLY THE PHENOMENON OF A SPLITTING
C  OF THE DEGENERACY  (LONGITUDINAL AND TRANSVERSE) FOR THE INFRARED
C  ACTIVE OPTIC VIBRATION. FOR CONVENIENCE, WE HAVE ARBITRARILY ARRANGED
C  THAT IF K = (0,0,0), WE SHALL CHOOSE THIS DIRECTION OF APPROACH TO BE
C  ALONG THE X-AXIS.  THIS IS DONE BY SETTING K(1) =1.E-10 IF KSQ
C  IS EQUAL TO ZERO.
C
C
C-----------------------------------------------------------------------
```

II-5

```
C  NEXT, WE WILL EVALUATE THE COULOMB CONTRIBUTION TO THE D MATRICES.
C  THE METHOD EMPLOYED FOR CALCULATING THE COULOMB CONTRIBUTION TO THE
C  MATRIX D USES TECHNIQUES DEVELOPED BY NIJBOER AND DE WETTE  (IN PAR-
C  TICULAR, REFER TO 'ON THE CALCULATION OF LATTICE SUMS,' PHYSICA, VOL
C  XXIII, 309-321, 1957).
C
C  THE ENTIRE MATRIX D-COUL(K,KAP1,KAP2)  CAN BE CALCULATED FROM A
C  KNOWLEDGE OF THREE SYMMETRIC DYADS, SO WE WILL FOCUS OUR ATTENTION
C  BELOW ON THE CALCULATION OF THREE MATRICES, X(1), X(2), AND X(3).
C  WE WILL PROCEED TO CALCULATE THE UPPER TRIANGULAR HALF OF THESE THREE
C  MATRICES, WHICH HAVE THE FOLLOWING SIGNIFICANCE--THEY ARE THE COULOM-
C  BIC DYADS THAT FIT INTO THE TOTAL D-COUL(K,KAP1,KAP2) MATRIX AS
C  FOLLOWS--
C
C
C
C                         CA        F1        F2
C                     :-------------------------:
C                     :       : X X X :         :
C                  CA :       :   X X :         :    MATRIX X(1) FOR (CA-F1)
C                     :       :     X :         :
C                     :-------------------------:
C                     :       : X X X :         :
C             D =  F1 :       :   X X :         :    MATRIX X(2) FOR (F1-F1)
C                     :       :     X :         :
C                     :-------------------------:
C                     :       : X X X :         :
C                  F2 :       :   X X :         :    MATRIX X(3) FOR (F2-F1)
C                     :       :     X :         :
C                     :-------------------------:
C
C  THE RELATION BETWEEN D-COUL AND THE THREE X-MATRICES BECOMES CLEAR
C  FROM CALCULATION STATEMENTS BELOW.
C
C  CLEAR THESE MATRICES TO ZERO INITIALLY--
C
      DO 99 J1 = 1,3
      DO 99 J2 = 1,3
      DO 99 KS = 1,3
   99 X(KS,J1,J2) = (0.,0.)
C
C  WE HAVE MADE USE OF THE FACT THAT KZ=2 FOR ALL OF THE MATRICES WE ARE
C  CALCULATING (SEE DIAGRAM ABOVE).  THUS, A(2)(L) = B(L,K1) = B(L,K2)
C  = B(L,K3), BY OUR CHOICE OF B(L,2) = 0.
C
      DO 8  K1 = 1,3
C
                     DO 4  L = 1,3
    4                A(2)(L) = B(L,K1)
C
      DO 8  L1 = 1,MAX
            M1 = L1 - (MAX + 1)/2
            N1 = L1 - (L1/2)*2
C
```

II-6

```
      DO 5        L2 = 1,MAX
                  M2 = L2 - (MAX + 1)/2
                  N2 = L2 - (L2/2)*2
C
      DO 3              L3 = 1,MAX
                        M3 = L3 - (MAX + 1)/2
                        N3 = L3 - (L3/2)*2
C
C
               N = L1 + L2 + L3
               N = N - (N/2)*2
               NTEST = (N1.EQ.N2).AND.(N2.EQ.N3)
C
C  IF M1 + M2 + M3 = EVEN, THEN N = 1 AND (M1,M2,M3) IS AN ALLOWED REAL
C  LATTICE VECTOR (XLATTICE). IF NTEST (A LOGICAL VARIABLE) IS TRUE,
C  THEN (M1,M2,M3)*PI IS AN ALLOWED RECIPROCAL LATTICE VECTOR (XLAMBDA).
C  WE ARE PRESENTLY INTENDING TO USE THE SAME GRID OF VARIABLES, (M1,M2,
C  M3) TO REPRESENT BOTH THE REAL AND RECIPROCAL LATTICES (RECALL THAT
C  WE SET THE F-F DISTANCE TO UNITY).  IN THIS WAY, WE CAN USE THE SAME
C  NEST OF DO LOOPS TO CARRY OUT BOTH REAL AND RECIPROCAL LATTICE SUMS--
C  ALL THAT IS NECESSARY IS THAT WE TEST EACH POINT IN THE GRID,
C  (M1,M2,M3), WITH 'N' AND 'NTEST' TO DETERMINE WHETHER IT IS ACCEPTA-
C  BLE FOR THE LATTICE SUM UNDER CONSIDERATION.
C
               M(1) = M1
               M(2) = M2
               M(3) = M3
C
      IF(N.EQ.0)  GO TO 5
C
C  IF N IS NOT 1, THEN THIS PARTICULAR TRIPLET (M1,M2,M3) IS NOT AN
C  ACCEPTABLE 'XLATTICE', SO WE THEN GO TO 5, WHERE A TEST IS MADE AS TO
C  THE ACCEPTABILITY OF (M1,M2,M3) FOR USE IN THE RECIPROCAL LATTICE SUM
C
C
C---------------- CONTRIBUTION FROM REAL LATTICE SUMS ------------------
C
C
                     DO 6  L = 1,3
    6                V(L) = M(L) + A(2)(L)
                     VSQ = V(1)*V(1) + V(2)*V(2) + V(3)*V(3)
C
                     IF(VSQ.GT.12.) GO TO 5
                     IF(VSQ.EQ.0.)  GO TO 4
C
C  THE CONDITIONAL  IF(VSQ.GT.12)  INSURES THAT WE DO THE SUM SPHERI-
C  CALLY--IT HAS THE EFFECT OF CUTTING THE CORNERS OFF OF THE CUBICAL
C  SPACE THAT WE ARE SUMMING OVER.  THE CHOICE OF VSQ = 12 FOR A CUT-OFF
C  DISTANCE WAS DECIDED BY THE FACT THAT THE FACTOR GAMM BELOW BECOMES
C  OF ORDER 5.*E-7 FOR VSQ GREATER THAN 12.
C
      VO = SQRT(VSQ)
      Z = CMPLX(0.,0., -(K(1)*V(1) + K(2)*V(2) + K(3)*V(3)))
      PHASE = CEXP(Z)
      T = PI*VSQ/2.
      RADT = SQRT(T)
```

II-7

```
      GAMM = (1. - EXP(-ADT))   (2.*AADT/EXDT(1+E)1. + 2.*T/3.)*E(XP1-7)
C
            DO 1  J1 = 1,3
            DO 1  J2 = J1,3
                  DELTA = 1.0
                  IF(J1.NE.J2) DELTA = 0.0
    1             A(K1,J1,J2) = A(K1,J1,J2) - PHASE*GAMM*(3.*U(J1)*U(J2)
     1            /USQ - DELTA)/RO**3
C
C
C------------ CONTRIBUTION FROM RECIPROCAL LATTICE SUMS ---------------
C
C
    5 IF(.NOT.M(1)) GO TO 3
C
C   IF .NOT.M(1) IS TRUE, THEN IT MEANS THAT M1,M2, AND M3 ARE NOT ALL
C   EQUAL--THAT IS, M1, M2, AND M3 ARE NOT ALL OF THE SAME PARITY (EVEN
C   OR ODD). IN THAT CASE, THE TRIPLET (M1,M2,M3) IS NOT ACCEPTABLE FOR
C   THE RECIPROCAL LATTICE SUM, AND WE GO TO 3.
C
                    DO 13 L = 1,3
   13               U(L) = R(L) - Q(L)/PI
                    USQ = U(1)**2 + U(2)**2 + U(3)**2
                    IF(USQ.GT.10.) GO TO 3
C
C   IN THE RECIPROCAL LATTICE SUM, THERE OCCURS A FACTOR EXP(-PI*USQ/2),
C   WHICH BECOMES LESS THAN 5.E-7 IF USQ IS GREATER THAN 10.
C
      Z = CMPLX(0.0, -PI*(M1*A1(2)(1) + M2*A1(2)(2) + M3*A1(2)(3)))
      PHASE = CEXP(Z)
C
            DO 8  J1 = 1,3
            DO 8  J2 = J1,3
                  DELTA = 1.0
                  IF(J1.NE.J2)  DELTA = 0.
    8             A(K1,J1,J2) = A(K1,J1,J2) + (2.*PI/3.)*PHASE*
     1            EXP(-PI*USQ/2.)*(3.*U(J1)*U(J2)/USQ - DELTA)
C
    3 CONTINUE
C
C   WE HAVE NOW CALCULATED THE UPPER TRIANGULAR PART OF THE THREE SYMME-
C   TRIC QUADS THAT ARE SUFFICIENT FOR PRODUCING THE (COULOMB CONTRIBU-
C   TION) FOR THE ENTIRE 9 X 9 MATRIX D(R).
C
      DO 15 K1 = 1,3
      DO 15 J1 = 1,3
      DO 15 J2 = J1,3
   15 A(K1,J2,J1) = A(K1,J1,J2)
C
      DO 16 J1 = 1,3
      DO 16 J2 = 1,3
C
            D(J1,1,J2,1) = (4./MCA)*(D(J1,1,J2,1) + ZSQ*A(2,J1,J2))
            D(J1,2,J2,2) = D(J1,2,J2,2) + ZSQ*A(2,J1,J2)
            D(J1,3,J2,3) = D(J1,2,J2,2)
            D(J1,1,J2,2) = -(2./SQRT(MCA))*(D(J1,1,J2,2)+ZSQ*A(1,J1,J2))
```

II-8

```
            D(J1,1,J2,3) = CONJG(D(J1,1,J2,2))
            D(J1,2,J2,3) = D(J1,2,J2,3) + ZSQ*CONJG(A(3,J1,J2))
C
   16 CONTINUE
C
C   WE SHALL USE A SHARE LIBRARY SUBROUTINE TO OBTAIN EIGENVALUES AND
C   EIGENVECTORS--SDIEIAR, COTAG.  THE MATRIX D(3,3,3,3) HAS BEEN LISTED
C   IN EQUIVALENCE WITH A SQUARE ARRAY, DG(9,9), WHICH SHALL BE USED IN
C   THE CALLING SEQUENCE FOR COTAG.  SINCE COTAG ASSUMES THE INPUT MATRIX
C   TO BE HERMITIAN, IT IGNORES THE DR(M1,M2) WITH M1.GT.M2, ASSUMING
C   THEM TO BE EQUAL TO CONJG(DR(M2,M1)).  HENCE, THOSE VALUES NEED NOT
C   BE SUPPLIED.
C
      IF(MU.NE.3) GO TO 999
C
C-------WRITE OUT THE A(1), A(2), A(3), AND DR MATRICES BEFORE DIAG-----
C
      DO 20 I = 1,9
      DO 20 J = 1,9
   20 DR(J,I) = CONJG(DR(I,J))
C
      WRITE (6,101) Q,AA,AQ,M2
C
      WRITE (6,104)
  105 FORMAT(1H0,37HTHE MATRICES A(1), A(2), A(3), AND DR ARE THE FOLLOW
     1ING--,///)
C
      WRITE (6,104) (((A(K,I,J),J=1,3),I=1,3),K=1,3)
  104 FORMAT(  3(3(2X,2F12.7,3X,2F12.7,3X,2F12.7,/),/ ))
C
      WRITE (6,102)  ((DR(I,J), J = 1,5), I = 1,9)
      WRITE (6,103)  ((DR(I,J), J = 6,9), I = 1,9)
C
C
C---------------------------------------------------------------------
C
C                    ****************************
C
  999               CALL COTAG(DR,9,WR,1,9,1.E-8)
C
C                    ****************************
C
C   THE ARRAY W(ALPHA, KAPPA, SIGMA) = W(3,3,9) ARE THE COMPLEX EIGEN-
C   VECTORS.  THE ARRAY W(3,3,9) IS EQUIVALENT TERM-FOR-TERM WITH WR(9,9)
C   BUT SINCE W APPEARS IN THE CALLING SEQUENCE OF THIS SUBROUTINE,
C   IT CANNOT BE USED IN AN 'EQUIVALENCE' STATEMENT.
C
C
      E = 4.803
      MEC2 = .0266
      SCALE = (2.*PI**2*1.E+4*E**2/A**3)/MEC2
C
C   THE COTAG ROUTINE RETURNS THE EIGENVALUES ON THE DIAGONAL OF DR.
C
      DO 11 I = 1,9
      OMEGA2(I) = SCALE*ABS(REAL(DR(I,I)))
```

II-9

```
      OMEGA(I) = SQRT(OMEGA2(I))
            DO 11 J = 1,9
            K1 = 1 + (J-1)/3
            J1 = J - 3*(K1-1)
            W(J1,K1,I) = WR(J,I)
   11 CONTINUE
C
C
C   THE EIGENVALUES ARE NOW GIVEN DIRECTLY IN INVERSE CENTIMETERS
C
      IF(MU.EQ.0)  GO TO 10
C
C---------------------------------------------------------------------
C
      WRITE (6,101) Q,AQ,AT,AE
  101 FORMAT(1H1, 22X, 82HTHE Q-VECTOR IS GIVEN BY 'Q-VECTOR' = (PI/2.)(2.
     1[illegible])
C
      WRITE (6,100) (J,OMEGA(J), J = 1,9)
  100 FORMAT(      21X,12HTHE FOLLOWING ARE THE EIGENFREQUENCIES OMEGA(J),
     1[illegible])
C
      IF(MU.EQ.2)  GO TO 10
C
      WRITE (6,106)
  106 FORMAT(/,20X,60HTHE FOLLOWING IS THE ARRAY OF (COMPLEX) EIGENVECTO
     1RS, CORRESPONDING TO THE ABOVE,/,20X,[illegible] THE J-TH
     2EIGENFREQUENCY HAS A COLUMN EIGENVECTOR IN COLUMN J.,///)
C
      WRITE (6,102) [illegible]
  102 FORMAT([illegible])
C
      WRITE (6,103) [illegible]
  103 FORMAT([illegible])
C
C---------------------------------------------------------------------
C
   10 RETURN
      END
```

III-1

```
      SUBROUTINE MODEL (T,A,WTO,WLO,WR,C11,C12,C44,MASS,ZSQ,ALPHA1,
     1ALPHA2,ALPHA3,BETA1,BETA2,BETA3,GAM2)
C
      REAL EST, MASS, MFC2, MFACT
C
C   T = TEMP IN DEGREES KELVIN, A = LATTICE CONSTANT (IN ANGSTROMS).
C   WTO = TRANSVERSE OPTIC FREQ. (IN CM-1), WLO = LONGITUD. OPTIC FREQ.
C   (IN CM-1), WR = RAMAN FREQUENCY (IN CM-1). C11, C12, C44 ARE THE
C   ELASTIC CONSTANTS (IN UNITS OF 1.E11 DYNES/CM**2) FOR A RIGID ION
C   MODEL (AS DEFINED BY GANESAN AND SRINIVASAN, CAN. J. OF PHYS.).
C   MASS = RATIO OF CATION MASS TO MASS OF FLUORINE, ZSQ, ALPHA1,... ARE
C   THE EFFECTIVE CHARGE (SQUARED) AND THE SHORT-RANGE FORCE-CONSTANTS
C   FOR THE RIGID ION MODEL.  MFC2 = REST ENERGY OF FLUORINE (IN [illegible]).
C   E = 4.803 REPRESENTS THE CHARGE OF AN ELECTRON IN CGS UNITS (X 1.E10).
C   EST IS THE LYDDANE-SACHS-TELLER RATIO, V = A**3/4 IS 1/4 OF THE VOLUME
C   OF THE PRIMITIVE CELL (IN ANGSTROM**3).
```

III-2

```
      RO = A/2.
      MFC2 = .0266
      PI = 3.14159
      E = 4.803
      V = RO**3
      UNIT = E**2/V * 1.E4
C
      WLO2 = WLO**2
      WTO2 = WTO**2
      WR2 = WR**2
      EST = WLO2/WTO2
      MFACT = MFC2/(2./MASS + 1.0)
C
      ZSQ = PI*WTO2*MFACT*(EST-1.)/2.
      ALPHA1 = (PI**2/3.0)*WTO2*MFACT*(EST + 2.0)
      ALPHA2 = 0.
      ALPHA3 = (PI**2)*MFC2*WR2 - ALPHA1
C
      ROC11 = RO*C11*1.E3
      ROC12 = RO*C12*1.E3
      ROC44 = RO*C44*1.E3
C
      BETA2 = .5*(ROC11 - ALPHA1 - ALPHA3 - 1.6*ZSQ)
      B = (ALPHA1 + ALPHA3)*(ALPHA1 + BETA2 - 1.9*ZSQ - ROC44)
      BETA1 = 3.*ZSQ + SQRT(B)
      BETA3 = 0.
      GAM2 = .5*(2.*BETA1 - ALPHA1 - BETA2 - 5.5*ZSQ - ROC12)
      ZSQ = ZSQ/UNIT**2.
C
      WRITE(6,100)  T,MASS,A, C11,C12,C44,WTO,WLO,WR,ZSQ,ALPHA1,BETA1,
     1ALPHA3,BETA2,GAM2
C
  100 FORMAT(1H1,[illegible] TEMPERATURE T = ,F6.0,19H THE EXPERIMENT
     1[illegible] PARAMETERS ARE GIVEN BY--,///,[illegible]
     2[illegible] LATTICE   C11 (E1.E-11  C12 (E1.E-..  C44 (E1.E-11  OM
     3EGA TO (CM-1)  OMEGA LO (CM-1)  OMEGA RAMAN,/,[illegible]CONSTANT (A),
     4[illegible]DYNES/CM**2),[illegible]
     5[illegible] PARAME
     6TERS FOR THE RIGID-ION MODEL ARE--,///,[illegible]ZSQ,[illegible]ALPHA1,[illegible]
     7[illegible]
     8[illegible]///)
C
      ALPHA1 = ALPHA1/UNIT
      BETA1 = BETA1/UNIT
      ALPHA3 = ALPHA3/UNIT
      BETA2 = BETA2/UNIT
      GAM2 = GAM2/UNIT
C
      WRITE (6,101)  ZSQ, ALPHA1, BETA1, ALPHA3, BETA2, GAM2, UNIT, RO
C
  101 FORMAT([illegible] PARAMETERS IN UNITS OF (E**2/RO**3)--,///
     1[illegible]
     2[illegible]
     3[illegible] DYNES/CM,/,[illegible] IS THE
     4N-F SEPARATION = A/2 = ,0PF8.3, (IN ANGSTROMS))
C
   98 RETURN
      END
```

IV-1

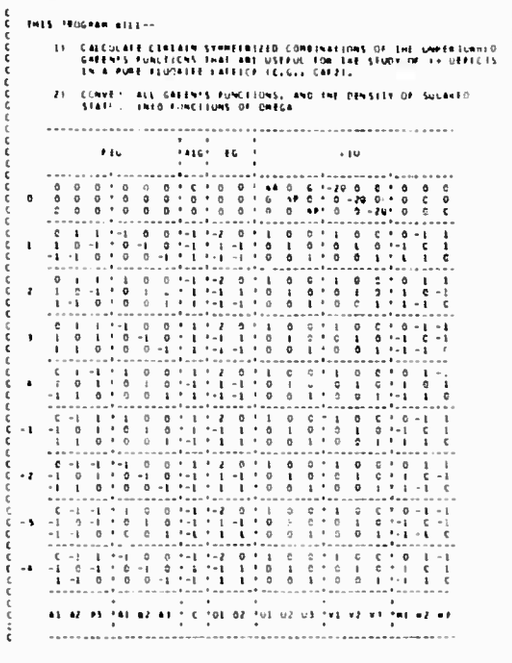

IV-2

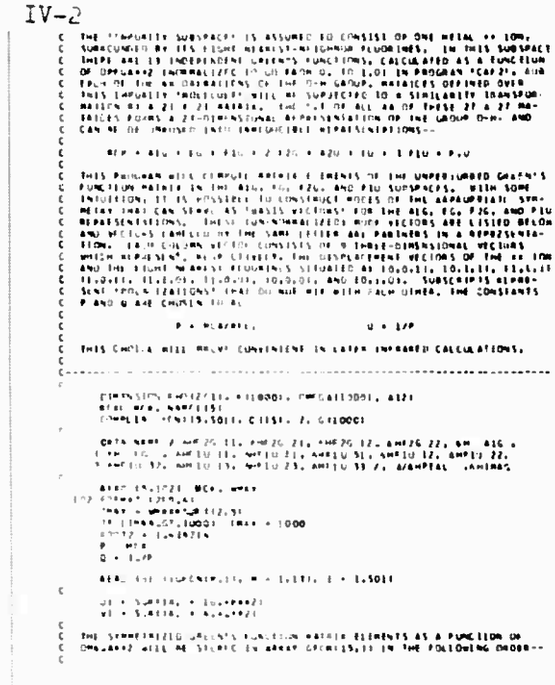

IV-3

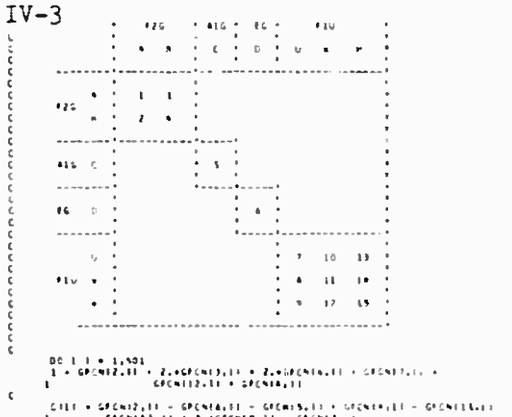

IV-4

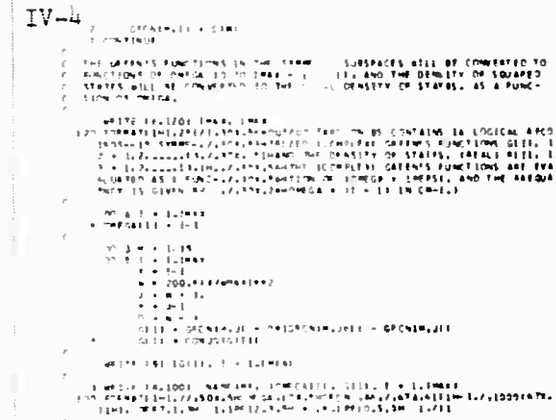

V-1

```
      DIMENSION V(3,3), UNIT(3,3), OMEGA(741)
      REAL MCA, MSR, MFL, LS1, NAME(15)
      COMPLEX G(3,3,741), A(2,2), B(3,3), A(3,6), C(3), PSE
C
C  THIS PROGRAM WILL CALCULATE MATRIX ELEMENTS OF THE PERTURBED GREEN'S
C  FUNCTION IN THE A1G, EG, F2G, AND F1U SYMMETRY SUBSPACES OF THE DE-
C  FECT SUBSPACE.  THE (COMPLEX) EIGENVALUES OF THE MATRIX [illegible] WILL
C  ALSO BE CALCULATED (AS A FUNCTION OF OMEGA) FOR EACH OF [illegible] SYMME-
C  TRIES.  THESE FUNCTIONS ARE ESPECIALLY USEFUL FOR DISCUSS[illegible] LOCAL
C  AND RESONANCE MODES, AND ARISE NATURALLY IN THE DECOMPOSITION OF
C  (I - GO(W) V)(EXP)-1.  THE GFCN'S TO BE USED IN THE PRESENT PROGRAM
C  ARE FROM TAPE NO.      , GIVEN AS A FUNCTION OF OMEGA = I-1 IN CM-1.
C  THE 'BASIS VECTORS' FOR EACH OF THESE SYMMETRY SUBSPACES WERE GIVEN
C  IN PROGRAM 'GFCN'.
C
      DATA UNIT / 1., 0., 0., 0., 1., 0., 0., 0., 1. /
      RC012 = 1.41421
      P = MCA/MFL
      Q = 1./P
      PI = 3.14159265
      U1 = SQRT(6. * (4.*P+Y2))
      A1 = SQRT(6. * (4.+Q+Y2))
C
      DATA NAME / AMGA2G11, AMGP2G21, AMGF2G12, AMGF2G22, AMG A1G ,
     1 AMG EG  , AMGF1U11, AMGF1U21, AMGF1U31, AMGF1U12, AMGF1U22,
     2 AMGF1U12, AMGF1U11, AMGF1U23, AMGA1U11 /,TITLE1, TITLE2 /
     2 AMPSEF2G, AMPSEF1U  /
C
C  THE DEFECT MATRIX SHALL CONTAIN THE FOLLOWING ASSUMPTIONS--WE ASSUME
C  (IN ORDER TO APPLY THE FORMALISM FOR ISOLATED, LOCAL DEFECTS), THAT
C  THE EFFECTIVE CHARGE (WHICH AFFECTS THE LONG-RANGE COULOMB FORCES)
C  DOES NOT CHANGE.  THIS IS REASONABLE, BECAUSE WE WOULD EXPECT THAT
C  IONS OF CA, SR, OR B. ARE QUITE SIMILAR AS FAR AS ELECTRICAL PROPER-
C  TIES ARE CONCERNED.  IN ORDER TO MAKE THE SIZE OF THE IMPURITY SUB-
C  SPACE MANAGEABLE, WE ASSUME THAT BETA2 AND GAMMA2 ALSO REMAIN
C  UNCHANGED--THIS IMPLIES THAT THE IMPURITY SUBSPACE CONTAINS ONLY ONE
C  METAL ION SURROUNDED BY ITS EIGHT NEAREST-NEIGHBOR FLUORINE IONS. THE
C  V MATRIX WILL THEREFORE DEPEND UPON CHANGES IN ALPHA1, BETA1, AND
C  ALPHA3.  THE CHANGE IN ALPHA1 IS CALCULATED FROM THE EXPERIMENTAL
C  VALUE OF W1O AT K=0, USING THE FIXED VALUE FOR ZSQ.  BETA1 IS EVALU-
C  ATED FROM THE ELASTIC CONSTANT C12, AND ALPHA3 FROM THE RAMAN
C  FREQUENCY.  THE EQUATIONS FOR CALCULATING W1O, C12, WR, ETC. ARE
C  GIVEN IN GANESAN AND SRINIVASAN, CAN. J. OF PHYS., 40, 74 (RIGID-ION)
C
C  ALL GREEN'S FUNCTIONS HAVE BEEN CALCULATED IN UNITS OF 1/(MFL*WMAX2),
C  SO THE V-MATRIX WILL BE EXPRESSED IN UNITS OF (MFL*WMAX2) BY GIVING
C  THE FORCE CONSTANT CHANGES IN TERMS OF THESE UNITS.
C
C----------EXPERIMENTAL PARAMETERS AND FORCE CONSTANT CHANGES---- ------
C
C  THE FOLLOWING EXPERIMENTAL PARAMETERS CORRESPOND TO T = 4 DEG. K.
C
      DATA ZSQ,   ALPHA1,   BETA1,    ALPHA3,    BETA2,    GAMMA2,    MFL  /
     1    .0085, 1.7328E4,  E.0858E4, 1.2301E4,  3.582E3-  3.124E3,   1.0  /
```

V-2

```
      DATA MCA,    W0CA,    WRCA,    W10CA,    C12CA /
     1      2.1096, 2.725,   378.2,   281.3,    5.80  /
C
      DATA MSR,    W0SR,    WRSR,    W10SR,    C12SR /
     1      4.612,  2.88,    289.5,   225.0,    4.748 /
C
      WMAX = 472.3
      WMAX2 = WMAX**2
C
      A1 = (2.*PI/3.0)*ZSQ*(4.7784E3) + PI**2*W10SR**2*.0206/(2./MSR+1.)
      DALPH1 = A1 - ALPHA1
      DALPH3 = -DALPH1 + PI**2*.0208*(WR3R**2 - WRCA**2)
      A3 = ALPHA3 + DALPH3
      B1 = (4OSR*C12SR*1.E3+2.*GAMMA2+4(*BETA2+5.5*ZSQ*4.7784E3)/2.
      DBETA1 = B1 - BETA1
C
      F = 4.*PI**2*.0208*WMAX2
C
      DALPH1 = DALPH1/F
      DBETA1 = DBETA1/F
      DALPH3 = DALPH3/F
C
      DM = MSR - MCA
C
      WLO2 = (2./MSR+1.)/(PI**2*.0208)*(A1+(4.*PI/3.)*ZSQ*(4.7784E3))
      WLO = SQRT(WLO2)
      LS7 = WLO2/W1CS**2
      C11 = (A1 + 2.*BETA2 + A1 + 4.*ZSQ*4.7784E3)/4OSR*1.E8
      C44 = (A1 + BETA2 - [illegible](A1 - B1*5.*ZSQ*4.7784E3)*2/
     1        (A1 + B1))/4OSR*1.E4
C
      WRITE(6,150) A1,B1,A3,WLO,LS7,C11,C44,DALPH1,DBETA1,DALPH3
C
  150 FORMAT(1H1,[illegible],40X,43HTHE FOLLOWING VALUES ARE CALCULATED FOR ,/
     1,45X,41HPURE SRF2 LATTICE IF WE USE FORCE CONSTANTS,/,40X,40HCONSE
     2STENT WITH THE SIMPLE DEFECT MODEL ,/,40X, 34HUSED IN THE PRESENT
     3CALCULATIONS--,///,45X,9HALPHA1 = ,1PE10.3,2X,9HDYNES/CM ,/,45X,
     49HBETA1  = ,1PE10.3,2X,9HDYNES/CM ,/,45X,9HALPHA3 = ,1PE10.3,2X,
     58HDYNES/CM,//,45X,6HWLO = ,0PF6.2,2X,4HCM-1,/,45X,29HLYDDANE-SACHE
     6 TELLER RATIO = ,F6.3,//,45X,6HC11 = ,1PE10.3,2X,9HDYNES/CM2,
     7/,45X,6HC44 = ,1PE10.3,2X,9HDYNES/CM2,///,40X,4C(1H-),//,45X,9HDAL
     8PH1 = ,1PE10.3,/,45X,9HDBETA1 = ,1PE10.3,/,45X,9HDALPH3 = ,1PE10.3
     9,//,40X,40(1H-))
C
C-----------------------------------------------------------------------
C
C                         F2G CALCULATIONS
C
          V(1,1) = -(DALPH1 + DBETA1)
          V(2,1) = RC012*DBETA1
          V(1,2) = V(2,1)
          V(2,2) = -(DALPH1 + DALPH3)
C
C  NOTICE THAT V IS EXPRESSED IN UNITS OF (MFL*WMAX2), BECAUSE DALPH1,
C  DBETA1, AND DALPH3 WERE EXPRESSED IN THESE UNITS.
```

V-3

```
      WRITE (6,101) V(1,1), V(1,2), V(2,2)
C
  101 FORMAT (1H1,//,[illegible],6HV11 = ,1PE10.3,/,50X,6HV12 = ,1PE10.3,/,50X,
     16HV22 = ,1PE10.3,//,26X,5HOMEGA,20X 28HEIGENVALUES OF GO*V (LAMBDA
     2),/,20X,40(1H-),/)
C
      DO 90 N = 1,2
      DO 90 M = 1,2
   90 READ (4)  (G(M,N,I), I = 1,741)
C
      DO 1 I = 1,741
          OMEGA(I) = I-1
C
          DO 2 M = 1,2
          DO 2 N = 1,2
          A(M,N) = G(M,1,I)*V(1,N) + G(M,2,I)*V(2,N)
          A(M,N+2) = UNIT(M,N)
    2     B(M,N) = UNIT(M,N) + A(M,N)
C
C
C  CARRY OUT THE INVERSION OF (I+GO*V) WITH CSIMEQ--SDA3064. SUBROUTINE
C  CSIMEQ WILL PLACE THE INVERSE OF THE MATRIX (I+GO*V) INTO THE RIGHT
C  HAND ROW NEXT TO THE INPUT MATRIX.
C
          CALL CSIMEQ(A,2,2)
C
C  WE SHALL NEXT CALCULATE THE EIGENVALUES OF THE MATRIX GO*V.  THIS IS
C  ACCOMPLISHED USING SHARE SUBROUTINE SDA1441, WHICH IS CAPABLE OF
C  DIAGONALIZING AN ARBITRARY (COMPLEX), NON-HERMITIAN MATRIX.
C
          CALL ALLMATRX(C,2,2)
C
C
          DO 3 M = 1,2
          DO 3 N = 1,2
    3     A(M,N) = A(M,3)*G(1,N,I) + A(M,4)*G(2,N,I)
C
          PSE = 4.*WMAX2*(V(2,1)*A(1,N) + V(2,2)*A(2,N))
C
          DO 4 M = 1,2
          DO 4 N = 1,2
    4     G(M,N,I) = A(M,N)
C
          G(1,3,I) = PSE
          G(2,3,I) = C(1)
          G(3,3,I) = C(2)
C
        WRITE (6,101) OMEGA(I), C(1), C(2)
  101 FORMAT(1H ,22X, F5.1,2X,2(1H(,4X, F10.3,5H + I*, F10.3,5H)))
C
    1 CONTINUE
C
        DO 80 N = 1,2
        DO 80 M = 1,2
        L = N+2*(M-1)
```

V-4

```
        WRITE (8) (G(M,N,I), I = 1,741)
   80 WRITE(6,100) NAME(L), NAME(L),NAME(L),(OMEGA(I), G(M,N,I), I=1,741)
  100 FORMAT (1H1,//,5X,1H1,5HOMEGA,11X,4A,[illegible],/,5X,(2(1H-1.),741)(0,
     1[illegible],3X,0PF6.0,2X,1H(,1PE12.3,5H + I*,1PE10.3,2H),/))
C
        WRITE (8) (G(2,2,I), I = 1,741)
        WRITE (8) (G(3,3,I), I = 1,741)
        WRITE (8) (G(1,3,I), I = 1,741)
C
        WRITE(6,100) (TITLE1,TITLE2,TITLE1,(OMEGA(I), G(1,3,I), I=1,741)
C
C
C---------------------- A1G CALCULATION------------------------------------
C
        V(1,1) = -(DALPH1 + DALPH3 + 2.*DBETA1)
C
        READ (4) (G(1,1,I), I = 1,741)
        WRITE(6,105) V(1,1), NAME(5)
  105 FORMAT(1H1,50X,6HV = ,1PE10.3,//, 26X,5HOMEGA,17X,6HLAMBDA,20X,9A,
     17,20X,40(1H-),/)
C
        DO 5 I = 1,741
             C(1) = G(1,1,I)*V(1,1)
             G(1,1,I) = G(1,1,I)/(C(1) + 1.)
             G(2,2,I) = C(1)
    5   WRITE (6,101) OMEGA(I), C(1), G(1,1,I)
        WRITE (8) (G(1,1,I), I = 1,741)
        WRITE (8) (G(2,2,I), I = 1,741)
C
C
C--------------------- EG CALCULATION--------------------------------------
C
        V(1,1) = DBETA1 - DALPH1 - DALPH3
C
        READ (4) (G(1,1,I), I = 1,741)
        WRITE(6,105) V(1,1), NAME(6)
C
        DO 6 I = 1,741
             C(1) = G(1,1,I)*V(1,1)
             G(1,1,I) = G(1,1,I)/(C(1) + 1.)
             G(2,2,I) = C(1)
    6   WRITE (6,101) OMEGA(I), C(1), G(1,1,I)
        WRITE (8) (G(1,1,I), I = 1,741)
        WRITE (8) (G(2,2,I), I = 1,741)
C
C
C----------- ---------- F1U CALCULATIONS ----------------------------------
C
C
             V(3,1) = -4.*(4.*P-1.)*DBETA1/U1
             V(3,2) = 4.*(2.*Q + 1.)*DBETA1/U1
             V(1,3) = V(3,1)
             V(2,3) = V(3,2)
             V(3,3) = -DBETA1 - DALPH1 - DALPH3
C
        WRITE (6,104)  V(1,3), V(2,3), V(3,3)
```

V-5

```
106 FORMAT(1H1,//,50X,6HV11 = ,1PE10.3,/,50X,6HV22 = ,1PE10.3,/,50X,
   16HV33 = ,1PE10.3,/,/, 3X,5HOMEGA,6X,4H V11,10X,4H V12,10X,4H V22,
   E31X,27HEIGENVALUES OF GOXP (LAMBDA),/,13X(1H-),/)
C
      DO 70 M = 1,3
      DO 70 N = 1,3
   70 READ (8) (G(M,N,I), I = 1,741)
C
      DO 2 I = 1,741
            W2 = (OMEGA(I)/WMAX)**2
C
            V(1,1) = 8.*(2.*P**2-2*D*W-16.*R-1.)**2*DALPH1)/U)**2
            V(2,1) = 8.*(-D*W**2+16.*P-2.*Q*?.)*DALPH1)/(U*V))
            V(1,2) = V(2,1)
            V(2,2) = 4.*(G**2*D*W**2-2.*(2.*G+1.)**2*DALPH1)/V)**2
C
            DO 8 M = 1,3
            DO 8 N = 1,3
            B(M,N) = G(M,1,I)*V(1,N) + G(M,2,I)*V(2,N) + G(M,3,I)*V(3,N)
            A(M,N+3) = UNIT(M,N)
    8       A(M,N) = UNIT(M,N) + B(M,N)
C
            CALL CSIMEQ (A,3,3,3)
            CALL ALLMAT (B,C,3,3)
C
            DO 12 M = 1,3
            DO 12 N = 1,3
   12       B(M,N) = A(M,4)*G(1,N,I) + A(M,5)*G(2,N,I) + A(M,6)*G(3,N,I)
C
            DO 11 M = 1,3
            DO 11 N = 1,3
   11       G(M,N,I) = B(M,N)
C
            G(2,1,I) = C(1)
            G(3,1,I) = C(2)
            G(3,2,I) = C(3)
C
      WRITE (6,107) OMEGA(I), V(1,1), V(1,2), V(2,2), C(1), C(2), C(3)
  107 FORMAT(1H ,1X,0PF6.0,2X,1H(,3(1PE12.3,2X),1H),3X    0PE12.3,2H, ,
     1 0PE10.3,2H))
C
    2 CONTINUE
```

V-6

```
      DO 40 M = 1,3
      DO 40 N = 1,3
      J = 6*M+3*(N-1)
      IF(M.GT.N) GO TO 40
      WRITE (8) (G(M,N,I), I = 1,741)
      WRITE (6,100) NAME(J),NAME(J),NAME(J),(OMEGA(I),G(M,N,I),I=1,741)
      GO TO 40
   40 WRITE (8) (G(N,M,I), I = 1,741)
      WRITE (6,100) NAME(J),NAME(J),NAME(J),(OMEGA(I),G(N,M,I),I=1,741)
   80 CONTINUE
C
      WRITE (8) (G(2,1,I), I = 1,741)
      WRITE (8) (G(3,1,I), I = 1,741)

      WRITE (8) (G(3,2,I), I = 1,741)
C
      DO 9 I = 1,741
            W2 = (OMEGA(I)/WMAX)**2
C
            V(1,1) = 8.*(2.*P**2*W2*D*W-16.*P-1.)**2*DALPH1)/U)**2
            V(2,1) = 8.*(-D*W2*16.*P-2.*D-?.)*DALPH1)/(U*V))
            V(1,2) = V(2,1)
            V(2,2) = 4.*(G**2*D*W**2-2.*(2.*G+1.)**2*DALPH1)/V)**2
C
            C(1) = -(G(1,1,I)*V(1,2)+ G(1,2,I)*V(2,2) + G(1,3,I)*A(3,2))
            C(2) = 1.-(G(1,2,I)*V(1,2)+G(2,2,I)*V(2,2)+G(2,3,I)*V(3,2))
            C(3) = -(G(1,3,I)*V(1,2)+ G(2,3,I)*V(2,2) + G(3,3,I)*V(3,2))
            PSE = V(2,1)*C(1) + V(2,2)*C(2) + V(3,2)*C(3)
            PSE = PSE*16.*4.*Q**2)*WMAX2/(2.*4.*Q**2)
            G(1,1,I) = PSE
    9 CONTINUE
C
      WRITE (8) (G(1,1,I), I = 1,741)
      WRITE (6,100) TITLE2, TITLE2, TITLE2, (OMEGA(I),G(1,1,I), I=1,741)
C
C  TAPE 45 CONTAINS 24 RECORDS, EACH WITH 741 COMPLEX NUMBERS. THE ORDER
C  WAS F2G(6 GFCN'S, 2 LAMBDA'S, , PSE), AIG (1 GFCN, 1 LAMBDA), EG (6
C  GFCN, 1 LAMBDA), FIW (6 GFCN'S, 3 LAMBDA'S, 1 PSE).
C
C------------------------------------------------------------------------
C
      RETURN
      END
```

VI

```
      DIMENSION DATA(1024), OMEGA(3,9), WSIG(8), AXESIN(3), TITLE(3)
      COMPLEX A(3,3,N)
      REAL KX, KY, KZ, MCA
      COMMON N,ALPHA1,ALPHA2,ALPHA3,BETA1,BETA2,BETA3,GAM2,ZSD,MCA,A
      DATA TITLE, 5HKX/PI , 5HKY/PI , 5HKZ/PI /
      READ (5,101) Z, W10, W20, WR, C11, C12, C44, MCA
      CALL MODEL (4., 4, W10, W20, WR, C11, C12, C44, MCA, ZSD, ALPHA1,
     1ALPHA2, ALPHA3, BETA1, BETA2, BETA3, GAM2)
  101 FORMAT (8E9.4)
      CALL PLOTS (DATA(1), 1024)
      CALL PLOT (3., .5, -3)
   75 READ (5,100) N1, N2, N3, N
  100 FORMAT (4I2, I1)
      IF (N1.EQ.99) GO TO 99
      EN = N
      NMAX = MAX0(N1,N2,N3)
      II = 1
      IF (N1-NMAX) 7,8,9
    8 II = 2
      IF (N2-NMAX) 7,9,9
    7 II = 3
    9 EN1 = N1
      EN2 = N2
      EN3 = N3
      ENMAXS = NMAX
      ENSUM = (EN1 + EN2 + EN3)/1.5
      R = AMAX1(EN1,EN2,EN3,ENSUM)
      DMAX = 1./R
      M = N+1
      DO 1 K = 1,M
      R = K-1
      KX = RDMAX*EN1
      KY = RDMAX*EN2
      KZ = RDMAX*EN3
      CALL KSPACE (KX, KY, KZ, WSIG, N, 2)
         DO 2 J = 1,9
    2    OMEGA(K,J) = WSIG(J)
    1 AXESIN(K) = DMAX*R*ENMAXS/EN
      AXESIN(M+1) = 0.
      AXESIN(M+2) = .1
      WIDTH = AXESIN(M)/AXESIN(M+2)
      DO 3 J = 1,8
      OMEGA(M+1,J) = OMEGA(1,J)
    3 OMEGA(M+2,J) = OMEGA(1,J)
      NPTS = 9*(M + 2) - 2
      CALL PLOT (22., -11., -3)
      CALL PLOT (0., .5, -3)
      CALL SCALE (OMEGA, 10., NPTS, 1, 10.)
      DO 4 J = 1,9
      OMEGA(M+1,J) = OMEGA(M+1,8)
      OMEGA(M+2,J) = OMEGA(M+2,9)
    4 CALL LINE (AXES, OMEGA(1,J), M, 1, -1, 4)
      CALL AXIS (0.,0.,TITLE(II),-4,WIDTH,0.,AXESIN(M+1),AXESIN(M+2),10.)
      CALL AXIS (0.,0.,28HPHONON FREQUENCIES IN CM-1, 26, 10., 90.,
     1 OMEGA(M+1,8), OMEGA(M+2,9), 10.)
      CALL PLOT (WIDTH, 0., 3)
      CALL PLOT (WIDTH, 10., 2)
      CALL PLOT (0., 10., 2)
      A = WIDTH - 3.2
      CALL SYMBOL (0., 1., .14, 21HDISPERSION CURVES FOR, 0., 21)
      CALL SYMBOL (A+.05, .7, .14, 23H(  ,  ,  )-DIRECTION, 0., 20)
      CALL NUMBER (A+.18, .7, .14, FLOAT(N1), 0., -1)
      CALL NUMBER (A+.54, .7, .14, FLOAT(N2), 0., -1)
      CALL NUMBER (A+.80, .7, .14, FLOAT(N3), 0., -1)
      GO TO 75
   99 CALL PLOT (0, 0, 999)
      RETURN
      END
```

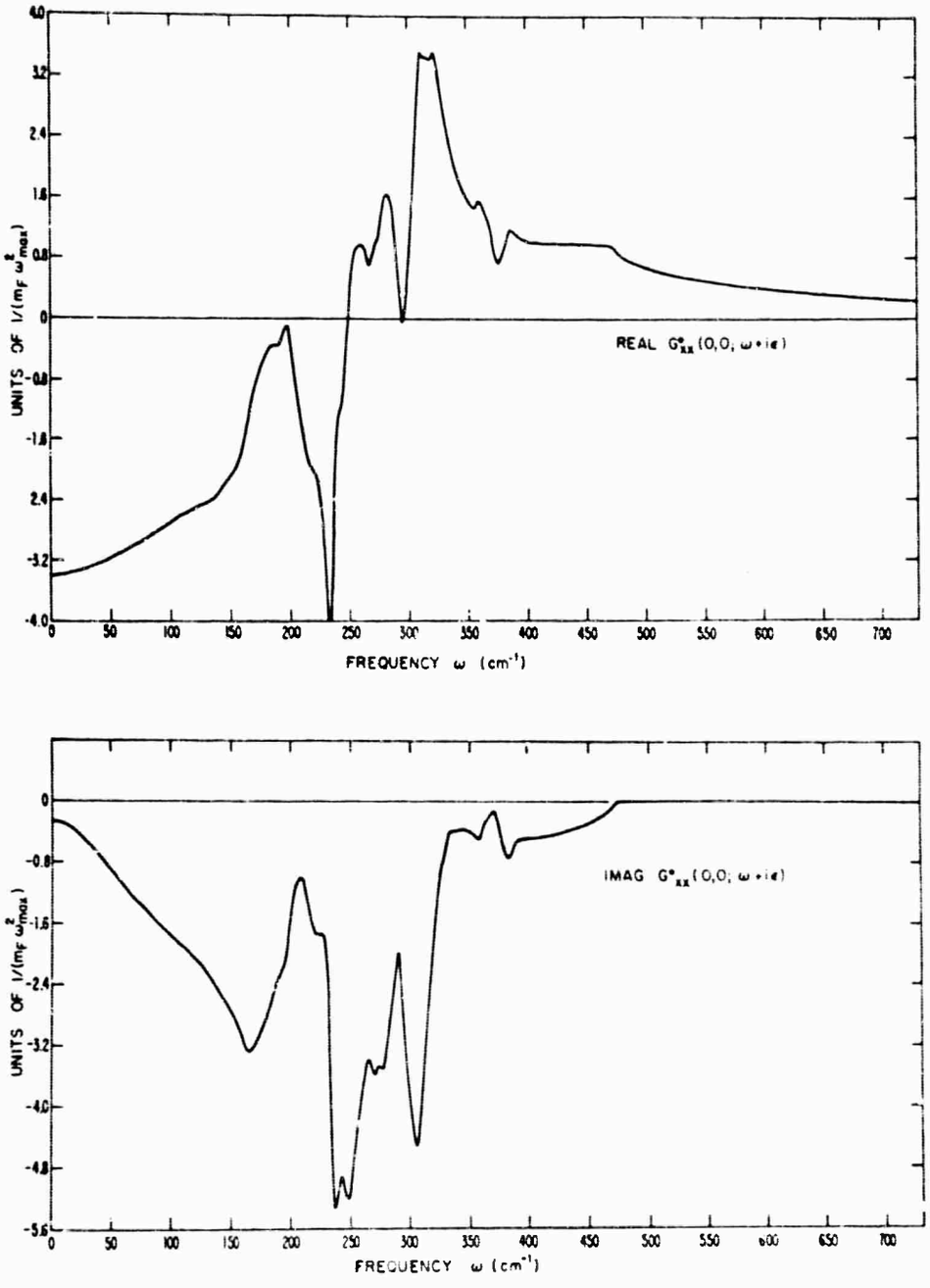

Fig. A-1: Real and imaginary parts of the 1st Green's function, $G^{o}_{xx}(0,0,\omega+i\epsilon)$ = "A" (cf. Fig. 6.8)

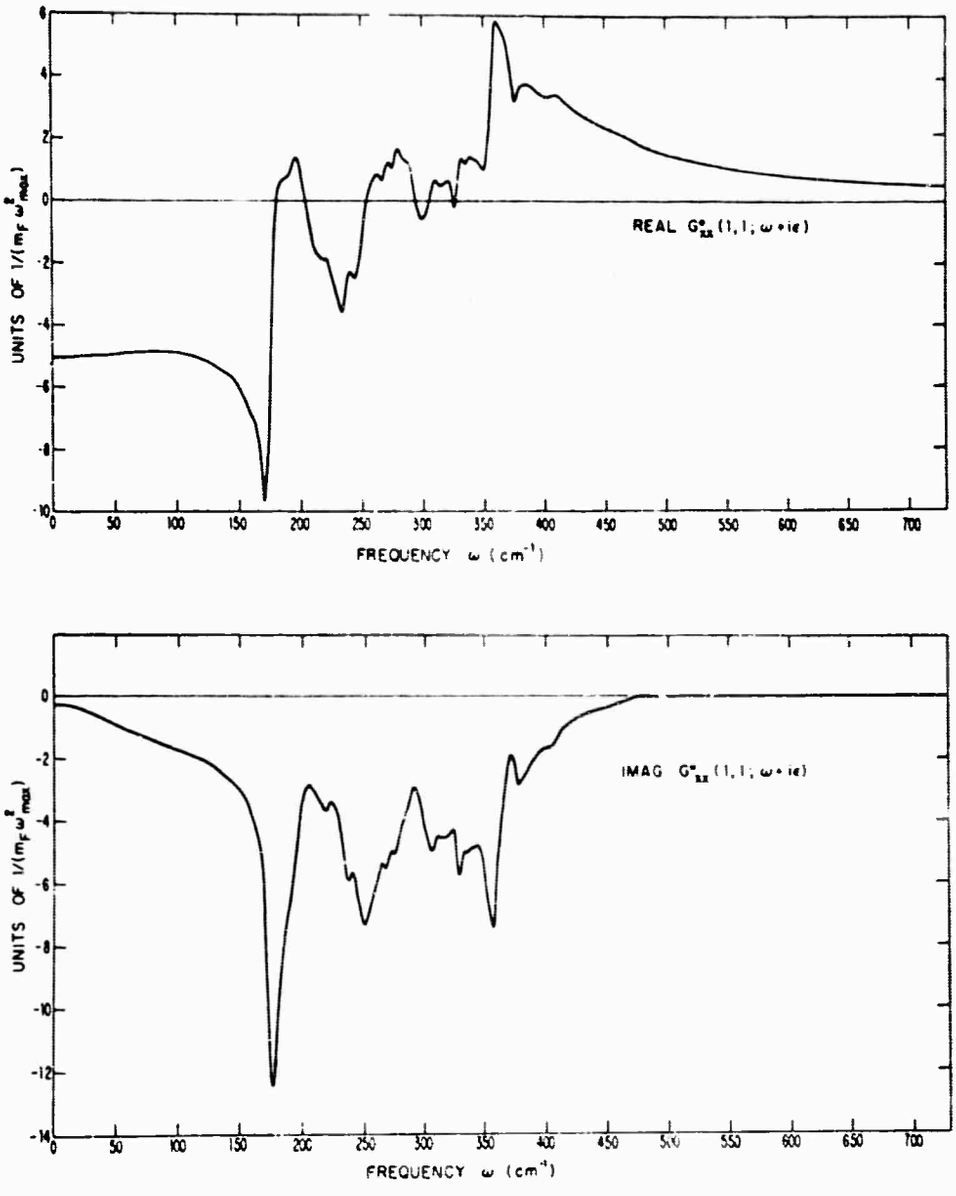

Fig. A-2: Real and imaginary parts of the 2nd Green's function, $G^{o}_{xx}(1,1;\omega+i\varepsilon)$ = "B" (cf. Fig. 6.8)

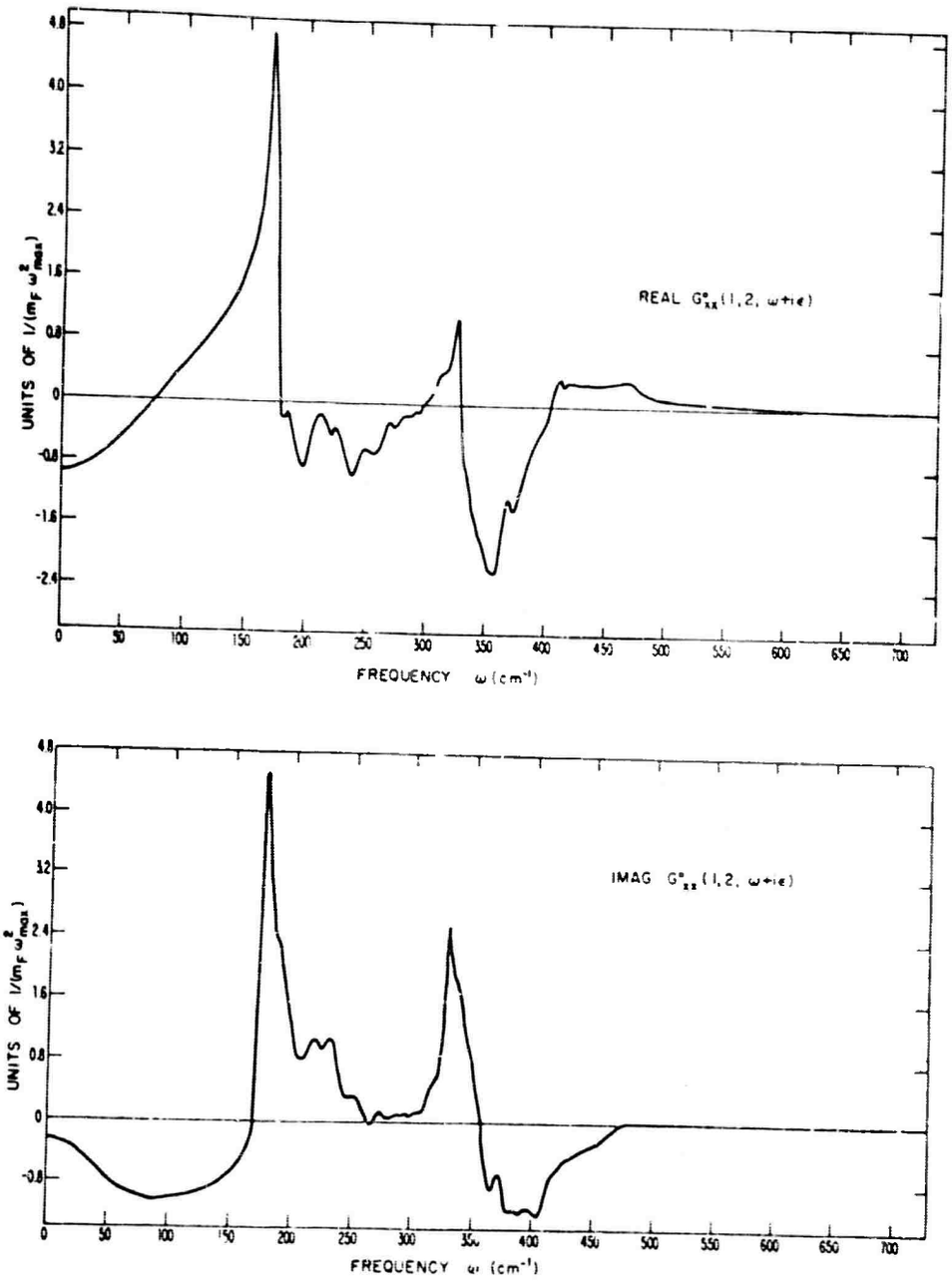

Fig. A-3: Real and imaginary parts of the 3rd Green's function, $G^{o}_{xx}(1,2;\omega+i\epsilon)$ = "M" (cf. Fig. 6.8)

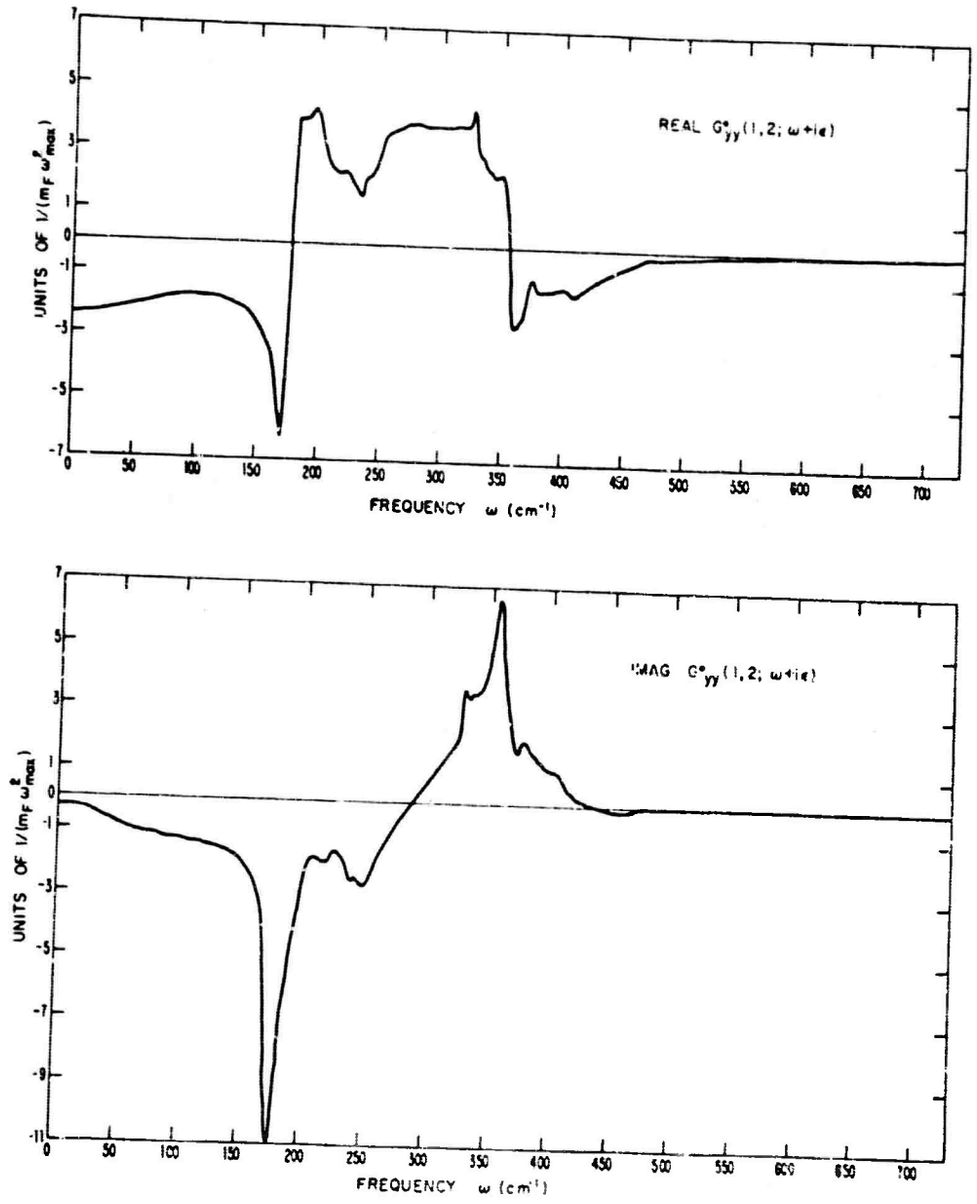

Fig. A-4: Real and imaginary part of the 4th Green's function, $G^{o}_{yy}(1,2;\omega+i\varepsilon)$ = "F" (cf. Fig. 6.8)

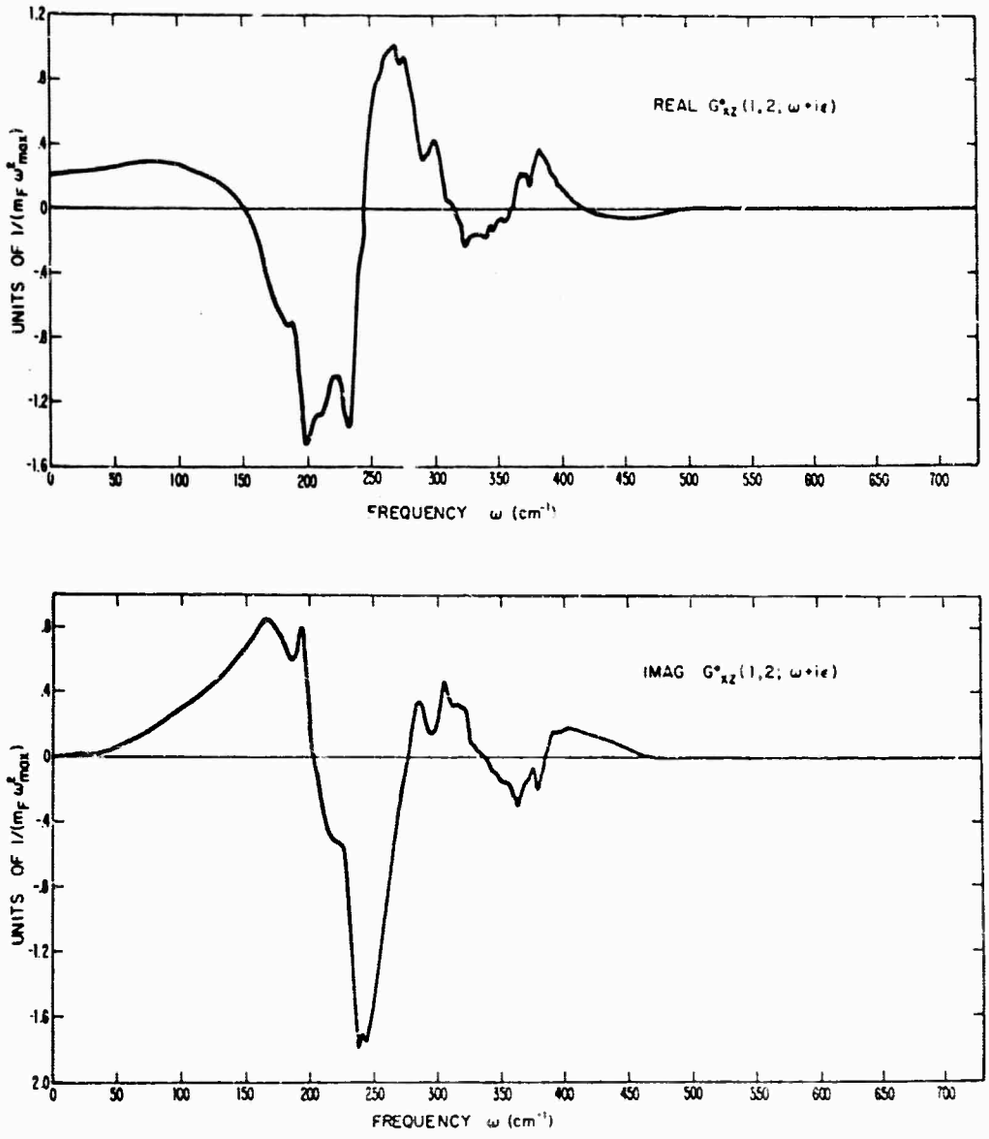

Fig. A-5: Real and imaginary parts of the 5th Green's function, $G^{o}_{xz}(1,2;\omega+i\varepsilon)$ = "H" (cf. Fig. 6.8)

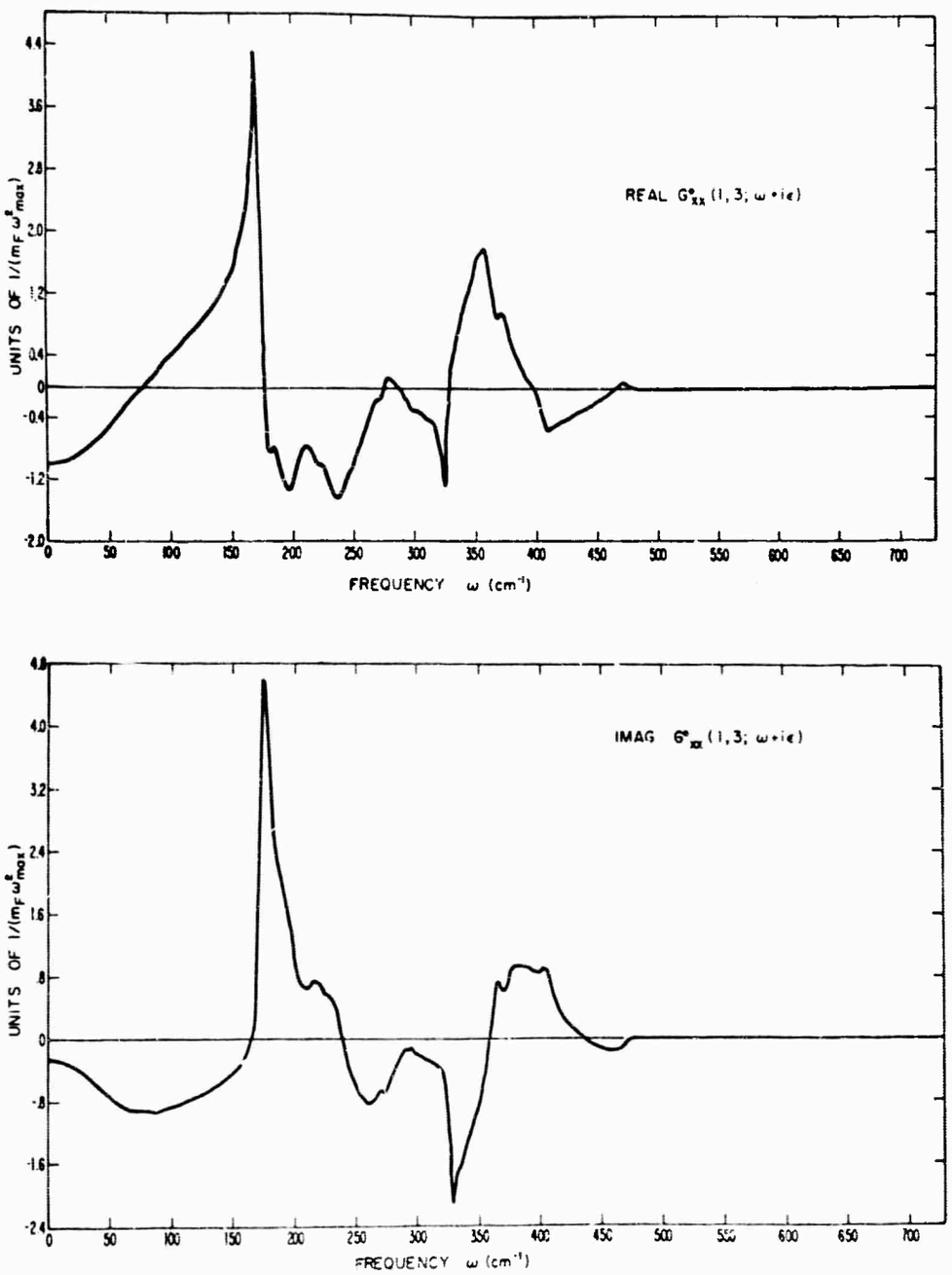

Fig. A-6: Real and imaginary parts of the 6th Green's function, $G^{o}_{xx}(1,3;\omega+i\epsilon)$ = "P" (cf. Fig. 6.8)

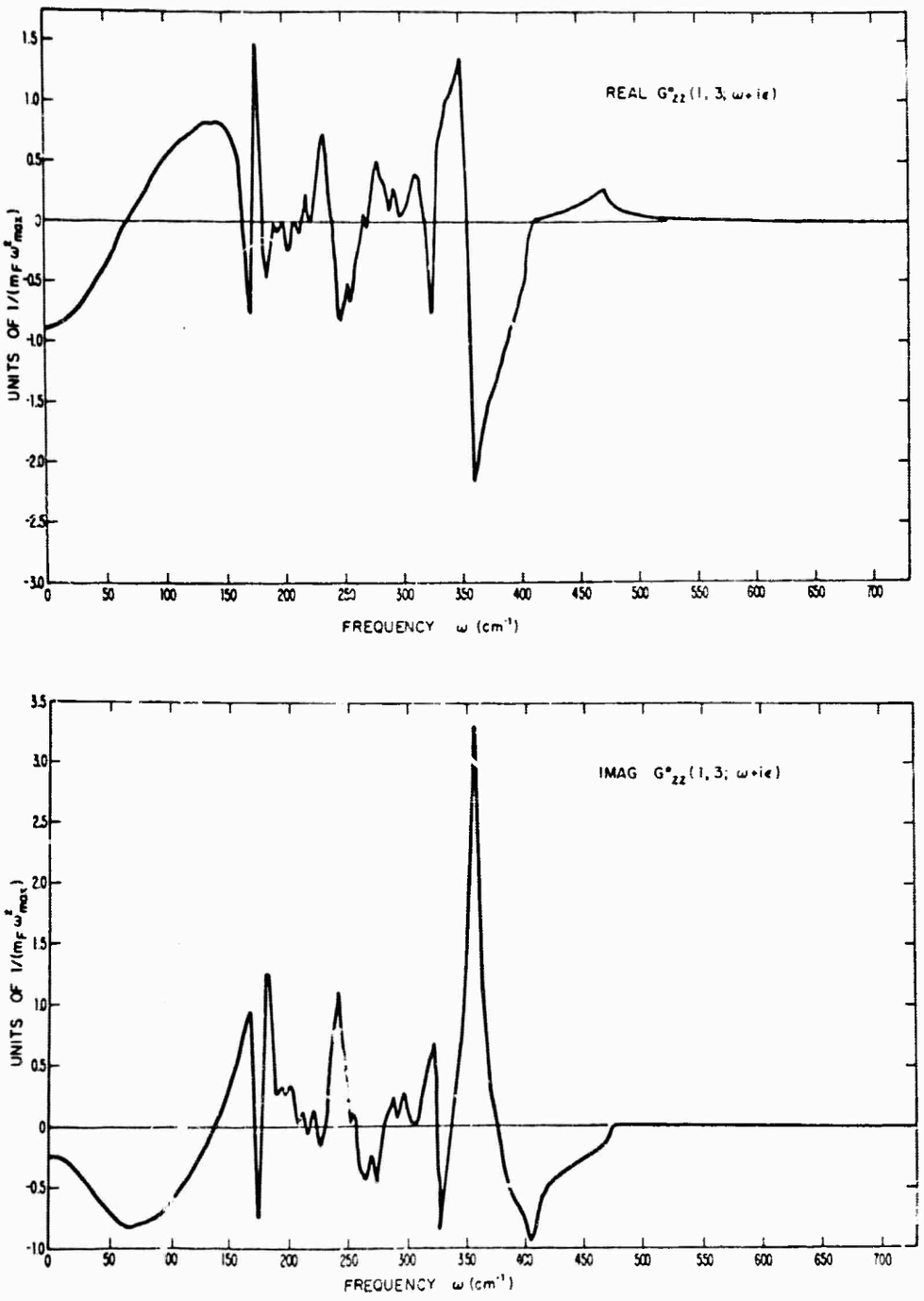

Fig. A-7: Real and imaginary parts of the 7th Green's function, $G^{o}_{zz}(1,3;\omega+i\varepsilon)$ = "Q" (cf. Fig. 6.8)

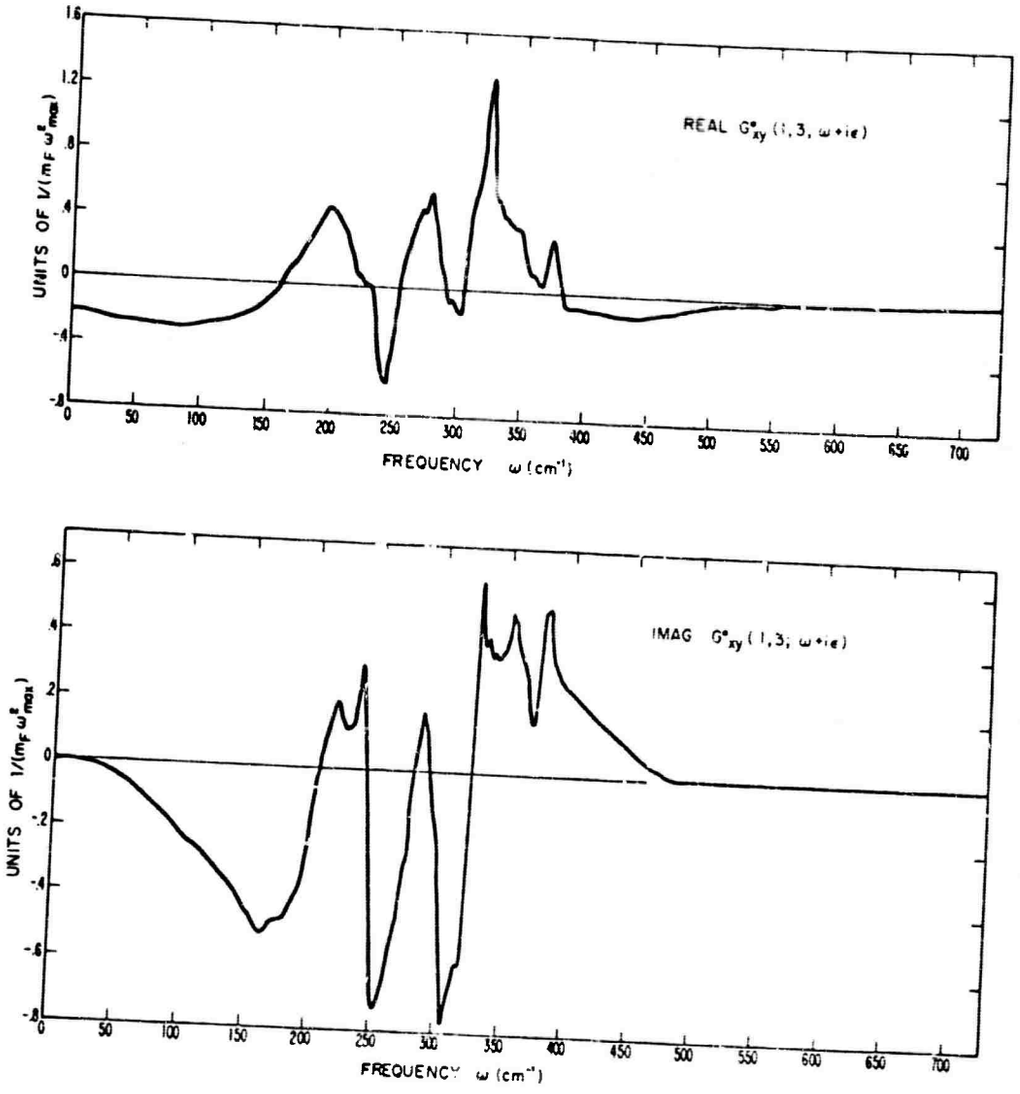

Fig. A-8: Real and imaginary parts of the 8th Green's function, $G^{\circ}_{x,y}(1,3,\omega+i\varepsilon)$ = "R" (cf. Fig. 6.8)

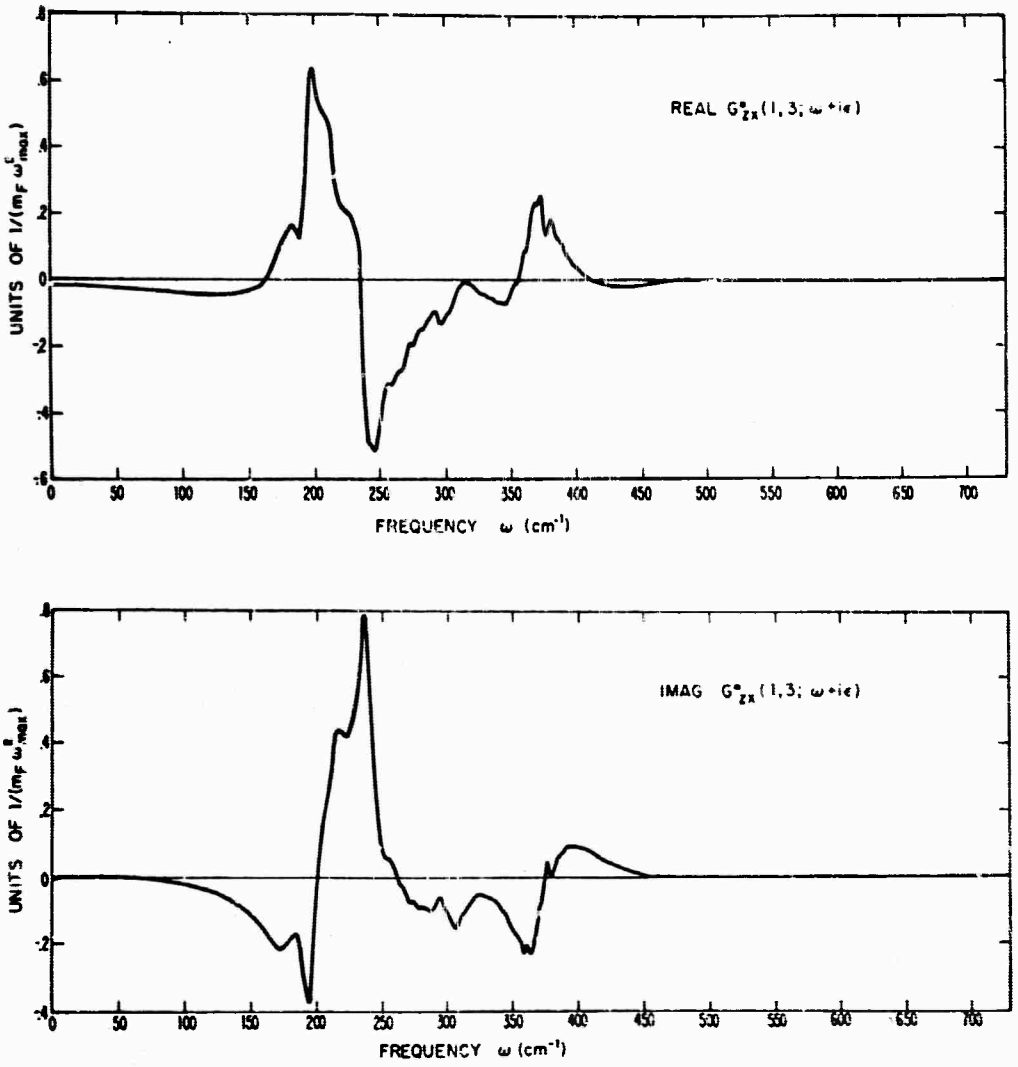

Fig. A-9: Real and imaginary parts of the 9th Green's function, $G^{o}_{zx}(1,3;\omega+i\epsilon)$ = "ζ" (cf. Fig. 6.8)

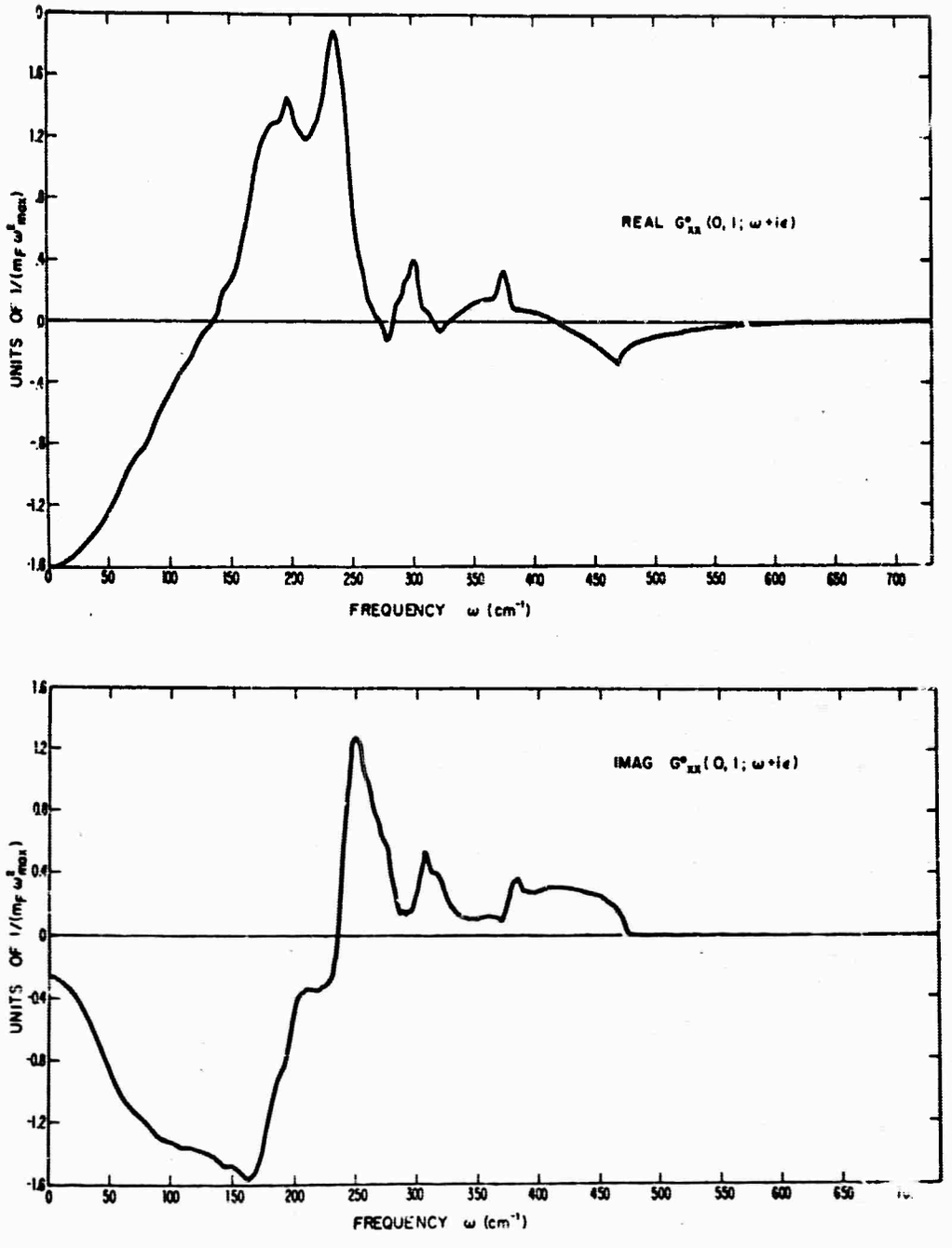

Fig. A-10: Real and imaginary parts of the 10th Green's function, $G^{o}_{xx}(0,1;\omega+i\epsilon)$ = "C" (cf. Fig. 6.8)

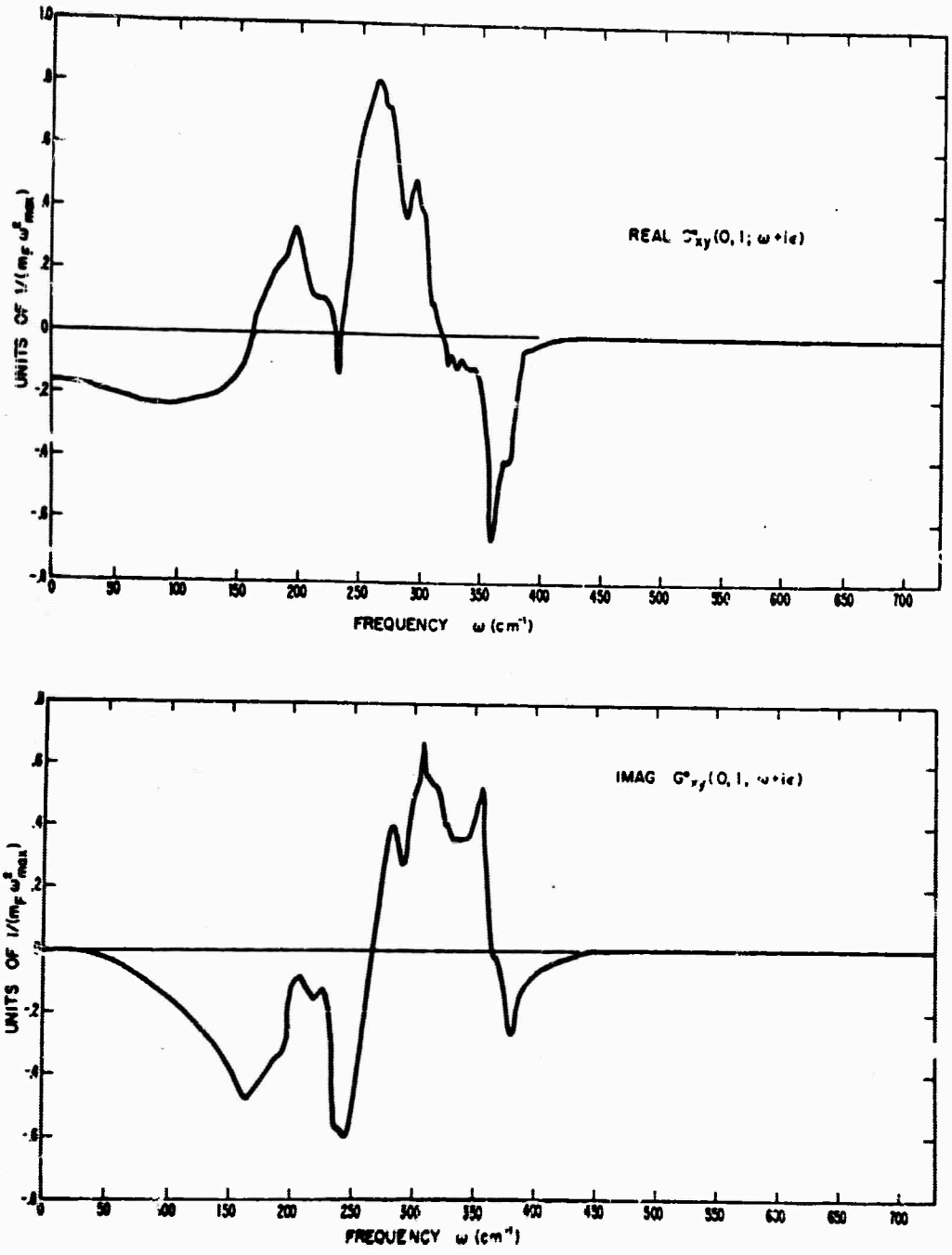

Fig. A-11: Real and imaginary parts of the 11th Green's function, $G^{o}_{xy}(0,1;\omega+i\epsilon)$ = "D" (cf. Fig. 6.8)

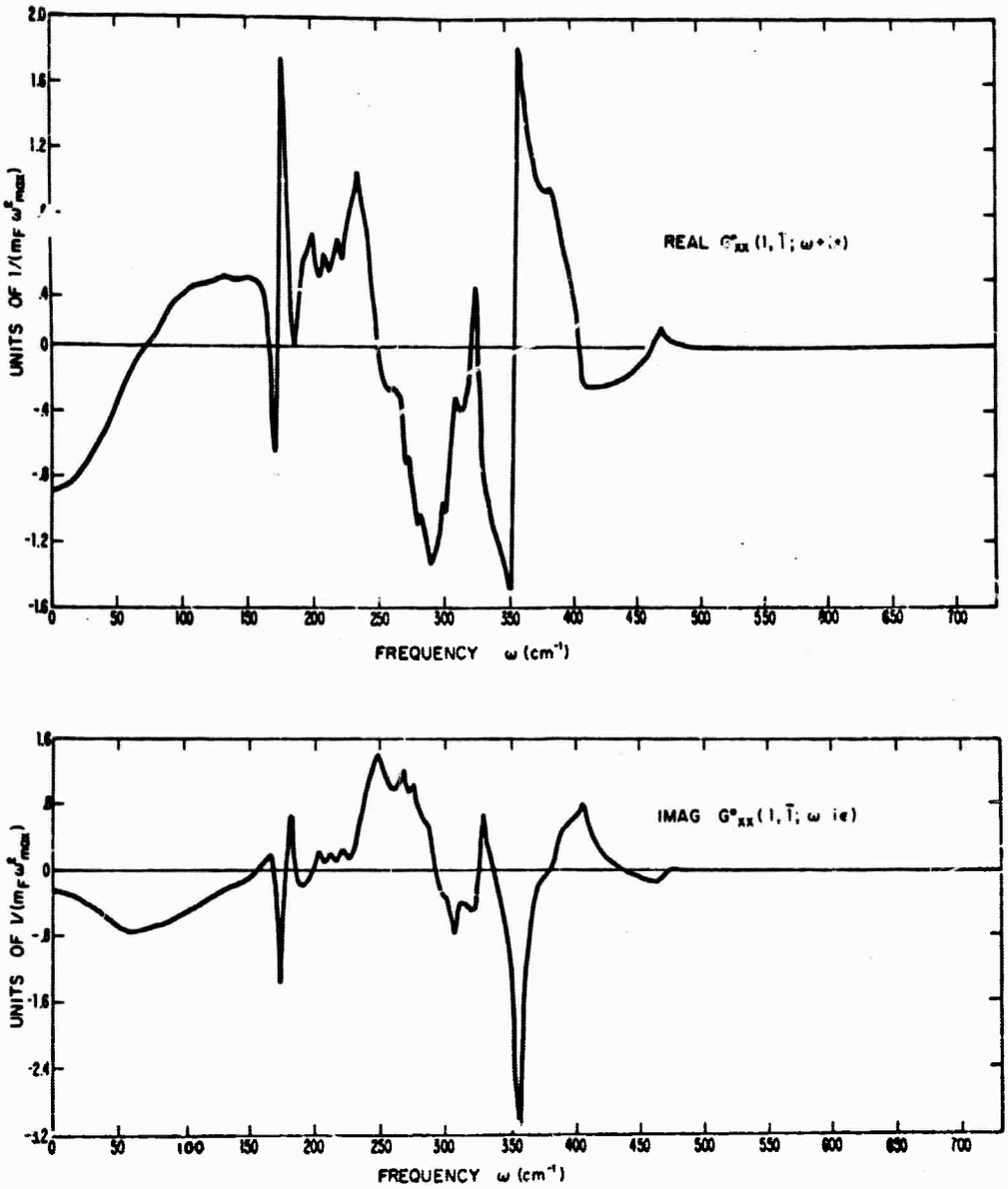

Fig. A-12: Real and imaginary parts of the 12th Green's function, $G^{o}_{\bar{x}x}(l,\bar{l};\omega+i\varepsilon)$ = "U" (cf. Fig. 6.8)

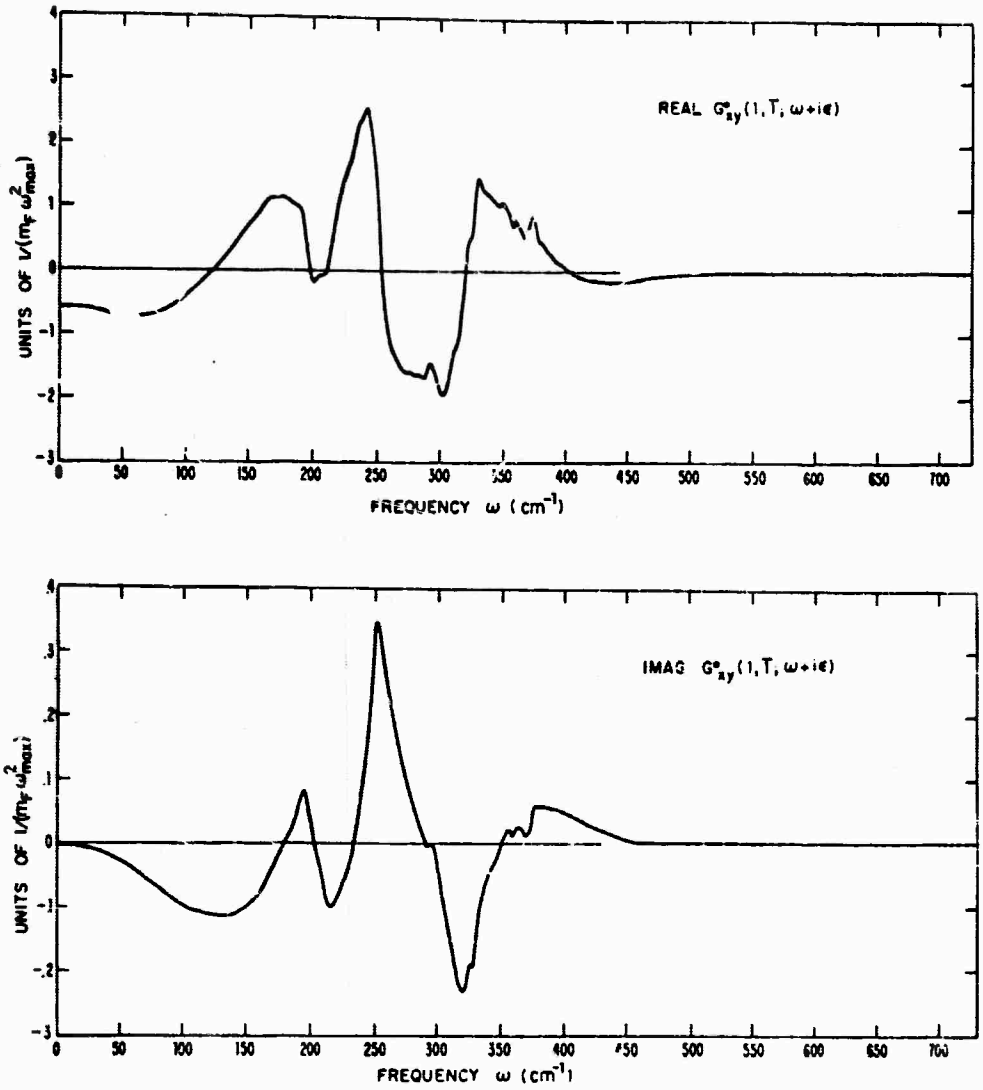

Fig. A-13: Real and imaginary parts of the 13th Green's function, $G^{o}_{xy}(1,\bar{1};\omega+i\epsilon)$ = "V" (cf. Fig. 6.8)

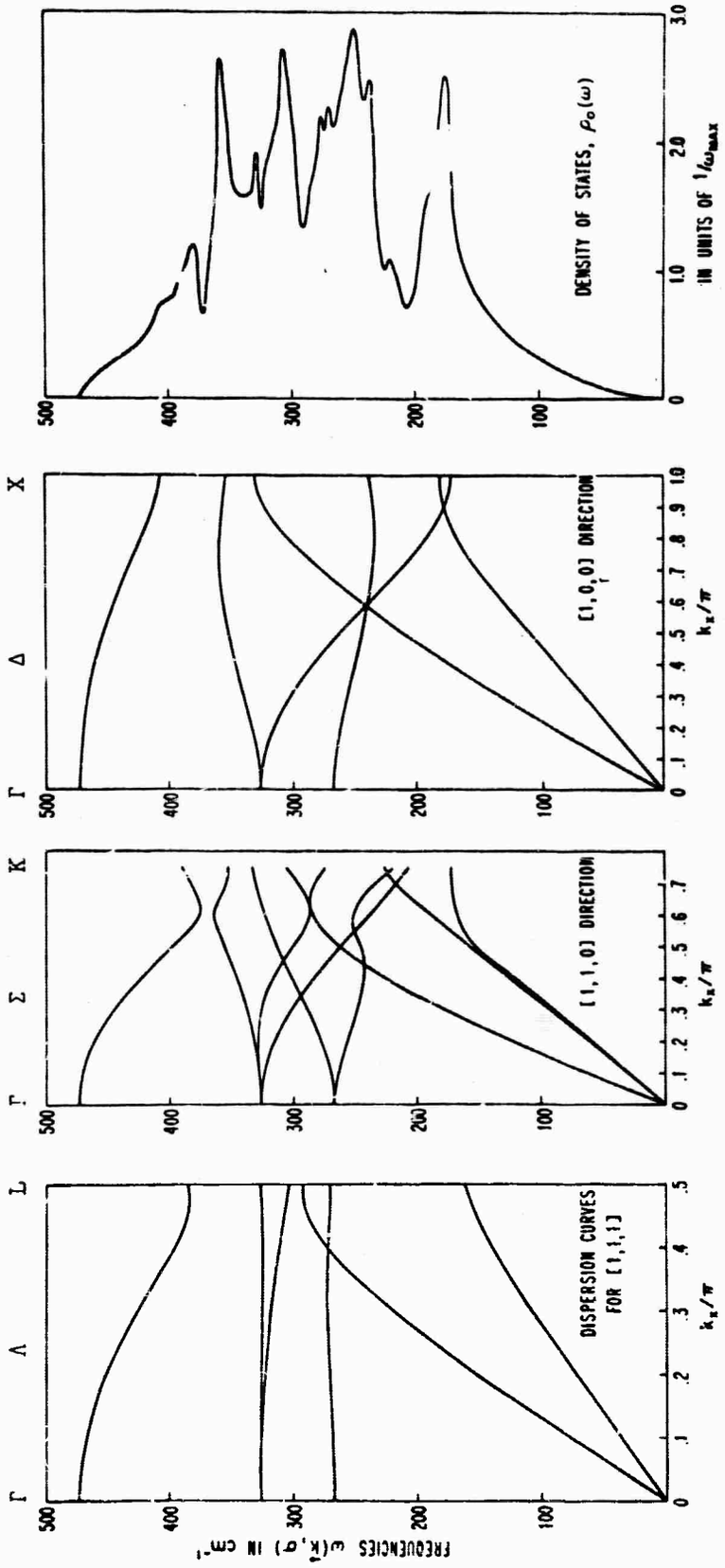

Fig. A-14: Calculated phonon density of states and dispersion curves for CaF_2, based on the rigid ion model described in Sec. 6.2.

REFERENCES

1. A. A. Maradudin, in Solid State Physics, edited by F. Seitz and D. Turnbull (Academic Press, N. Y.), 18, 273 (1966); 19, 1 (1967)
2. R. K. Chang, B. Lacina, and P. S. Pershan, Phys. Rev. Lett. 17, 755 (1966)
3. H. W. Verleur and A. S. Barker, Jr., Phys. Rev. 164, 1169 (1967); Solid State Commun. 5, 695 (1967)
4. R. F. Potter and D. L. Stierwalt, in Proc. of the Internat'l. Conf. on the Physics of Semiconductors, Paris, 1964 (Academic Press, N. Y., 1965), p. 1111
5. P. J. Gielisse, J. N. Plendl, L. C. Mansur, R. Marshall, S. Mitra, R. Mykolajewycz, and A. Smakula, J. Appl. Phys. 36, 2446 (1965)
6. G. Lucovsky, E. Lind, and E. A. Davis, in Proc. of the Internat'l. Conf. on the Physics of II-VI Semiconductors (W. A. Benjamin, Inc., N. Y., 1967)
7. O. Brafman, I. F. Chang, and S. S. Mitra (unpublished); cf. Ref. 21 below.
8. F. Kruger, O. Reinkoler, and E. Koch-Holm, Ann. Physik 85, 110 (1928)
9. A. Mitsuishi (unpublished); cf. Ref. 21 below.
10. A. S. Barker, J. A. Ditzenberger, H. J. Guggenheim, Phys. Rev. 175, 1180 (1968)
11. D. W. Feldman, M. Ashkin, and J. H. Parker, Phys. Rev. Lett. 17, 1209 (1966)
12. F. Oswald, Z. Naturforsch., 14A, 374 (1959)
13. Y. S. Chen, W. Shockley, and G. L. Pearson, Phys. Rev. 151, 648 (1966)
14. H. W. Verleur and A. S. Barker, Jr., Phys. Rev. 149, 715 (1966)

15. M. Balkanski, R. Beserman, and J. M. Besson, Solid State Commun. 4, 201 (1966)

16. J. Parrish, C. H. Perry, O. Brafman, I. F. Chang, and S. S. Mitra, in Proc. of the Internat'l Conf. on the Physics of II-VI Semiconductors (W. A. Benjamin, Inc., N. Y., 1967)

17. H. W. Verleur and A. S. Barker, Jr., Phys. Rev. 155. 750 (1967)

18. O. Brafman, I. F. Chang, G. Lengyel, S. S. Mitra, and E. Carnall, Phys. Rev. Lett. 19, 1120 (1967); in Proc. of the Internat'l. Conf. on Localized Excitations in Solids (Plenum Press, Inc., N. Y.,1968)

19. M. V. Klein and H. F. MacDonald, Phys. Rev. Lett. 20, 1031 (1968)

20. S. S. Jaswal and J. R. Hardy, Phys. Rev. 171, 1090 (1968)

21. G. Lucovsky, E. Burstein, and M. Brodsky, in Proc. of the Internat'l. Conf. on Localized Excitations in Solids (Plenum Press, Inc., N. Y., 1968)

22. I. F. Chang and S. S. Mitra, Phys. Rev. 172, 924 (1968)

23. J. M. Ziman, Theory of Solids (Cambridge, 1964); Electrons and Phonons (Oxford, 1963)

24. A. A. Maradudin, E. W. Montroll, and G. H. Weiss, in Solid State Physics, edited by F. Seitz and D. Turnbull (Academic Press, Inc., N. Y., 1963), Suppl. 3: "Theory of Lattice Dynamics in the Harmonic Approximation"

25. M. Born and K. Huang, Dynamical Theory of Crystal Lattices (Oxford, 1966)

26. A. A. Maradudin, Rept. Prog. in Phys. 28, 331 (1965)

27. R. S. Knox and A. S. Gold, Symmetry in the Solid State (W. A. Benjamin, Inc., N. Y., 1964) (contains many useful reprints)

28. M. Tinkham, Group Theory and Quantum Mechanics, (McGraw-Hill, Inc., N. Y., 1964)

29. V. Heine, Group Theory in Quantum Mechanics (Macmillan, N. Y., 1964)

30. J. S. Lomont, Applications of Finite Groups (Academic Press, Inc., N. Y., 1959) (contains an extensive bibliography on the application of group theory to physics.)

31. C. Herring, Jour. Franklin Inst. 233, 525 (1942) (reprinted in Knox and Gold, Ref. 27)

32. G. F. Koster, in Solid State Physics, edited by F. Seitz and D.Turnbull (Academic Press, Inc., N. Y.) 5, 173 (1957)

33. L. Chen, R. Berenson, and J. L. Birman, Phys. Rev. 170, 639 (1968)

34. J. L. Birman, Phys. Rev. 127, 1093 (1962)

35. J. L. Birman, Phys. Rev. 150, 771 (1966)

36. A. A. Maradudin and S. H. Vosko, Rev. Mod. Phys. 40, 1 (1968)

37. J. L. Warren, Rev. Mod. Phys. 40, 38 (1968)

38. E. Wigner, Nach. der Akad. Wiss. zu Gött., Math-Kl. Phys., Berlin, 1930, p. 133 (translated in Knox and Gold, Ref. 27)

39. C. Kittel, Quantum Theory of Solids (John Wiley, Inc., N. Y., 1963)

40. N. S. Gillis and N. R. Werthamer, Phys. Rev. 167, 607 (1968); D. R. Fredkin and N. R. Werthamer, Phys. Rev. 138, A1527 (1965)

41. P. Nozieres, Interacting Fermi Systems (W. A. Benjamin, Inc., N. Y., 1964), Chapter 2, 3

42. A. A. Abrikosov, L. P. Gorkov, and I. E. Dzyaloshinski, Methods of Quantum Field Theory in Statistical Physics (prentice-Hall, N. J., 1963)

43. G. Baym, Ann. of Phys. 14, 1 (1961)

44. V. M. Galitskii and A. B. Migdal, Zhur. Eksp. i. Teor. Fiz. 34, 139 (1958); Engl. trans., Soviet Physics-JETP 34, 96 (1958)

45. P. C. Martin and J. Schwinger, Phys. Rev. 115, 1342 (1959)

46. D. N. Zubarev, Usp. Fiz. Nauk., 71, 71 (1960); Engl. Trans., Soviet Phys.-Uspekhi 3, 320 (1960)

47. Nguyen Xuan Xinh, Westinghouse Research Report No. 65-9F5-442-P8 (1965); J. Phys. (France) 28, Suppl. No. 2, C1-103 (1967)

48. T. Timusk and M. V. Klein, Phys. Rev. 141, 664 (1966)

49. W. Hayes, G. D. Jones, H. F. Macdonald, C. T. Sennett, and R. J. Elliott, Proc. Roy. Soc. A289, 1 (1965)

50. E. Burstein, in Phonons and Phonon Interactions, edited by T. A. Bak (W. A. Benjamin, Inc., N. Y., 1964)

51. R. A. Cowley, in Phonons in Perfect Lattices and in Lattices with Point Imperfections, edited by R. W. H. Stevenson (Plenum Press, Inc., N. Y., 1966)

52. R. A. Cowley, Adv. in Phys. 12, 421 (1963)

53. A. A. Maradudin, Ann. of Phys. 30, 371 (1964)

54. Y. A. Izyumov, Adv. in Phys. 14, 569 (1965)

55. R. J. Elliott and D. W. Taylor, Proc. Roy. Soc. A296, 161 (1967)

56. A. A. Maradudin, in Astrophysics and the Many-Body Problem (W. A. Benjamin, Inc., N. Y., 1963); in Phonons and Phonon Interactions, edited by T. A. Bak (W. A. Benjamin, Inc., N. Y., 1964)

57. A. A. Maradudin, Rept. Prog. in Phys. 28, 331 (1965)

58. R. J. Elliott, in Phonons in Perfect Lattices and in Lattices with Point Imperfections, edited by R. W. H. Stevenson (Plenum Press, Inc., N. Y., 1966)

59. R. J. Elliott, Argonne Nat'l. Laboratory Report ANL-7237 (1966)

60. R. J. Elliott, in Proc. of the Internat'l. Conf. on Lattice Dynamics, Copenhagen, 1963

61. G. J. Koster and J. C. Slater, Phys. Rev. 95, 1167 (1954); 95, 1436 (1954); 96, 1208 (1954)

62. P. A. Wolff, Phys. Rev. 124, 1030 (1961)

63. A. M. Clogston, Phys. Rev. 125, 439 (1961)

64. J. Kanamori, J. Appl. Phys. 36, 929 (1965)

65. J. Friedel, Nuovo Cimento 2 (Suppl.), 287 (1958)

66. P. G. Dawber and R. E. Turner, Proc. Phys. Soc. 88, 217 (1966)

67. F. Gautier and P. Lenglart, Phys. Rev. 139A, 705 (1965)

68. M. Lax, Rev. Mod. Phys. 23, 287 (1951); Phys. Rev. 85, 621 (1952)

69. D. A. Greenwood, Proc. Phys. Soc. 71, 585 (1958)

70. F. Nakano, Prog. Theor. Phys. 15, 77 (1956)

71. R. Kubo, J. Phys. Soc. (Japan) 12, 570 (1957)

72. S. F. Edwards, Phil. Mag. 3, 1020 (1958)

73. R. Klauder, Ar . of Phys. 14, 43 (1961)

74. T. Matsubara and Y. Toyozawa, Prog. Theor. Phys. 26, 739 (1961)

75. F. Yonezawa, Prog. Theor. Phys. 31, 357 (1964)

76. F. Yonezawa and T. Matsubara, Prog. Theor. Phys. 35, 357 (1966)

77. J. Beeby, Proc. Roy. Soc. A279, 82 (1964); S. F. Edwards and J. Beeby, Proc. Roy. Soc. A274, 395 (1962)

78. S. F. Edwards, Proc. Roy. Soc. A267, 518 (1962)

79. P. Soven, Phys. Rev. 15 , 539 (1966); 156, 809 (1967)

80. I. M. Lifshitz, Adv. in Phys. 13, 483 (1964)

81. E. A. Stern, Phys. Rev. 168, 730 (1968)

82. B. Velicky, S. Kirkpatrick, and H. Ehrenreich, Phys. Rev. 175, 747 (1968)

83. T. Wolfram and J. Callaway, Phys. Rev. 130, 2207 (1963)

84. D. Hone, H. Callen, and L. R. Walker, Phys. Rev. 144, 283 (1966)

85. S. Takeno, Prog. Theor. Phys. 30, 731 (1963)

86. Y. Wang and H. Callen, Phys. Rev. 160, 358 (1967)

87. Y. Izyumov, Proc. Phys. Soc. 87, 505 (1966)

88. D. Hone (to be published)

89. S. W. Lovesey, Proc. Phys. Soc. 91, 658 (1967); J. Phys. Chem.: Proc. Phys. Soc. 1, 102, 118 (1968)

90. A. Oseroff and P. S. Pershan, Phys. Rev. Lett. 21, 1593 (1968)

91. L. F. Johnson, R. E. Dietz, and H. H. Guggenheim, Phys. Rev. Lett. 17, 13 (1966); A. Misetich and R. E. Dietz, Phys. Rev. Lett. 17, 392 (1966); P. Moch, G. Parisot, R. E. Dietz, and H. J. Guggenheim, Phys. Rev. Lett. 21, 1596 (1968)

92. W. J. L. Buyers, R. A. Cowley, T. M. Holden, and R. W. H. Stevenson, Solid State Commun. 6, 145 (1968)

93. M. Motokawa and M. Date, J. Phys. Soc. (Japan) 23, 1216 (1967)

94. M. V. Klein, Phys. Rev. 131, 1500 (1963); 141, 716 (1966)

95. G. Benedek and G. F. Nardelli, Phys. Rev. 155, 1004 (1967)

96. M. Wagner, Phys. Rev. 131, 2520 (1963); 133, A750 (1964)

97. G. Blaesser, J. Peretti, and G. Toth, Phys. Rev. 171, 665 (1968)

98. G. Lehman and R. E. de Wames, Phys. Rev. 131, 1008 (1963)

99. I. M. Lifshitz, J. Phys. USSR 7, 211, 249 (1943); 8, 89 (1944); Zhur. Eksp. i. Teor. Fiz. 17, 1017, 1076 (1947); 18, 293 (1948); Suppl. Nuovo Cimento 3, 716 (1956)

100. E. W. Montroll and R. B. Potts, Phys. Rev. 100, 525 (1955)

101. R. E. Shamu, W. M. Hartmann, and E. L. Yasaitis, Phys. Rev. 170, 822 (1968)

102. I. G. Nolt, R. A. Westwig, R. W. Alexander, and A. J. Sievers, Phys. Rev. 157, 731 (1967)

103. R. Brout and W. M. Visscher, Phys. Rev. Lett. 9, 54 (1962)

104. W. M Visscher, Phys. Rev. 129, 28 (1963)

105. R. J. Elliott and D. W. Taylor, Proc. Phys. Soc. 83, 189 (1964)

106. Y. M. Kagan and Y. A. Iosilevskii, Zhur. Eksp. i. Teor. Fiz. 42, 259 (1962); Engl. Trans., Soviet Phys.-JETP 15, 182 (1962)

107. S. Takeno, Prog. Theor. Phys. 29, 191 (1963); 28, 33 (1962); 29, 328 (1963)

108. B. Mozer and A. A. Maradudin, Bull. Am. Phys. Soc. (II) 8, 193 (1963)

109. P. G. Dawber and R. J. Elliott, Proc. Phys. Soc. 81, 453 (1963); Proc. Roy. Soc. A273, 222 (1963)

110. J. A. Krumhansl and J. A. D. Matthew, Phys. Rev. 166, 856 (1968)

111. J. Van Krankendonk and J. H. Van Vleck, Rev. Mod. Phys. 30, 1 (1958)

112. E. Merzbacher, Quantum Mechanics (John Wiley, Inc., N. Y., 1961)

113. N. Bloembergen, Nonlinear Optics (W. A. Benjamin, Inc., N. Y., 1965)

114. F. G. Bass and M. I. Kaganov, Zhur. Eksp. i Teor. Fiz. 37, 1390 (1959); Engl. Trans. Soviet Phys. - JETP 10, 986 (1960)

115. R. J. Elliott and R. Loudon, Phys. Lett. 3, 189 (1963); P. A. Fleury and R. Loudon, Phys. Rev. 166, 514 (1968)

116. J. T. Hougen and S. Singh, Phys. Rev. Lett. 10, 406 (1963); Proc. Roy. Soc. A277, 193 (1964)

117. Das Gupta, Phys. Rev. Lett. 3, 38 (1959); Phys. Rev. 128, 2181 (1962)

118. I. I. Sobel'man and E. L. Feinberg, Soviet Phys.-JETP 34, 339 (1958)

119. R. Loudon, Adv. in Phys. 13, 423 (1964)

120. L. N. Ovander, Soviet Phys.-Solid State 3, 1737 (1962); 4, 1078 (1962); 6, 290 (1964)

121. R. Loudon, Proc. Roy. Soc. A275, 218 (1963)

122. R. Loudon, Proc. Phys. Soc. 82, 393 (1963)

123. V. L. Strizhevskii, Soviet Phys.-Solid State 3, 2141 (1962)

124. M. Lax and E. Burstein, Phys. Rev. 97, 39 (1955)

125. M. Born and M. Bradburn, Proc. Roy. Soc. A188 1 (1947)

126. F. Stern, in Solid State Physics, edited by F. Seitz and D. Turnbull (Academic Press, Inc., N. Y.), 15, 299 (1963)

127. D. K. Martin, Adv. in Phys. 14, 39 (1964)

128. R. Kubo, in Boulder Lectures in Theoretical Physics (Academic Press, Inc., N. Y., 1958), Vol. 1

129. H. Bilz, in Phonons in Perfect Lattices and in Lattices with Point Imperfections, edited by R. W. H. Stevenson (Plenum Press, Inc., N. Y., 1966)

130. T. P. Martin, Phys. Rev. 160, 686 (1967); 170, 779 (1968)

131. R. S. Wilson, W. T. King, S. K. Kim, Phys. Rev. 175, 1164 (1968)

132. F. J. Dyson, Phys. Rev. 92, 1331 (1953)

133. R. Bellman, Phys. Rev. 101, 19 (1956)

134. J. des Cloizeaux, J. Phys. Rad. 18, 131 (1957)

135. R. Englman, Nuovo Cimento 10, 615 (1958)

136. H. Schmidt, Phys. Rev. 105, 425 (1957)

137. R. L. Agacy, Proc. Phys. Soc. 83, 591 (1964)

138. J. Hori and T. Asahi, Prog. Theor. Phys. 17, 523 (1957)

139. J. Hori, Prog. Theor. Phys. 18, 367 (1957)

140. J. Mahanty, Nuovo Cimento 19, 46 (1961)

141. A. A. Maradudin, P. Mazur, E. W. Montroll, and G. H. Weiss, Rev. Mod. Phys. 30, 175 (1958)

142. C. Domb, A. A. Maradudin, E. W. Montroll, and G. H. Weiss, Phys. Chem. Solids 8, 419 (1959); Phys. Rev. 115, 18, 24 (1959)

143. P. Dean, Proc. Phys. Soc. 73, 413 (1959); Proc. Roy. Soc. A254, 507 (1960); A260, 263 (1961)

144. P. Dean and J. L. Martin, Proc. Roy. Soc. A259, 409 (1960)

145. P. Dean and M. D. Bacon, Proc. Phys. Soc. 81, 642 (1963)

146. J. L. Martin, Proc. Roy. Soc. A260, 139 (1961)

147. M. D. Bacon, P. Dean, and J. L. Martin, Proc. Phys. Soc. 80, 174 (1962)

148. H. B. Rosenstock and R. E. McGill, J. Math. Phys. 3, 200 (1962)

149. D. N. Payton, III, and W. M. Visscher, Phys. Rev. 154, 802 (1967); 156, 1032 (1967); 175, 1201 (1968)

150. J. S. Langer, J. Math. Phys. 2, 584 (1961)

151. H. Poon and A. Bienenstock, Phys. Rev. 141, 7105 (1966); 142, 466 (1966)

152. P. L. Leath and B. Goodman, Phys. Rev. 148, 968 (1966); 175, 963 (1968)

153. S. Takeno, Prog. Theor. Phys. 25, 102 (1961); 28, 33 (1962); 29, 328 (1963)

154. R. Kubo, J. Phys. Soc. (Japan) 17, 1100 (1962)

155. P. S. Pershan and W. B. Lacina, Phys. Rev. 168, 725 (1968)

156. R. W. Davies and J. S. Langer, Phys. Rev. 131, 163 (1963)

157. D. W. Taylor, Phys. Rev. 156, 1017 (1967)

158. P. L. Leath, Phys. Rev. 171, 725 (1968)

159. R. J. Elliott, R. N. Aiyer, and P. L. Leath (to be published)

160. I. M. Lifshitz, Zhur. Eksp. i. Teor. Fiz. 44, 1723 (1963); Engl. Trans., Soviet Phys.-JETP 17, 1159 (1963)

161. C. V. Raman, Ind. J. Phys. 2, 387 (1928)

162. E. Rumpf, Z. Physik. Chem. (Leipzig) B7, 148 (1930)

163. E. Beck, Metallurgie 5, 514 (1908)

164. E. G. Chernevskaya and G. V. Anan'eva, Fiz. Tverd. Tela 8, 216 (1966); Engl. Trans., Soviet Phys.-Solid State 8, 169 (1966)

165. S. Ganesan and R. Srinivasan, Can. J. Phys. 40, 74 (1962); 40, 91 (1962)

166. R. Srinivasan, Proc. Phys. Soc. 72, 566 (1958)

167. D. Cribier, Ann. Phys. 4, 333 (1959)

168. T. Shimanouchi, M. Tsuboi, and M. Miyazawa, J. Chem. Phys. 35, 1597 (1961) (these authors do not consider the Coulomb field)

169. J. D. Axe, Phys. Rev. 139, A1215 (1965)

170. W. Cochran, Adv. in Phys. 9, 387 (1960); Proc. Roy. Soc. A253,260 (1959)

171. R. A. Cowley, Proc. Roy. Soc. A268, 109, 121 (1962)

172. A. D. B. Woods, W. Cochran, and B. N. Brockhouse, Phys. Rev. 119, 980 (1960); R. A. Cowley, W. Cochran, A. D. B. Woods, and B. N. Brockhouse, Phys. Rev. 131, 1030 (1963)

173. B. R. A. Nijboer and F. W. De Wette, Physica 23, 309 (1957); 24, 422 (1958); 24, 1105 (1958); F. W. De Wette, Physica 25, 1225 (1959); Phys. Rev. 123, 103 (1961)

174. K. Huang, Proc. Roy. Soc. A208, 352 (1951); E. R. A. Report L/T 239 (1950)

175. R. H. Lyddane and K. F. Herzfeld, Phys. Rev. 54, 846 (1938)

176. R. H. Lyddane, R. G. Sachs, and E. Teller, Phys. Rev. 59, 673 (1941)

177. W. Cochran and R. A. Cowley, J. Phys. Chem Solids 23, 447 (1962)

178. W. Kaiser, W. G. Spitzer, R. H. Kaiser, and L. E. Howarth, Phys. Rev. 127, 1950 (1962) (CaF_2)

179. D. R. Bosomworth, Phys. Rev. 157, 709 (1967) (Ca, Sr, Ba, CdF_2)

180. J. D. Axe, J. W. Gaglianello, and J. E. Scardefield, Phys. Rev. 139, A1211 (1965) (CdF_2)

181. L. V. Berman and A. G. Zhukov, Opt. i. Spektroskopiya 19, 783 (1965); Engl. Trans., Opt. Spect. 19, 433 (1965) (CaF_2)

182. A. Hadni, Ann. Phys. (Paris) 9, 9 (1964) (CaF_2, SrF_2)

183. D. R. Huffman and M. H. Norwood, Phys. Rev. 117, 709 (1960) (CaF_2)

184. D. Gerlich, Phys. Rev. 136, A1366 (1964) (SrF_2)

185. D. Gerlich, Phys. Rev. 135, A1331 (1964) (BaF_2)

186. W. E. Bron and M. Wagner, Phys. Rev. 167, 841 (1968)

187. K. Lakatos and J. A. Krumhansl, Phys. Rev. 175, 841 (1968)

ACKNOWLEDGEMENTS

I wish to thank Professor Peter Pershan for his helpful supervision of this work from its conception to its completion, and for many stimulating conversations during my research tenure. I have appreciated his continuing interest in my project, and his ready willingness to be available for helpful discussions whenever I needed assistance.

I am indebted to Dr. Richard Chang and to Dr. Geoffrey Brooker for giving me much helpful advice on experimental techniques; to Mr. Robert Callender for collaboration in taking some of the low temperature data (Argon laser and Spex system); and to Mr. Howard Goldberg for his work related to the problem of spectrometer slit convolution.

Dr. Hargreaves of Optovac, Inc. supplied all of the crystal samples used in this study, and kindly loaned us some of the samples during the initial stages of the investigations.

Unclassified

Security Classification

DOCUMENT CONTROL DATA - R & D

(Security classification of title, body of abstract and indexing annotation must be entered when the overall report is classified)

1. ORIGINATING ACTIVITY (Corporate author)
Division of Engineering and Applied Physics
Harvard University
Cambridge, Mass. 02138

2a. REPORT SECURITY CLASSIFICATION
Unclassified

2b. GROUP

3. REPORT TITLE
PHONON OPTICAL PROPERTIES OF MIXED FLUORITE SYSTEMS: RAMAN SCATTERING FROM $Ca_{1-x}Sr_xF_2$ AND $Ba_{1-x}Sr_xF_2$

4. DESCRIPTIVE NOTES (Type of report and, inclusive dates)
Interim technical report

5. AUTHOR(S) (First name, middle initial, last name)
William Bradley Lacina

6. REPORT DATE
March 1969

7a. TOTAL NO. OF PAGES
217

7b. NO. OF REFS
187

8a. CONTRACT OR GRANT NO.
ARPA SD-88

b. PROJECT NO.

c.

d.

9a. ORIGINATOR'S REPORT NUMBER(S)
Technical Report No. ARPA-36

9b. OTHER REPORT NO(S) (Any other numbers that may be assigned this report)

10. DISTRIBUTION STATEMENT
Reproduction in whole or in part is permitted by the U. S. Government.
Distribution of this document is unlimited.

11. SUPPLEMENTARY NOTES

12. SPONSORING MILITARY ACTIVITY

13. ABSTRACT

The general problem of the effects of impurities on the vibrational, electronic, and magnetic properties of crystalline solids has currently attracted much interest. One aspect of this problem has been the study of random disordered systems, and in recent years, there have been numerous experimental and theoretical investigations of the phonon optical properties of mixed crystal systems. We have studied experimentally the Raman scattering (at $\sim 4^{o}K$, $77^{o}K$, and $300^{o}K$) from the mixed fluorite systems, $Ca_{1-c}Sr_cF_2$ and $Ba_{1-c}Sr_cF_2$, using laser excitation and a photon counting detection system. Analogous work on the far-infrared reflectivity spectra for these systems has been carried out by Verleur and Barker.

The Green's function methods which have been extensively employed for the isolated defect and random disorder problems are reviewed, and it is shown how the phonon optical properties can be expressed using this formalism. These techniques have been very useful for qualitative and quantitative understanding of impurity effects, although they usually involve combersome computational difficulties for physically realistic models of the impurity and the host lattice. A low concentration theory for Raman scattering and infrared absorption in mixed crystals, based on an average Green's function $\langle G \rangle$, is described and applied to the $Ca_{1-c}Sr_cF_2$ system; theoretical calculations are presented and compared with experimental measurements. The "proper self-energy" functions which arise in this formalism are calculated to first order in the concentration c, and involve certain unperturbed phonon Green's functions $G^{o}_{\alpha\beta}(\ell K, \ell' K'; \omega + i\varepsilon)$, which have been computed numerically for a rigid ion model of a harmonic fluorite lattice. These Green's functions, which would be useful for many other studies of phonon impurity properties in CaF_2, are included in an appendix.

DD FORM 1 NOV 65 1473 (PAGE 1)

S/N 0101-807-6811

Unclassified

Security Classification

A-31408

14

KEY WORDS	LINK A		LINK B		LINK C	
	ROLE	WT	ROLE	WT	ROLE	WT
Phonon Optical Properties						
Mixed Fluorite Systems						
Green's function						
Raman Scattering						
Disordered Systems						